



Christoph Zöphel

Flexibility Options in Energy Systems

The influence of Wind - PV ratios and sector coupling on optimal combinations of flexible technologies in a European electricity system

IMPRESSUM

Herausgeber:

Technische Universität Dresden
Fakultät der Wirtschaftswissenschaften
Lehrstuhl für Energiewirtschaft
01062 Dresden

Tel.: +49 351 463-33297

Fax: +49 351 463-39763

E-Mail: ee2@mailbox.tu-dresden.de

Internet: <http://www.ee2.biz>

ISBN: 978-3-86780-698-5

URN : [urn:nbn:de:bsz:14-qucosa2-781290!](https://nbn-resolving.org/urn:nbn:de:bsz:14-qucosa2-781290)

Stand: 02/2022

Alle Rechte vorbehalten.

Flexibility Options in Energy Systems

The influence of Wind - PV ratios and sector coupling on optimal combinations of flexible technologies in a European electricity system

DISSERTATION

zur Erlangung des akademischen Grades Dr. rer. pol.
vorgelegt an der Fakultät Wirtschaftswissenschaften
der Technischen Universität Dresden von

Christoph Zöphel

Geboren am 30. November 1988 in Eisenach

BETREUER

Prof. Dr. Dominik Möst

Professur für BWL, insb. Energiewirtschaft

GUTACHTER

Prof. Dr. Dominik Möst

Professur für BWL, insb. Energiewirtschaft

Prof. Dr. Thilo Bocklisch

Professur für Energiespeichersysteme

Eingereicht: 16.07.2021

Verteidigt: 02.02.2022

Foreword

The European Union Fit for 55 program intends to reduce greenhouse gas emissions by 55% by 2030. One prominent measure is to increase the extension of renewable energy sources, especially for electricity supply. Beyond 2030, a further significant increase of renewable energy sources is foreseen. However, the feed-in from the majority of the added renewable systems is weather-dependent. Since electricity demand and supply must be balanced at all times, the weather-dependent feed-in comes with the challenge of how renewable energies can be well integrated into the overall system and how flexibility can be provided to balance supply and demand.

- But what flexibility is required in the system?
- And how do different feed-in profiles of renewable technologies affect flexibility needs?
- How can this flexibility be provided cost-effectively in the overall system?

Mr Zöphel devotes his work to these topics, particularly to the questions of which flexibility options are required depending on the different proportions of wind power and photovoltaics in the overall system and what contributions the different flexibility options can make. Accordingly, the aim of his work is the systematic analysis of the need for and provision of flexibility in the future European energy system and the answering of the overarching research question:

- How do different Wind-PV ratios in the future expansion of intermittent renewable energy sources affect the optimal flexibility provision in a multi-coupled European energy system?

With this question, Mr Zöphel addresses an extraordinarily relevant and essential question in connection with the transformation of the electricity system in his dissertation and subdivides it into several sub-questions.

To do this, he translates these relevant challenges into methodologically sophisticated models to provide quantitative answers to the questions mentioned above. He developed extensive preliminary analyzes with the help of models for a cost-optimized renewable expansion in Europe and a techno-economic electricity market model. The strength of the work is the clear and precise analysis of different renewable pathways – especially higher shares of photovoltaic compared with higher percentages of wind energy – and their impact on flexibility needs. Mr Zöphel has chosen a highly topical and relevant topic studied at many institutions. Despite the extensive work in this field, he succeeds due to his approach and the scope of modelling – both spatially for throughout Europe as well as on an hourly basis – making his work a unique selling proposition. Anyone who has read

Christoph Zöphels' dissertation understands much better than before how significant higher shares of photovoltaic and wind energy impact the residual load and the flexibility needed to balance supply and demand. That makes this book helpful for policymakers but also for researchers and practitioners.

I hope you enjoy reading this informative dissertation!

Prof. Dr. Dominik Möst

Danksagung

Für die Erstellung dieser Dissertation möchte ich zuallererst meinen Dank an Professor Dominik aussprechen. Sein Wissen, seine Unterstützung und sein Vertrauen haben es mir ermöglicht, meine Arbeit zu reflektieren und stetig zu verbessern. Ich danke außerdem meinem Zweitgutachter Herrn Professor Thilo Bocklisch für den Austausch und die zusätzlichen Perspektive auf meine Arbeit. Als Mitglieder der Promotionskommission gilt mein Dank außerdem Frau Professor Susanne Strahinger und Herrn Professor Alexander Kemnitz.

Für die prägenden Jahre am Boysen-TU Dresden-Graduiertenkolleg möchte ich Herrn Professor Antonio Hurtado, Herrn Professor Lutz Hagen und Dr. Anna Martius sowie allen betreuenden ProfessorInnen des 2. Graduiertenkollegs danken. Mein besonderer Dank gilt außerdem den Stiftern des Boysen-TUD-Graduiertenkollegs, der gemeinnützigen Friedrich und Elisabeth Boysen-Stiftung sowie der Technischen Universität Dresden.

An die Zeit mit meinen Kolleginnen und Kollegen sowohl am Graduiertenkolleg als auch am Lehrstuhl für Energiewirtschaft werde ich immer in freundschaftlicher Dankbarkeit denken. Die Professionalität, Expertise und die Offenheit haben mich stets inspiriert und motiviert. Der berufliche und private Austausch hat zum erfolgreichen Abschluss meiner Promotion bedeutend beitragen.

Ohne meine Eltern, meine Schwester und meine ganze Familie wäre alles schwerer und vieles unmöglich. Ich danke Ihnen von Herzen dafür, dass sie in jeder Lebenssituation immer für mich da sind.

Por último, me gustaría dar las gracias especialmente a Carmen, que ha hecho posible la realización de mi tesis en primer lugar. Ha acompañado mi trabajo con una paciencia y una comprensión impresionantes, endulzando los éxitos y suavizando los descensos, incluso cuando nuestra hija ya formaba parte de nuestra familia. Os quiero.

Dresden, 21.02.2022

Abstract

Within the present work, the main objective is to identify interactions between flexibility demand and flexibility supply. Therefore, three research fields regarding the future transformation of the European energy system are addressed. First, an expansion of intermittent renewable energy sources (iRES) is discussed taking the potentials of wind and PV technologies into account. The analysis is based on fundamental considerations of generation characteristics as well as available potentials across 17 countries in central-western Europe. To emphasize the differences in electricity generation between wind and PV, an iRES expansion model is developed coping for geographically highly resolved weather data as well as for limitations of iRES potentials due to land-use restrictions and for energy-policy constraints. Three scenarios with varying Wind-PV ratio in total iRES electricity generation are evaluated. Second, the options to provide flexibility to balance the flexibility demand are introduced and mathematically implemented in ELTRAMOD. Therefore, the model was adjusted to represent multiple flexible technologies for upward, downward and shifting flexibility provision to cover the residual load. In a system perspective and a greenfield approach, the linear electricity market model enables the analysis of cost-optimal combinations of flexibility options against the background of scenarios with different flexibility demands. In addition, the third research field addresses the emerging developments of sector coupling by including selected Power-to-X technologies. A second scenario dimension analyses the role of energy storages in the energy end-use sectors for a more flexible sector coupling. The results underline the importance of the Wind-PV ratios in electricity generation when assessing flexibility demand and flexibility supply in model-based energy system analysis. Due to the higher seasonality of PV, the residual load parameter indicate higher iRES integration challenges in terms of flexible capacity requirements. Particularly the provision of spatial and temporal balancing flexibility is significantly influenced by a higher wind or a higher PV share in the iRES mix. With sector coupling, the value of temporal shifting is increasing. Hourly storages are not only highly sensitive to the Wind-PV ratio, but in addition strongly impacted by sector coupling. In both dimensions, a higher PV share is increasing the value for short-term shifting. Furthermore, sector coupling increases the need for additional electricity generation. Thereby, for peak-load capacity provision gas-fuelled power plant are optimal in the present work increasing the total emissions especially with higher PV shares. The sensitivity analysis shows the value of additional iRES capacities as well as of storage cost reductions to further reduce emissions.

Contents

Contents.....	V
List of Figures	IX
List of Tables.....	XVII
Abbreviations	XXI
Nomenclature: iRES expansion model	XXIII
Nomenclature: Investment and dispatch model for flexibility options.....	XXV
1 Introduction	1
1.1 Scope and research questions.....	3
1.2 Outline of the work.....	5
2 Fundamentals of flexibility demand and provision in the energy system.....	9
2.1 Flexibility requirements in an energy system with high shares of variable renewable energy sources	9
2.1.1 Characteristics of electricity generation from wind and PV systems	10
2.1.2 Definition and parameters of the flexibility demand by means of the residual load	12
2.1.3 Impact of intermittent renewable energy expansion on the flexibility demand	14
2.1.3.1 Impacts on the residual load – an example for Germany	14
2.1.3.2 Further challenges regarding the intermittent renewable energy expansion ..	17
2.1.4 Derivation of PV and wind onshore expansion scenarios.....	18
2.2 Options for providing flexibility in the energy system	20
2.2.1 Back-up and load shedding flexibility	21
2.2.2 Spatial and temporal shifting flexibility	23

2.2.3	Load increase flexibility and sector coupling	24
3	Potential-based optimal wind and PV expansion in Europe.....	27
3.1	Determination of wind onshore and PV potentials.....	28
3.1.1	Identification of a representative weather year.....	29
3.1.2	General steps for the weather data accessing	30
3.1.3	Calculation of Wind onshore potentials.....	31
3.1.4	Calculation of PV potentials	34
3.1.5	Area analysis for wind onshore and PV installations	35
3.2	Model-based optimal expansion of varying renewable energies	40
3.2.1	Model requirements and general assumptions.....	40
3.2.2	Model formulation for wind onshore and PV expansion.....	42
3.2.3	Further data input	46
3.2.4	Limitations of the modelling approach	48
4	Influence of different Wind-PV ratios on the flexibility demand.....	51
4.1	Results on overall installed iRES capacities and annual generation.....	51
4.2	Evaluation of sorted residual load parameters	57
4.3	Evaluation of time-dependent residual load parameters	62
4.4	Total costs of iRES investments and iRES cost potentials.....	69
4.5	Summary and qualitative assessment of the potentials of flexibility options	73
5	Modelling Investment and Operations Decision for Flexibility Options	77
5.1	Modelling framework and general assumptions.....	77
5.1.1	Basic structure of ELTRAMOD and underlying main assumptions.....	78
5.1.2	Model requirements and adaptations of ELTRAMOD for the implementation of flexibility options	80
5.1.3	Representation of selected sector coupling approaches and derivation of scenarios for the flexibility supply side	83

5.2	ELTRAMOD-based investment and dispatch model	86
5.2.1	Objective and cost-related equations.....	86
5.2.2	Electricity balance	88
5.2.3	Constraints for the electricity sector	89
5.2.3.1	Dispatchable power plants	89
5.2.3.2	Storages and demand-side-management processes	91
5.2.4	Constraints for the representation of sector coupling.....	93
5.2.4.1	Constraints for the district heating sector	93
5.2.4.2	Constraints for the electrolyser-based hydrogen production.....	94
5.2.4.3	Constraints for the private passenger transport sector	95
5.3	Data input	97
5.3.1	Electricity sector	97
5.3.2	Sector coupling technologies.....	104
5.4	Limitations of the modelling approach.....	111
6	Techno-economic analysis of optimal combinations of flexibility options.....	115
6.1	Aggregated results for the whole region observed	116
6.2	Detailed analysis of the role of different flexibility options.....	121
6.2.1	Evaluation of the role of sector coupling technologies	121
6.2.1.1	Overall results on capacity and dispatch	121
6.2.1.2	Temporal dispatch of sector coupling	125
6.2.2	Evaluation of the role of technologies for shifting flexibility in the electricity system.....	130
6.2.2.1	Electricity storages.....	130
6.2.2.2	Electricity transmission capacity	135
6.2.3	Evaluation of the role dispatchable power plants	140
6.2.3.1	Overall results on capacity and dispatch	140

6.2.3.2	Temporal dispatch of power plants.....	146
6.2.4	Analysis of further flexibility options.....	148
6.3	Interplay of flexibility options on country level.....	150
6.4	Total system costs evaluation	154
6.5	Comparison of CO ₂ -emissions.....	158
6.6	Additional scenarios	162
6.6.1	Increase of total iRES share in the observed region.....	163
6.6.2	Higher share of electricity in the energy demand sectors.....	165
6.7	Sensitivities for selected input assumptions.....	168
7	Conclusion.....	175
7.1	Summary and research questions	175
7.2	Limitations and further research.....	179
7.3	Implications and recommendations resulting from the insights.....	181
	Bibliography.....	185
	Appendix.....	203
A	Literature on model-based analysis of flexibility demand and provision	203
B	Additional calculations and results for the iRES expansion model	205
B.1	Derivation of wind onshore generation time series.....	205
B.2	Derivation of PV time series	207
B.3	Additional data and results of the iRES expansion	209
B.4	Impact of selected model equations on the optimal iRES expansion.....	214
C	Additional data input for the investment and dispatch model	219
C.1	Additional data.....	219
C.2	Derivation of heating profiles.....	226
D	Additional results for the investment and dispatch model.....	227

List of Figures

Figure 1.1: Literature examples and contribution of the present work.....	2
Figure 1.2: Structure of the present thesis.....	6
Figure 2.1: Hourly (left) and monthly (right) normalized average country-specific capacity factors of iRES and electricity demand across Europe.....	11
Figure 2.2: Exemplary residual load with time-dependent parameters of the flexibility requirement.....	12
Figure 2.3: Exemplary sorted residual load duration curve with parameters of the cumulated flexibility requirements	13
Figure 2.4: Installed iRES capacities (left) and resulting sorted residual loads (right) for linear iRES expansion in Germany (ceteris paribus of all other influencing factors)	14
Figure 2.5: Overview and theoretical application for flexibility options	21
Figure 2.6: European energy consumption of different sector and CO ₂ emissions	25
Figure 3.1: Steps for the potential analysis of wind onshore and PV	28
Figure 3.2: Steps of data acquisition	30
Figure 3.3: Potential capacity factors for wind onshore in the observed region	33
Figure 3.4: Potential capacity factors for PV in the observed region	35
Figure 3.5: a) available area based on Corine land cover, b) area excluded based on elevation and slope, c) area excluded based on protected areas	37
Figure 3.6: Share of area available for iRES installations compared to overall country area	38
Figure 3.7: Cost-potential curves for wind onshore (left) and PV (right) for selected countries	40
Figure 3.8: Country-specific electricity demand in the year 2012	46
Figure 4.1: Cumulative generation (left) and capacities (right) from iRES in the scenarios for the whole region observed	52
Figure 4.2: Scenario-specific generation and iRES share on country level	53

Figure 4.3: Scenario-specific comparison of PV share and total iRES share	54
Figure 4.4: Scenario-specific iRES capacity on country level	55
Figure 4.5: Distribution of total wind onshore and PV capacities per raster in the scenarios	56
Figure 4.6: Duration curve of iRES electricity generation in the scenarios	58
Figure 4.7: Normalised combination of selected parameter of iRES expansion and sorted residual load parameter per country and scenario	59
Figure 4.8: Unsorted residual load (left) and sorted residual load (right) for each scenario	60
Figure 4.9: Country-specific normalised sorted residual loads	61
Figure 4.10: Boxplots of country-specific residual load parameters with normalised range of residual load (left), surplus energy (middle) and hours with surplus (right)	62
Figure 4.11: Normalised combination of selected parameter of iRES expansion and time-dependent residual load parameter for each country and scenario ...	63
Figure 4.12: Residual load of the whole observed region cumulated per month (left) and per hour (right)	64
Figure 4.13: Duration and energy content of single country-specific surplus phases (black dots) and respective medians and quartiles (red dashed lines)	65
Figure 4.14: Average energy and duration of surplus periods	66
Figure 4.15: Periodogram spectral power density of the aggregated country specific residual loads	67
Figure 4.16: Correlation coefficients of the pairwise country-specific residual loads ...	68
Figure 4.17: Simultaneous surplus phases in the countries during the year	69
Figure 4.18: Scenario-specific total costs of the overall iRES installation in the observed region (left) and boxplot of country-specific investments (right)	70
Figure 4.19: Complete and scenario-specific cost-potential curves for wind onshore (left) and PV (right) in the whole region observed	72

Figure 4.20: Theoretical applications of flexibility options in the High PV and High Wind scenario	75
Figure 5.1: System boundaries and implemented technologies	81
Figure 5.2: Dimensions of the scenario framework	86
Figure 5.3: Maximum potentials of the selected DSM processes per country	102
Figure 5.4: Availability of DSM processes in an exemplary summer week in Germany	103
Figure 5.5: Overview on data requirements for PtX technologies	105
Figure 5.6: Annual district heat demand per country in the target year	106
Figure 5.7: Exemplary time series of daily average heat demand in Germany and France for the target year	107
Figure 5.8: Hydrogen demand per country in the target year	108
Figure 5.9: Exemplary normalised daily (immediately) charging profiles and availability profiles of BEV car fleet in Germany and France	108
Figure 5.10: Annual electricity consumption including minimum additional electricity demand of the sector coupling technologies	110
Figure 6.1: Sorted residual load and corresponding dispatch of flexibility options in the scenarios for the whole region observed	117
Figure 6.2: Composition of residual electricity demand and supply (without iRES) in times with positive (pos) and negative (neg) original residual load	118
Figure 6.3: Sum of monthly dispatch of flexibility options (without iRES generation) to meet the residual load across all countries observed	120
Figure 6.4: Optimal sector coupling capacities installed and dispatch across the whole region observed	121
Figure 6.5: Total storage investments (bars) and sum of storage charging (points) across the whole region observed	123
Figure 6.6: Boxplot of country-specific full load hours of heat pumps, electrolyser and BEV	124

Figure 6.7: Country specific relative change of full load hours and capacity in HF compared to LF as function of the PV share on total electricity demand...	125
Figure 6.8: Monthly sums of electricity consumption of the sector coupling technologies across the whole region observed	126
Figure 6.9: Hourly sums of electricity consumption of the sector coupling technologies across the whole region observed	127
Figure 6.10: Exemplary daily dispatch of PtX technologies in France	128
Figure 6.11: Total installed storage capacity across the whole region observed	131
Figure 6.12: Boxplot of country-specific full load hours of the storage mix	132
Figure 6.13: Monthly total sums of net charging across the whole region observed ...	133
Figure 6.14: Hourly total sums of net charging across the whole region observed	134
Figure 6.15: Mean country- and storage type-specific maximum electricity storage charging and discharging amount relative to the installed storage power capacity	135
Figure 6.16: Optimal expansion of the electricity transmission grid and corresponding export flows across the whole region observed	136
Figure 6.17: Scenario-specific maps of optimal NTC expansion and country-specific net export flows	137
Figure 6.18: Boxplot of transmission line-specific utilisation rates	139
Figure 6.19: Daily export (positive values) and import (negative values) flows for selected countries	139
Figure 6.20: Total installed power plant capacities by technology	141
Figure 6.21: Mean of the country-specific ratios between secured capacity investments and peak electricity demand	143
Figure 6.22: Total electricity generation of controllable power plants	144
Figure 6.23: Boxplot of fuel-type specific full load hours in the 17 countries observed	145
Figure 6.24: Monthly sum of electricity generation by controllable power plants for the whole region observed	146

Figure 6.25:Hourly sum of electricity generation by controllable power plants for the whole region observed	147
Figure 6.26:Daily dispatch of power plants in selected countries	148
Figure 6.27:Overall amount of curtailment and share on total iRES generation across the whole region observed	149
Figure 6.28:Total shedded load and corresponding number of activations	149
Figure 6.29:Optimal investments in DSM capacity and sum of load reduction	150
Figure 6.30:Mean of pairwise correlation between country-specific dispatch of flexibility options and residual load time series	152
Figure 6.31:Exemplary week in Italy illustrating the dispatch of flexibility options	153
Figure 6.32:Exemplary week in Great Britain illustrating the dispatch of flexibility options	154
Figure 6.33:Annualised system costs in the electricity system and comparison with total costs including sector coupling	155
Figure 6.34:OPEX in the electricity system and total OPEX including sector-specific benchmark technologies	156
Figure 6.35:Specific system costs per country and scenario as function of the PV share on the electricity demand	158
Figure 6.36:Calculation of sector specific emissions	159
Figure 6.37:Total sector-specific emissions	160
Figure 6.38:Specific emissions per country and sector as function of the PV share on electricity demand	162
Figure 6.39:Percentage change of PtX capacities and electricity demand in <i>iRES+</i> compared to original results	163
Figure 6.40:Absolute change of CO ₂ emissions in <i>iRES+</i> compared to original results	165
Figure 6.41:Percentage change of PtX capacities and electricity demand in <i>PtX+</i> compared to original results	167
Figure 6.42:Absolute change of CO ₂ emissions in <i>PtX+</i> compared to original results .	168

Figure 6.43:Change of installed capacities of flexibility options in the sensitivity with lower CAPEX for sector coupling technologies	169
Figure 6.44:Sector-specific changes in emissions in the sensitivity with lower CAPEX for sector coupling technologies	170
Figure 6.45:Change of installed capacities of flexibility options in the sensitivity with lower CAPEX for electricity storages	171
Figure 6.46:Sector-specific changes in emissions in the sensitivity with lower CAPEX for electricity storages	172
Figure 6.47:Change of installed capacities of flexibility options in the sensitivity with higher CO ₂ -prices	173
Figure 6.48:Sector-specific changes in emissions in the sensitivity with higher CO ₂ -prices	174
Figure B.1: Original manufactures (dotted lines) and smoothed (solid lines) power curves of the two reference farms.....	206
Figure B.2: Distribution of cumulated wind onshore and PV generation per raster ...	211
Figure B.3: Energy amount and duration of connected deficit periods	212
Figure B.4: Exemplary periodogram for Denmark (High Wind) and Italy (High PV)	213
Figure B.5: Change in iRES capacities compared to the original results for both relaxations.....	215
Figure B.6: Scenario-specific distribution of iRES generation without constraining maximum and minimum iRES share per country (S-ALL)	216
Figure B.7: Comparison of sorted residual load for Denmark and Portugal with and without selected model restrictions	216
Figure B.8: Costs-potential curves without restriction of the raster densitiy (S-RAST)	218
Figure B.9: cost-potential curve without restriction of the raster density as well as maximum and minimum iRES share (S-ALL)	218
Figure D.1: Boxplots of absolute change in storage capacities in LF and HF compared to NO	232

Figure D.2: Hourly storages level of PSP in three selected countries	233
Figure D.3: Boxplot of country-specific NTC investments	233
Figure D.4: Exemplary import and export flows for Denmark and Great Britain	234
Figure D.5: Geographical presentation of transmission line utilisation and share of export on each country's electricity demand	235
Figure D.6: Boxplot of country-specific increase in power plants capacities compared to the NO scenario	238
Figure D.7: Comparison of optimal expansion of power plants by technology with existing capacities	239
Figure D.8: Country-specific share of curtailment on total iRES generation as function of the PV share on total electricity demand	239
Figure D.9: Average activated DSM measures per country normalised to capacities installed as function of the PV share on the electricity demand	240
Figure D.10: Share of technology-specific CAPEX on total CAPEX	240
Figure D.11: Absolute change in controllable power plant capacity in iRES+ compared to the original results	243
Figure D.12: Absolute change in electricity storage capacity in iRES+ compared to the original results	243
Figure D.13: Absolute change in NTC in iRES+ compared to the original results	244
Figure D.14: Absolute change in CAPEX in iRES+ compared to the original results ...	244
Figure D.15: Absolute change in controllable power plant capacity in PtX+ compared to the original results	245
Figure D.16: Absolute change in electricity storage capacity in PtX+ compared to the original results	245
Figure D.17: Absolute change in NTC in PtX+ compared to the original results	246
Figure D.18: Absolute change in CAPEX in PtX+ compared to the original results	246

List of Tables

Table 2.1: Mean country-specific pairwise correlation of iRES electricity generation in Europe.....	12
Table 2.2: Aggregated parameter of the residual load resulting from an exemplary iRES expansion in Germany.....	15
Table 2.3: Time-dependent parameter of the residual load resulting from an exemplary iRES expansion in Germany.....	16
Table 2.4: Deviation of scenarios with different Wind-PV shares based on literature	19
Table 3.1: Comparison of average values of full load hours for PV, wind onshore and offshore for the weather years 2006 to 2015.....	29
Table 3.2: Categorization of wind classes.....	32
Table 3.3: Assumptions on technical data for current and future wind turbines.....	32
Table 3.4: Comparison of average capacity factors for wind onshore in the present work with existing values in the literature.....	33
Table 3.5: Comparison of average capacity factors for PV in the present work with existing values in the literature.....	35
Table 3.6: Applied GIS data for the area analysis.....	36
Table 3.7: Assignment of CLC land use categories to iRES technologies.....	36
Table 3.8: Data required for the illustration of cost-potential curves for PV and wind onshore.....	38
Table 3.9: Model requirements and assumptions.....	41
Table 3.10: Country-specific iRES data.....	47
Table 4.1: Scenario-specific residual load parameter cumulated for the whole region observed.....	61
Table 4.2: Generalised relationships between the demand for flexibility and the potential provision of flexibility.....	74
Table 5.1: Overview of flexibility supply side scenarios with corresponding main assumptions.....	84

Table 5.2:	Technical data for fossil fuel-based power plants.....	98
Table 5.3:	Economic data for fossil fuel-based power plants	98
Table 5.4:	Technical data for RES	100
Table 5.5:	Economic data for controllable RES	100
Table 5.6:	Techno-economic data for electricity storages.....	101
Table 5.7:	Techno-economic data of DSM processes	104
Table 5.8:	Techno-economic data of PtX technologies.....	109
Table 5.9:	Techno-economic data of energy storages for sector coupling	110
Table 6.1:	Standard deviation of the hourly dispatch of PtX technologies in France .	129
Table 6.2:	Overview of system costs and resulting specific costs in the electricity system.....	157
Table 6.3:	Comparison of resulting CO ₂ emissions in the HF scenario with values of the year 1990	161
Table 6.4:	Overview of differences regarding electricity demand due to sector coupling in <i>PtX+</i> compared the original scenarios	166
Table 7.1:	Summary of main results for the mix of flexibility options.....	178
Table A.1	Overview of literature discussing flexibility requirements and provision.	203
Table B.1:	Studies included with varying Wind-PV ratio	209
Table B.2:	iRES generation in the FD scenarios per iRES technology type and country	210
Table B.3:	Installed capacities in the FD scenarios per iRES technology type and country.....	211
Table B.4:	Normalisation procedure for correlation analysis	212
Table B.5:	Investments in iRES per country and scenario	213
Table B.6:	Description of sensitivity analysis.....	214
Table B.7:	Sensitivity analysis for selected model equations and impact on total costs and LCOE.....	217

Table C.1: Capacity and Generation Restrictions for controllable RES	219
Table C.2: Assignment of DSM processes (Data: Gils 2016, Gils 2014).....	220
Table C.3: Existing static NTC values for the model region of 2019	221
Table C.4: Total and share of heating demand in the residential and tertiary sector..	222
Table C.5: Data table on hydrogen demand in the countries observed.....	223
Table C.6: Data input for BEV	224
Table C.7: Parameter for calculating the levelised costs of the benchmark processes	225
Table D.1: Installed capacity of heat pumps in the FD scenarios	227
Table D.2: Installed capacity of electrolyser in the FD scenarios	228
Table D.3: Installed BEV	229
Table D.4: Installed electricity storage capacity in the NO scenario	230
Table D.5: Installed electricity storage capacity in the LF scenario	231
Table D.6: Installed electricity storage capacity in the HF scenario	232
Table D.7: Installed power plant capacity in the NO scenario.....	236
Table D.8: Installed power plant capacity in the LF scenario	237
Table D.9: Installed power plant capacity in the HF scenario.....	238
Table D.10: Scenario-specific residual load parameter cumulated for the whole region observed in the iRES+ scenario	241
Table D.11: iRES generation for the additional scenario iRES+ in the FD scenarios per iRES technology type and country	241
Table D.12: Installed capacities for the additional scenario iRES+ in the FD scenarios per iRES technology type and country	242

Abbreviations

BEV	Battery-Electric-Vehicle
CAPEX	Capital Expenditures
CCGT	Closed Cycle Gas Turbine
CHP	Combined Heat and Power
CSP	Concentrated Solar Power
DAY	Daily Storage
EC	European Commission
ENTSO-E	European Network of Transmission System Operators for Electricity
EROI	Energy Returned on Energy Invested
EU	European Union
FD	Flexibility Demand Scenarios
FS	Flexibility Supply Scenarios
GIS	Geographic Information System
HF	Scenario with High Flexibility in sector coupling
HOU	Hourly Storage
ICE	Internal Combustion Engine
LCOE	Levelised Costs Of Electricity
LF	Scenario with Low Flexibility in sector coupling
NECP	National Energy and Climate Plan
NO	Scenario without sector coupling
NTC	Net Transfer Capacity
OCGT	Open Cycle Gas Turbine
OPEX	Operational Expenditures
PSP	Pump Storage Plant

PtG	Power-to-Gas
PtH	Power-to-Heat
PtX	Power-to-X
PV	Photovoltaic
REF	Reference Wind-PV Ratio Scenario
RES	Renewable Energy Sources
SEA	Seasonal Storage
SoC	State of Charge
UN	United Nations
iRES	intermittent Renewable Energy Sources
VWF	Virtual Wind Farm Model

Nomenclature: iRES expansion model

Sets

Element/Symbol	Subset	Description
$c \in C$		Countries
	$cl \in C$	Countries with additional restrictions regarding the PV share
$r \in R$		Raster
$on \in ON = \{PVro, PVgr, WON\}$		Onshore iRES technologies including PV roof-top, PV ground-mounted and Wind onshore

Mappings

Symbol	Set	Description
$mr(c)$	R	Set of raster assigned to country C

Parameter

Symbol	Unit	Description
an_{on}	-	Annuity of investment in onshore technology on
an_{woff}	-	Annuity of investment in wind offshore power plant
$area_{r,on}$	[m ²]	Available area for onshore technology on in raster r
$capmin_{c,on}$	[MW]	Minimum capacity of onshore technology on in country c
$capmin_{woff_c}$	[MW]	Minimum capacity of wind offshore in country c
ext	-	Extension factor for minimum iRES expansion in each country
$flh_{r,on}$	[h]	Full load hours of onshore technology on in raster r
flh_{woff_c}	[h]	Full load hours of wind offshore in country c
$gmax$	-	Maximum share of electricity generation of PV or wind onshore on total iRES generation
lu_{on}	[MW/m ²]	Land-use of onshore technology tr
$smax_c$	-	Maximum share of iRES generation on electricity demand in country c
$sres$	-	Share of iRES on total electricity demand
spv	-	Share of PV on iRES electricity generation
$swoff$	-	Maximum share of wind offshore on iRES electricity generation
$wvlh_{r,on}$	-	Weighting factor to control density of onshore technology on in raster r

Variables

Symbol	Unit	Description
$CAP_{r,on}$	[MW]	Capacity of onshore technology on in raster r
CAP_{WOFF_c}	[MW]	Capacity of wind offshore power plants in country c
DEM_c	[MWh]	Electricity demand in country c
INV_c	[EUR]	Investments per country c
$PEN_{r,on}$	[MW]	Penalty for iRES density relaxation for onshore technology tr in raster r
$TCAP_{c,on}$	[MW]	Total capacity of onshore technology tr in country c
$TDEM$	[MWh]	Total electricity demand
$TGEN_c$	[MWh]	Total electricity generation of iRES in country c

Nomenclature: Investment and dispatch model for flexibility options

Sets

Element/Symbol	Subset	Description
$c, cc \in C$		Countries/Market zones
$dsm \in DSM = \{shi, she\}$		DSM processes including processes for shifting demand and shedding demand
$li \in L$		Lines (connection between two countries)
$pt \in P = \{pth, ptg, ev\}$		Power-to-X technologies including power-to-heat (heat pumps), power-to (electrolyser), electric vehicles
$tech \in TE$		Technologies
	$chp \in TE$	CHP plants
	$s \in TE$	Electricity storages technologies
	$ramp \in TE$	Technologies with ramping restrictions
	$dres \in TE$	Dispatchable renewable power plants
	$csp \in TE$	CSP
	$bio \in TE$	Biomass based power plants
	$geo \in TE$	Geothermal power plants
$t, tt \in T$		Time step

Parameter

Symbol	Unit	Description
η	-	Efficiency of a technology or process
an	-	Annuity of investment in a technology or process
$cap_{c,cc}^{NTC}$	[MW _{el}]	Existing NTC from country c to country cc
co_{fix}	[EUR/MW _{el}]	Fixed costs of a technology or process
co_{var}	[EUR/MW _{hel}]	Variable costs of a technology or process
$dhe_{c,t}$	[MW _{hth}]	Heat demand at time step t in country c
$dhy_{c,t}$	[MW _{h2}]	Hydrogen demand at time step t in country c
epr_s^{stor}	-	Energy-to-power ratio of storage technology s
epr_{pt}^{PTX}	-	Energy-to-power ratio of storages for PTX technology pt
ev^c	[MW _{hel}]	Storage capacity of EV
ev^p	[MW _{el}]	Charging/Discharging power of EV
ev^{km}	[km]	Yearly traveling distance of EV

Symbol	Unit	Description
f^{chp}	-	CHP factor
$fl_{tech,c}$	[h]	Maximal full load hours (for reservoir technology)
ff	-	Flexibility factor adjusting equations for sector coupling
i	[%]	Interest rate
$li_{ma,c,cc,li}$	-	Adjacency matrix dedicating line li connection between two countries c and cc
$max_cap_{tech,c}$	[MW _{el}]	Maximal installable capacity for selected technologies $tech$ in country c
$max_{dsm,c}$	[MWh _{el}]	Maximal installable capacity of DSM process dsm in country c
$norm_{c,t}^{solar}$	-	Normalised times series of solar radiation at time step t in country c
$norm_{c,t}^{ev,cha}$	-	Normalised times series of charging profile of EV at time step t in country c
$norm_{c,t}^{ev,p}$	-	Normalised times series of available charging power of EV at time step t in country c
$norm_{dsm,c,t}$	-	Normalised times series of DSM process dsm availability at time step t in country c
$rde_{c,t}$	[MWh _{el}]	Residual load at time step t in country c
sc	-	Minimum share of electricity for sector coupling
t_{dsm}^{shi}	[h]	Maximal shifting time of DSM process dsm
t_{dsm}^{daylim}	[h]	Recovery time of DSM process dsm

Variables

Symbol	Unit	Description
$BP_{c,t}$	[MWh _{th}]	Dispatch of benchmark process in time step t in country c
$CAP_{tech,c}$	[MW _{el}]	Installed capacity of technology $tech$ in country c
$CAP_{dsm,c}$	[MW _{el}]	Installed capacity of DSM process dsm in country c
$CAP_{pt,c}$	[MW _{el}] or [-]	Installed capacity of PTX technology pt in country c
$CAP_{c,cc}^{NTC}$	[MWh _{th}]	Installed NTC from country c to country cc
CO_{INV_c}	[EUR]	Total investments in country c
CO_{FIX_c}	[EUR]	Total fix costs in country c
CO_{DC_c}	[EUR]	Total dispatch costs in country c
CO_{BP_c}	[EUR]	Total costs of benchmark processes in country c
$CURT_{c,t}$	[MWh _{el}]	Curtailed electricity in time step t in country c
$CHA_{s,c,t}$	[MWh _{el}]	Charging of electricity of storage s in time step t in country c

Symbol	Unit	Description
$CSP_{csp,c,t}$	[MWh _{el}]	CSP-based electricity generation in time step t in country c
$DSM_{dsm,c,t}$	[MWh _{el}]	Load reduction or increase (effective) of DSM process dsm in time step t in country c
$DSM_H_{dsm,c,t,tt}$	[MWh _{el}]	Load reduction or increase (on hold) of DSM process dsm for time step t in time step tt in country c
$GEN_{tech,c,t}$	[MWh _{el}]	Electricity generation of technology $tech$ in time step t in country c
$EXP_{c,cc,t}$	[MWh _{el}]	Electricity export from country c in country cc in time step t
$HECSP_{csp,c,t}$	[MWh _{th}]	CSP heat storage charging or discharging in time step t in country c
$IMP_{cc,c,t}$	[MWh _{el}]	Electricity import from country cc in country c in time step t
$PTX_{pt,c,t}$	[MWh _{el}]	Dispatch of PTX technology pt in time step t in country c
$PTX_STOR_{pt,c,t}$	[MWh _{el}]	Charging or discharging of storages for PTX technology pt in time step t in country c
$RAMP_{tech,c,t}$	[MWh _{el}]	Ramping up or down of technology $tech$ in time step t in country c
$SL_{s,c,t}^{STOR}$	[MWh _{el}]	Storage level of storage s in time step t in country c
$SL_{pt,c,t}^{PTX}$	[MWh _{th}]	Storage level of storages for PTX technology pt in time step t in country c
$SL_{csp,c,t}^{CSP}$	[MWh _{th}]	CSP heat Storage level in time step t in country c
TC	[EUR]	Total system costs

1 Introduction

Following the Paris Agreement of the year 2015 signed by 189 countries until February 2020 (UNFCCC 2020), ambitious national climate protection targets are formulated to reduce emissions by up to 70 % in each country until 2030 compared to the reference years 2005 or 1990 (UN Climate Summit 2020). In the so called Green Deal, the European Union aims to be climate neutral with net-zero emissions by 2050 (EU 2020). For the target to decrease CO₂ emissions in worldwide energy systems, the substitution of fossil fuels by renewable energy sources (RES) is seen as the most promising strategy (IPCC 2011). Due to the energy policy driven support for RES, the different technologies historically benefitted from overall declining costs resulting in a significant increase of RES capacities in Europe particularly in the electricity sector (IRENA 2020). Following the clean energy package of the European Commission, a maximal deployment of RES until 2050 is a priority (EC 2019). With regard to the energy policy triangle (EC 2007), the targeted energy system transformation with iRES has been assessed to be sustainable, competitive and feasible on global (see e.g. Bogdandov et al. 2019), international (see e.g. Zappa et al. 2019) and national scale (see e.g. Child & Breyer 2016). Focusing on the energy sector in a techno-economic perspective, three overlapping key developments of this system transformation can be identified forming the drivers for the present analysis:

1. Expansion of wind and PV capacities
2. Integration of iRES electricity in the European energy system
3. Sector coupling to decarbonise further energy demand sectors

First, the weather-dependency and the varying distribution of generation potentials as key characteristics of the iRES are defining the challenge of the energy system integration. With wind and PV, two intermittent renewable energy sources (iRES) with very contrasting electricity generation characteristics are in the focus of iRES expansion. Since several factors can

influence the future iRES development (e.g. costs, security of supply or acceptance), an expansion pathway with of either more wind or more PV can lead to strongly contrasting flexibility demands for iRES system integration. Second, to achieve ambitious targets for emission reductions and integrate higher shares of iRES in the power plant mix, the formerly electricity demand following energy system increasingly becomes a weather-dependent supply following one. To balance the iRES flexibility demand, a suitable mix of flexible technologies is required. And third, to further decrease emissions in the energy system, *sector coupling* is a targeted option. By coupling the energy demand end-use sectors with the electricity sector, (carbon-free) electricity can be supplied to meet the energy demand. With sector coupling, RES based electricity can be used to supply the energy demand in further sectors substituting fossil fuels with renewable fuels.

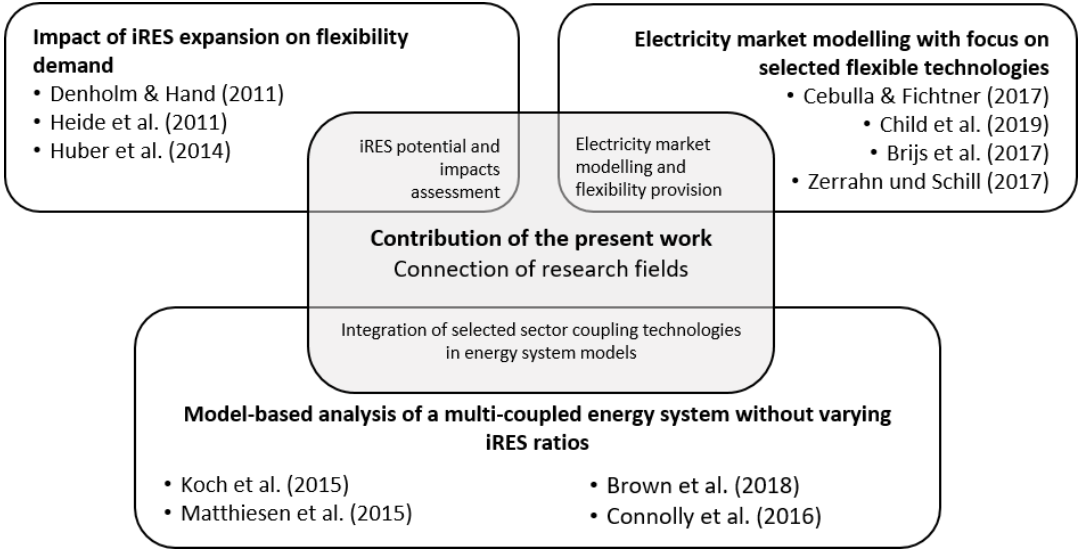


Figure 1.1: Literature examples and contribution of the present work (Own illustration)

The interplay of the introduced challenges and drivers of the energy system transformation requires a structured analysis of interactions between flexibility demand and flexibility supply. Therefore, iRES potential assessments and energy system modelling are the central methods applied in the present work. Energy system models enable the analysis and comparison of possible future transformation pathways based on predefined assumptions (Zöphel et al. 2019). For the examination of various aspects regarding flexibility requirements and provision, different model-based approaches exist in the literature. Table A.1 in Appendix A gives an overview of selected peer-reviewed publications with different foci on the aspects discussed before. In Figure 1.1 additionally the contribution of the present work based on this literature analysis is illustrated. A branch of the literature focusses on the development of various parameters regarding the flexibility needs due to iRES expansion. While these studies underline

the increasing challenges of high iRES shares for the electricity system, the influence of the findings on the flexibility provision is of lower interest (see e.g. Huber et al. 2014). In contrast, a further part of literature analysing the optimal flexibility provision. Although different Wind-PV ratios at total iRES electricity generation are part of the analysis, the minority implicitly puts the modelling results in context with aspects of flexibility requirements (e.g. Gils et al. 2017, Weitemeyer et al. 2015, Steinke et al. 2013). In addition, most of the studies focus on selected technologies or on the competition between flexibility options with similar applications, while a broader range of flexible technologies is included less frequent (as e.g. Child et al. 2019). The publications of the third branch analyse not only the electricity system but multi-coupled energy systems. Thereby, scientific literature often focusses on national analysis (e.g. Koch et al. 2015, Matthiesen et al. 2015), particularly when sector coupling is part of the analysis. Most studies analyse the dispatch of a broad range of flexibility options without examining optimal capacity expansions. Additionally, since the focus is put on interactions between different energy supply and demand sectors, the influence of different iRES technologies on the need for flexibility is less common (see e.g. Brown et al. 2018 or Connolly et al. 2016).

1.1 Scope and research questions

The overview above emphasises the possibilities and challenges of the model-based analysis of the transformation of the European energy system. The present work aims to connect three different research fields:

- (1) *iRES potential and future flexibility demand assessment*
- (2) *Electricity market modelling for the analysis of optimal flexibility provision*
- (3) *Evaluation of the impact of selected sector coupling technologies*

The objective is to systematically analyse flexibility requirements and provision in the future European energy system with a techno-economic focus to answer the overarching research question:

How are different Wind-PV ratios in the future iRES expansion effecting the optimal flexibility provision in a multi-coupled European energy system?

Based on the research question the three research fields are analysed taking up the drivers as discussed before. Regarding the first research field, the analysis of spatially and temporally differences in the wind and PV feed-in characteristics results in a need to examine iRES expansion and resulting flexibility requirements in a wider region observed. Therefore, the

present work covers a European energy system including 17 countries¹ of western and central Europe. To cope for the temporally variations of iRES electricity generation, an hourly resolution is necessary. Furthermore, since the challenges for flexibility provision in the electricity system particularly occur with high shares of iRES, the total share of wind and PV generation will be set to 80 % of the today's electricity demand in the observed region. This share is chosen to account for a significant increase of iRES technologies with a respective enormous transformation requirement for the energy system. While the total iRES shares are fixed, the Wind-PV ratio will change based on the scenarios defined in this work. Thus, a first scenario dimension is developed in the present work, representing the set of flexibility demand (FD) scenarios. As part of research field (1), wind and PV generation potentials are derived and applied in an iRES expansion model. This model application enables the scenario-specific examination of the need for flexibility to answer the question:

How do varying Wind-PV ratios in the iRES electricity generation influence the flexibility needs of a transnational European energy system?

The results of the iRES expansion model serves as input for the model-based analysis of interactions of different flexible technologies against the background of different Wind-PV ratios in the energy system (see research field (2)). Again, explicit transformation pathways of the energy system are beyond the scope of the present work. Instead, a greenfield approach is used to isolate the interplays between flexibility requirements and flexibility provision. Thereby, the analysis of optimal combinations of a broad range of relevant technologies in a transnational energy system is in the focus. A further central research question is:

Are different Wind-PV ratios in a transnational European energy system and the resulting flexibility demand influencing the optimal provision of flexibility in the electricity market?

Finally, in the third research field the present work contributes to literature in further shedding light on the interactions of different sector coupling technologies. A policy-driven introduction of higher levels of electrification in energy end-use sectors is assumed to analyse the interactions between available flexibility options in a multi-coupled energy system. With the analysis of the mix of flexibility options under the influence of sector coupling, a second scenario dimension, namely the flexibility supply scenarios (FS) complementing the FD scenarios introduced before. In modelling perspective, the clear focus on the power market is kept, while a simplified

¹ In the following, country codes as in ISO-3166-1 are used for the 17 countries included in this work: Austria – AT, Belgium – BE, Switzerland – CH, Czech Republic – CZ, Germany – DE, Denmark – DK, Spain – ES, France – FR, Great Britain – GB, Ireland – IE, Italy – IT, Luxembourg – LU, The Netherlands – NL, Norway – NO, Poland – PL, Portugal – PT, Sweden - SE

approach for coupling technologies is developed. Therefore, selected sector coupling technologies are identified, which are most likely to be exploited in the mid- to long-term. This allows to answer the following additional research question:

How does sector coupling influence the optimal flexibility provision in the European electricity market?

All three research fields and the corresponding scenario dimensions are interacting. By holistically analysing flexibility requirements and provision in the future European energy system in an appropriate scenario and modelling framework, a research gap can be filled. The purpose of the present work is to contribute on the one side by presenting suitable modelling frameworks for the representation of urgent energy system transformation challenges for both, the iRES expansion as well as the iRES integration by flexibility options and sector coupling. On the other side, with focusing on varying Wind-PV shares crucial interactions in a multi-coupled multi-national energy system dominated by weather-dependent renewable energy sources can be identified. This enables a better understanding of the role of relevant flexibility options. IN addition, the objective of the examination is to emphasise techno-economic differences between the scenarios, instead of identifying optimal pathways. This perspective is of high importance since the modelling results should be used to complement further research with additional perspectives on the energy system transformation. To increase transparency, the applied model formulation and gathered input data is made available in a data repository available at: <https://github.com/CZoephel/Flexibility-in-a-European-Energy-system>.

1.2 Outline of the work

Besides the present chapter, this work is divided into six chapters. The fundamentals of flexibility demand and flexibility provision are discussed in Chapter 2 to further emphasise the characteristics of wind and PV electricity generation as well as to present relevant flexible technologies. As a result, the most important aspects of an iRES based energy system transformation relevant for the present work are presented. The following Chapters 3 to 6 are taken up the research field introduced before as illustrated in Figure 1.2.

For the inclusion of spatially and temporally differences in the wind and PV feed-in characteristics, a suitable dataset is required. Therefore, in Chapter 3, the derivation of wind and PV generation time series is based on the selection of a representative weather year as well as on the technology-specific weather data gathering and processing taking technological progress and available land into account. Furthermore, for the analysis of different future wind and PV installation scenarios, a model is developed which implements temporally and spatially highly-resolved iRES data and additionally includes relevant energy-policy aspects. These

restrictions are introduced to take current and future challenges regarding the iRES expansion in Europe into account increasing the cost-optimal model solution based on techno-economic characteristics. Limitations of the present approach and comparisons with existing literature are thereby part of the discussion.

As a further contribution to research field (1), the results of the model application and the scenario-specific examination of the need for flexibility are discussed afterwards. In Chapter 4, besides the analysis of the location of wind and PV capacities across 17 European countries, the flexibility requirements will be assessed regarding multiple parameters describing the need for flexibility. Additionally, the influence of the assumed costs data on the overall costs for iRES expansion in the scenarios will be discussed. Furthermore, possible interactions of the outcomes regarding the flexibility demand with the role of single flexibility options are evaluated qualitatively.

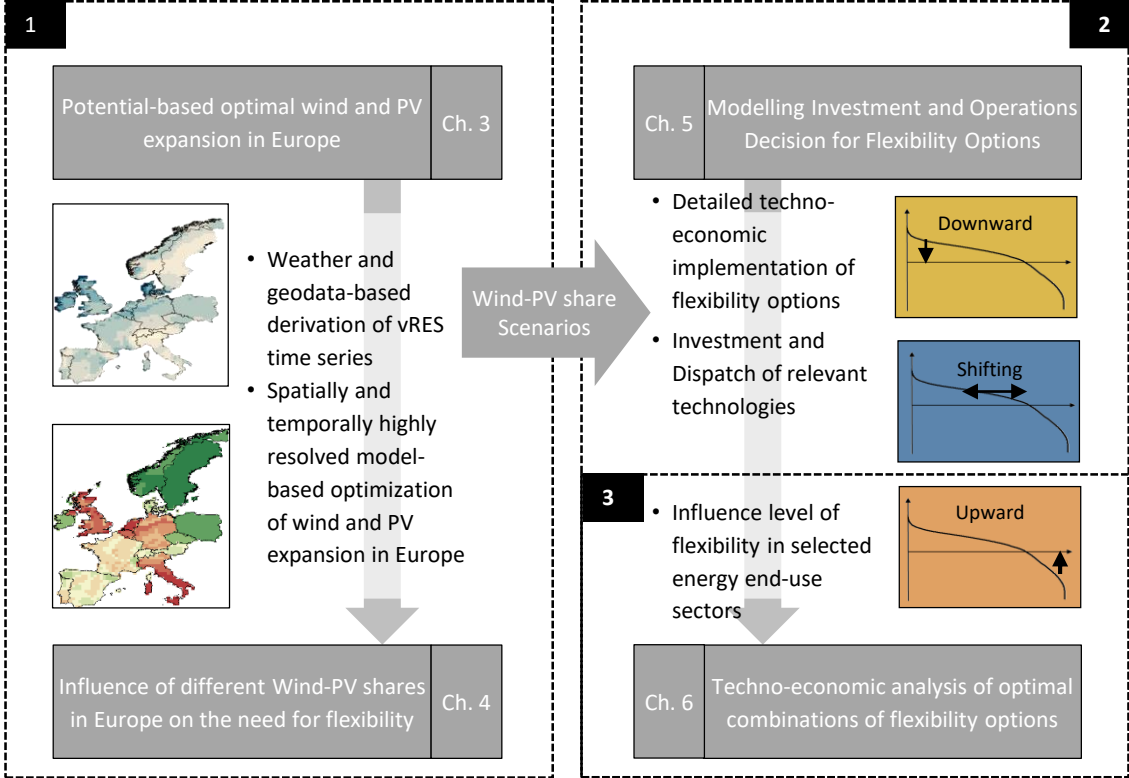


Figure 1.2: Structure of the present thesis (Own illustration)

The connection of the flexibility demand analysis with the optimal flexibility provision is realised in research field (2). The results of the iRES expansion model serves as input for the model-based analysis of interactions of different flexible technologies. Therefore, in Chapter 5 the ELTRAMOD electricity market model is introduced and relevant adjustments to cope for

the present research design are presented. This part is of high importance since it narrows down the research framework regarding the modelling of flexibility supply. On the one side, this includes the identification and implementation of relevant flexibility options with various application potentials in the electricity market. On the other side, a suitable representation of further energy end-use sectors is introduced to analyse possible interactions due to sector coupling. An important aspect refers to the availability of energy storages for the sector coupling technologies theoretically allowing for a more flexible sector coupling. Both, the mathematical model formulation as well as a description of data input requirements and processing will be presented in this part.

In Chapter 6, the results on the model-based analysis of optimal investment and dispatch decisions for flexibility options including PtX technologies are discussed combining research field (2) and (3). Thereby, two dimensions are taken into account. First, the influence of different flexibility demand scenarios is assessed. Second, the optimal mix of flexibility options including sector coupling measures is compared. Besides the technical feasibility to integrate high amount of iRES electricity, further factors of the future transformation pathway, like the system costs and realisable emission reductions are analysed. The insights are complemented by additional scenarios and sensitivity analysis shedding light on major influencing factors on the results.

Finally, Chapter 7 summarises the findings and answers the research questions. Both, the outcomes as well as the limitations of the present work are discussed and used to give outlooks on possible further research. In addition, the results will be discussed regarding required preconditions for an efficient realisation the targeted energy system transformations driven by the challenges discussed above. In doing so, policy recommendations can be derived.

2 Fundamentals of flexibility demand and provision in the energy system

To address the interplay between iRES expansion and necessary transformation measures, the present chapter discusses the fundamentals of the need and the provision of flexibility in the energy system. Thereby, crucial definitions and interrelations will be introduced to facilitate the understanding in the course of the present work. At first, the focus lies on the flexibility needs resulting from an assumed high long-term ambition for achieving decarbonisation goals by deploying particularly iRES technologies in Europe in the present and future energy systems. Based on the analysis of fundamental characteristics of iRES technologies, the term flexibility is discussed and major impact factors on the flexibility needs are analysed exemplarily. As the future mix of iRES technologies in the electricity generation is uncertain, different key scenarios for the present work are derived. In the second part of Chapter 2, the technologies available to meet changing flexibility needs in the energy system and their potential applications are presented.

2.1 Flexibility requirements in an energy system with high shares of variable renewable energy sources

Generally, two main characteristics influence the iRES electricity generation, namely, the temporal as well as spatial availability. In the following, the discussion of flexibility requirements is presented in a generalized perspective to give an overview of different aspects describing the impact of iRES on flexibility demand.

2.1.1 Characteristics of electricity generation from wind and PV systems

While fossil fuels such as natural gas or coal can be stored and transported, the kinetic wind energy as well as the radiation energy of the sun causes a temporal fluctuation in the supply of electricity². The resulting output of iRES plants fluctuates within a very short time as well as seasonally (see Brunner et al. 2020, Olauson & Bergkvist 2016, Heide 2010, Bremen et al. 2008). For the present analysis, wind onshore and offshore as well as PV (rooftop and utility scale) are defined as iRES. In the northern hemisphere, wind and PV systems usually show typical electricity supply patterns over the course of one year. Figure 2.1 illustrates the variability exemplarily for Germany using the monthly and hourly mean values of electricity generation from PV as well as wind onshore and offshore installations³. Electricity generation from wind energy is generally higher in winter. This seasonality is more pronounced for wind onshore installations than for offshore installations. The normalised electricity demand shows a similar trend but with comparably lower fluctuations. In contrast, seasonal PV generation correlates negatively with the load with on average more than ten times the maximum in summer compared to the minimum in winter. The average daily fluctuation of the PV generation depicts a significant midday peak due to the earth's rotation and missing feed-in the night hours. Although again lower, this rather correlates with the daily demand for electricity. In contrast, wind has hardly any daily fluctuations in Germany. With regard to these feed-in patterns, temporal smoothening effects can be observed due to seasonal and daily correlations of the iRES with the electricity demand. However, depending on the installed capacity the weather-related fluctuations of wind and PV generation are stronger than those of the load resulting in a need for flexibility to balance the temporal variability of iRES generation and electricity demand (see chapter 2.1.3) (Heide (2010), Bremen et al. (2008)).

² In addition to solar and wind-based electricity generators further weather-dependent electricity sources. While established hydro power plants (such as reservoir, run-of-river and pump storage plants) as well as solarthermal and geothermal plants will be addressed in the present work separately, further technologies as for example tidal power plants are excluded due to their low relevance (see also introduction).

³ Each iRES line is normalized to the respective monthly or hourly average of the 30-year EMHIRES weather data set (EMHIRES 2020). In addition, the demand for electricity based on hourly normalized demand profiles of ENTSO-E is also shown (ENTSO-E, 2018).

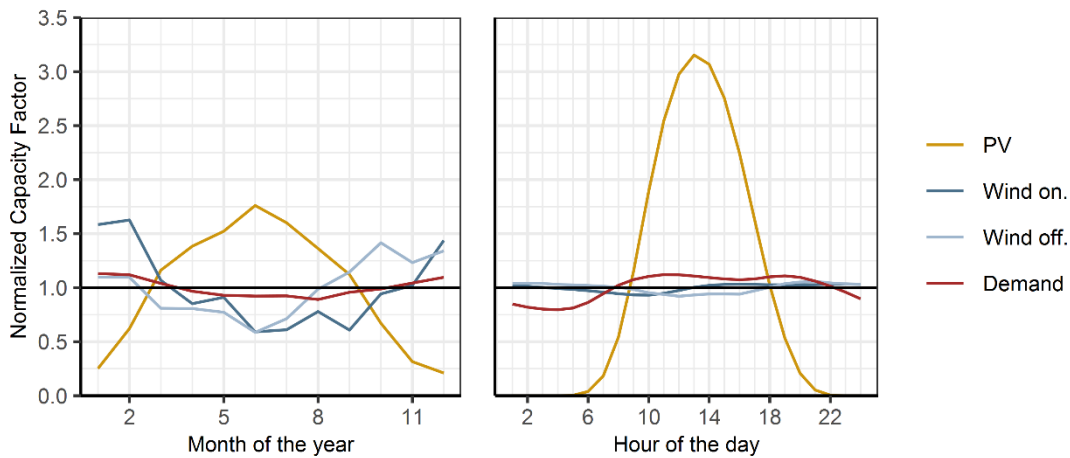


Figure 2.1: Hourly (left) and monthly (right) normalized average country-specific capacity factors of iRES and electricity demand across Europe (Own illustration based on the 30 years of EMHIRES weather data (2020))

In addition to differences in the temporal fluctuations in the iRES electricity generation, the weather-dependency of wind and solar energy furthermore affects the spatial potentials of wind and PV systems in terms of full load hours. Based on the 30-year EMHIRES dataset (EMHIRES, 2020), average full load hours for PV systems of 1,025 h can be calculated for Europe. In contrast, wind has a higher availability. On average, wind onshore installations in the European countries reach full load hours of 1,788 h. Furthermore, for wind offshore installations higher average full load hours of 3,132 h can be achieved, due to the lower roughness of the earth's surface at sea. Furthermore, different geographic conditions as well as meteorological influences result in unequal distribution of PV and wind generation potentials in the European countries. Due to the increasing sun altitude from north to south and the associated increase in solar radiation energy, the potential for PV systems in southern Europe is higher than in the north. In contrast, the kinetic wind energy in altitudes usable for the hub heights of wind turbines is mainly influenced by the surface texture, i.e. roughness. Accordingly, the best wind conditions prevail close to the coast and at offshore locations. These geographical influences also lead to spatial fluctuations of the iRES electricity generation. Due to the predominant dependence of PV electricity generation on the temporal course of the seasonal and daily amount of solar radiation, even geographically more distant areas in Europe show similar PV feed-in patterns. The influence of the weather, such as cloud cover, is often overlapped by the Earth's movement. Table 2.1 shows that both the pairwise country-specific mean hourly and seasonal correlations for the PV electricity feed-in in Europe are high. In contrast, wind has a higher stochasticity due to regionally different and more frequent changes of meteorological conditions (Olauson & Bergkvist 2016). Compared to PV, the short-term correlation of electricity

generation from wind energy between spatially distant areas is much lower. Nevertheless, also for wind a seasonal effect can be observed in Table 2.1 indicating a similar feed-in over the course of the year in even more distant regions in Europe.

Table 2.1: Mean country-specific pairwise correlation of iRES electricity generation in Europe (Data: EMHIRES, 2017, 2018)

iRES-technology	Mean hourly correlation	Mean seasonal correlation
PV	0,78	0,98
Wind onshore	0,25	0,72
Wind offshore	0,29	0,75

2.1.2 Definition and parameters of the flexibility demand by means of the residual load

The balancing of electricity supply and electricity demand is necessary in interconnected networks even without the supply of iRES electricity to ensure adequate and secure electricity supply (Hirth and Ziegenhagen 2015, Stoft 2002). On the generation side, mostly dispatchable power plants with different reaction times ensure this balance. As mentioned before, these iRES feed-in characteristics cause flexibility requirements in an energy system particularly when the share of weather dependent electricity generation capacity increases. By defining the residual load in the following chapter, specific parameters of the need for flexibility will be discussed in order to further narrow down this term (Huber et al. 2014, Lund et al. 2015).

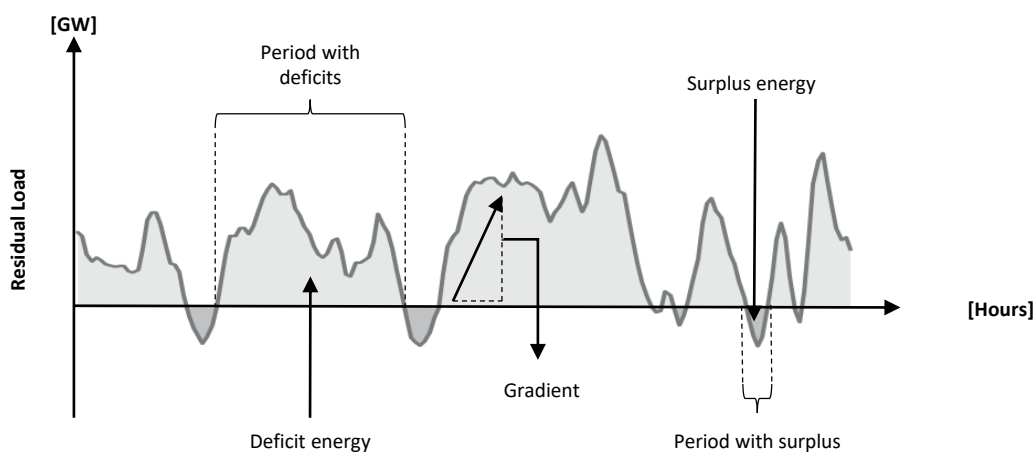


Figure 2.2: Exemplary residual load with time-dependent parameters of the flexibility requirement (Own illustration)

In order to estimate the need for flexibility, usually the residual load is applied, i.e. the difference between the electricity load and the weather-dependent electricity generation that has to be covered by flexible technologies. The variability of electricity generation from iRES as well as the only weakly correlated electricity demand, influences the pattern of the residual load. Figure 2.2 illustrates the parameters of an exemplary residual load. With low iRES capacities installed, mainly situations with positive residual load (demand for electricity exceeding the weather-dependent generation) occur to be covered by dispatchable power generation. In contrast, with higher iRES capacities, the corresponding electricity generation can exceed the demand for electricity, resulting in surpluses in which the residual load is negative. The power required and the duration of these periods determine the amount of deficit or surplus energy that must be provided by flexible technologies. In addition to sufficient power and energy provision, additional flexibility requirements are imposed to these technologies due to load changes or residual load gradients.

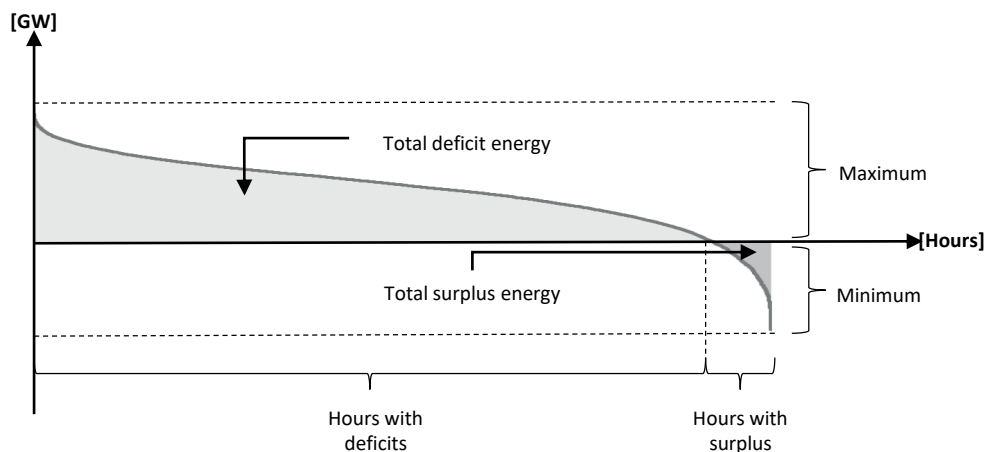


Figure 2.3: Exemplary sorted residual load duration curve with parameters of the cumulated flexibility requirements (Own illustration)

While the time-dependent parameters of the residual load are directly influencing the dispatch of potential flexibility options, parameters that reflect the aggregated flexibility requirements of a year are suitable for estimating the electricity deficits and surpluses in a comprehensive system perspective. By sorting the residual load of a year in a descending order from the maximum to the minimum, estimates on the total flexible capacities required to provide the deficit or surplus energy can be deduced. Figure 2.3 shows the residual load duration curve with the associated parameters of the flexibility requirement. The maximum represents the maximal additional capacity needed in the time with the greatest difference between electricity demand and iRES generation. If the annual minimum is negative, its level indicates the need for capacity to increase load to cover the iRES surpluses if iRES curtailment has to be avoided.

Furthermore, it is possible to estimate the potential hours of operation of different technologies based on the pattern of the residual load duration curve as well as the hours with deficits and surpluses.

In addition to the level and the pattern of the electricity demand, the residual load and the associated parameters of the need for flexibility are strongly influenced by the expansion of the iRES capacities. In order to illustrate this effect, the following section examines exemplarily for Germany the need for flexibility against the background of an expansion of wind and PV systems.

2.1.3 Impact of intermittent renewable energy expansion on the flexibility demand

2.1.3.1 Impacts on the residual load – an example for Germany

With increasing shares of fluctuating electricity generation, the need for flexibility is changing and new requirements occur for the energy system. Possible impacts will be presented exemplarily for an assumed iRES expansion in Germany with focus on the parameters of the residual load as introduced before.

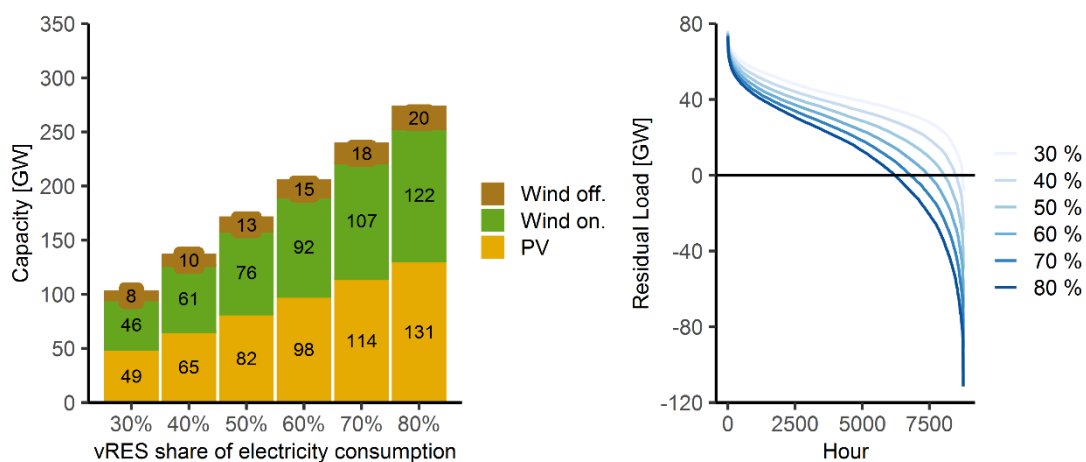


Figure 2.4: Installed iRES capacities (left) and resulting sorted residual loads (right) for linear iRES expansion in Germany (ceteris paribus of all other influencing factors) (Own illustration)

While in Germany in the year 2019, the total RES generation amounted up to 244 TWh covering 42 % of the electricity demand, the share of iRES was 30 %. Around 49 GW PV plants, 53 GW wind onshore and 8 GW wind offshore plants were installed, generating in total around 174 TWh of electricity (UBA 2020). Based on these capacities and assuming a constant demand for electricity (580 TWh), in Figure 2.4 (left) a linear expansion is extrapolated to higher iRES

shares⁴. To theoretically cover 80 % of the electricity demand, 131 GW PV, 122 GW wind onshore and 20 GW wind offshore capacities are required. This represents almost a three-fold increase in capacity compared to 2019 and is in the range of various studies on renewable energy development scenarios in Germany⁵. Figure 2.4 (right) shows the sorted residual load curves. Higher iRES shares lead to a steeper pattern of the residual load. However, the maximum of the sorted residual load changes only slightly. Due to the weather dependency of the iRES and the fluctuating electricity load, low iRES electricity generation often coincides with winter months and a respective high electricity demand. In general, the expansion of iRES requires rather similar dispatchable capacities for generation adequacy, but can substitute substantial amount of conventional generation (Zöphel and Möst 2017). However, due to the weather-dependency increasing wind and PV capacities cause an increases in surplus hours with corresponding surplus energy. While in the year 2019, almost no iRES surpluses can be seen for the aggregated values for Germany, with a share of 80%, surpluses of more than 100 GW are possible in this exemplary calculation (see also Table 2.2).

Table 2.2: Aggregated parameter of the residual load resulting from an exemplary iRES expansion in Germany (Data: EMHIRES, 2020; ENTSO-E, 2020)

Share of iRES	Maximum [GW]	Minimum [GW]	Mean [GW]	Standard deviation [GW]	iRES surplus hours [h]	iRES surplus energy [TWh]
30 %	77	1	43	12	0	0,0
40 %	76	-16	38	14	73	0,4
60 %	75	-51	28	19	758	9,5
80 %	74	-86	18	25	1893	36,8

In Table 2.2, the most important aggregated parameters of the residual load for different iRES shares can be compared. With linear wind and PV expansion up to a theoretical iRES share of 80%, the mean residual load decreases from 43 GW to 18 GW. At the same time, the standard deviation increases from 12 GW to 25 GW and the iRES surpluses occur in more than 1,800 hours. During these hours, a total amount of almost 37 TWh iRES surplus electricity is fed-in corresponding to 8 % of total iRES generation.

⁴ For this analysis, normalised feed-in curves of the iRES plants based on the EMHIRES data as well as the electricity demand based on ENTSO-E data for the year 2015 are used (EMHIRES, 2020; ENTSO-E, 2020).

⁵ see e.g. Agora (2014), Öko-Institut / ISI (2015): -95% scenario or Fraunhofer ISE (2015): -90% emission

Under the assumptions made, some extreme maximum values for the flexibility demand can be observed when analysing the time-dependent parameters of the residual load in Table 2.3. In the case of an 80% share, the low correlation of iRES electricity generation with the demand results in a maximum surplus phases of 174 hours in which almost 7 TWh surplus electricity is generated. On the other hand, a period of nearly two weeks with constantly positive residual load and around 12 TWh of electricity demand would have to be covered by additional electricity supply. In Figure 2.4 (right), the steeper decline of the sorted residual load with increasing iRES share also indicates the larger gradients of the residual load. With an increasing share of weather-dependent electricity generators, in particular the day-night cycle of PV supply leads to increasing hourly residual load changes. In Table 2.3, the level of maximum residual load gradients doubles (one-hour gradients) or almost triples (four-hour gradients) compared to the situation in 2019.

Table 2.3: Time-dependent parameter of the residual load resulting from an exemplary iRES expansion in Germany (Data: EMHIRES, 2017, 2018, ENTSO-E, 2018)

iRES share	Maximal period with iRES surplus		Maximal period with iRES deficit		Maximal residual load gradients	
	[h]	[TWh]	[h]	[TWh]	1h [GW]	4h [GW]
30 %	0	0,0	8760	378,2	12	30
40 %	9	0,1	1777	70,9	12	39
60 %	141	2,8	757	30,3	17	56
80 %	174	6,9	333	11,6	23	74

The development of the iRES expansion and the respective need for flexibility are frequently discussed in the literature at the national level, as exemplified above (e.g. Bauknecht et al. 2016, Denholm & Hand 2011). However, national energy systems differ from each other. Not only different demand structures, but also local weather conditions as well as unequally distributed iRES potentials lead to different flexibility requirements for existing energy systems (Zöphel et al. 2018). Power systems connected by transmission grids potentially enable regional balancing effects and reduce the flexibility requirement of the overall system. Additionally, a linear extrapolation of iRES capacities is a major simplification, which might over- or underestimate the impact on the flexibility requirements. Although this linear up-scaling is commonly used in iRES potential analysis, the approach neglects changes in national iRES feed-in characteristics due to technological progress and the exploitation of additional locations. Therefore, in the present work, both a large geographical scope as well as higher spatial resolution are applied to overcome those simplifications (see Chapter 2.3 for further specifications).

2.1.3.2 Further challenges regarding the intermittent renewable energy expansion

Of high importance for the integration of iRES electricity into the (existing) energy system are furthermore electricity markets. To give an overview about the impact of the expansion of RES on these markets, challenges will be discussed briefly.

The different electricity sub-markets introduced with the liberalization of the electricity system (EU 1997) are structured to provide both, planning security as well as time-dependent flexibility (Zöphel and Müller 2016). Accordingly, the flexibility requirements as well as flexibility provision in energy systems includes different time-dependent perspectives. While in the power derivatives market long-term supply contracts are traded to hedge against price risks, the short-term clearing of electricity demand and supply is realised at the day-ahead and intraday wholesale markets, with settlements on the following day and the same day, respectively. The market-clearing price is derived by sorting the short-term marginal costs of the participating power plants into the Merit-Order. The merit-order effect of iRES in the electricity spot market caused by RES expansion and marginal cost close to zero for wind and PV, is extensively discussed in the literature (e.g. Sensfuß et al. 2007). On the one side, the marginalisation of conventional electricity generators not directly benefitting from energy policy support schemes can cause refinancing issues for the more expensive yet often less carbon-intensive technologies, like gas power plants (Zöphel and Müller 2016). This contradicts the need for secured dispatchable generation capacity also required with iRES expansion. Similarly, the decrease in electricity market prices caused by the iRES with no marginal costs lowers the revenues for the iRES operators itself, leading to the so called self-marginalisation of iRES and casting doubts of a market-based integration (under current market design) of iRES without energy policy support (v. Selasinsky 2016). On the other side, the merit-order effect increases the costs for the RES support, since the difference of the electricity market wholesale prices and the feed-in tariff is compensated by the electricity end-users.

Regarding the impact of iRES capacities on the electricity markets, very short-term balancing of electricity demand and supply is further organized in the balancing reserve markets. These are regulated sub-markets due to their high importance for the security of supply. Since particularly the wind electricity supply is hardly to predict, very short-term iRES feed-in fluctuations need to be balanced within seconds and minutes by balancing power (Holtinen et al. 2013). In addition to unplanned plant or line outages and forecast errors in the electricity load prediction, the literature finds an increase in required balancing reserves up to 60 % per GW additional iRES capacity depending on the observed region, iRES technology as well as forecast quality (Hirth and Ziegenhagen 2015). Future improvements regarding the forecast accuracy of iRES feed-in can minimize the uncertainty of PV and wind electricity generation (Holtinen et al.

2013). Generally, the impacts of high shares of iRES in the European energy systems on the investment and dispatch of different flexibility options in the wholesale electricity market are in the focus of the present analysis, while potential adjustments of the electricity market design required to enable flexibility demand and provision are not in the focus of the present work.

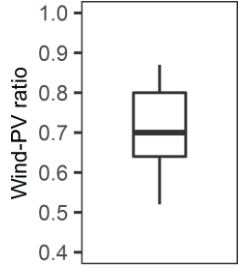
Besides the key techno-economical and market-policy related challenges to integrate the increasing amounts of iRES into the electricity markets and the energy system further uncertainties regarding the future expansion of iRES, particularly with regard to the share of wind and PV in future electricity generation. On the one side, the energy economical and energy political dimension is part of this uncertainty. On national level, the energy policy-driven expansion of the iRES is realized with different levels regarding the ambition and speed (Pruditsch & Zöphel 2018). Additionally, the political support for iRES in general as well as wind and PV separately is varying with increasing time horizon, depending particularly on the renewable energy governance (Pruditsch 2017). Different support schemes have led to a sustained reduction in the cost of wind and PV systems. On the other side, further socio-ecological parameters increase the range of criteria, which need to be taken in account for energy policy debates. Thus, aspects like life-cycle greenhouse gas emissions and recyclability, public and private participation potentials for iRES projects or possibilities for co-locating energy systems (e.g. building integration, agrivoltaic) as well as land-use discussions or noise issues have an influence on the perception of PV and wind onshore (ESYS 2020). In general, acceptance for iRES technologies strongly depends from public information and participation and may differ not only between countries, but also between regions within the same country (Ntanos et al. 2018). Bechberger et al. (2003) state that besides individual (national) ambitions in energy policy, further economic (e.g. fossil fuel prices, iRES costs degradation), political (e.g. formulation of expansion targets for wind and PV), technical (e.g. interactions between iRES generation and electricity grid expansion) and cognitive (e.g. public attitude towards wind power plants close to populated areas) factors influence the long-term success of instruments of iRES promotion. A change of focus or priority regarding these factors might influence the speed of iRES expansion in general as well as the preferences for either wind or PV specifically (Bechberger et al., 2003).

2.1.4 Derivation of PV and wind onshore expansion scenarios

However, the different feed-in characteristics of wind and PV systems can lead to different flexibility requirements. As discussed before, the aspect of Wind-PV share has received comparably low attention in the literature adopting an ambitious expansion of flexibility options in Europe. Nevertheless, publication-dependent differences in the explicitly or

implicitly assumed combination can be observed. In Table 2.4, the boxplot of the wind shares in relation to the total generation from wind and PV power plants (Wind-PV ratio) is plotted from a total of 21 studies. The studies included in this figure were selected according to three criteria. First, only studies that examine Europe as a transnational energy system and, second, develop scenarios with a high share of renewable energies, i.e. with a target year beyond the year 2030, were selected. Third, specific information on wind and PV electricity generation is necessary. If only capacities are provided, these were used to calculate the generation and the corresponding shares using the average full load hours from Chapter 2.1. In Table B.1 in Appendix B.3, a list of the studies included and the respective data are presented. In general, all studies assume a wind share of more than 50 % of the total iRES electricity generation. Half of the examinations have a share greater than or less than 70 %. In 2019, the Wind-PV ratio in the European Union was 74 % (EEA 2017). A large part of the studies scales the current iRES capacities, as in Chapter 2.1.3, up to the desired share (e.g. EU-Reference, Knopf 2013, ENTSO-E, BMU). The lowest wind share with almost 50 % can be found in the Distributed Generation Scenario 2040 of the ENTSO-E Ten Year Net Development Plan (ENTSO-E 2018). Within this study, a distributed iRES generation with a high penetration of PV rooftops systems is assumed. The highest share of wind can be observed in a study by the The Union of the Electricity Industry (Eurelectric) with 90 % wind generation in the iRES mix.

Table 2.4: Deviation of scenarios with different Wind-PV shares based on literature

	Scenario Name	Abbreviation	Wind-PV ratio
	High Wind	HP	0.9
	REF	REF	0.7
	High PV	HW	0.5

As this literature analysis has a broad mix of political, scientific and industrial background, the findings are used to develop three key scenarios in the course of the present work. To investigate the impact on the need for flexibility, three different Wind-PV ratios are set up covering the range as shown in Table 2.4. The Wind-PV ratio represents the percentage of wind (onshore and offshore) generation in the cumulated wind and PV feed-in in the key scenarios, hereafter named High PV, REF and High Wind. Furthermore, in each of these scenarios, a total iRES share of 80 % of the electricity consumption for the transnational energy system analysis is assumed. In Chapter 3, based on these preliminary considerations, scenario-specific iRES expansion

decisions are modelled, which are based on regionally high-resolved weather data as well as geo-information restricting the land-use. The derived detailed time series of wind and PV electricity feed-in are applied to discuss flexibility demand resulting from an optimal iRES expansion with varying Wind-PV ratios.

2.2 Options for providing flexibility in the energy system

Following the definition of flexibility for energy systems as in IEA (2008), these flexible technologies are meant to maintain a reliable and rapid response to large forecasted and unexpected fluctuations of energy demand and supply by adjusting their output. With Ma et al. (2013), describing flexibility as the “the ability of a power system to cope with variability and uncertainty in both generation and demand, while maintaining authors a satisfactory level of reliability at a reasonable cost, over different time horizons.”, the authors add the economic and temporal dimension to the definition of energy system flexibility. Thus, for the flexibility provision of the electricity system, the challenges can be summarised into two main requirements. First, flexibility options must provide sufficient flexibility to cope with the volatility and uncertainty of iRES generation on different time scales. Second, back-up capacity is required to compensate for weather-dependent low iRES feed-in phases. As introduced before, various categorisation options for the consideration of flexibility provision can be found. While in general, flexibility can be related to the ability of the electricity system to manage changes (Hillberg & Oleinikova 2019), a crucial distinction is the perspective of flexibility assessment. In a more local perspective, aspects regarding bus voltage maintenance and redispatch measures are highly relevant. However, in the present work the targeted overall system perspective rather relates to secure energy supply in general.

Since the climate protection targets necessitate comparably rapid and significant transformation measures, both exploiting the flexibility potential of today’s technology mix as well as additional flexibility options are required. For flexibility provision and sector coupling, a broad range of technologies with both high and low technology readiness level as well as varying contribution are available to be introduced. The different techno-economic characteristics and applications of the options suggest that no single technology can meet the future need for flexibility. Thus, the consideration of individual technologies and their use, only provides limited information on the potentials of the various options to meet the need for flexibility (Zöphel et al. 2018). An adequate model formulation for the present object of research should allow for long-term planning and at the same time combine a short-term resolution to take the fluctuating character of wind and PV into account. The following discussion of available flexibility options focusses on potential applications of single technologies as well as on possible

synergies and competitions between relevant technologies based on existing literature. Although interactions in a mix of flexibility options discussed in the literature are taken up, the detailed analysis of specific synergies and competitions between technologies including relevant technical parameters is the aim of the model-based analysis in the later chapters of this work (see Chapter 5 and 6).

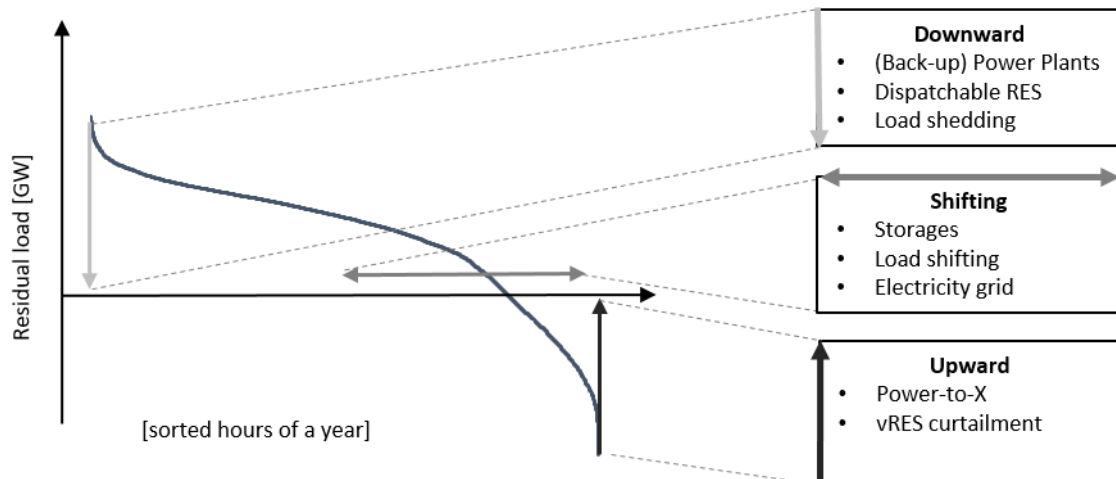


Figure 2.5: Overview and theoretical application for flexibility options (Own illustration)

Technologies to provide flexibility in the electricity system can be categorised differently (see for instance Huber 2017, Lund et al. 2015). In Figure 2.5, relevant flexibility options are presented together with their theoretical effect on the residual load (based on Michaelis et al. (2017)).

2.2.1 Back-up and load shedding flexibility

With a flexible electricity generation, the fluctuation of the residual load is compensated by adjusting the electricity supply. The historically and currently largely positive residual load forms the basis for electricity demand-oriented electricity generation in the existing power plant mix. This power plant portfolio is currently characterized by fossil fuels in most European countries. With hydropower, biomass, geothermal and solar thermal power plants, power plants with renewable fuel exist as well (Papaefthymiou et al. 2014). The different flexibility requirements and applications are coordinated in several electricity markets and thus enable security of supply. An alternative to additional electricity supply is load shedding, e.g. of industry processes, to decrease the residual load. Since often this process shedding results in loss of profits, the respective incentives, i.e. electricity prices, at the energy markets need to be high enough to compensate for this reduction (Michaelis et al. 2017).

The changing need for flexibility with the expansion of the iRES has three central effects on flexible electricity generation. Since the maximum of the residual load changes only slightly with an increase in the share of iRES in electricity generation, a need for dispatchable generation capacities will be necessary theoretically in order to provide sufficient back-up capacity and maintain security of supply, especially in times of low iRES electricity supply (Zöphel & Müller 2015). At the same time, however, it was shown that an increase of iRES installations leads to decreasing residual loads and thus realisable full load hours for power plants. Especially base load power plants, i.e. power plants, which are built to run steadily due to their technical and economic characteristics (high investment, comparatively low fuel costs), can thus lose importance. Not least, this has economic reasons, since with a lack of full load hours, the refinancing of investments is difficult (Zöphel et al. 2018)⁶. A third challenge regarding flexible electricity generation can be found in the increase of variance of the residual load, due to the weather-dependent electricity generation. The corresponding higher gradients influence the requirements on the load change behaviour of thermal power plants. Ramping up or down often increases abrasion and maintenance costs (Troy et al. 2011). In contrast to nuclear thermal and coal-fired power plants, gas turbines and gas and steam power plants as well as engine power stations can operate comparatively flexible and are therefore more suitable for energy systems with a high share of iRES (Michaelis et al. 2017). However, thermal power plants are currently often the reason for additional flexibility needs. Power plants that provide their output to the reserve power markets must ensure a certain level of availability. Combined heat and power (CHP) plants are also often tied to the heat supply. Both examples increase the share of so-called must-run capacities, which also run in times with a high iRES feed-in (Zöphel & Müller 2015). Thus, in addition to the comparatively low reaction times of some power plant types, commitment obligations in other energy submarkets are further limiting the flexibility of these technologies.

In the present work, the pattern of the residual load as well as a combined heat and power supply are subject of the model-based analysis to evaluate the role of flexible generation capacities and load shedding in a mix of flexibility options against the background of scenario-specific Wind-PV ratios.

⁶ The need for secured capacity in the presence of weather-dependent iRES electricity generation and the simultaneous displacement of dispatchable generation capacities from the electricity markets are the starting point of the discussion on the incentive potential of today's electricity market design (so-called energy-only market, short EOM) compared to capacity markets. An overview regarding the discussion of the current market design against the background of increasing shares of iRES can be found in *iea* (2016) and *BMW* (2015).

2.2.2 Spatial and temporal shifting flexibility

Both the fluctuations and simultaneity of electricity generation influence the potential of electricity-shifting technologies. As shown in Figure 2.5, storages, load management measures and electricity grids are suitable for this application. The latter are crucial assets of the national and European electricity systems, in order to connect the locations of the electricity generation with those of the electricity consumption. Sufficient interconnection capacity decreases electricity price differences in connected electricity market areas and enables the export of surplus iRES electricity (at low prices), instead of curtailing it (Verzijlbergh et al. 2017). As iRES capacities increase, electricity grids enable spatial balancing effects of the regionally unevenly distributed weather-dependent electricity generation (Rodriguez et al. 2014). Thus, electricity grids reduce the aggregated iRES feed-in variance and smoothen the residual load on a transnational scale (Olauson & Bergkvist 2016). The regional balancing effects are stronger with larger geographical size of the connected power system (Huber 2014). Against this background, the expansion of electricity grids is discussed as a crucial source of flexibility (Schlachtberger et al. 2017) and an important target of European Union (EU 2019).

On the other hand, electricity storage systems shift energy over time, thus balance times with surplus and deficit electricity. These storages are technically characterized primarily by their energy capacity and by their power capacity. While larger charging and discharging capacities can compensate for higher deficits and surpluses, higher storage capacities allow longer balancing between surplus and deficit phases. The different technologies with different possible applications are usually divided into the categories of chemical, mechanical and electrical storage based on the stored energy form. In the present work a distinction is also made with regard to a cross-sectoral application. Electricity storages are accordingly defined as storages charging and discharging electricity, while energy storages refer to technologies using electricity to cover cross-sectoral energy demand. Pumped hydro storages are widely used today. However, particularly battery storages are considered to have great potential due to their compatibility with decentralized energy systems (Verzijlbergh et al., 2017). By balancing load and generation fluctuations, storages can integrate iRES-based electricity and compensate for its variability. They are also able to provide system services due to their fast response times (Michaelis et al. 2017). This means that electricity storages not only compete with conventional electricity generation but also with electricity grids. Especially the discussion of possible synergies and competitions between electricity grids and electricity storage is the subject of a large body of scientific literature (see for instance Cebulla 2017, Gils et al. 2017, Schlachtberger et al. (2017), Matthiesen et al. 2015, Denholm & Hand 2011). For instance, Cebulla (2017) and Gils et al. (2017) conclude, that electricity grids and storages can either substitute or complement

each other, strongly depending from the iRES share. In the present thesis, the model-based analysis also assesses the role of storages against the presence of further flexibility options and sheds light on the influence of the iRES feed-in characteristics on the need for different storage types.

A further option for temporal shifting is demand side management (DSM). Particularly non-time critical electrical loads can reduce their electricity demand in times with low iRES feed-in (positive residual load) and postpone it to times with iRES surpluses, thus show a similar application compared to storages. In contrast to load shedding, the shifted electricity demand needs to be compensated later on (Michaelis et al. 2017, Zerrahn & Schill 2015). On the one hand, DSM measures are discussed as promising in literature, as they are considered as cost-effective approach for iRES integration. On the other hand, e.g. Ladwig (2018) shows, that techno-economical restrictions (e.g. opportunity costs, realisable shifting times) particularly for industry processes limit the potential of DSM.

2.2.3 Load increase flexibility and sector coupling

Curtailling iRES electricity to balance wind and PV surplus generation is a flexibility option to provide upward flexibility by increasing the residual load. However, this approach counteracts the climate policy aim to exhaustively consume the iRES electricity. Nevertheless, the complete integration of iRES electricity is not cost efficient in a system perspective (Rodriguez et al. 2014). An alternative is using the surplus energy by increasing the electricity demand. In a multi-coupled energy system, further energy storages like heat or hydrogen storages are increasingly important (Mathiesen et al. 2015). Thus, relevant flexibility options improve ideally the iRES integration by covering surpluses as well as replace carbon-intensive processes and technologies, while allowing for additional flexibility from other energy demand sectors (Brown et al., 2018, Eller 2015). To enable the integration of the electricity sector with the energy end-use sectors, issues regarding techno-economic (e.g. cost competitiveness), policy and regulatory barriers (e.g. electricity market price signals and grid charging methods) have to be met, while at the same time negative effects for the consumers benefit and comfort have to be avoided (Van Nuffel et al. 2018). Figure 2.6 illustrates the potentials for electricity in the industry, buildings and transport sector and compares the respective CO₂ emissions.

Sector coupling in the heating sector is already established today in the form of combined heat and power plants (CHP). By using waste heat for the heat supply, the efficiency of fuel consumption can be increased. In contrast, heat pumps and electric boilers use electricity

directly for heat production (power-to-heat – PtH)⁷. Combined with a heat storage, iRES surpluses can be transferred flexibly to the heating sector. Compared with further sector coupling approaches, linking the heating and electricity sector is considered as promising, since technologies for electricity-based heat generation and heat storage are mature technologies with relatively low costs (Bloess et al. 2017, Agora 2014).

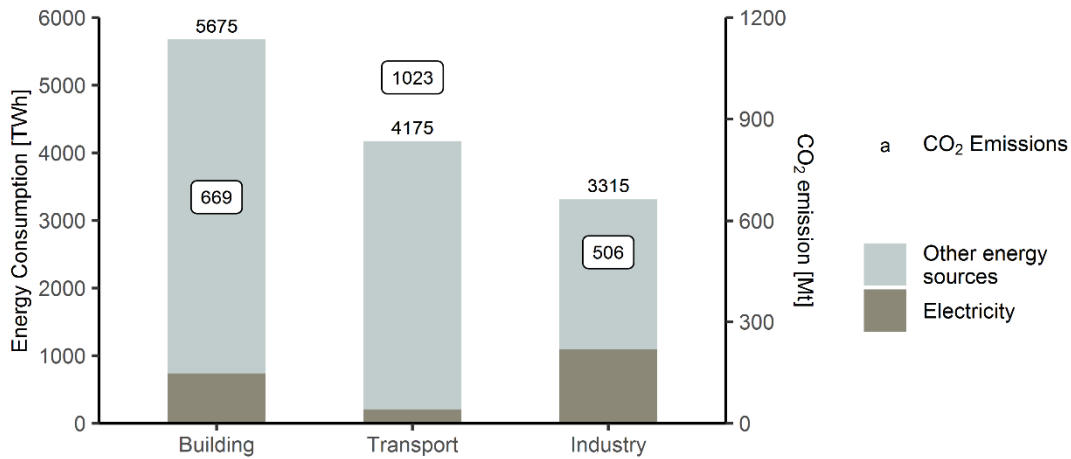


Figure 2.6: European energy consumption of different sector and CO₂ emissions (Own illustration based on Agora 2019)

Regarding the transport sector, electromobility is one of the major options for the electrification particularly of the motorised private transport (Kasten & Hacker 2014). Since the direct use of electricity in vehicles realised by batteries (battery electric vehicles – BEV) is considered as promising⁸, the available storage capacity has a high value as flexibility option. Ideally, the BEV can be charged in times with low residual load and discharged when there are deficits of iRES electricity generation (Heinrichs 2013). Nevertheless, this is only possible, when the BEV is available, i.e. connected with a charging station. Additionally, the already mentioned challenges for the electricity system regarding the increased electricity demand and resulting system peak load are part of the scientific discussion (see e.g. Trost 2016, Schill & Gerbault 2015, Heinrichs 2013). Here the potential and acceptance of electricity market-oriented or grid-oriented charging of BEV are in the focus of (see e.g. Hu et al. 2016, Fraunhofer IWES 2014). By coupling the electricity sector with the gas sector by producing iRES based hydrogen via water electrolysis⁹

⁷ For an overview of different PtH applications and concepts the reader may be referred to Bloess et al. (2017).

⁸ Further approaches for the electrification of the transport sector can be found in Martino et al. (2019) and Richardson (2013).

⁹ A detailed overview about the electrolysis technology can be found in Götz et al. (2016).

(power-to-gas – PtG) further flexible storage potential can be exploited. Hydrogen is assessed to play an increasing role in the decarbonisation of the energy demand due to multiple application potentials in the heating, transport and industry sector. In addition, hydrogen can be stored and transported relatively easily. This also enables the substitution of fossil fuels and the iRES integration in all end-use sectors with a gas demand (besides direct electrification), while similar infrastructures can be used. However, challenges regarding costs and efficiency remain (Staffell et al. 2019). Nevertheless, the potential role of hydrogen in the energy system transformation is also taken up by current national roadmaps, like the German National Hydrogen Strategy (BMWi 2020) or the Japanese Basic Hydrogen Strategy (METI 2017).

In general, the applications for the electrification of energy end-use sectors (Power-to-X – PtX) are often compared with established benchmark processes (e.g. gas boiler in the heating market, internal combustion engine for private transport or gas reforming for hydrogen production in industry). Particularly for PtG concepts, existing analysis show a rather low competitiveness (Michaelis et al. 2017, Brunner & Müller 2015). Nevertheless, against the background of ambitious climate protection targets in energy end-use sectors, energy policy guidelines or directives explicitly or implicitly supporting PtX technologies are likely. Reasons for a respective development are besides others, the often limited application of electricity in distinct energy end-use sectors (e.g. high-temperature for industry, non-road transport). In addition, a multi-coupled energy system offers the opportunity to access additional energy storages like heat or hydrogen storages (Matthiesen et al. 2015). Ideally, both an improvement of iRES integration as well as the exploitation of further flexibility potentials are resulting synergies (Brown et al., 2018, Eller 2015). Nevertheless, this strongly depends from the available flexibility of the underlying processes and applications in the heating, transport and industry sector. An (inflexible) increase in electricity demand based on sector coupling potentially result in additional challenges for the electricity system and increase the flexibility requirements in this sector (Sterchele et al. 2020, Lindberg et al. 2019). With sector coupling forming the third driver for the present work, the range of interacting technologies and required infrastructure is further broadened, resulting in a higher electricity demand (despite efficiency gains) and most likely influence the flexibility requirements for the entire energy system also in dependence of available energy storages.

3 Potential-based optimal wind and PV expansion in Europe

Since the iRES potential derivation has direct influence on the model formulation, the present chapter first looks at the required data gathering and processing. This includes the identification of a representative weather year, followed by the presentation of the weather data used. For the data access, databases are available online (see for example Pfenninger & Staffel 2020), which however only provide data for single point coordinates or aggregated country-specific time series. However, to improve the assessment of the need for flexibility by mapping the regional and time-dependent characteristics of wind and PV a temporally and regionally high resolved analysis of the iRES electricity generation is required (Zerrahn and Schill 2017). Thus, it is necessary to collect relevant data to cope for an adequate spatial and temporal detail. The results below are additionally compared with existing literature for validation purposes. For the calculation of the potentials, the focused region is central-western Europe with in total 17 countries (see list of countries in Chapter 1.3). Furthermore, GIS-based area potentials are calculated in order to be able to limit the areas available for iRES installations. In the second part of Chapter 3, these potentials serve as input parameters for the model-based optimal expansion of fluctuating renewable energies to cover high shares of the electricity demand in different Wind-PV ratio scenarios. After presenting the model description, additional data, like electricity demand and technology cost assumptions will be presented in Chapter 3.2.3 before the chapter concludes with a discussion of the limitations of this model approach. Chapter 4 then presents the scenario-specific results of the wind and PV expansion.

3.1 Determination of wind onshore and PV potentials

In the present work, the focus of the potential analysis lies on wind onshore and PV, since for these two iRES technologies, the optimal distribution of capacities is most influenced by local conditions. Additionally, wind onshore and PV compete with one another as the available areas for the installations are often limited. In contrast, this limitation of area might increase the potential for distant wind offshore installations despite techno-economic challenges. Nevertheless, although time series for wind offshore can be gathered with the same steps as presented below, the future technology potentials (e.g. realisable distance to shore, sea depth or floating offshore wind farms) are more difficult to estimate compared to the other iRES (WFO 2019). These trends strongly influence the installation potentials and costs for wind offshore capacities (Caglayan et al. 2019). As it is beyond the scope of the present work to focus on these uncertainties, the wind offshore technology is included in a simplified approach by exogenously implemented time series. Based in cost data and these generation time series, wind offshore can contribute to the iRES mix on country level in competition with wind onshore and PV.

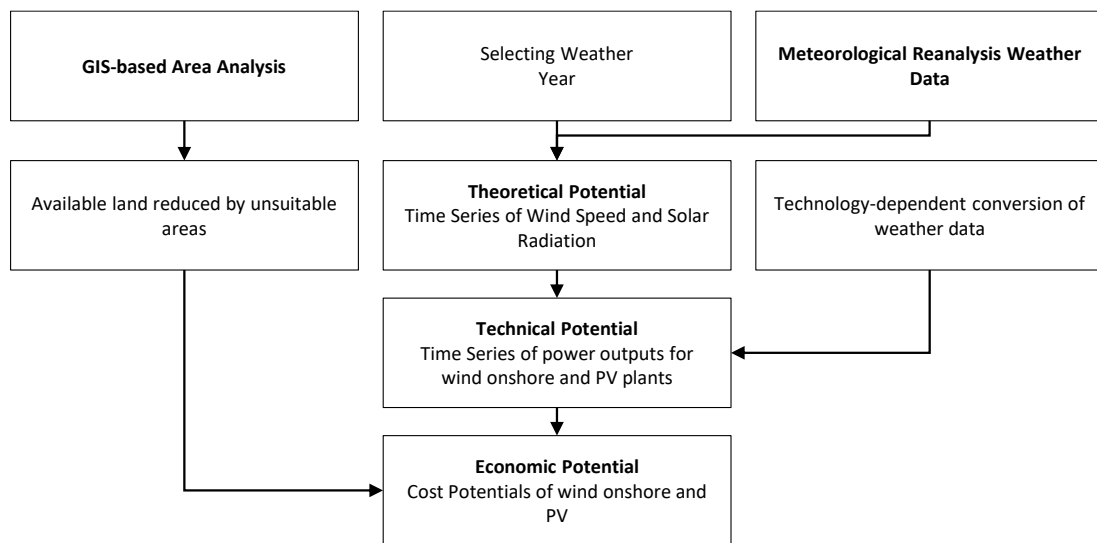


Figure 3.1: Steps for the potential analysis of wind onshore and PV (Own illustration)

To represent the spatial and temporal potential for wind onshore and PV, meteorological simulations and satellite datasets are used to convert wind speeds and solar radiation to the respective (normalised) power output of each technology. In Figure 3.1, the required steps are presented, structuring the following subchapters and narrowing down the respective categories of potentials as in Fiukowski et al. (2016). Accordingly, based on a selected weather year, the theoretical potential for wind onshore and PV is the physical energy supply contained in the wind speed and solar radiation. The required time series are gathered by using meteorological historic and simulation-based weather data. In a next step, this data is converted to time series

of power outputs for wind onshore and PV, forming the technical potentials. Furthermore, Geographic Information System (GIS) Data is used to analyse the available area, which results in cost potentials for the respective technologies, here defined as economic potentials. A further restriction of this potential is applied by the model formulation in Chapter 3.2. The steps illustrated in Figure 3.1 are validated against similar work in the existing literature

3.1.1 Identification of a representative weather year

The choice of the weather year as basis for all subsequent investigations is crucial, because only by including the knowledge of the annual deviations of wind and PV power generation from the long-term mean, the results of the present work can be assessed validly. However, years with high, medium or low wind yields may differ from the solar years. The aim of the present work is to identify a representative reference year for both electricity generation technologies. With regard to the optimal mix of flexibility options, the flexibility requirement in the present work is therefore determined on the basis of a medium-yielding year for all electricity generation technologies which may under- or overestimate the demand depending on the actual weather year. Particularly extreme wind and solar years are thus excluded as weather year, although they are challenging regarding the security of electricity supply and flexibility provision (van der Wiel et al., 2019). However, as this analysis focuses on providing flexibility on the wholesale electricity market and does not include any additional options for maintaining security of supply (e.g. reserve power market), this approach is considered as valid.

Table 3.1: Comparison of average values of full load hours for PV, wind onshore and offshore for the weather years 2006 to 2015 (Data: EMHIRES, 2020)

	2006	2007	2008	2009	2010	2011	2012	2013	2014	2015	Ø
PV	1,011	1,033	991	1,021	1,003	1,069	1,016	956	1,009	1,046	1,015
Wind onshore	1,801	1,970	1,952	1,820	1,731	1,826	1,857	1,844	1,809	1,956	1,857
Wind offshore	2,436	2,563	2,619	2,399	2,208	2,525	2,485	2,432	2,434	2,630	2,473

EMHIRES data covering ten years (2006 to 2015) is used to compare the weather years and the average full-load hours for PV, wind onshore and offshore of the 17 countries in the observed region (EMHIRES 2020, Gonzales Aparicio et al. 2017, 2016) (see Table 3.1). For each technology, and thus in total, the deviation is lowest in 2012 and is therefore selected as the reference year for the following study.

3.1.2 General steps for the weather data accessing

Meteorological data not only offers high resolution and global coverage, but are also often freely available, in contrast to commercially available historical data (Staffell 2016). Long-term meteorological datasets can be created based on global atmospheric simulations. In the literature (see for instance Bosch et al., 2017, Pfenninger et al., 2017, Staffell 2016), NASA's MERRA-2 (Modern-Era Retrospective Analysis for Research and Applications, Version 2) dataset is frequently used (NASA 2020), due to both very good historical (1980 - present) and geographical (global) coverage as well as regional resolution ($0.5^\circ \times 0.625^\circ$) and temporal resolution (hourly). In the present work, the resolution of the MERRA-2 dataset is applied for the analysis, not only of wind onshore and PV generation time series, but also for the assessment of available land for iRES installations.

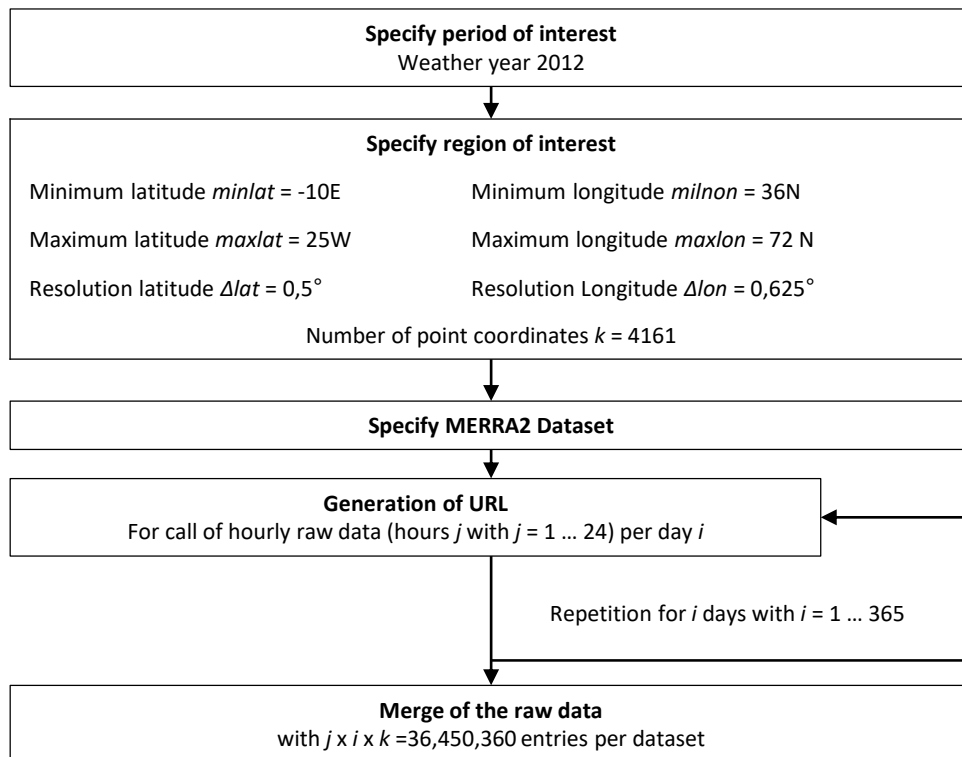


Figure 3.2: Steps of data acquisition (Own illustration)

Due to the aimed large geographic coverage with regionally high-resolution iRES power generation data, in the present work the raw data gathering is automated by using the NASA earth data portal (NASA 2020) and the OPeNDAP 4 Data Server of the Earth System Grid II (OPeNDAP 2020). Figure 3.2 shows the relevant steps for each parameter to generate the wind and PV power generation time series. For the automated data provision, the minimum and

maximum latitude and longitude covering the whole region observed is required. The MERRA-2 grid with a resolution of 0.5 ° in width and 0.625 ° in length gives a total of 4,161 raster points for the present region of interest. By specifying these parameter, the URL for retrieving the relevant dataset can be generated. The call is made for each day in hourly resolution and is repeated in a loop until the data can be merged for an entire year. For each dataset, more than 36 million data points are available. Subsequently, a reduction and assignment of the coordinate points to national borders takes place. Accordingly, the number of coordinate points is reduced to 1,481 rasters representing an onshore area of 6,848,144 km².

Chapters 3.1.3 and 3.1.4 illustrate the technology-specific time series derivation in more detail first for wind onshore and second for PV. Thereby, technological progress is taken into account and the main steps for the transformation of the weather data into generation time series is presented.

3.1.3 Calculation of Wind onshore potentials

For the calculation of wind electricity generation time series, power curves of wind turbines are used, describing the power output of the wind turbine as function of the wind speed. To cope for future developments, major trends are included, namely an increase in power density, in rotor diameter and in hub height. The increase of power density (W/m²) will be taken into account when calculating the land-use for wind power plant installations. Furthermore, for future turbine configuration the following assumptions are made taking different wind classes with different wind-yield qualities into account. According to DIN EN 61400 (IEC 2019) three classes IEC I to III are defined with decreasing locational wind speeds (see Table 3.2). Anticipating the analysis below, the wind class I with average yearly wind speeds > 10 m/s are not existing onshore in the observed region. In Ryberg et al. (2019) a turbine categorised as IEC II class is selected for the target year 2050. In the present work, the improvements of turbine design will be applied by scaling existing wind turbines to the configuration in Ryberg et al. (2019) for both wind classes IEC II and III. While this can be done directly for the IEC II turbine, the relative growth rates between the existing and the projected turbine will be also used for the IEC III class. An Enercon E101 (Enercon 2015) and a GE 120 (GE 2014) serve as reference turbine for wind class II and IEC III, respectively. The results of the scaling are illustrated in Table 3.3.

Table 3.2: Categorization of wind classes (Data: based on IEC 2019)

Wind class	Mean wind speed w
IEC III	$w < 7,5$ m/s
IEC II	$7,5$ m/s $\leq w \leq 10$ m/s
IEC I	$w > 10$ m/s

Table 3.3: Assumptions on technical data for current and future wind turbines (Data: Ryberg et al. 2019, Enercon 2015, GE 2014)

	Wind class IEC II			Wind class IEC III	
	Existing turbine	Target turbine*	Growth rate	Existing turbine	Target turbine**
Name manufacturer	Enercon E101			GE 120	
Hub height [m]	92	120	30 %	110	143
Rotor diameter [m]	101	136	35 %	120	162
Nameplate capacity [MW]	3.05	4.20	38 %	2.50	3.45

To determine the wind onshore potential, time series of the power generation for each raster are created. Based on the Virtual Wind Farm Model (Staffell & Green 2014), the following steps are included (see Appendix B.1 for a detailed step description):

1. Extraction of wind speeds and roughness lengths from the MERRA-2 weather data
2. Transformation of the wind speed to turbine hub height by applying the logarithm height formula using roughness lengths
3. Conversion of wind speeds to normalized generation time series based on manufacture power curves of reference wind turbines

As a result, wind onshore capacity factors (CF) can be calculated as potentials which are represented for the study area in the geographical resolution ($0.5^\circ \times 0.625^\circ$) based on the MERRA-2 data in Figure 3.3. The increase in CF close to the coast becomes apparent with full-load hours of more than 4,000 h/a. Particularly high mean wind speeds are possible in Denmark and Great Britain.

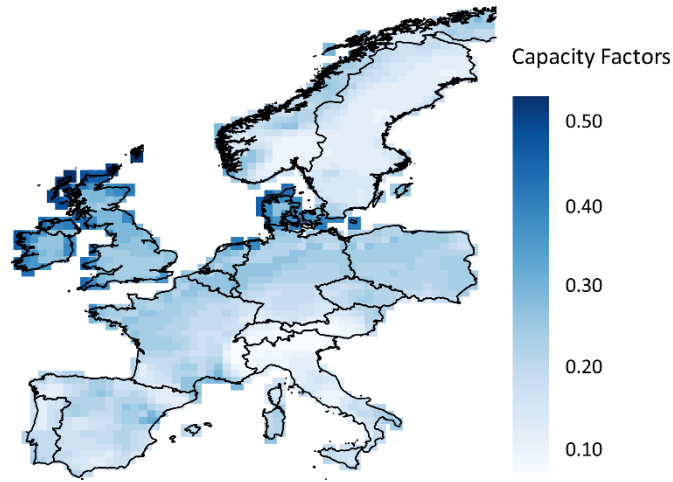


Figure 3.3: Potential capacity factors for wind onshore in the observed region (Own illustration)

In Table 3.4 the average achievable CF are compared with literature values with similar scope, i.e. weather data based analysis of wind onshore potentials in Europe. In general, differences can occur based on the weather data applied and the assumed technical characteristics of the wind onshore technology. The CF in the present work show similar values with those of Ryberg et al. (2019) and Stetter (2012), both using MERRA data and assuming technical progress in wind turbine design. The latter assumptions directly result in higher CF compared to those of the other authors in Table 3.4.

Table 3.4: Comparison of average capacity factors for wind onshore in the present work with existing values in the literature

Source	Average capacity factors	Weather Data	Future Turbine Design
Present cf	28.1 %	MERRA-2	⊙
Ryberg et al. (2019)	29.2 %	MERRA-2	⊙
Bosch et al. (2017)	21.8 %	MERRA-2	---
Eurek et al. (2017)	24.2 %	CFDDA*	---
McKenna et al. (2015)	23.0 %	ECMWF**	---
Scholz (2012)	24.0 %	HELIOSAT	⊙
Stetter (2012)	28.2 %	MERRA	⊙

* Dataset: Climate Four Dimensional Data Assimilation of National Center for Atmospheric Research (NCAR); ** Dataset: ERA of European Centre for Medium-Range Weather Forecasts (ECMWF)

3.1.4 Calculation of PV potentials

Similar to the discussion of future trends regarding the wind turbine design, the performance of PV systems will also be affected by technological progress in the future. These trends mainly concern the use of alternative materials to improve efficiency. Besides the widespread crystalline silicon, low cost and low to medium efficiency cells based on nano-crystalline concepts as well as high efficient so called third generation PV cells are discussed as promising (Obeidat 2018). These developments concerning the cell efficiencies are taken into account implicitly by assuming improved power densities and decreased investment costs (see Chapter 3.1.5). A distinction regarding different power densities is made for rooftop and utility PV systems. For the inverter, as part of the PV module transforming the PV cells DC current into AC, a further increase in efficiency is expected due to material and controller improvements. While today losses of around 10 % are standard, it was shown experimentally, that efficiencies up to 99.7 % are achievable (Obeidat 2018). For the present work, an inverter efficiency of 95 % is assumed. Additional impact factors on the efficiency of PV modules are the ambient temperatures (Huld et al. 2010). Therefore, a temperature-dependent efficiency calculation approach is applied.

The PV potential in the observed region is based on the solar radiation data, which is converted to PV electricity generation time series for each of the 1,481 rasters using the following steps as in Pfenninger & Staffell (2016) (see Appendix B.2 for a detailed step description):

1. Extraction of horizontal solar radiation data and temperature time series from the MERRA-2 database
2. Conversion of the horizontal radiation data to the inclined plane
3. Calculation of the normalized feed-in time series with the aid of the module efficiency and temperature time series

Analogous to the presentation for the standardised wind time series, Figure 3.4 shows the theoretical CF for PV based on the MERRA-2 weather data for the region observed and the weather year 2012. The solar radiation and the resulting CF clearly increase from north to south. The highest potentials occur accordingly in the south of Portugal, Spain and Italy.

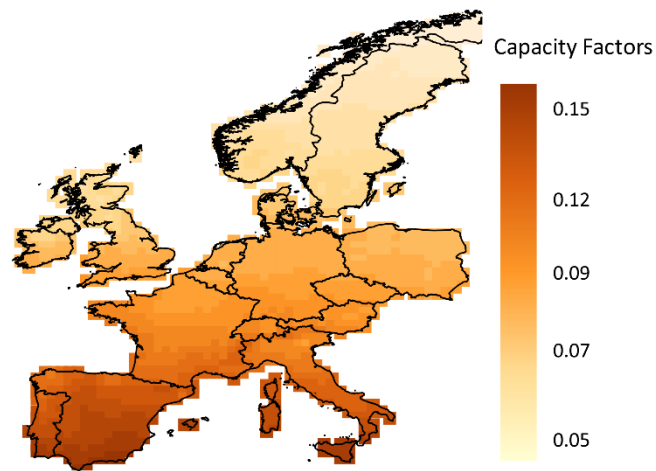


Figure 3.4: Potential capacity factors for PV in the observed region (Own illustration)

The average CF is compared to the values found in literature in Table 3.5. The present CF show the lowest values, mainly due to the higher geographical scope of the other studies which include additional countries in the southwest of Europe. Compared with Pfenninger & Staffell (2016), a single country comparison shows better results.

Table 3.5: Comparison of average capacity factors for PV in the present work with existing values in the literature

Source	Average Capacity Factors	Weather Data
Present CF	11.4 %	MERRA-2
Pfenninger & Staffell (2016)	12.9 %	MERRA-2
Scholz (2012)	12.9 %	HELIOSAT
Stetter (2012)	14.4 %	MERRA

The capacity factors shown in Figure 3.3 and Figure 3.4 are theoretical potentials, which may be limited by further restrictions with regard to the actual expansion of the iRES. Since the target of high shares of renewable energy is expected to lead to a strong expansion of wind onshore and PV plants, questions of social acceptance become increasingly important. Possible restrictions are implicitly part of the present work through corresponding constraints in the model formulation (see chapter 3.2.1). First, the previously determined potential is limited to areas suitable for IRES installations.

3.1.5 Area analysis for wind onshore and PV installations

In the literature several further restrictions are introduced, such wind turbine offset regulations, estimates on buffer zones around areas excluded from the available land for iRES or suitability

factors (see McKenna et al 2015 and Scholz 2012). McKenna et al. (2015) apply small-scale analysis with very high resolution excluding the available land. In order to include further constraints and decrease the potential not just for a single technology and a single country, more detailed high-resolution land use and housing stock analyses are needed for all the countries studied. For the present work, no data set exists covering the whole observed region. Additionally, future regulations regarding offset and buffer zones are highly uncertain, particularly since significant installations are required for the future iRES expansion pathways. Therefore, additional techno-economic and socio-ecological restrictions are observed in the implementation of the model-based expansion of the iRES (see Chapter 3.2) implicitly restricting the available land to cope for the limitations above as well as to include energy policy considerations discussed in the model description of the iRES expansion below.

To determine the area potential for the iRES with GIS data, various area categories are processed and merged to assign suitable areas for the installation of wind onshore and PV systems. In the present area analysis, three layer are used based on Scholz (2012). In Table 3.6, the respective layers, the information on the resolution and sources of the respective GIS data are presented.

Table 3.6: Applied GIS data for the area analysis

Data	Resolution	Dataset	Source
Land Cover	0.0083 ° × 0.0083 °	CORINE Land Cover	CLC 2012
Elevation and Slope	0.0083 ° × 0.0083 °	GTOPO30 digital elevation Model	USGS 1996
Protected Areas	varying	World Database on Protected Areas	WDPA 2014

Table 3.7: Assignment of CLC land use categories to iRES technologies (Data: CLC 2017)

	Category	Nomenclature in CLC*
Wind onshore	Forests	31
	Scrub and/or herbaceous vegetation associations	32
PV	Artificial surfaces	111, 112, 121-124, 131-133
Shared areas	Arable land	211-213
	Pastures	231
	Open spaces with little or no vegetation	33

To estimate the land cover, GIS data from the CORINE Land Cover Set (CLC) are applied classifying land use in Europe. Out of five main groups (built-up areas, agricultural areas, forests and semi-natural areas, wetlands, water) with a total of 44 subcategories, the categories relevant for wind onshore and PV installations were included (see Table 3.7), as in Scholz (2012). While forests and scrub and/or herbaceous vegetation areas are only suitable for wind onshore

installations, artificial areas, i.e. roof areas, are exclusively assigned to PV systems. For the areas that are considered suitable for both technologies, the model-based iRES expansion decision (see chapter 3.2) involves an endogenous distribution of the available area for the installation of PV or wind turbines. In the extension model, PV rooftop systems will be expanded for built-up areas, while the installation of PV utility systems will be assumed in the case of shared areas.

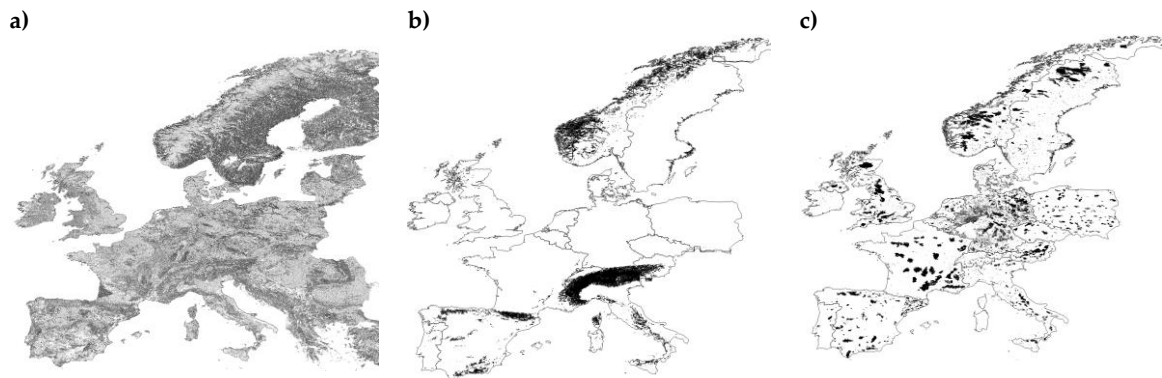


Figure 3.5: a) available area based on Corine land cover, b) area excluded based on elevation and slope, c) area excluded based on protected areas (Own illustration)

These available areas are further restricted. According to Scholz (2012), areas with an elevation above 2000 m and/or a slope greater than 20° are considered unsuitable. The altitude of the area observed is analysed based on the digital elevation model GTOPO30 (USGS 1996) and corresponding slopes are calculated using the QGIS Terrain Analysis Tool. Furthermore, protected areas with protection status I to IV in the IUCN (International Union for Conservation of Nature) are extracted from the dataset of the World Database of Protected Areas and excluded from the potential iRES areas. In Figure 3.5 the different GIS layer show the areas suitable for iRES installations based on land cover (Figure 3.5a) as well as the areas excluded based on the criteria elevation, slope (Figure 3.5b) and protected areas (Figure 3.5c). Finally, these different datasets are merged and assigned to the grid cells with the MERRA-2 resolution of $0.5^\circ \times 0.625^\circ$.

Above all, the population density has a major influence on the area potential, which affects both the total area potential and the PV potential. Figure 3.6 shows the resulting distribution of accumulated areas for wind onshore and/or PV installations in proportion to the area of the respective country. For example, for Germany, values ranging between 2% to 15% of the country's national territory are reported in the literature for wind onshore potential (Matthes et al. 2018, BMVI 2015). Here, different constraints (e.g., wind turbine offset distance regulations) and conflict risks (e.g. competition between PV and solar thermal roof-top use or agricultural land use for food production or electricity generation) are accounted for, explaining the range

of area potentials in the literature. Thus, the data on generation potential based on available land as presented here are rather technical potentials.

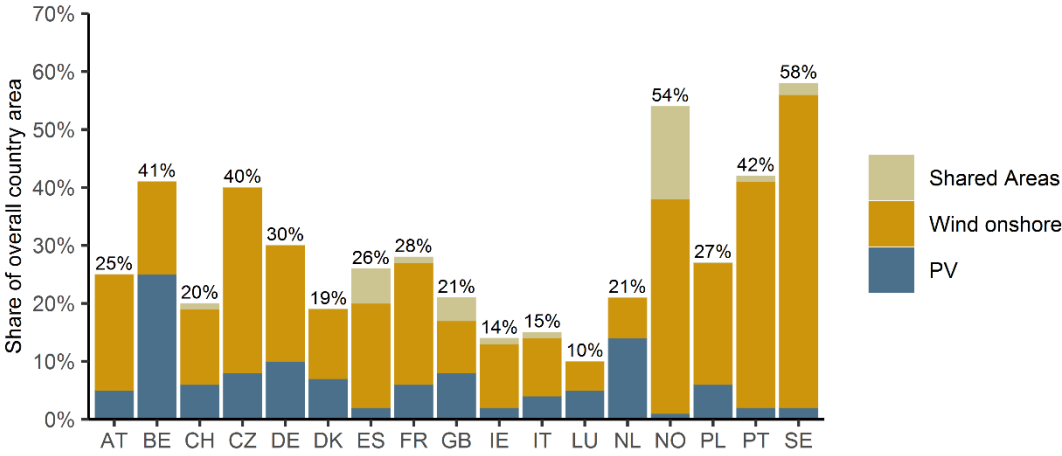


Figure 3.6: Share of area available for iRES installations compared to overall country area (Own illustration)

The data generation of the present chapter enables the calculation of iRES cost-potential curves across the observed region. These curves illustrate the relation between specific generation costs and the generation potential. Thereby, the costs are expressed as levelised costs of electricity (LCOE) based on the CF in each raster and the assumed cost data, while the generation potential reflects the available land. To generate these curves Table 3.8 presents the required data.

Table 3.8: Data required for the illustration of cost-potential curves for PV and wind onshore (Data: Ryberg et al. 2019, Vartiainen et al. 2020, Fraunhofer ISE 2018, Rinne 2018, Zappa & van den Broek 2018, Schröder et al. 2013)

		PV rooftop	PV utility	Wind IEC II	Wind IEC III
CAPEX	EUR/kW _p	760	420	854	1,300
OPEX	EUR/kW _p	4	4	30	30
WACC	%	7	7	7	7
Economic Lifetime	years	25	25	25	25
Power density	MW/km ²	211	167	6.0	4.2

For the costs data, values for the target year 2050 estimated in literature are applied. As most of the specific investment costs in the present work, the CAPEX (total capital expenditure) are derived from Schröder et al. (2013). The values found here are comparable with more current works (e.g. Zappa et al. 2019, Vartiainen et al. 2020, JRC 2015). Nevertheless, this source is preferred since also further cost data for the model-based analysis of flexibility provision (see Chapter 5) can be retrieved. Additionally, the distinction of the cost data in PV rooftop and

utility as well in the two wind onshore classes are based on Zappa & van den Broek (2018) and Rinne et al. (2018), respectively. Economic lifetime and the weighted average cost of capital (WACC) are based on Fraunhofer ISE (2018) and Vartiainen et al (2020). The LCOE are calculated for each technology rt and raster r as sum of $CAPEX_{r,rt}$ and yearly $OPEX_{r,rt,t}$ (for the whole lifetime N discounted by the $WACC$) divided by the discounted raster- and technology specific-yield $Y_{r,rt,t}$ (see equation (xx)). Since the cost values are specific values (in EUR/kWp), the yield is included as full load hours.

$$LCOE_{r,rt} = \frac{CAPEX_{r,rt} + \sum_1^N \frac{OPEX_{r,rt,t}}{(1+WACC)^t}}{\sum_1^N \frac{Y_{r,rt,t}}{(1+WACC)^t}}$$

Finally, the power density in MW/km² are based on Ryberg et al. (2020) for wind and Zappa and van den Broek (2018) for PV. These values do not include offset distance regulations.

In Figure 3.7 the cost-potential curves for wind onshore (left) and PV (right) are illustrated for selected countries, with higher generation potentials for wind onshore compared to PV. This is a result of higher CF as well as more area suitable for wind onshore for the countries shown in Figure 3.7. For most of the selected countries, the wind onshore potential is starting with low LCOE reflecting the locations close to the sea with good wind conditions. This becomes especially obvious for Great Britain. In contrast, the spread of LCOE of the PV cost-potential curves is lower due to the less varying solar radiation in the countries. Particularly France and Spain are characterised with high potentials and comparably low LCOE for both iRES technologies. The presented cost-potential curves show a good match in comparison with existing literature. While for PV, Fraunhofer ISE (2015) estimate a similar range of LCOE, Vartiainen et al. (2020) calculate lower LCOE of 9 to 15 EUR/MWh from southern to northern European countries mainly due to higher FLH assumed and the focus on utility PV systems. Fraunhofer ISE (2018) calculate for PV and wind onshore a range of LCOE of 20 – 70 EUR/MWh and 30 – 70 EUR/MWh for Germany. Regarding the PV and wind onshore generation potentials (in TWh), Scholz (2012) estimates slightly lower values. McKenna et al. (2015) identifies cost-potential curves for wind onshore for different countries. The authors illustrate similar curves for most of the countries in Figure 3.7, while for Great Britain a higher potential for wind onshore is estimated. Reasons for deviating results can be found in the methodology and the data used. Besides the aforementioned inclusion of buffer zones, particularly the resolution of the weather data has an impact on the cost potential curves with the averaging of wind speeds or solar radiation per raster, a lower resolution flattens the cost-potential curve (McKenna et al.

2015). In addition, the assignment of coastlines and national borders is increasingly difficult with lower resolved weather data.

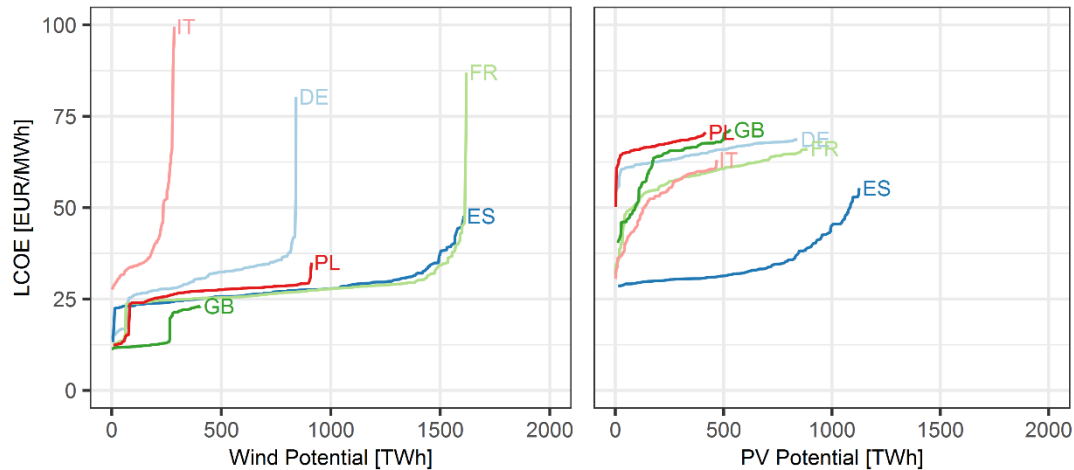


Figure 3.7: Cost-potential curves for wind onshore (left) and PV (right) for selected countries (Own illustration)

3.2 Model-based optimal expansion of varying renewable energies

Based on the iRES potentials, the model for the optimal expansion of wind and PV capacities as well as the associated data will be presented below. While in this model formulation the focus lies on weather-dependent RES expansion, further RES are seen as flexibility option and will be included in the second model for optimal investment decisions in flexible technologies. Before presenting the mathematical description of the developed optimization model, the model approach is derived based on requirements arising from energy policy considerations¹⁰.

3.2.1 Model requirements and general assumptions

The optimal expansion of the iRES is driven by its potentials, as these directly influence the electricity generation costs of the wind and PV systems. Various studies are examining the optimal model-endogenous iRES expansion together with conventional power plants and other flexibility options (as for example in Brown et al., 2018, Gils et al., 2017, Zerrahn and Schill 2017, Scholz 2012). These approaches can be used to derive insights into interactions between, for example, power plant decommissioning (for example, by phasing-out electricity generation based on fossil fuels) or a limited CO₂ budget on the value of iRES technologies. In the present work, the expansion of the iRES is calculated separately from the expansion of any flexibility

¹⁰ The applied model formulation and gathered input data is made available in a data repository available at: <https://github.com/CZoepfel/Flexibility-in-a-European-Energy-system>.

options. Accordingly, this is based on the assumption of a continuation of the iRES support including remuneration for iRES operators and feed-in priority for iRES electricity as an incentive system for the investment in iRES capacities. This support also includes the assumption of an energy policy-driven target for iRES expansion to reduce CO₂ emissions in the energy supply. Based on this, the achievement of various expansion goals is defined according to the previously defined scenarios in the model formulation. However, with the support of the iRES, energy policy challenges for regional, national and international energy systems are emerging. With the target of high shares of iRES in the energy supply both techno-economic factors and increasingly socio-ecological restrictions influence the optimal iRES expansion (Schubert 2015). In the following, an overview of the derived requirements included in this work is given (see also Table 3.9).

Table 3.9: Model requirements and assumptions

Scope	Assumptions and requirements	Restrictions in model formulation
European energy policy	<ul style="list-style-type: none"> Limited coordinated European iRES expansion 	<ul style="list-style-type: none"> Minimal and maximal iRES shares per country
National energy policy	<ul style="list-style-type: none"> Limitation of iRES expansion density in single areas of the countries Technology diversity 	<ul style="list-style-type: none"> Restriction of iRES concentration in each country Maximum share of each iRES technology
Socio-ecologic	<ul style="list-style-type: none"> Environmental and land use concerns in the public 	<ul style="list-style-type: none"> Land-use restrictions Exclusion of protected areas
Techno-economic	<ul style="list-style-type: none"> Affordable iRES expansion 	<ul style="list-style-type: none"> Generation potentials Investments and O&M costs

First of all, despite the multinational European area observed in the present work, national individual interests are of great importance, particularly with regard to energy policy (Pruditsch and Zöphel 2017). According to Unteutsch (2014) and Del Río (2005), particularly the conflict with other national socio-economic and ecological goals are the reasons for the divergent national iRES expansion targets in Europe. While an optimal iRES deployment across Europe could optimally exploit the unevenly distributed iRES potentials, a European-wide cooperation can be considered unrealistic due to these national preferences as well as to potentially unequal distributions of iRES integration costs (Del Río 2005). Although it is generally assumed that there is a homogenous interest in expanding the iRES in each of the countries considered, the model formulation specifies minimum and maximum iRES shares for each country while maintaining a share of 80 % iRES-based power generation on total electricity demand for the entire area observed. Furthermore, the expansion of the iRES capacities based on the sites with

the highest potential, can lead to a high concentration of iRES technologies in a comparably small part of the respective country, especially with sufficient total area available. This has both, techno-economic and social conflict potential. As an example of these, the wind onshore expansion in Germany can be listed, where the high concentration of wind turbines in the north of the country causes electricity grid reinforcement and redispatch needs with corresponding economic costs. Due to current regulatory framework conditions, this also leads to an unequal distribution of these costs and thus, on the other hand, to potential acceptance problems (Möst et al., 2015). Therefore, in the model formulation a high a concentration of wind and PV installations is avoided. Another assumption refers to a targeted technology diversity, since an expansion of single iRES technology in the model has to be avoided (for example due to optimal techno-economic characteristics). As further model requirement, the expansion should take the techno-economic restrictions within the countries into account. Accordingly, the previously identified wind and PV potentials as well as the iRES-specific investments serve as input for the determination of optimal locations for each of the technologies. With regard to socio-economic factors, questions of limited areas and acceptance play an increasing role (Wolsink 2018, Höltinger et al., 2016). With the area potential analysis carried out in the previous chapter, ecologically sensitive nature reserves and areas that are not suitable for the iRES installations have been excluded.

In the following, respective constraints are formulated taking these requirements into account. In addition, the effect of these restrictions will be discussed by comparing the results presented in Chapter 4 with and without main constraints.

3.2.2 Model formulation for wind onshore and PV expansion

In general, the model formulation presented below uses the spatially highly resolved wind onshore and PV potentials derived before as well as additional wind offshore data to calculate cost optimal iRES extension pathways taking into account the scenarios as well as the energy policy restriction discussed before. While the wind offshore technology is included in a simplified representation on country level, the data gathering and processing of the wind onshore and PV potentials on raster level leads to different requirements regarding their model implementation. Regarding wind onshore, two different wind turbine types (wind class IEC II and IEC III) are exclusively assigned suitable for each raster based on the respective average wind speed. In contrast, the two PV technologies, rooftop and utility systems, depend on the area available (urban or rural areas) in each raster. Furthermore, potential PV capacities on rural areas are assigned to land available for both wind and PV power plants (see chapter 3.1.5, Table 3.9). The model description first introduces the objective function and further general equations,

followed by restrictions limiting the installable capacity, by equations concerning the realisable iRES generation and concludes by presenting the mathematical representation of the energy policy restriction.

Objective

The objective function (3.1) of the iRES expansion model minimizes total investment costs, composed by the annualized (an_{ton}) costs of investments in the onshore technologies $CAP_{r,ton}$ (see equation (3.2). Thereby, set ton representing the onshore technologies includes two PV technologies, namely roof-top $PVro$ and ground-mounted $PVgr$ as well as wind onshore WON . Due to the alternative representation of wind offshore, this technology is listed differently (CAP_WOFF_c). Additionally, the variable $PEN_{r,ton}$ are introduced penalizing the relaxation of the equation (3.15) which restricts the concentration of iRES capacities in each raster.

$$MIN \left[CORES = \sum_{c \in C} INV_c \right] \quad 3.1$$

$$INV_c = \sum_{tr \in TR} \sum_{r \in mr(c)} (CAP_{r,on} + PEN_{r,on}) \cdot an_{on} + CAP_WOFF_c \cdot an_woff \quad \forall c \in C \quad 3.2$$

Equations (3.3) sums up the wind onshore and PV installations, respectively, to total country-specific capacities. Furthermore, equation (3.4) defines the total generation of one country as the sum of the installed wind onshore as well as PV capacities in each raster multiplied by the raster- and technology-specific full load hours plus the country-specific wind offshore generation. Additionally, equation (3.5) describes the summation of the country-specific electricity demands DEM_c to total demand $TDEM$ in the observed region.

$$TCAP_{c,on} = \sum_{on \in ON} \sum_{r \in mr(c)} CAP_{r,on} \quad \forall c \in C \quad 3.3$$

$$TGEN_c = \sum_{on \in ON} \sum_{r \in mr(c)} CAP_{r,on} \cdot flh_{r,on} + CAP_WOFF_c \cdot flh_woff_c \quad \forall c \in C \quad 3.4$$

$$TDEM = \sum_{c \in C} DEM_c \quad 3.5$$

Restrictions of the iRES generation

The scenarios with different Wind-PV-ratios are mathematically implemented by equations (3.6) and (3.7). While the former one fixes the total iRES electricity generation to the desired share $sres$ of the electricity demand $TDEM$. The latter one introduces the PV share spv and limits the scenario-specific share of PV generation (as product of capacities and raster-specific full load hours vlh_r^{PV}) regarding total iRES generation. Furthermore, in equation (3.8) an upper bound for the total share of wind offshore generation $swoff$ is formulated and set to 0.3, based on Gils et al. (2017).

$$\sum_{c \in C} TGEN_c = sres \cdot TDEM \quad 3.6$$

$$\sum_{r \in R} (CAP_r^{PVgr} + CAP_r^{PVro}) \cdot vlh_r^{PV} = sres \cdot spv \cdot TDEM \quad 3.7$$

$$\sum_c CAP_WOFF_c \cdot flh_woff_c \leq sres \cdot swoff \cdot TDEM \quad 3.8$$

Restrictions of the iRES capacity

Regarding the installable wind onshore, PV and wind offshore power plants, minimum capacities are introduced to cope for historical iRES expansion pathways. For each country and technology, equations (3.9) and (3.10) set these lower bounds for the onshore technologies and wind offshore based on the ENTSO-E Ten Year Net Development Plan (ENTSO-E 2018a, 2018b). Furthermore, the potential wind onshore and PV capacities are characterized by their land-use ($lu_{r,on}$) restricted by the available area per raster (equation (3.11)).

$$TCAP_{c,on} \geq capmin_{c,on} \quad \forall c \in C, \forall on \in ON \quad 3.9$$

$$CAP_WOFF_c \geq capmin_woff_c \quad \forall c \in C \quad 3.10$$

$$\frac{CAP_{r,on}}{lu_{r,on}} \leq area_{r,on} \quad \forall r \in R \quad 3.11$$

Energy policy restrictions

The considerations regarding the energy policy based restrictions are mathematically implemented below. Firstly, equations (3.12) and (3.13) restrict the minimal and maximal iRES share for each country respectively. While $smin_c$ is based on the EU reference scenario 2020 (see

data description in Chapter 3.2.3) the extension of this share ext is defined by 30 %, forcing a iRES expansion in each country based on existing capacities. The maximal iRES share of each country $smax_c$ is set to 110 % of the today's electricity demand per country.

$$TGEN_c \geq (smin_c + ext) \cdot DEM_c \quad \forall c \in C \quad 3.12$$

$$TGEN_c \leq smax_c \cdot DEM_c \quad \forall c \in C \quad 3.13$$

Assuming at least two different iRES technologies in each country, the complete coverage of the iRES share by a single technology is seen unreasonable within a country. Thus, the maximum share ($gmax$) of wind onshore and PV of a country is set to 90% in the equation (3.14). The remaining 10% can be covered accordingly by PV or Wind or, if possible, by wind offshore without violating the specifications of the scenario-specific Wind-PV ratios.

$$\sum_{on \in ON} \sum_{r \in mr(c)} CAP_{r,on} \cdot vlh_{r,on} \leq gmax \cdot GEN_c \quad \forall c \in C, \forall on \in ON \quad 3.14$$

As formulated in the requirements for the model, a strong concentration of onshore iRES capacities within single raster is discussed as critical, due to potential techno-economic as well as socio-ecological issues. Nevertheless, a corresponding restriction should enable higher iRES densities particularly for raster with high iRES potentials. Therefore, in equation (3.15) all raster-specific full load hours of wind onshore and PV of each country are weighted from 0 to 1. These weights ($wvlh_{r,on}$) are used to limit the installable capacity of each raster as share of the country's total capacity. To additionally cope for good raster-specific potentials the relaxation of these constraints is allowed by the variables $PEN_{r,on}$, resulting in costs double as high as the normal raster-specific investment costs (see cost equation (2)).

$$CAP_{r,on} - PEN_{r,on} \leq wvlh_{r,on} \cdot TCAP_c \quad \forall r \in R, \forall c \in C, \forall on \in ON \quad 3.15$$

To improve the comparability of the Wind-PV ratio scenarios and the resulting need for flexibility, it is finally necessary to avoid extreme shifts in the country-specific iRES capacities caused by the scenario definitions. A change in the Wind-PV ratio assigned for the whole region leads to tipping points for iRES capacity expansions in single countries resulting in major shifts in optimal iRES locations. As a result, this strongly impacts the need for flexibility across the study area. Based on evaluations within the present work, this occurs especially in countries with high electricity demand and/or both high wind onshore and PV potentials. These countries with the aforementioned characteristics are mainly France (FR) and Spain (ES). Particularly the high potentials can also be seen in the Figure 3.7 depicting the cost-potential curves. To enable a rather smooth gradation between the scenarios, the scenario-specific PV shares spv serve as

upper bounds for the PV generation in these two countries (combined in subset CL) (see equation (3.16)).

$$\sum_{r \in mr(cl)} (CAP_r^{PVro} + CAP_r^{PVgr}) \cdot vlh_r^{PV} \leq sres \cdot spv \cdot DEM_c \quad \forall cl \in C \quad 3.16$$

Particularly the last equations, implementing energy-policy restrictions based on discussions on reasonable iRES expansion pathways, are limiting the unrestricted optimal installation of wind and PV in the observed region. In general, the outcomes are highly sensitive with regard to the constraints, in particular restricting the iRES expansion in the countries. To emphasise the impact of these constraints, two relaxations of the iRES expansion model are calculated in the Appendix B.4. There, the results of an exclusion of the introduced expansion restrictions are compared with the results discussed in Chapter 4. This analysis underlines, that imposing the energy policy related restriction, as implemented in the developed model, is forcing the iRES expansion to more realistic scenarios regarding the distribution of the capacities. As a result, an under- or overestimation of the flexibility demand is reduced.

3.2.3 Further data input

In Chapter 3.1, hourly resolved time series of PV and wind onshore feed-in based on regional weather data were determined. In addition, an analysis of the available area using GIS data was performed. For the analysis of cost-potential curves, cost data as well as power densities were depicted (see Chapter 3.1.5). In the following, further data input for the previously introduced model are presented. This concerns data on the country-specific electricity demand, on the wind-offshore turbines as well as values for existing iRES capacities.

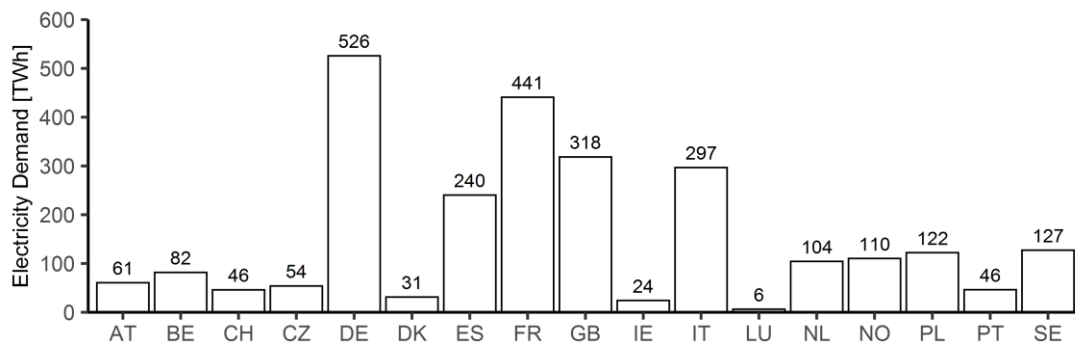


Figure 3.8: Country-specific electricity demand in the year 2012 (Own illustration based on ENTSO-E, 2019; Eurostat, 2019)

Figure 3.8 shows the sum of country-specific electricity demand based on historic hourly demand data from ENTSO-E (2019). In addition, incomplete values were supplemented by

values from Eurostat (2019). The year 2012 was also chosen as the reference year to form a consistency with the selected weather year. In the present paper it is assumed that electricity demand in the electricity sector (in contrast to the further energy end-use sectors considered afterwards) remains the same in terms of level and pattern up to the target year 2050. In total, the electricity demand in the observed region adds up to 2,636 TWh. The hourly resolved country-specific electricity demand time series serve as input for the hourly analysis of the flexibility requirements in Chapter 4 as well as for the model-based analysis of the optimal investment in flexibility options in the remaining chapters.

Table 3.10: Country-specific iRES data

Parameter	Full Load Hours*	Existing Capacities**		
		PV	Wind onshore	Wind offshore
	vlh_{woff_c}	$cap_{min_c}^{PV}$	$cap_{min_c}^{WON}$	$cap_{min_c}^{WOFF}$
Unit	[h]	[MW]	[MW]	[MW]
AT	0	2,000	3,880	0
BE	3,340	4,050	2,709	2,191
CH	0	1,750	120	0
CZ	0	2,560	580	0
DE	3,370	46,860	46,821	9,249
DK	3,660	840	3,905	2,135
ES	3,340	8,090	27,650	0
FR	3,340	8,500	12,267	1,633
GB	2,228	7,460	12,350	13,900
IE	2,228	10	3,600	0
IT	3,370	24,580	12,966	434
LU	0	120	90	0
NL	3340	5,100	2,889	3,011
NO	3,660	0	2,080	0
PL	3,370	500	6,005	445
PT	3,340	720	5,243	57
SE	3,660	0	7,675	165
SUM		113,140	150,831	33,219

*(EMHIRES, 2019; Troen & Lundtang 1989),** ENTSO-E TYNDP (2018)

For the electricity generation of offshore wind farms for 2012, hourly resolved feed-in time series from the EMHIRES (2020) data set are used as a basis. Time series are only available for the countries, with more than two offshore wind farms in 2015. In Table 3.10, these countries and associated full load hours are highlighted. For the remaining countries with wind offshore

potential, the available full load hours are assigned, based on their classification in the European Wind Atlas (Troen & Lundtang 1989). As further shown in Table 3.10, the existing capacity of iRES are used to take current developments in the country-specific expansion of wind and PV systems into account. The values are based on data on the expected progress for the year 2020 of the ENTSO-E Ten Year Net Development Plan (ENTSO-E 2018a, 2018b).

3.2.4 Limitations of the modelling approach

The future expansion pathways are most likely influenced by various further factors with more complex interactions between iRES technology characteristics and location of PV and wind power plants. An analysis of iRES expansion purely based on techno-economic parameters therefore always builds on simplifications. In addition, the results of the presented optimisation approach are highly sensitive with regard to the modelling framework and the underlying assumptions. First, this concerns techno-economical characteristics like future technology developments and costs. These parameters generally influence the role of iRES technologies and might change the optimal shares and spatial distribution of PV and wind power plants. As emphasised before, particularly the potential of wind offshore is highly uncertain and broadly discussed in literature. Second, although discussions beyond purely techno-economic characteristics and resulting expansion decision are introduced, the future iRES development pathway is influenced by multiple uncertainty factors ranging from future approaches for iRES promotion and the underlying level of technology-neutrality to effects of stakeholder preferences in the energy system transformation or the degree of cross-national cooperation. The possibilities to identify optimal parameter adjustments taking each aspect into account is limited and can only be solved by further scenario analysis. Third, the regional and technological coverage within the present model framework for the analysis of iRES expansion can be seen as basis for further improvements. On the one side, with the 17 central-western countries, countries with shares regarding energy consumption and iRES expansion in Europe are selected. However, iRES potentials in the south-east of Europe but also in the North-African region are high and potentially accessible. On the other side, while the focus of the present work is on most established iRES technologies PV and wind, further iRES and controllable RES technologies exist with uncertain share in the future generation mix. Here, impacts on computational effort have to be taken into account if larger system boundaries are desired. In general, the resulting solutions influence the cost-optimal solution and might increase or decrease the total costs as well as the iRES capacity requirements. In the present work, a selection of a reasonable set-up is required to achieve the overall target of a comparison of flexibility demand and flexibility supply. Therefore, the flexibility demand (FD) scenarios, data gathering and the developed iRES expansion model are assessed to cover the characteristics of

the iRES technologies as well as to cope for geographically highly resolved weather data, for limitations of iRES potentials due to land-use restrictions as well as for selected energy-policy restrictions of wind and PV expansion. With the analysis above, central influencing factor on the flexibility demand are emphasised. While the further examination in the present work build up on the introduced scenarios, the results are based on a iRES expansion model developed within the present work.

4 Influence of different Wind-PV ratios on the flexibility demand

In Chapter 2, initial insights into the change of flexibility demand based on the development of iRES in a single country were gained. In the present chapter, the effect of an expansion of wind- and PV-based electricity generation in 17 European countries is observed. For this purpose, the previously determined potentials of the iRES and the developed model for optimal iRES expansion planning are applied, taking into account varying Wind-PV ratios as well as the introduced energy policy restrictions. With the High PV, the REF and the High Wind scenario, three different Wind-PV ratios of 0.5, 0.7 and 0.9 respectively are assumed. Thereby, the impacts of central differences of the PV and wind electricity generation regarding simultaneity and availability are of particular interest. This poses the question of how much and where capacities are optimal to cover the defined iRES share of 80 % of the region today's electricity demand. In addition, impacts on spatial and temporal effects of iRES surplus and deficit phases are discussed. The scenarios are compared with regard to their flexibility requirements on the basis of the residual load parameter introduced before. This chapter finally summarizes the flexibility needs and derives generalised relationships between the observed flexibility demand and the potential of various flexibility options presented in Chapter 2.

4.1 Results on overall installed iRES capacities and annual generation

The iRES-based electricity generation covers 80% (2,162 TWh) of the electricity demand with varying shares of wind onshore and offshore as well as PV in each scenario, as shown in Figure 4.1, on the left. Country- and scenario-specific results on iRES generation and capacity can be found in Appendix B.3, Table B.2 and B.3. While in the High PV scenario almost

1,080 TWh of electricity is generated by PV systems, in the High Wind scenario this is 215 TWh. With a total installed capacity of 1,386 GW in the High PV Scenario, around 257 GW or 477 GW additional iRES capacities are required for the same amount of electricity compared to the REF or High Wind Scenario illustrating the lower availability of PV in the observed region (see Figure 4.1, on the right). As a result, with a decreasing PV share the average iRES full-load hours across the area observed are increasing from 1,567 to 1,915 and 2,380 h, respectively.

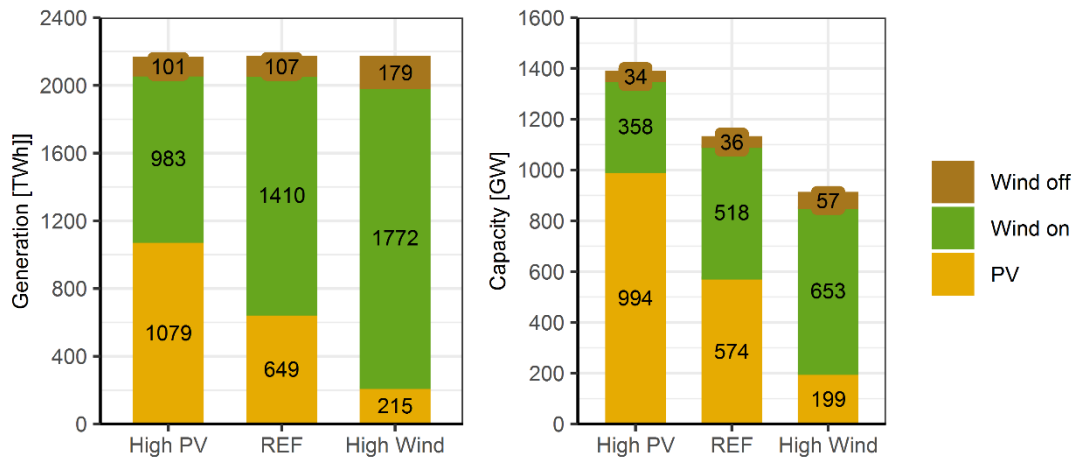


Figure 4.1: Cumulative generation (left) and capacities (right) from iRES in the scenarios for the whole region observed (Own illustration)

When comparing the scenario-specific capacities for the optimal iRES expansion in the present work with similar studies, the present results are comparable, although the bandwidth is large mainly due to differences in the exact region observed, the iRES expansion target as well as assumed development of the electricity demand. Since the EU-Reference scenario (Capros et al. 2016) has a lower iRES share (around 55 %) assumed for Europe, the present values for the countries included here are 1.4 to 2.1 times as high. For the “A Clean Planet for all” strategy, the European Commission assesses possible future strategies for a European long-term greenhouse gas emissions reduction. With wind and solar shares at electricity generation of around 75 % the cumulative wind and PV capacities are in the range of 1,200 (EE scenario) to 2,170 GW, whereas in the latter scenario (P2X) a strong increase in electricity demand due to expansion of sector coupling is assumed (EC 2018). In the REFLEX project two ambitious decarbonisation scenarios were developed with iRES capacities of 1,143 to 1,325 GW for a total iRES share of 80 % in the EU-28 countries (Zöphel et al. 2019).

The results on iRES generation and capacity on country level illustrate the interplay of spatially distributed iRES potentials and restricted installable iRES capacities based on the country-

specific electricity demand¹¹. The country level perspective is of high importance, since the amount and location of the iRES strongly influences the respective residual loads and thus, the flexibility demand. In the following, at first further results regarding the iRES generation are evaluated on country level followed by additional details on the required capacities.

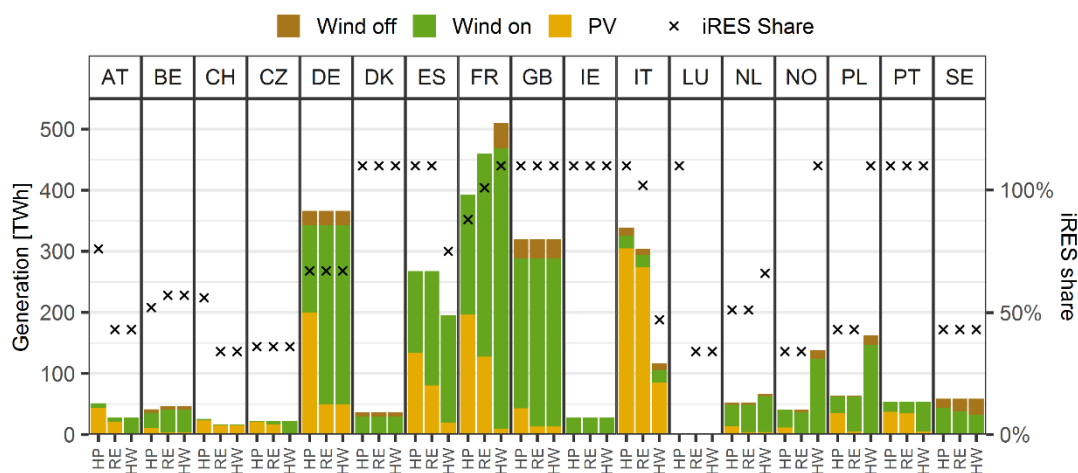


Figure 4.2: Scenario-specific generation and iRES share on country level (Own illustration)

Generally, the countries with high electricity demand contribute most to the overall iRES generation. Due to the defined minimum PV share in each scenario, Spain and France influence most significantly the differences in the overall iRES technology mix (see Figure 4.2). Italy, as a country with high PV potentials but comparably small wind potentials is contributing most with PV-based electricity generation in each scenario. In contrast, in some countries (e.g. Denmark, Great Britain or Ireland) the mix of iRES generation shows rather small differences. Particularly in these countries the wind generation is often significantly higher compared to PV, since the wind potential is more cost-beneficial. These countries also exploit the maximal RES share of 110 % of the country-specific electricity demand (see crosses depicting the iRES share in Figure 4.2). In comparison, Portugal has a constant iRES share of 110 % although their Wind-PV mix is varying, due to comparable costs of both, PV and wind onshore. In contrast, in this potential-based optimal iRES expansion, single countries, like Czech Republic and Sweden, show no significant increase in generation compared to today's iRES shares.

¹¹ In Chapter 4.5, the influence of a relaxation of both, the constraints for limiting the concentration of capacities within the raster as well as the maximum and minimum iRES share per country will be discussed in detail.

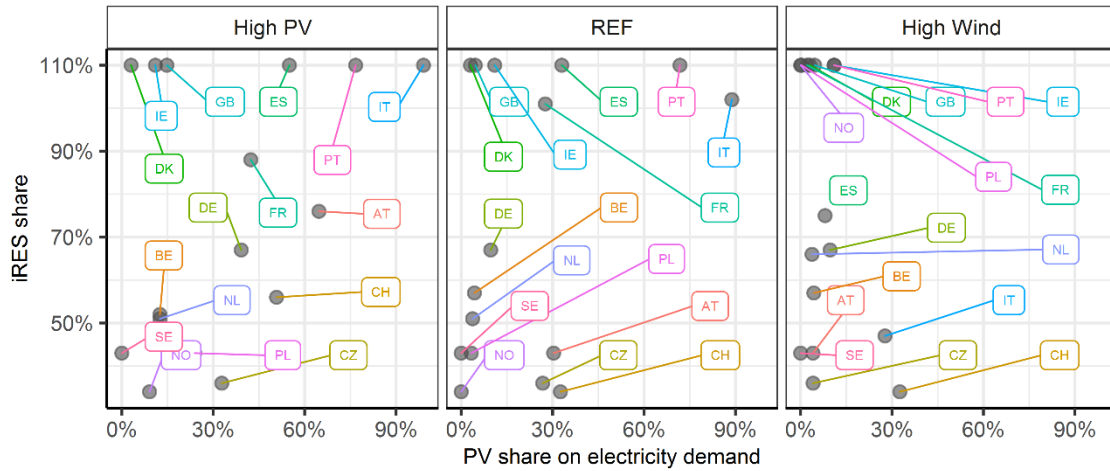


Figure 4.3: Scenario-specific comparison of PV share and total iRES share (Own illustration)

To give an additional perspective on the results regarding the iRES shares in the countries, Figure 4.3 compares the PV share on total electricity demand with the total iRES share. This is of interest, since very high iRES shares potentially lead to more extreme residual load parameters and an increasing flexibility need. The regional distribution of iRES generation is expected to have a high impact on the demand for spatial balancing flexibility. In each of the flexibility demand (FD) scenarios, in total 7 countries have a iRES share higher than 100 %. In High PV, countries with high iRES share in combination with both high PV share and high wind share can be observed. In addition, in this scenario the resulting iRES generation is also spatially distributed most evenly. While high amounts of PV generation can be found in the south (Portugal, Spain and Italy) as well as in the Alpine countries (Austria and Switzerland), the wind-based electricity generation is located in the north with high country-specific shares in Ireland, Great Britain, France and Denmark. In the High Wind scenario, no country with a PV share on total electricity demand above 30 % can be found. Especially the northern countries Denmark, Great Britain and Ireland but now also France, Poland and Norway are characterised by high iRES shares with contributions from almost exclusively wind power plants. With REF, a gap between these countries with low and high PV share (namely Italy and Portugal) as well as with low and high iRES share occurs, increasing the differences between the (north-) western countries with wind generation centres and the southern countries dominated by PV installations. Figure B.2 in Appendix B.3 additionally shows the spatial distribution of the iRES generation.

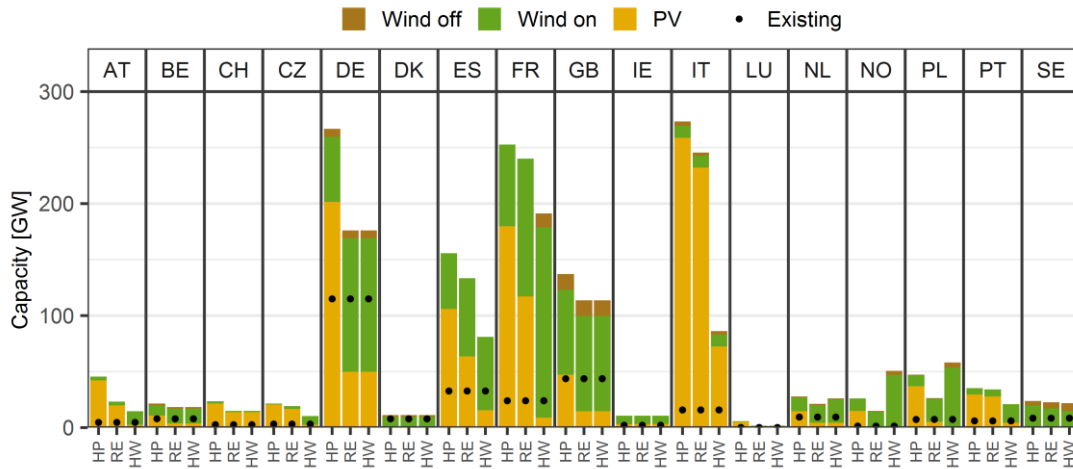


Figure 4.4: Scenario-specific iRES capacity on country level (Own illustration)

The corresponding capacities, depicted in, also clearly show main contributions of single countries. Most of the countries show decreasing capacities with higher Wind-PV ratios, following the trend of the overall capacities. Only Norway and Poland have the highest installed capacities in the High Wind scenario, since the PV and wind offshore potentials or costs are comparably high. Generally, these overall capacity requirements reflect an enormous expansion requirement for the 17 countries observed. Compared to the existing capacities based on ENTSO-E data of the year 2019 (see Table 3.10 in Chapter 3), the required overall increase in PV capacities is highest in the High PV scenario with 776 %, while for the REF scenario this increase is 406 % and 74 % for the High Wind scenario. For wind onshore the expansion of overall capacities compared to the TYNDP data of the year 2019 is 133 %, 239 % and 325 % respectively. The total values for wind offshore are 18 %, 24 % and 97 % respectively.

The results presented above indicate, that the country-specific yearly electricity demand (limiting the potential iRES generation) as well as the country size are of high importance for the spatial distribution of the cumulated iRES capacity. Figure 4.5 shows the installed capacity per raster in the region observed. In the High PV scenario, countries with high electricity demand and high PV potentials but a relatively small country area (e.g. Italy) show comparably high iRES installations per raster. In contrast, although for example Spain has very high wind onshore and PV potentials, the electricity demand is lower, while at the same time the country size is larger. For the High PV scenario Italy has very high iRES capacities with around 270 GW (thereof 259 GW PV), followed by France (262 GW) and Germany (255 GW). In the REF scenario, the high (PV-) capacities in Italy become obvious compared to the decreasing density in most of the remaining countries. Due to the higher availability of wind power plants, the

installed capacities and their respective distribution is generally decreasing with higher wind shares.

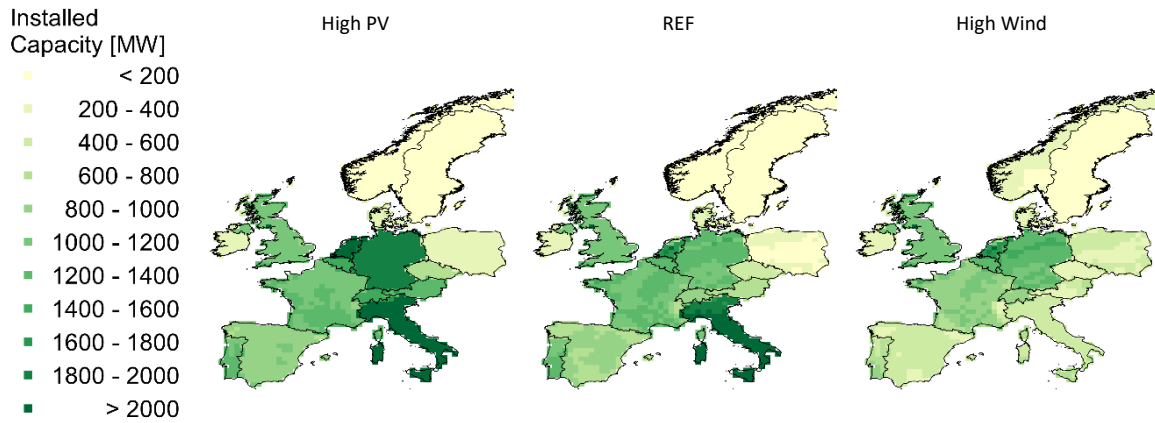


Figure 4.5: Distribution of total wind onshore and PV capacities per raster in the scenarios (Own illustration)

An exception can be observed in the north-eastern countries (e.g. Norway and Poland), where a slight increase in some of the country-specific raster occurs in the High Wind scenario. In this scenario, with 191 GW France has the highest iRES capacities installed (thereof 170 GW Wind onshore). Additionally, Germany and Great Britain have significant capacities in the High Wind scenario (164 GW and 108 GW, respectively). As it was mentioned before, the structure of iRES expansion in Germany, France, Italy and Spain is changing most significantly with the scenarios, since they play an important role in the observed region (high electricity demand and/or high iRES potentials).

The comparison between the optimal capacity expansions and the existing wind and PV installations indicate both that the contribution of single countries has to increase significantly, to achieve ambitious expansion targets as well as that the expansion is only partly driven by cross-national iRES potentials assessments. Independently from the results on optimal wind and PV expansion in the present work, the required increase in effort is also noted on European level (EC 2019b). However, the national energy-policy support for selected technologies is not stable and can change foci in short-term (Renn & Marshall 2016). Thus, a linear continuation (or even increasing ambition) of today's energy policy is also uncertain. The optimal iRES expansion clearly differs from iRES expansion ambitions of national energy policies. This becomes most obvious when comparing the existing with the optimal capacities in the scenarios for Germany and Italy. In Germany a significant iRES expansion was realised in the last years although iRES potentials are comparably low. This can be seen with regard to the optimal iRES share in the FD scenarios not exceeding 60 % since Wind-PV installations in other countries are

optimal (see Figure 4.4). As a result, in High PV Germany would increase its capacities by 132 % compared to today's capacities. In contrast, very high solar radiation in Italy results in high PV installations particularly in High PV. Compared with existing capacities, very high expansions of up to 1633 % would be required to exploit these potentials. Although this might reflect the limitedness of a model-based optimal iRES expansion based on potentials, the scenarios are seen as valuable for the present work, since with the aim to analyse the interactions between flexibility demand and flexibility supply extreme scenarios are useful to isolate certain effects, while future developments most likely are in between this scenario frame.

As mentioned before, the total installed iRES capacity and the respective generation is influencing the flexibility requirements due to the input assumptions regarding the scenario-specific Wind-PV shares. Thereby, the optimal expansion is based on the specific investments of the iRES technologies as well as the derived iRES potentials and the available area. However, the wind and PV generation characteristics as well as the underlying spatial and temporal differences across the 17 countries observed are additionally influencing the need for flexibility. These characteristics are expected to strongly affect the residual load, thus the resulting flexibility requirements regarding the integration of the iRES electricity. In the following chapters, the parameter for the sorted (Chapter 4.2) and for the time dependent (Chapter 4.3) residual load are discussed by taking the differences between the wind and PV technology into account. Thereby the aim is to identify main influencing factors on the residual load pattern.

4.2 Evaluation of sorted residual load parameters

For the analysis of differences of the scenario-specific need for flexibility, the country specific iRES generation and residual loads are firstly further aggregated to the entire region observed. Figure 4.6 shows the aggregated sorted generation from wind onshore and offshore as well as PV systems for the whole observed region. The power supply is normalised to the overall scenario-specific iRES capacity, to illustrate the availability and simultaneity of iRES in the scenarios. The scenario with the highest PV generation shows the largest decline of the curve. In almost 1,200 hours of the year with more than 40 % of the installed capacity, the overall electricity output is highest in the High PV scenario. In the remaining hours, the High Wind scenario shows the highest values. In almost 80 % (6,924 h) of the year, the availability of iRES capacities in this scenario is over 20 %, while in the REF or High PV scenario this is true for around 38 % and 26 % of the hours, respectively (see marking lines in Figure 4.6). For the entire year, the average availability increases from 18 % in High PV over 20 % in REF to 27 % in High Wind.

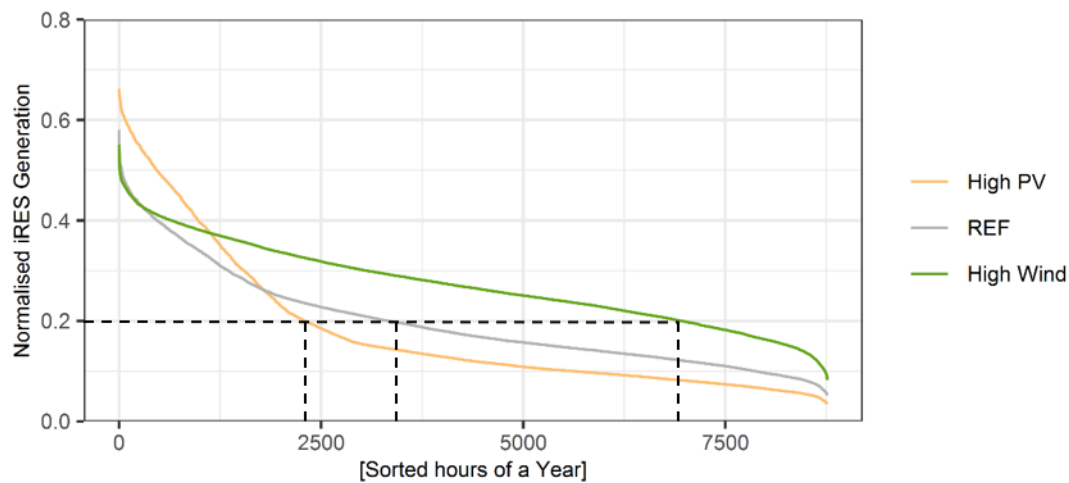


Figure 4.6: Duration curve of iRES electricity generation in the scenarios (Own illustration)

For the analysis of the sorted residual load, as difference between the iRES generation and the electricity demand, the most important parameters are the maximum and minimum residual load as well as the cumulated surplus energy and surplus hours. To identify main correlations, the influence of the country-specific iRES share as well as the Wind-PV share on these parameters is assessed. In Figure 4.7, these interrelations for 17 countries and three scenario-specific results (in total $n = 51$ observations per graph) are displayed including a fitted linear regression line. For better comparability, the results are normalised to enable a comparison between the country- and scenario-specific residual loads¹². A high wind share on total iRES generation reduces the maximum residual load in a range between 10 and 40 % compared to the country-specific peak electricity demand. This load reduction potential is clearly reduced with higher PV capacities. While a higher PV share leads to a high seasonality of electricity generation with peaks in the summer month (in Europe), wind is correlating with the seasonal electricity demand. Thus, it is more likely to have iRES feed-in during the highest demand (in winter), resulting on average in a more significant maximum peak residual load reduction with higher wind shares. Although a correlation can be seen regarding the minimum residual load in Figure 4.7, the R value is lower. Since an increase in iRES share reduces the residual load, very high shares result in more iRES surplus hours (up to 60 % of the hours of the years) and energy (almost 60 % of iRES generation) in single countries.

¹² The normalisation is done as described in Table B.4 in Appendix B.

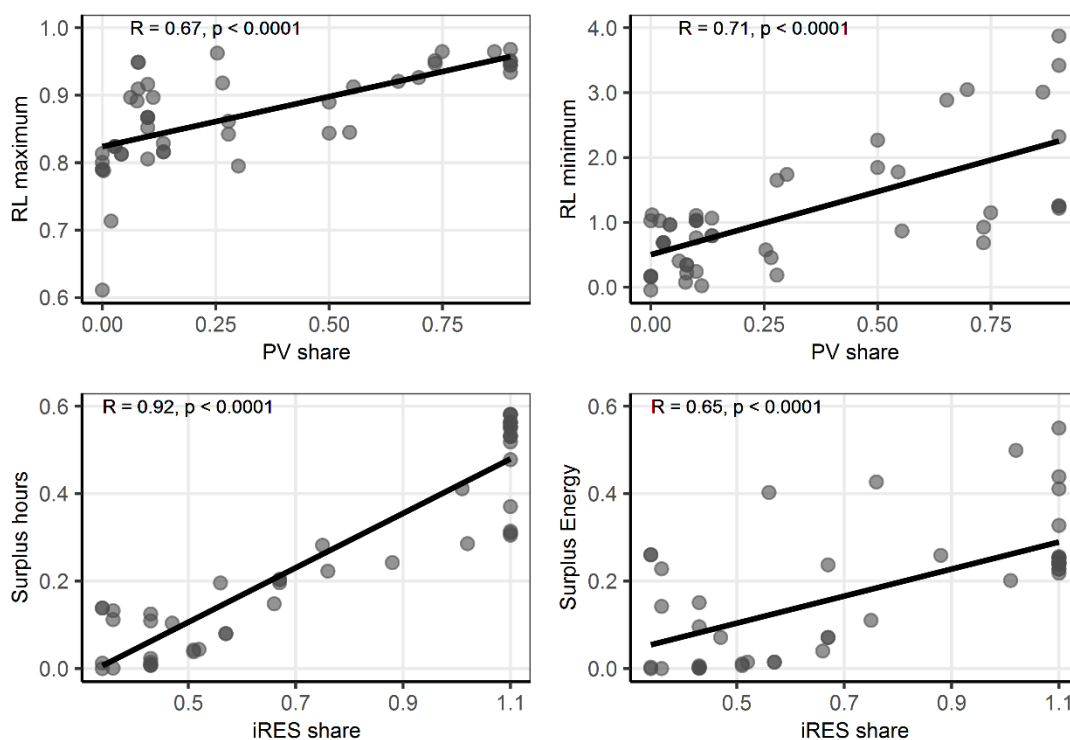


Figure 4.7: Normalised combination of selected parameter of iRES expansion and sorted residual load parameter per country and scenario (RL maximum and minimum normalised to country's maximum electricity demand; surplus hours normalised to 8760 hours of a year; surplus energy normalised to total iRES generation) (Own illustration)

The differently distributed availability and simultaneity as well as the resulting impacts on the residual load parameter are reflected in the pattern of the residual load aggregated for the entire region as shown in Figure 4.8 on the left. All scenarios show a seasonality with a higher residual load (mainly due to a higher electricity demand) in the winter months. The more concentrated PV feed-in, especially in the High PV scenario, leads to large excesses of iRES of more than 400 GW in the summer months, supporting the correlation analysis before. At the same time, the periods with high residual load are also highest in the High PV scenario. With increasing wind share in iRES generation, the range between maximum and minimum residual load decreases, while additional surplus phases can be observed also in the winter month due to higher wind feed-in. Compared to the High PV scenario with a standard deviation of the aggregated residual load of 186 GW, the values are reduced to 115 and 75 GW in the REF or High Wind Scenario.

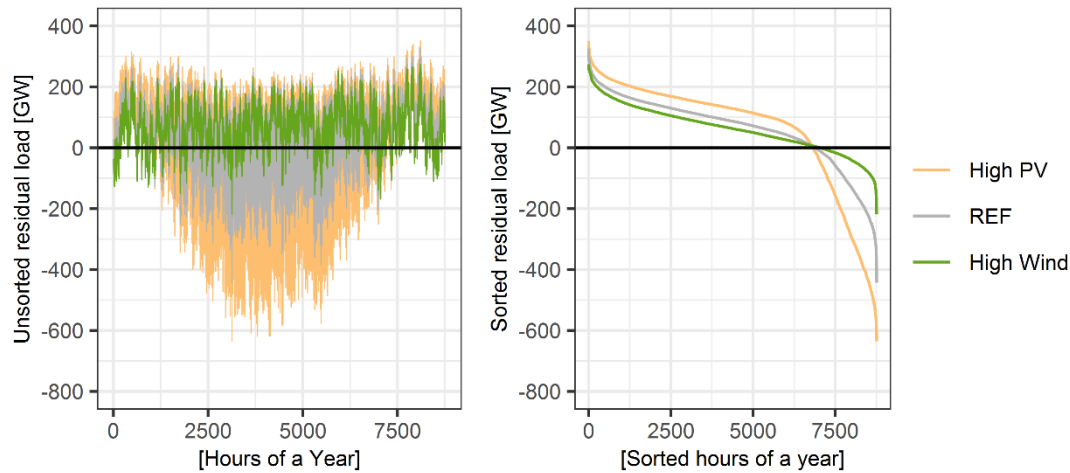


Figure 4.8: Unsorted residual load (left) and sorted residual load (right) for each scenario (Own illustration)

If the aggregated residual load for each scenario is sorted from the highest to the lowest value (see Figure 4.8, right), the differences in the maximum and minimum residual load peaks become obvious. As discussed before, this perspective allows for estimations regarding the potential of technologies providing downward, upward and shifting flexibility. The positive maximum residual load is lowest in the High Wind scenario but in a similar range across all scenarios. Compared with the peak electricity load of 441 GW in the observed region, the maximum residual load decreases by 21 %, 27 % and 39 % with increasing wind share. Thus, although with more wind in the total iRES generation the peak load can be reduced most, the contribution of iRES to reduce the required secured generation capacity is rather limited in each scenario. In contrast, the analysis of the remaining hours shows that the simultaneity of iRES power generation and electricity demand varies stronger in the scenarios. The negative peak increases from 218 GW in the High Wind scenario over 442 GW (REF) to 635 GW in the High PV scenario. Thus, the characteristics of PV-based electricity generation result in high hourly feed-in peaks, while iRES generation during the night is limited to wind energy. As a result, the sorted residual load for High PV has the sharpest decrease. In contrast, more wind capacities lead to a flatter pattern of the residual load and fewer hours with high (positive and negative) residual loads. The average positive (negative) residual load decreases from 149 GW (244 GW) in High PV to 110 GW (117 GW) in the REF and 88 GW (43 GW) in the High Wind Scenario. As further depicted in Table 4.1, the largest surpluses occur in the High PV scenario with 473 TWh, while this surplus decreases with increasing wind share to 219 TWh (REF) and 74 TWh (High Wind) respectively. Although the total iRES share has the highest correlation with the iRES surpluses, a higher PV share in the Wind-PV ratio clearly increases the iRES deficit and surplus amounts. While the cumulated deficits in High PV are exceeding those of the High Wind

scenario by 65 %, this value increases to 539 % when applied for the surpluses, indicating a higher iRES integration challenge particularly regarding the surplus balancing.

Table 4.1: Scenario-specific residual load parameter cumulated for the whole region observed

		High PV	REF	High Wind
Total iRES generation	[TWh]	2,162	2,162	2,162
iRES deficits of cumulated residual load	[TWh]	1,020	763	617
iRES surplus of cumulated residual load	[TWh]	473	219	74
Share of deficits on total iRES generation	[%]	47	35	29
Share of surplus on total iRES generation	[%]	23	10	3

In Figure 4.9, the influence of the Wind-PV ratio (depicted as PV share on the electricity demand) as well as implicitly the iRES share on the country-specific residual load can additionally be examined. To compare the residual loads, each curve is normalised to its maximum. This illustration further emphasises, that the residual loads with the highest surplus energy can be found in countries with high PV shares particularly in the High PV scenarios (Spain, Italy, Portugal but also Austria and Switzerland). In countries with very high wind shares, like Denmark, Great Britain and Ireland, a large number of surplus hours can be seen in each FD scenario (around 5,000 h), while the aforementioned analysed lower range of the residual load can be confirmed as well.

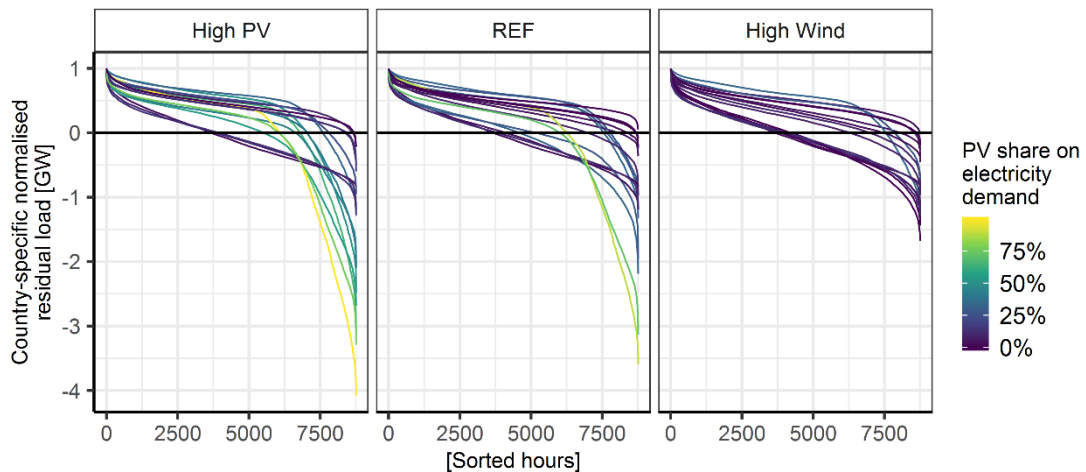


Figure 4.9: Country-specific normalised sorted residual loads (Own illustration)

Figure 4.10 summarises main observations, depicting boxplots of country-specific parameter of the sorted residual load for each FD scenario. This illustration again applies normalised parameter (see y-axis) to improve the comparability of the results. On the left in Figure 4.10, the

range of the country-specific residual load (from maximum to minimum) normalised with the country-specific peak load is illustrated. While in each scenario only a small number of countries has a ratio of less than one (e.g. Luxembourg and Sweden), the range of the residual load ranges decreases with increasing wind share. In the middle of Figure 4.10, the country-specific sum of surplus electricity is normalized with the annual iRES-based generation of each country. The decrease in the median from High PV to REF and High Wind is mainly caused by Italy, Spain and Portugal, reflecting the influence of the decreasing PV share in each country's iRES technology mix. Finally, the share of hours with surplus energy (see Figure 4.10 on the right) is varying differently compared to the parameters discussed before. From High PV to High Wind, the spread of the country-specific values is increasing. While in these two scenarios the median is at around 20 % of the hours of a year, it is lower in REF since the countries with large PV installations are reduced. However, high wind shares result in a high number of surplus hours as it has been observed before.

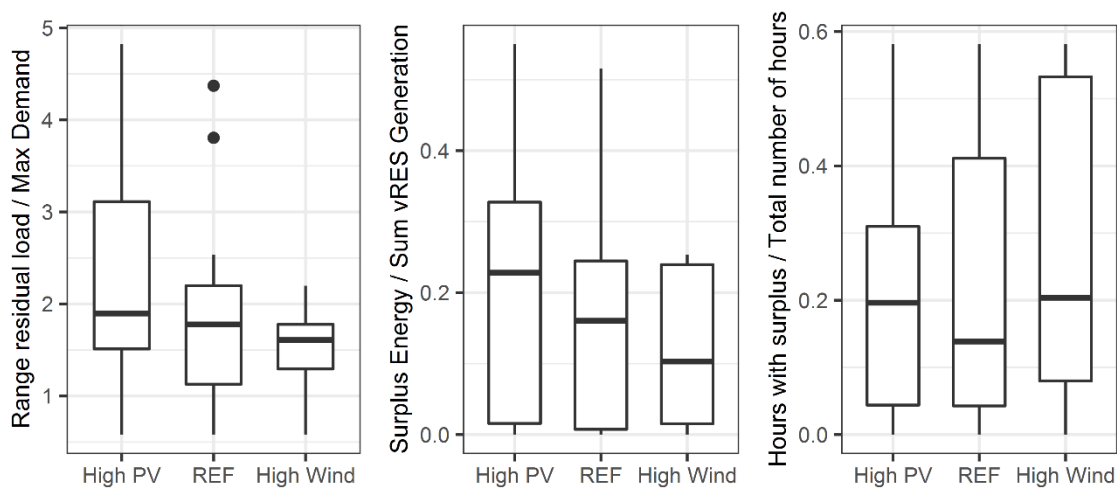


Figure 4.10: Boxplots of country-specific residual load parameters with normalised range of residual load (left), surplus energy (middle) and hours with surplus (right) (Own illustration)

4.3 Evaluation of time-dependent residual load parameters

In addition to the sorted duration curve, the time-dependent analysis of residual load gradients as well as iRES surpluses and deficits periods offers further insights to the assessment of the flexibility demand in the scenarios. Similar to the correlation analysis for the sorted residual load parameter, the overall iRES share as well as the PV share on the electricity demand show a high interrelation with the time-dependent parameter. In Figure 4.11, a normalised combination of the country-specific PV share and the iRES share is compared with the average

one- and four-hourly gradient as well as mean connected surplus energy and hours. Again, a normalisation is applied to improve the comparability of the resulting country- and scenario-specific residual loads (see Appendix B.3 Table B.4 for the normalisation approach). Particularly, the PV share on total electricity demand has a high correlation regarding the mean gradients. While with very low PV shares the mean 1 hourly gradients are around 3 % of the installed capacity, very high PV shares result in average gradients of around 5 %. This correlation further increases with 4 hourly gradients, where with PV shares of around 90 % average four hour gradients of up to 20 % of the country's installed iRES capacity can be observed. In contrast, the interrelation between the iRES share with the duration and amount of iRES surplus phases is comparably low (see lower R-values in Figure 4.11), since the time-dependent residual load is additionally influenced by the countries load curve. With increasing iRES share on the country's electricity demand, the mean connected surplus phases can last up around one day (24 h).

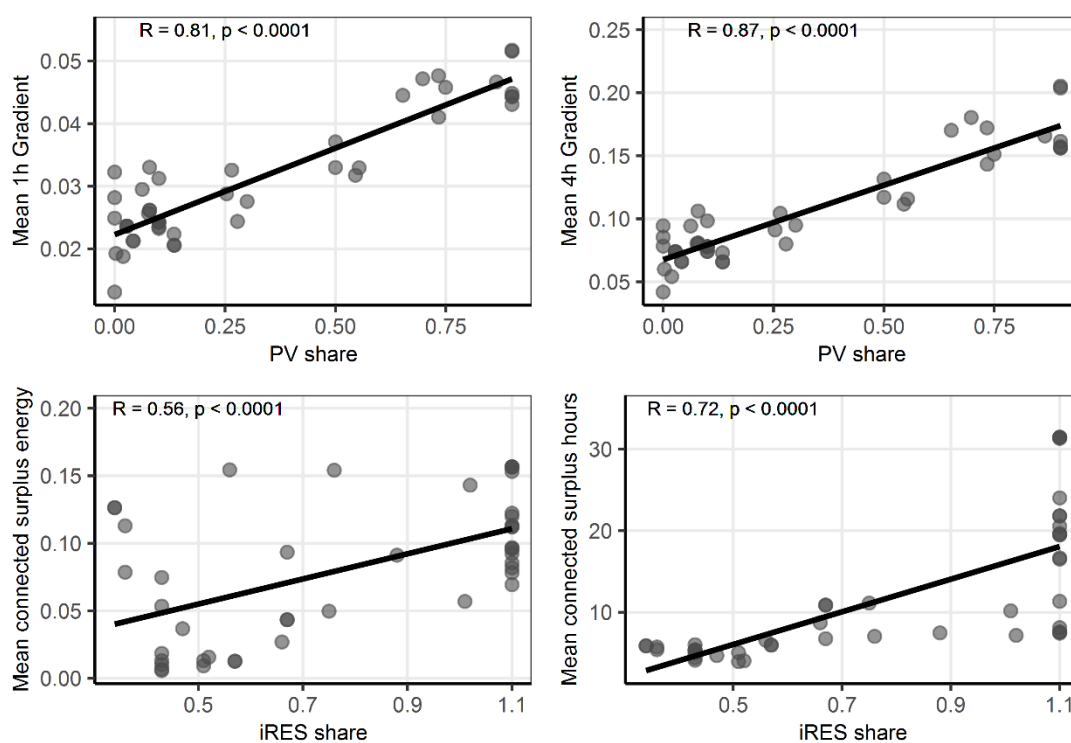


Figure 4.11: Normalised combination of selected parameter of iRES expansion and time-dependent residual load parameter for each country and scenario (Gradients normalised to installed iRES capacity per country; mean connected surplus energy normalised to total iRES surplus energy ($\times 100$); mean connected surplus hours not normalised) (Own illustration)

Figure 4.12 illustrates the residual load aggregated for the 17 countries and cumulated per month as well as hour of the entire year. Here, the increasing range between the positive and negative residual load peaks in both, the seasonal as well as the daily perspective is once again emphasised. The seasonal availability of PV leads to cumulated iRES surplus energy of up to 30 TWh in the summer month in the High PV scenario. With increasing Wind-PV ratio the overall residual load is increasing as well. Thus, in the High Wind scenario, the monthly residual load deficits range between 20 TWh in February and nearly 75 TWh in September. Similar observations can be made when looking at the hourly sums. The lowest daily residual load variability can be seen for the High Wind scenario, reflecting the high wind shares and the underlying wind feed-in characteristics. The aforementioned diurnal increasing or decreasing generation by PV systems are resulting in increasing gradients with a lower Wind-PV ratio in the observed region. For the aggregated residual load across all 17 countries, maximum values of 62 GW for one-hourly gradients and 188 GW for four-hourly gradients can be found in the High PV scenario, illustrating a high demand for power output adjustments within hours in this scenario. Besides the daily and seasonal feed-in characteristics of wind and PV, the temporal simultaneity is also affecting the total residual load of the whole region observed (see explanation below).

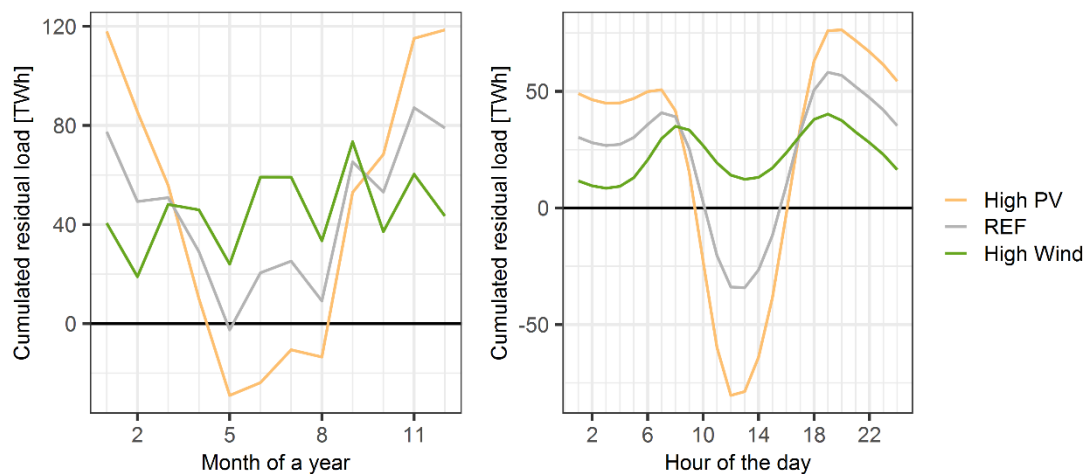


Figure 4.12: Residual load of the whole observed region cumulated per month (left) and per hour (right) (Own illustration)

Furthermore, the iRES surpluses investigated in the previous section are examined in more detail with respect to duration and energy content of the related phases for each country. A connected surplus period is defined as successive hours with negative residual load. For the three scenarios in Figure 4.13, each point shows the duration and the corresponding amount of

energy of a country-specific surplus phases¹³. In each scenario, the tendency of increasing amount of energy with increasing duration of surplus phases becomes obvious, resulting in surpluses of over 200 hours and more than 4 TWh (4×10^6 MWh) occur in single countries, with the highest values in the High Wind scenario. In the High PV scenario, however, due to the day-night rhythm, shorter excess periods in the range of 5 to 9 hours occur more frequently in the residual load of the 17 countries, but with comparatively high amounts of energy (see red dashed lines). With increasing share of wind-based generation, the number of shorter and (more significantly) longer surplus periods increases.

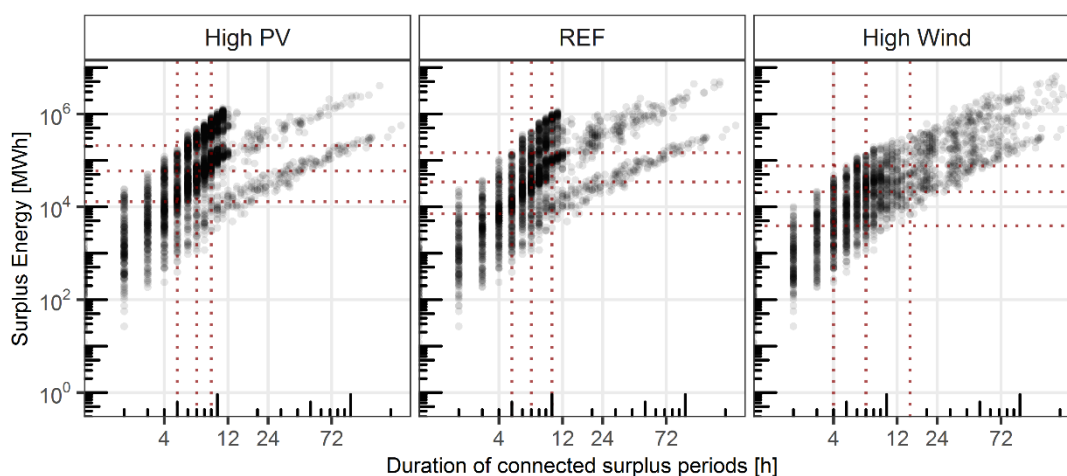


Figure 4.13: Duration and energy content of single country-specific surplus phases (black dots) and respective medians and quartiles (red dashed lines) (Own illustration)

Apart from the extreme phases mentioned above, the amount of energy in these country-specific connected surpluses decreases in average (see horizontal red dashed lines). While the median surplus phase duration is similar in each scenario (around 7 h), the corresponding median country-specific hourly surplus energy decreases strongly with increasing wind share from the High PV scenario (59 GWh) to REF (32 GWh) to the High Wind scenario (18 GWh), confirming the findings regarding the seasonal and daily pattern of the aggregated residual load also on country level. Regarding the surplus duration, particularly the upper quartile is affected most by the wind share with increasing values from High PV (9 h) and REF (10 h) to High Wind (16 h). Figure B.3 in Appendix B.3 shows the same figure for the deficit phases of the study area. In

¹³ Due to the large bandwidth of the data, the axes are scaled logarithmically for better readability. In addition, the red dotted lines show the distribution of the scenario-specific point pairs (25th percentile, median and 75th percentile) of the duration of the phases and their amount of energy.

comparison to the surpluses there are similar relationships. The phases with positive residual load tend to be longer and with higher energy deficits.

Figure 4.14 depicts the resulting average country-specific surplus energy [GWh] as well as the average surplus duration. Surplus periods are of particular interest, since they are valuable for both flexibility options for upward as well as for shifting flexibility. Due to the low costs of electricity in these times, the cost efficiency for arbitrage as well as sector coupling is increasing. Italy, France and Germany, the countries with the highest installed PV capacities in the High PV scenario have the highest average surplus energy of more than 300 GWh in a single surplus period, while the mean duration is lower than 8 hours in these countries. In the REF scenario, the high PV capacities in Italy are also leading to comparably short surplus periods. With higher share of wind power in the country's iRES generation (see High Wind), especially Great Britain, France and Norway show large and long average surplus periods of more than 20 h and 200 GWh. Denmark, as wind-dominated country shows the longest periods on average in each FD scenario. Besides, with higher PV shares in the scenarios, the amount of countries with mean surplus periods of less than 100 GWh and shorter than 10 hours is increasing.

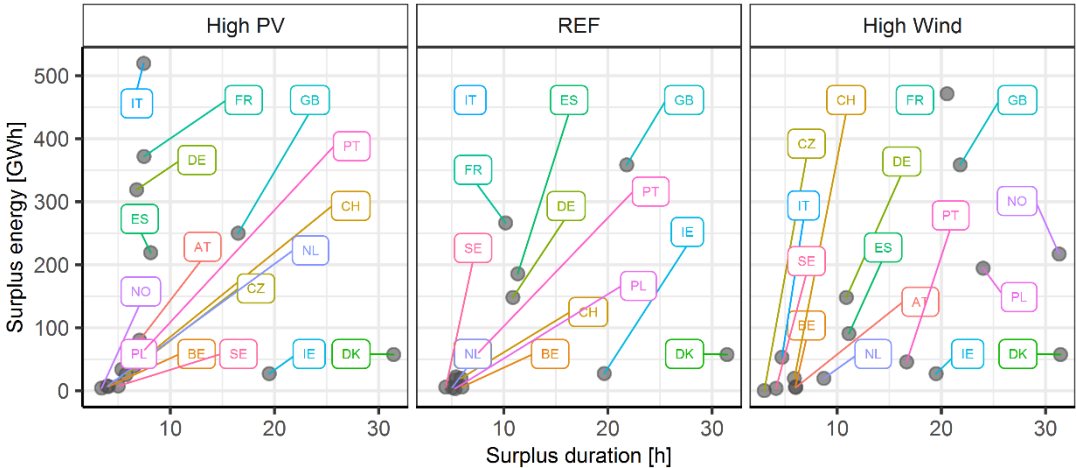


Figure 4.14: Average energy and duration of surplus periods (Own illustration)

Besides the average surplus periods the country- and scenario-specific residual loads are further characterised by periodical patterns. Structures can be found in the representation of the so-called spectral density estimation in a periodogram. In the present study, the approach is applied to the country-specific residual loads¹⁴. This allows for the identification of frequencies

¹⁴ In the literature, the estimation of the spectral density is often used for electronic signal processing. However, it is also used for the time series analysis and time series generation of iRES (Belderbos et al., 2017, Zhao et al., 2015). For the purpose in the present work, the residual load time series are decomposed into underlying sine

with high intensity to determine important periodicities of the scenario-specific and country-specific residual loads, as illustrated in Figure 4.15. In High PV the periods with the highest amplitude can be found for 24 hours followed by 12 hours and a strong seasonal period of a year (8760 hours), clearly reflecting the daily and seasonal generation characteristics of PV further enhanced by the electricity load patterns.

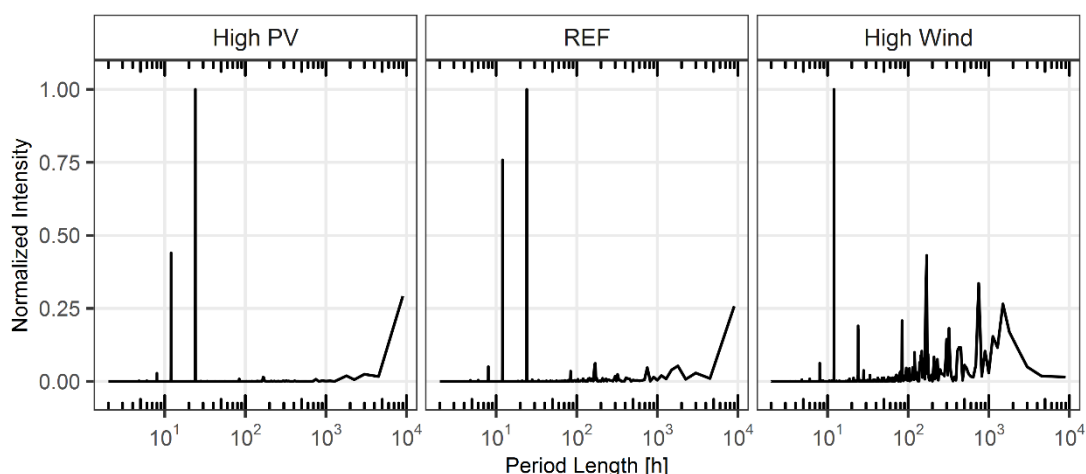


Figure 4.15: Periodogram spectral power density of the aggregated country specific residual loads (Own illustration)

These periodicities are changing with higher overall Wind-PV ratio. For the High Wind scenario, the strongest frequency occurs at 12 hours followed by peaks at around one week (168 hours) and one month (1,000 hours). Compared with High PV and REF, further peaks can be identified mainly in the range between a week and a month, while the 24 hour as well as the overall annual period is significantly lower in High Wind. The total residual load aggregated over 17 countries is smoothing the period intensity with regard to countries with very high Wind or PV installations due to high potentials. In Figure B.4 in Appendix B.3, two periodograms for Denmark with high wind installations and Italy with high PV installations is presented. Additionally, the intensity is not normalised. The comparison shows again the high intensity of the 24-hour period in Italy as well as in Denmark, whereas in Italy the intensity is significantly higher. Additionally, while in Italy further peaks only occur in the 12 hour and in the yearly period, the Danish periodogram clearly shows multiple additional period length.

and cosine functions of different frequencies with the aid of the Fourier transformation. Thereby, the normalised intensity (with regard to the maximum) is displayed as a function of period duration (as reciprocal of the frequency).

In addition to the time-dependent analysis, the spatial distribution of the iRES surpluses and deficits regarding the simultaneity of the residual load is finally investigated. This helps to assess the application potential of spatial shifting flexibility via transmission grids. By analysing the correlation, the differences in the simultaneity of the residual loads can be summarised. Figure 4.16 shows a box plot of the pairwise country-specific correlation coefficients for each scenario. The High PV scenario has the widest spread of coefficients and the highest median. The characteristics of the solar radiation discussed in Chapter 2 and its daily and seasonal behaviour also influence the corresponding residual loads across countries and are particularly dominant in this scenario. As a result, a relatively strong correlation with a coefficient of more than 0.5 can be observed for around 50 % of all 17 countries. Both the median and the bandwidth of the observed correlation coefficients decrease with higher wind shares in the iRES electricity generation. Here, the increasing influence of spatial balancing effects of the wind-based electricity generation leads to a decrease of the correlation of the residual load between the countries. While in the High Wind scenario the bandwidth between the 25 and 75 percentile is lowest, the lowest median of country-specific residual load correlation can be found in the REF scenario.

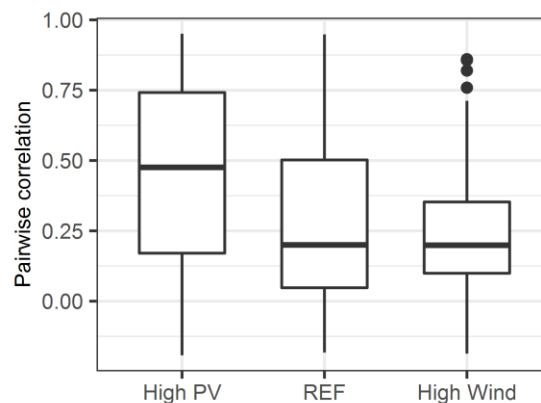


Figure 4.16: Correlation coefficients of the pairwise country-specific residual loads (Own illustration)

As displayed in Figure 4.17, surpluses occur most frequently in the summer months in the High PV scenario. With increasing wind share, the number of hours with simultaneous surpluses decreases for the majority of countries. In total, the number of hours with surpluses in more than 50 % of the countries is highest in High PV (1471 h), while in REF and High Wind these values halve (738 and 746 h). Only in High PV, simultaneous surplus hours in maximal 15 countries can be observed. Additionally, the hours with no surpluses across the whole region observed (thus, deficits in all 17 countries) is highest in High PV (903 h), followed by REF (647 h) and High Wind (194 h). While for High PV, these times occur most frequently in the winter month, this is true for High Wind during the summer month, reflecting the general electricity

generation characteristics of wind and PV. Furthermore, in each scenario simultaneous surpluses in three or four countries are most frequent (around 30 % of the hours of a year). Thus, the simultaneity of the surpluses discussed here additionally influences the pattern of the cumulated residual load for the entire region and leads to higher iRES surpluses with increasing PV share in electricity generation in the observed region.

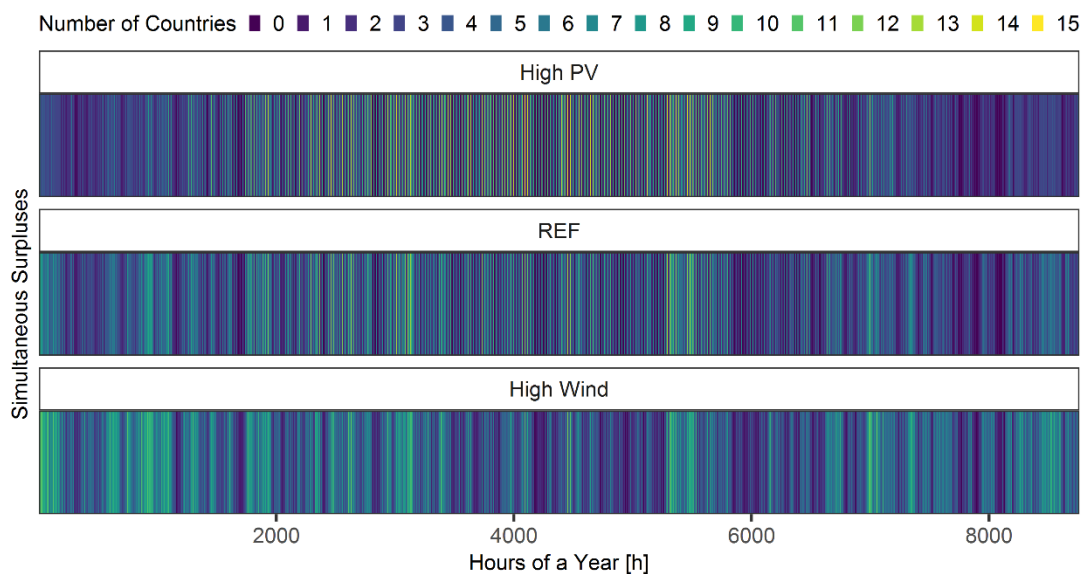


Figure 4.17: Simultaneous surplus phases in the countries during the year (Own illustration)

4.4 Total costs of iRES investments and iRES cost potentials

When linking the optimal iRES installation of the different Wind-PV ratio scenarios with the investment data for residential and utility scale PV systems as well as the two wind turbine classes of Chapter 3.1.5, the total iRES costs sum up as illustrated in Figure 4.18 on the left. Since the specific investment costs for PV (residential 760 EUR/kW_p, utility 420 EUR/kW_p) are lower compared to wind turbines (854 – 1,300 EUR/kW_p), the former ones have a comparably lower share in total costs in each scenario. Note, that here the investments are used without including follow-up or integration costs. While in the High PV scenario the installed PV capacities account for 74 % (thereof 85 % utility scale) of total capacities to cover 50 % of iRES generation, the costs for PV installations account for the half of the total investments. In each scenario, utility scale PV systems make the major part of PV installation with an increasing share from 85 % in High PV over 91 % in REF and 94 % in High Wind. This is a result of the lower specific investment costs for utility PV systems, not only compared to residential ones, but also to wind power. With increasing wind share in the iRES generation, the costs for onshore technologies are decreasing slightly due to the lesser capacities required. However, since the wind offshore technologies

(with specific investment costs of 2,093 EUR/kW_p) play a more important role in the High Wind scenario, the total costs are the highest in this scenario (994 bn. EUR). The assumed costs parameters are highly uncertain and future cost reduction for PV or wind technologies can change the cost comparison. Depending from the scenario, a 10 % cost reduction for the PV systems (all other parameter taying equal) can reduce the total costs by 1 % (High Wind) to 5 % (High PV). In contrast, a 10 % cost reduction for onshore wind turbines results in 4 % (High PV) to 8 % (High Wind) lower total iRES installation costs. The wind offshore technology is contributing less to the iRES generation in the scenarios due to the cost competition with PV and wind onshore. Wind offshore has on average nearly twice as many full load hours compared to the average full load hours of wind onshore. However, the assumed cost data based on literature findings shows investments for wind offshore more than double as high as for the onshore technology. The wind onshore technology is therefore preferred in the present cost optimal iRES expansion. Nevertheless, for this technology, the future costs developments have the potential to significantly impact the iRES technology mix as well as the resulting iRES expansion cost (Jansen et al. 2020). However, higher wind offshore share in the iRES mix is not part of the analysis. Based on the findings in the present work, the influence of a potential stronger wind offshore expansion on the flexibility demand will be discussed qualitatively in Chapter 7.

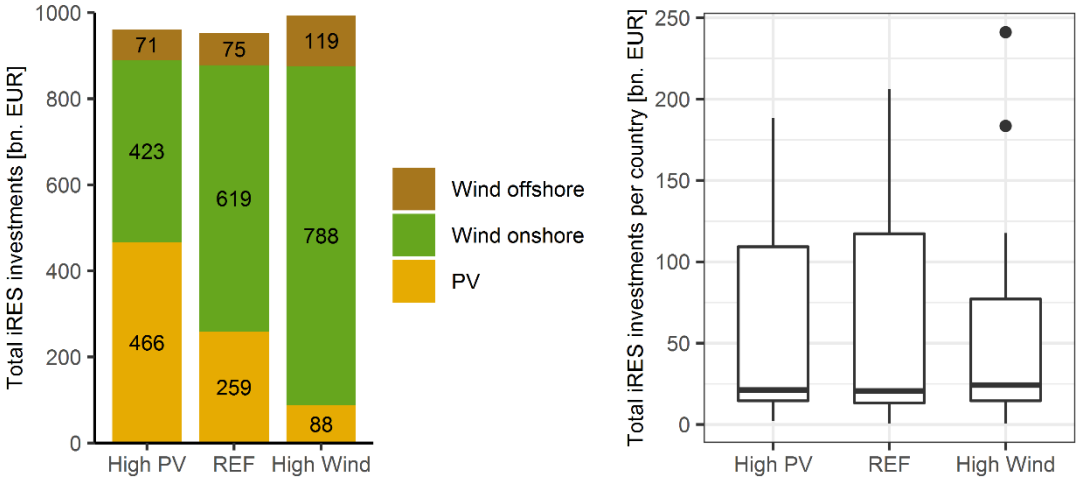


Figure 4.18: Scenario-specific total costs of the overall iRES installation in the observed region (left) and boxplot of country-specific investments (right) (Own illustration)

In Figure 4.18 on the right, the distribution of the country-specific investments under the assumed cost parameter is illustrated in boxplots (see country-specific values in Table B.5 in Appendix B.3). The lowest value in each scenario can be found for Luxembourg, the country with the lowest iRES installation. Nevertheless, countries with significantly decreasing PV

capacities from High PV to High Wind (e.g. Italy, Austria and Switzerland) reduce their iRES installation costs by up to 50 %. In contrast, countries like Norway and Poland with high wind capacities in the High Wind scenario have more than twice the investments compared to High PV. For example, Portugal, providing the same amount of iRES electricity in all scenarios, has 13 % higher costs (23 bn. EUR) in High Wind compared to High PV, illustrating the higher weight of the assumed specific investment costs for wind onshore capacities. In all scenarios, France has the highest cost with 175 bn. EUR in High PV, 206 bn. EUR in REF and 241 bn. EUR in the High Wind scenario, accounting for 18 % to 24 % of the total costs. As a comparison, in 2016 and 2017, France spent 2.6 bn. EUR and 2.8 bn. EUR respectively for wind onshore, wind offshore and PV installations (EurObserv'ER 2018). To install the capacities discussed here, the yearly iRES investments has to be two to threefold over a time horizon of 30 years. In contrast, in the EU the iRES investments accounted for 62 and 37 bn. EUR in the year 2016 and 2017, respectively (EurObserv'ER 2018). Assuming constant expenditures for the next 30 years, this range would be sufficient to cumulate total investment cost of around 1,000 bn. EUR. For this simplified calculation, no additional costs for iRES plant decommissioning and repowering are included, which further increase the iRES installation costs. Finally, when relating the country-specific costs in the present work to the corresponding population (data based on Eurostat 2019) evenly distributed across 30 years, the costs range between 26 EUR/capita and year in Poland to 422 EUR/capita and year in Norway both in the in the High Wind scenario to achieve the presented iRES capacities. The high value in Norway is an outlier across all scenarios due to the strong increase of wind onshore installation in the High Wind scenario. On average the REF scenario shows lowest values (65 EUR/capita·a), compared to High PV (73 EUR/capita·a) and High Wind (85 EUR/capita·a) following the same trend as the total costs. Furthermore, if the country-specific total costs of iRES installation are allocated to 30 years and related to the country-specific gross domestic product (GDP), the share of these costs at the country's GDP of the year 2018 ranges between 0.04 % (Switzerland) and 0.61 % (Norway) (Eurostat, 2020). Nevertheless, the figures underline two important points. First, a constantly high investment in iRES capacities is crucial to achieve high iRES share. Secondly, since the starting point of iRES installation within each country is very different, the increase in expansion rates as well as investment expenditures is very different and accordingly challenging in each country. A comparison with the ambitions communicated in the European Green Deal with targets of investing 1,000 bn. EUR in a sustainable European Union (thus not only investments in iRES) in the next decade may lead to the assumptions, that the European energy policy appreciates major investment requirements in the future. Additionally, in the Green Deal agreement, "just transition mechanisms" are foreseen to counteract unevenly distributed transition burdens across EU member states (EC 2019a).

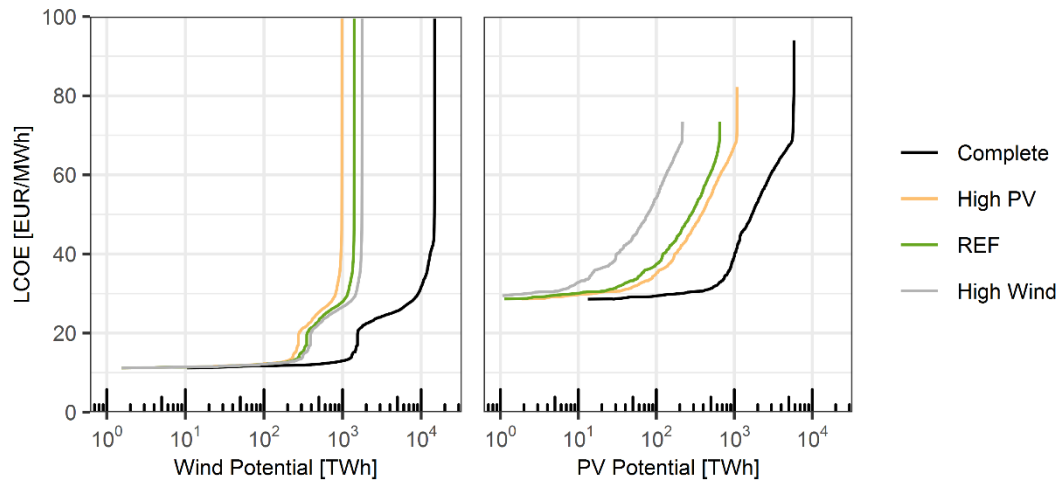


Figure 4.19: Complete and scenario-specific cost-potential curves for wind onshore (left) and PV (right) in the whole region observed (Own illustration)

The cost-potential curves, illustrated for selected countries in Chapter 3.1.5 (Figure 3.7), can give an overview, about the optimal least cost use of the available iRES potential. Nevertheless, as discussed before, the successively installation of iRES capacities exclusively based on potentials is assumed to be not realistic, due to possible restrictions in the power system and the society. Therefore, the energy policy restrictions (see equation (3.15) in Chapter 3.2.2) implemented in the model limit the concentration of iRES capacities in each raster. The impact of these restrictions on the cost-potential curves for wind onshore (left) and PV (right) can be seen in Figure 4.19 (note the logarithmic scaling of the x-axis). As a reference, the complete cost-potentials of the whole region observed are illustrated in black as a comparison for the scenario-specific curves. In general, wind onshore shows lower LCOE between 10 and 30 EUR/MWh compared to PV, while high cost increases can be observed for the last 10 % of the available potential. Also for PV, generation potentials of around 1,000 TWh are available at LCOE of around 30 EUR/MWh. The horizontal maximum of each scenario-specific realised cost-potential (-generation) curve represents the wind onshore and PV generation in each scenario (compare with Figure 4.1). The exploited potential is significantly lower compared to the available potential. The comparison of the range of the complete and scenario-specific LCOE validates the functioning of the implemented restrictions as intended. Instead of only exploiting the potential with lower LCOE (in the observed region, this would be coastal raster for wind onshore and southern raster for PV), the installation of the iRES capacities is well distributed across the available land. While for wind, almost each raster with wind onshore potentials has capacities installed, the lower maximal LCOE of the PV cost-potential curve indicate a higher amount of raster not exploited by PV capacities due to high costs.

4.5 Summary and qualitative assessment of the potentials of flexibility options

With the availability as well as the simultaneity of geographically distributed wind and PV electricity generation, the two central features of iRES technologies can be summarised. Both technologies differ significantly regarding these characteristics. A 50 % share of PV in total iRES electricity generation, significantly more capacity is required compared to a scenario with more wind turbines. Additionally, due to the higher availability of wind onshore in the observed region, the average installed capacity per square meter land used decreases with higher wind shares. In contrast, since wind turbines have a higher specific power density, the total land used for iRES installations is highest in the High Wind scenario. Furthermore, the energy policy constraints applied in the model regarding the regional distribution of iRES-based electricity generation indicate that in the High PV scenario, the contribution of each country to iRES power generation is the least scattered in the observed area, thus more evenly distributed. These results strengthen the requirement to assess future iRES expansion pathways by including not only techno-economic characteristics, but also socio-ecological. This is especially true, when the share of iRES in the energy system reaches very high value. When comparing the iRES-based capacity expansions in the presented scenarios with data of the TYNDP, single countries often show no significant increase of PV or wind installations. In contrast, the contribution of the whole region observed as well as of single countries to the iRES generation to theoretically cover 80 % of the electricity demand requires an enormous increase in installations in each scenario. It is crucial to take into account, that the resulting iRES expansion pathways are an outcome of model-based cost optimisation, while further potential restrictions and influencing factors are neglected and often not trivial to specify in a long-term time horizon (e.g. national iRES expansion ambitions and local public acceptance as well as further cost declines). Thus, the scenarios should be interpreted as range of possible futures also reflecting the underlying uncertainty of possible developments regarding the combination of iRES technologies in the future Europe. The presented iRES expansion model enables to analyse further sensitivities regarding the maximum iRES share as well as the distribution of the respective capacities with the corresponding impacts on the flexibility needs, as partly shown above. Nevertheless, an evaluation beyond the presented Wind-PV share scenarios will not be part of the following analysis to limit the research framework of the present work.

Table 4.2: Generalised relationships between the demand for flexibility and the potential provision of flexibility

Impact factors	Impact on residual load	Impact of increasing wind share	Relevant flexibility options	Potential application
Availability and simultaneity of iRES	Pattern of positive residual load	Decrease of positive residual load	Dispatchable power plants, load shedding	Increase of electricity supply (energy and power)
	Pattern of negative residual load	Decrease of negative residual load	Load increase, sector coupling	Increase of electricity demand (energy and power)
	Duration and content of surplus and deficit phases	Increasing maxima; tends to be longer with decreasing amount of energy	Storages, DSM, electricity grids	Temporal and spatial balancing of energy
Availability of iRES	Variance and seasonality of residual load	Decreasing variance	Dispatchable power plants, load shedding, Load increase, sector coupling	Increase of electricity supply or demand (energy and power)
			Storages	Temporal balancing of energy
Simultaneity of iRES	Correlation of regional residual loads	Decreasing variance	Storages, DSM	Temporal balancing of energy
			Electricity grids	Spatial balancing of energy

As it was shown, the availability and simultaneity of wind and PV generation cause significant differences in the need for flexibility. With regard to the optimal provision of flexibility as part of the model-based analysis in the following chapters, expectations of possible effects on the combinations of flexibility options can be derived. In the following, the value of different flexible technologies categorized in Chapter 2.2 (downward, shifting and upward flexibility) is assessed by an isolated comparison with the structure of the scenario-specific residual load. Thereby, the most important iRES characteristics impacting the residual load are availability (in terms of full load hours) and simultaneity (in terms of temporal distribution of iRES feed-in). Complemented by the spatially different distribution of iRES potentials, these aspects define the results of the iRES model as presented above. Table 4.2 summarizes the expected relationships between flexibility demand and flexibility provision. In addition, Figure 4.20 emphasises possible differences regarding the investments and dispatch of flexibility options based on the varying need for flexibility in the High PV and High Wind scenario. The illustration displays simplified

theoretically application potentials for both single countries as well as transnational analysis as in the present work.

The present chapter emphasises the increase in correlation and thus the simultaneity of the country-specific residual load curves with an increasing share of PV generation. Furthermore, the fluctuation of the iRES technologies results in periods of very high power demand coinciding with times of very low iRES power generation. In each scenario, this leads to high maxima of the residual loads. The flexibility to provide the lack of capacity and energy, has to be provided by additional dispatchable power plants during these hours or offset by reducing the electricity demand (load shedding). In the hours with a positive residual load, it was shown that an increasing share of wind and the resulting higher and more constant availability of iRES power generation decreases the power deficits compared to the scenario with a higher PV share. In this perspective, the value of additional capacities of dispatchable electricity generation decreases with increasing wind share, as also illustrated in Figure 4.20 (see different sizes of the arrows for downward flexibility).

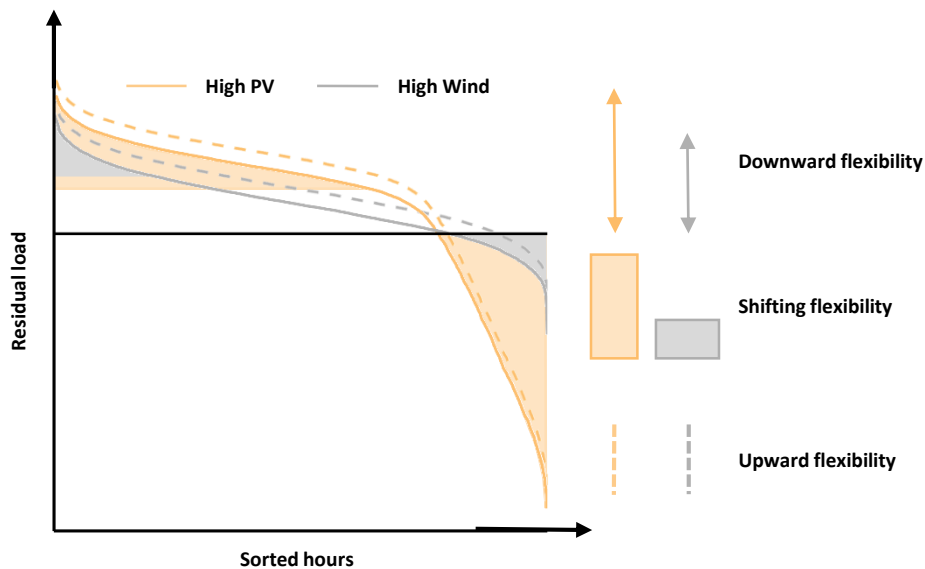


Figure 4.20: Theoretical applications of flexibility options in the High PV and High Wind scenario (Own illustration)

The country-specific analysis identified three further interactions. First, an increasing number of iRES surplus hours with increasing wind share can be observed on average. Second and in contrast, the high correlation of PV generation in the observed area and its daily feed-in peak leads to increasing annual surpluses with increasing PV shares in the total iRES generation.

Third, with an increasing PV share, the range of country-specific residual load parameters becomes larger. Particularly a higher share of surplus iRES electricity might facilitate the electrification of other energy demand sectors. Nevertheless, as mentioned before, this strongly depends on the flexibility of sector coupling. Assuming that these surpluses are used exclusively for load increase or sector coupling, more PV capacity might therefore increase the potential of these technologies. If the sector coupling is inflexible a rather parallel increase of the original residual is more likely, as illustrated in Figure 4.20 (dashed lines for the upward flexibility). The aspect of sector coupling flexibility is part of the third research field in the present work and analysed in detail in the following chapters.

At the same time, the surplus phases in the High Wind scenario tend to be longer, but are characterized by less surplus energy compared to the High PV scenario. In an isolated perspective, this influences the necessary capacity as well as the operating hours of the technologies to balance the surplus and deficit phases by increasing and decreasing the electricity load. The higher correlation of the country-specific residual loads with higher PV shares increases the number of hours with simultaneous surpluses in the countries and thus, the potential of storages and DSM. With regard to the surplus and deficit phases smaller storage energy capacities, but high storage power capacities seem to be beneficial in scenarios with higher PV share. This is again illustrated in Figure 4.20 by squares with different sizes indicating differences in capacity and energy required. For spatially shifting flexibility by electricity grids, a higher share of wind in iRES generation might increase the demand for larger transmission capacities to exploit the potential regional balancing effects of the less simultaneous wind generation. The observed distribution of iRES generation, implies scenario-specific differences regarding the locations and times with iRES surplus and iRES deficit, directly influencing the role of NTC for spatial balancing.

Nevertheless, by neglecting possible competitions and synergies between the available flexibility options, the limitations of this isolated assessment (both in terms of single technologies and in terms of single residual load parameters) become obvious. Although the evaluation facilitates the understanding of basic interactions, the need for a holistic analysis of the interdependencies between the need for flexibility as a function of the Wind-PV ratio in the generation of iRES-based electricity and the supply of flexibility is underlined. In addition, it is necessary to assess the combination of various flexibility options in the presence of energy market-based framework conditions (e.g. CO₂ emission prices). Therefore, in the following a detailed model for the analysis of optimal flexibility provision is presented. In this investment and dispatch model for flexibility options with different application fields the country-specific residual loads serve as exogenous data input.

5 Modelling Investment and Operations Decision for Flexibility Options

With the aim to decarbonise the conversion, supply and demand of energy, a significant expansion of less carbon-intensive technologies is required. As illustrated in the analysis of the flexibility demand, a high iRES share to theoretically cover 80 % of the electricity demand in the observed region most likely requires different flexibility options. The need for assessing the system transformation increases with the amount of options involved in the technology mix, including capital-intensive technologies with long lifetimes (e.g. power plants or electricity grids), large-scale and small-scale storage technologies as well as flexible energy demand. To determine synergies and competitions between different flexibility options, an electricity market model is applied. Therefore, in the following the modelling framework, the mathematical model description as well as the required input data is presented. Depending on the scenario-specific Wind-PV-ratio, the examination of combinations of flexibility options will enable specifying the role of selected technologies in the presence of different shares of wind and PV.

5.1 Modelling framework and general assumptions

The modelling objective is to determine optimal long-term system configurations with cost-minimising combinations of different flexibility options including sector coupling technologies and their respective dispatch. Since the analysis of structural interrelations and of structural changes is in the focus of the present work, fundamental models are the appropriate approach for the following analysis (Ringkjøb et al. 2018, Zerrahn & Schill 2015). To derive an appropriate

model framework for the present research design, the model requirements are described. Based on the electricity market model ELTRAMOD (Electricity Transshipment Model), the underlying general model approach and main assumptions are introduced, followed by the discussion of respective model adaptations and extensions. A critical discussion of the modelling approach is given in Chapter 5.4.

5.1.1 Basic structure of ELTRAMOD and underlying main assumptions

In the electricity market model ELTRAMOD the EU-28 countries, Switzerland and Norway, represent the available model regions with nationally aggregated generation and storage technologies. In its basic structure, the ELTRAMOD model family is a fundamental model that optimises the provision of electricity at an hourly resolution for a period of one year while electricity demand, fuel prices and CO₂-prices are implemented exogenously. Thereby, several important assumptions are included, which are commonly made in the formulation of electricity market models. On the one hand, the fundamental approach implies the explanation of the dispatch decision of all technologies involved based on minimal costs in a wholesale electricity market. The resulting electricity prices are furthermore based on the exogenous demand for electricity and other parameters such as technical restrictions or input prices. Accordingly, a perfect competition without the influence of uncertainty and market power is assumed.¹⁵ On the other hand, the application of the optimisation approach across the whole region observed is based on a perspective reflecting a rationally acting central planner with complete information. Thus, the central coordination of load balancing is a result of country-specific energy balances representing wholesale spot markets for electricity interconnected by transmission capacities. This is furthermore based on the assumptions of a perfect foresight for the optimization period as well as the willingness of transnational cooperation for cross-border trade. In addition, the assumption of perfect foresight involves a deterministic modelling approach. This means, that the input parameters are fixed and not influenced by external factors. This can be seen critically, as the influence of forecast uncertainties increases particularly against the background of increasing feed-in from iRES (Hirth and Ziegenhagen 2015). However, a long-term planning perspective poses additional challenges in estimating future uncertainties. Sets of scenarios and sensitivity analysis are therefore often a solution to illustrate the range of possible outcomes within a given modelling framework.

¹⁵ This means, besides large-scale power-plants also the different storage types, demand-side-management process as well as PtX technologies are dispatched optimally based on time-dependent price signals.

ELTRAMOD is furthermore formulated as a linear optimization model. This is possible because the implemented technologies form small units compared to the overall system. Thus, for example, on-off decisions of single power plants, which mathematically might lead to mixed-integer or non-linear model formulations, are aggregated. In ELTRAMOD, the objective function specifies the minimisation of the power generation costs for the entire region observed. Furthermore, the aforementioned balance between electricity demand and power generation as well as electricity trading in each time step is a crucial constraint for each model region. These region-specific energy balances form the basis for the minimum cost of electricity supply based on short-term marginal costs. The ELTRAMOD model family is built as a bottom-up model. The thermal and renewable power plant as well as storage technologies are represented in detail regarding their technical and economic characteristics. Accordingly, the constraints take different input parameters (e.g. efficiency, fuel prices, CO₂-prices, CO₂ emission factor, and variable costs) into account. In addition to the demand for electricity, the supply of electricity from wind and PV systems is given exogenously in hourly resolution reflecting the feed-in priorities for iRES as relevant energy policy. Furthermore, the EU emission trading system (ETS) is represented by specifying prices for emission allowances. Electricity trading between the model regions is a result of the model application, but is limited by exogenously specified maximum net transfer capacities (NTC). Electricity grids within the model regions, i.e. countries are neglected. This abstraction can reduce the model size and thus the computing time. ELTRAMOD is also applied for cost-effective investment decisions (as for example ELTRAMOD-INVEST in Schubert 2015) in addition to dispatch optimisation. Based on an existing power plant mix, this long-term expansion planning often analyses interactions between exogenously given development scenarios (e.g. iRES expansion) and optimal expansion (and decommissioning) of different technologies including annualised investments.

The applicability of ELTRAMOD for analysis regarding future developments in the electricity market was demonstrated in various works (e.g. Hobbie et al. 2019, Ladwig 2018, Schubert 2015). To verify the power of the model, calibration measures and back testing procedures are applied in these publications. When comparing ELTRAMOD results with historical parameters, the aforementioned literature shows good consistencies with historical data regarding electricity prices, import-export electricity flows and generation levels. In the following model requirements and adaptations are presented to adequately reflect the specifications of the present work.

5.1.2 Model requirements and adaptations of ELTRAMOD for the implementation of flexibility options

On the one hand, adjustments based on the research design are necessary to take aspects concerning flexibility provision as discussed in Chapter 2 into account. The target year for the analysis of the future electricity system is oriented at the year 2050. Specifying a target year for the long-term analysis facilitates the input data gathering, since required exogenous model parameter can be derived from existing literature. Furthermore, the application of a greenfield approach as well as of different scenarios and sensitivities is seen as appropriate modelling framework to cope for the uncertainties in the present work. This means, the analysis of the future system configuration is independent from the existing power plant mix and possible path dependencies¹⁶. Accordingly, the results should be interpreted as optimal benchmark, while real world market failures are neglected. When analysing the interdependencies between flexibility needs and supply with the help of scenarios and sensitivities, the interpretability of the model results and possible uncertainties is facilitated.

On the other hand, model expansions are required to implement various flexibility options. An overview is provided by Figure 5.1. First of all, with the application of a greenfield approach, the adaption of basic ELTRAMOD as model-endogenous investment and dispatch model is apparent. These model decisions thereby concern both, the implementation of electricity market based flexibility options as well as the representation of selected sector coupling technologies. The implementation of these technologies in an investment and dispatch model requires the formulation of additional equations with effects on the computational time. Particularly the introduction of additional storage and energy balances (see model description in Chapter 5.2) increases the required computational capacity. To keep the model tractable, the following abstractions are implemented. Regarding the model region, less countries are included compared to the ELTRAMOD basic version. Thus, the same 17 countries of Central-Western Europe as before form the present model region. To limit the calculation time but also due to uncertainties regarding the future ancillary service provision to secure system stability (source), which are not meant to be in the focus of the present work, further electricity markets are neglected in the present model analysis¹⁷. As a result, the dispatch decisions for the

¹⁶ An exception of the greenfield approach is made for hydropower plants, due to the high amounts of installed capacities across the region observed and their relevance for low-carbon electricity generation, and existing transmission capacities between the countries, due to their importance in providing flexibility today and in the future.

¹⁷ Nevertheless, further energy markets have the potential to improve the competitiveness of flexibility options, particularly regarding the provision of ancillary services. A highly flexible balancing of electricity demand or

corresponding flexibility options are solely based on a stylised wholesale electricity market, while further income potentials but also cost factors (see e.g. grid tariffs) are excluded.

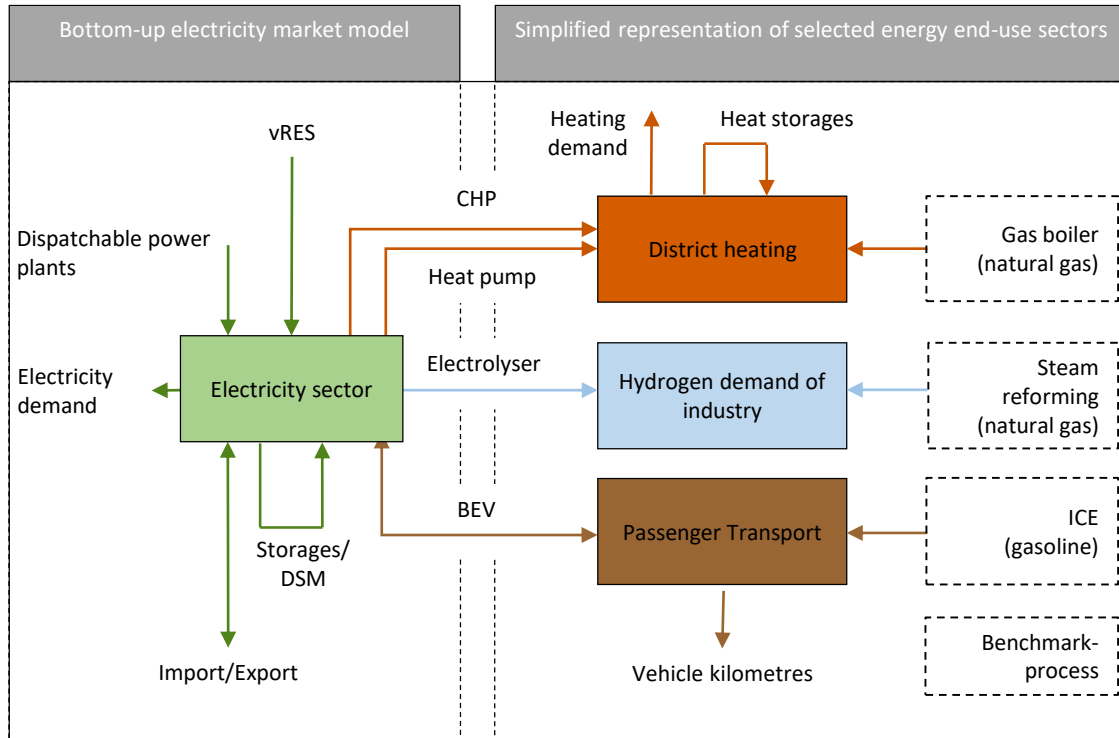


Figure 5.1: System boundaries and implemented technologies (Own illustration)

Various power plant technologies are included in the ELTRAMOD model family, distinguished by different techno-economic parameter. Flexibility aspects of dispatchable electricity generation to meet high residual load gradients are represented by load change costs, while the reduction in must-run capacities of CHP plants is made possible by the implementation of heat storages to decouple the electricity and heat generation. Furthermore, technologies for spatially and temporally shifting energy are comprehensively included in the model adaption. The spatial balance is represented by NTC allowing for import-export flows between the countries in the modelled region, as in the basis version of ELTRAMOD. In addition, three types of electricity storages are included, which correspond to the techno-economic characteristics of batteries, pumped storage power plants or compressed air energy storages (CAES). Based on different energy-to-power ratios, these storage types represent hourly, daily or seasonal storages respectively. The flexibility potential of DSM is implemented by four country-specific

supply is discussed as beneficial in literature, analysed for example for storages (e.g. Palizban & Kauhaniemi 2016), for DSM (e.g. Gils 2016, Paulus and Borggreffe 2011), or sector coupling technologies like heat pumps (Posma et al. 2019), electrolyser (Alshehri 2019) or BEV (Luca de Tena & Pregger 2018, Sarabi et al. 2016).

processes. However, by implementing DSM potentials, ELTRAMOD is further extended by a flexible electricity demand within the constraints defined in the model descriptions. The implementation of DSM in ELTRAMOD is described and applied in detail in Ladwig (2018) and Müller & Möst (2018). The present work builds on the work in these publications and adapts it for the respective model requirements and scenario framework.

While the electricity sector is represented by a more detailed bottom-up approach, additional electricity demand is introduced due to sector coupling as illustrated in Figure 5.1 (further details regarding the model-based representation of sector coupling technologies are given in the following chapter). As in the future the promotion of a multi-coupled energy system is expected, different options for the electrification of further energy demand sectors are included in the model formulation. However, since the technical, economic and ecological benefit of coupling the energy sectors strongly depends from the developments in the electricity sector (Lund et al. 2017), the modelling framework intends to identify the impacts of selected technologies on the additional electricity demand as well as on the flexibility provision in an electricity market perspective. Although further processes and measures exist to decarbonise these energy demand sectors independently from the electricity sector, the present work does not aim to setup an energy system model. To cope for possible competing technologies in the energy demand sectors respective benchmark processes for each sector are introduced. This simplified energy sector representation takes up a similar approach as in Zöphel et al. 2019, but is further adjusted and detailed for the present work. This enables a simplified representation of potential competition for these selected sector coupling technologies and allows for the determination of the cost-optimal provision of the sector-specific energy end-use demand as a model-endogenous results in a single model¹⁸. However, the developments regarding the future sector coupling are highly dynamic and the role of single technologies can change due to cost reductions, technological improvements or policy interventions (van Nuffel et al. 2018). Thus, the present work illustrates a part of future possible pathways from a today's perspective. Nevertheless, for the sector coupling technologies, the level of flexibility of the sector coupling itself is of high importance. Particularly an uncontrolled electricity demand from further energy end-use sectors induces new load peaks and increases the flexibility requirements in the electricity sector (van Nuffel et al. 2018). Due to the crucial role of sector coupling within the present work, in the following additional details are given. This includes the choice of sector

¹⁸ Recently, scientific projects like REFLEX deal with similar research foci in international and interdisciplinary research cooperation by combining joint work of various experts and extensive model couplings (see Möst et al. 2021).

coupling technologies, underlying assumptions regarding their implementation into the model formulation as well as the approach for analysing sector coupling flexibility.

5.1.3 Representation of selected sector coupling approaches and derivation of scenarios for the flexibility supply side

The choice of the select sector coupling technologies for the model-based implementation in the present work is driven by the rational of which technologies are most likely to be exploited in the mid- to long-term. These technologies are heat pumps, electrolyser and battery-electric-vehicles (BEV) as detailed in the following. In addition to the electrification of the heating supply by residential as well as large-scale heat pumps, district heating by cogeneration in CHP plants are main decarbonisation strategies (Kavvadias et al. 2019). For the residential and the tertiary sector accounting for almost two third of the final energy demand for heating in the EU (Fleiter et al. 2016), heat pumps are seen as most promising due to the comparably low costs, particularly for space heating and hot water provision (Bloess et al. 2017). Regarding PtG processes, the hydrogen production by electrolysis for industry processes is implemented, to reflect potential decarbonisation strategies in the industry. In general, applying hydrogen as fossil fuel substitute for the industry is seen as beneficial, since it is currently used in different processes in the chemical (ammoniac, methanol) and refinery industry as well as a reducing agent in metal production (EPRS 2019). Thereby, hydrogen often is the only alternative for the processes mentioned above (HC 2020). Although electricity and biofuels are central competitors for hydrogen in the heating and transport sector, hydrogen is discussed as important future fuel to allow for decarbonisation (if generated with low-carbon electricity) in these sectors where electricity as direct energy carrier has limited potential, such as (high temperature) heating and long-distance as well as heavy-duty transport via fuel cells. However, the cost competitiveness as well as performance regarding these further applications is assessed to be more challenging compared to industry processes (Staffell et al. 2019). Due to these reasons, the focus of the present work is laid on hydrogen production for the industry sector via PtG. Finally, the electrification of the passenger transport sector by battery-electric vehicles (BEV) is included, since various policy support programs to promote consumer adoption and increase convenience are introduced across Europe (Wappelhorst 2020). Compared to BEV, alternative low-carbon options for the private car sector are also assessed as less efficient (compared to fuel cell electric vehicle) or limited due to resource availability (regarding biofuels) (Michalski et al. 2018). For the analysis of the coupling of the electricity sector with the heat, industry and transport sector, the benchmark technologies gas boiler, steam reforming and internal combustion engine (ICE) are applied, respectively (see Figure 5.1). While for gas boiler and steam reforming natural gas is the corresponding fuel type, the ICE based passenger cars are

fuelled by gasoline. Thus, for the selected PtX technologies, the investment and dispatch decisions are electricity market driven and influenced by opportunity costs of investing in alternative technologies, while possible commitments in other energy markets are neglected.

Table 5.1: Overview of flexibility supply side scenarios with corresponding main assumptions

Scenario	Energy end-use sector		
	District Heating	Hydrogen for Industry	Passenger Transport
No sector coupling			
NO	Coverage of sectoral energy demand by benchmark processes		
Enforced sector coupling			
	Minimum 50 % of district heating demand based on heat pumps	Minimum 50 % of industries hydrogen demand based on electrolyser	Minimum 50 % of passenger cars as BEV
LF	Low flexibility		
	No heat storages	No hydrogen storages	Charge immediately
HF	High flexibility		
	Heat storages	Hydrogen storages	Bi-directional charging

Depending on the technology and the energy end-use sector, a significant investment in PtX technologies based on electricity market incentives is estimated to only be likely in scenarios with very favourable developments pathways of influencing parameters (e.g. further cost reductions and strong increase in fossil fuel costs) (Staffell et al. 2019, Michaelis 2018). While, the identification of optimal framework conditions for the investment in PtX technologies is not in the focus of the present work, it is assumed in the following that the future deployment of these technologies is promoted by energy policy programs. Based on this assumption, scenarios with a targeted sector coupling are introduced. To generally evaluate the impact of the enforced sectors coupling also with regard to the electricity market, a scenario with no sector coupling is introduced (see NO scenario in Table 5.1). In contrast, for the targeted sector coupling a minimum share of the selected energy end-use sectors is defined to be electrified. Note that, by setting a lower bound of the amount of electricity, the investment in the respective PtX technologies are model-endogenous decision variables. The minimum electrification share is set to 50 % for each of the sector-specific applications, as listed in Table 5.1. Instead of assuming 100 %, this lower bound induces that potential competing technologies (here represented as

benchmark processes) or alternatives (e.g. efficiency gains) are likely to be deployed as well in the future. At the same time, an electrification of the sector-specific energy demand exceeding these 50 % is allowed. With regard to the input data needed for the analysis of this enforced sector coupling, both, the annual as well as the time-dependent energy demand of the selected sector are required as presented in Chapter 5.3.

For the selected PtX technologies, two overlapping developments will be considered. On the one side, the increase in electricity demand will affect the provision of flexibility due to a change of the residual demand. On the other side, the level of flexibility of this sector coupling is further expected to influence the optimal mix of flexibility options in comparison to the NO scenario. With this perspective two scenarios are defined representing both extreme cases, a scenario with low flexibility (LF) and with high flexibility (HF) of sector coupling, as illustrated in Table 5.1. The key aspect of this distinction affects the access to energy storages within the sectors. As described for example in Matthiesen et al. (2015), the deployment of storages in a multi-coupled energy is crucial for a more efficient use of electricity. Whereas in the LF scenario this flexibility provision has to be realised solely in the electricity sector, in the HF scenario additional options to shift energy within the end-use sectors become available. Here, the modelling of the district heating and the hydrogen sector additionally allows for storage installations. With investments in BEV, where battery storages exist either way, the defined distinctions concerns the charging strategies, reflecting the priorities of the car fleet to either charge immediately or to provide flexibility by allow for bi-directional charging. Details on model formulation are presented in the following chapter.

As summarised in Figure 5.2, the modelling framework employs two scenario categories for the examination of the research questions. On the one hand, scenarios on the flexibility demand side (FD scenarios) with varying Wind-PV-ratios serve as input for the modelling of optimal investment and dispatch decisions for flexibility options. On the other hand, the scenarios discussed above represent the flexibility on the supply side (FS scenarios). In addition to flexibility provision in the electricity sector, the analysis will take the sector coupling approach of the selected technologies in comparison with the NO scenario into account. Here, interrelations between potentially low-cost storage technologies (e.g. thermal or hydrogen storages) and capital intensive PtX technologies (e.g. hydrogen production by electrolysis) will be discussed.

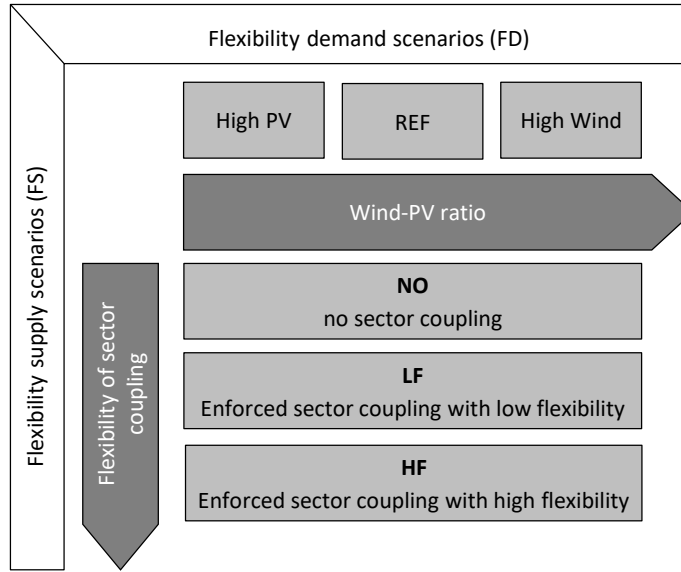


Figure 5.2: Dimensions of the scenario framework (Own illustration)

The resulting scenario matrix in Figure 5.2 is a product of the three Wind-PV share scenarios (High PV, REF, High Wind) and the three flexibility supply side scenarios (NO, LF, HF). Regarding the scenarios of the flexibility supply side, the corresponding model implementation will be described as well in the following mathematical model description¹⁹.

5.2 ELTRAMOD-based investment and dispatch model

5.2.1 Objective and cost-related equations

As depicted in equation 5.1, the objective of the linear optimization problem ELTRAMOD is the minimisation of the costs of electricity generation to cover the electricity demand in the power sector, as well as in parts of the heating, transport and industry sector across all 17 countries c in the modelled region. The total system costs are composed by four components, the investments CO_c^{INV} , the fixed cost CO_c^{FIX} , the dispatch costs CO_c^{DC} , and the costs resulting from the application of the benchmark processes $CO_{c,t}^{BP}$.

$$\text{Min} \left[\text{TotalCosts} = \sum_c CO_c^{INV} + \sum_c CO_c^{FIX} + \sum_c CO_c^{DC} + \sum_c CO_{c,t}^{BP} \right] \quad 5.1$$

¹⁹ The applied model formulation and gathered input data is made available in a data repository available at: <https://github.com/CZoepfel/Flexibility-in-a-European-Energy-system>.

Equation (5.2) defines the costs of capital. Here, the model-endogenously derived capacities (in general described as CAP with unit [MW]) address installations for different dispatchable power plants $tech$, for the interconnector capacity ntc between country c and country cc , for multiple DSM processes dsm , and for PTX technologies pt . While electricity storages are part of the $tech$ set, further energy storages are implemented, namely capacities assigned to the PTX technologies as well as heating storages for CSP plants $hecsp$. Each of the capacities are multiplied with a corresponding annuity factor to calculate on the basis of annual costs.

$$\begin{aligned}
 CO_c^{INV} = & \sum_{tech} CAP_{tech,c} * an_{tech} + \frac{1}{2} * \sum_{cc} CAP_{c,cc}^{NTC} * an^{NTC} \\
 & + \sum_{dsm} CAP_{dsm,c} * an_{dsm} + CAP_{pt,c}^{PTX} * an_{pt} \\
 & + CAP_{pt,c}^{PTX_STOR} * an_{pt}^{PTX_STOR} + CAP_c^{HECSP} * an^{HECSP}
 \end{aligned} \quad \forall c \in C \quad 5.2$$

Furthermore, in equation 5.3, the fixed costs, as product of the capacity installed and the fixed cost factor co^{fix} are defined as the sum of fixed costs for the dispatchable power plants and the selected PTX technologies. In contrast, fixed costs for energy storages are neglected.

$$CO_c^{FIX} = \sum_{tech} CAP_{tech,c} * co_{fix_{tech}} + CAP_{pt,c}^{PTX} * co_{fix_{pt}} \quad \forall c \in C \quad 5.3$$

The dispatch costs are calculated as in equation 5.4, by firstly including variable co_{tech}^{var} , fuel co_{tech}^{fuel} as well as emission costs $co_{tech}^{co_2}$ for generating electricity $GEN_{tech,c,t}$ of technology $tech$ in time step t . The latter two cost components depend of the generation efficiency η_{tech} . Secondly, ramping costs are implemented to illustrate different levels of flexibility to increase $RAMP_{tech,c,t}^{up}$ or decrease $RAMP_{tech,c,t}^{down}$ the power output of power plants. Thirdly, the activation of demand reduction $DSM_{dsm,c,t}^{red}$ and demand increase $DSM_{dsm,c,t}^{inc}$ for load shifting, as well as for load shedding $DSM_{c,t}^{she}$ is causing costs as well. For the sector coupling technologies, no additional dispatch costs are included, since the marginal costs for electricity in each time step t is implicitly causing costs for the load increase of PtX applications.

$$CO_c^{DC} = \sum_{tech,t} (GEN_{tech,c,t} * (co_{tech}^{var} + \frac{co_{tech}^{co_2} + co_{tech}^{fuel}}{\eta_{tech}})) \quad \forall c \in C \quad 5.4$$

$$\begin{aligned}
& + \sum_{ramp,t} (RAMP_{tech,c,t}^{up} * CO_{tech}^{ramp,up} + RAMP_{tech,c,t}^{down} * CO_{tech}^{ramp,down}) \\
& + \sum_{dsm,t} ((DSM_{dsm,c,t}^{red} + DSM_{dsm,c,t}^{inc}) * CO_{dsm}^{shi}) + (\sum_t DSM_{c,t}^{she} * CO^{she})
\end{aligned}$$

The fourth cost component is adding the costs for the benchmark processes BP (see equation 5.5), which serve as alternative energy source for the sector coupling technologies. For each of the energy end-use sectors included, the most cost-efficient substitute is implemented. While for the heating sector with gas boiler $BP_{c,t}^{gb}$ and the hydrogen production for the industry via steam reforming BP_c^{SR} , natural gas is consumed associated with costs depending on the efficiency of the process (CO^{gb} and CO^{SR}), for the passenger transport ICE BP_c^{ice} are fuelled with gasoline (CO^{ice}).

$$CO_c^{BP} = \sum_t BP_{c,t}^{gb} * CO^{gb} + BP_c^{SR} * CO^{SR} + BP_c^{ice} * CO^{ice} \quad \forall c \in C \quad 5.5$$

5.2.2 Electricity balance

Besides the cost terms forming the model objective, the energy balance is a crucial part in electricity market models, since here the required match between all sources of electricity demand and supply is secured. While for the constraints representing the selected PtX technologies further energy balances are defined for each represented energy end-use sector (see Chapter 5.2.4), equation (5.6) is depicting the central equation for matching electricity demand and supply and will be named electricity balance in the following. The hourly residual load $rde_{c,t}$, as difference between the exogenous input of the system load and the calculated iRES time series for each country, can be increased on the one side by exports $EXP_{c,cc,t}$, charging of electricity storages $CHA_{s,c,t}$ and load increase $DSM_{c,t}^{inc}$. In addition, surplus iRES generation can be curtailed $CURT_{c,t}$. On the other side, PTX technologies can also generate additional electricity demand. Due to differences in the model implementation of the sector coupling technologies, the three selected technologies are included separately in equation (5.6). Based on the discussion regarding the representation of sector coupling technologies, the level of sector coupling flexibility is introduced with the flexibility factor $ff = [0,1]$, which can be adjusted exogenously for the flexibility supply scenario calculation. ff is implemented to limit the flexibility of sector coupling and mainly influences the equations in Chapter 5.2.4. However, while the electrification with heat pumps $PTX_{pth,c,t}$ and electrolyser $PTX_{ptg,c,t}$ directly increases the electricity demand, for EV different ff also affect the energy balance, resulting in either direct charging $EV_{c,t}$ (with $ff = 0$) or bi-directional charging $PTX_STOR_{ev,c,t}^{CHA}$ and discharging $PTX_STOR_{ev,c,t}^{DIS}$ in the EV battery (with $ff = 1$). Besides the discharging of EV batteries, electricity

supply or demand reduction for each hour and country can be provided by power plants $GEN_{tech,c,t}$ (including electricity storage discharging), DSM-based load reduction $DSM_{dsm,c,t,tt}^{red}$ (for shifting) or load shedding $DSM_{c,t}^{she}$, as well as imports $IMP_{cc,c,t}$.

$$\begin{aligned}
 0 = & rde_{c,t} + \sum_{cc} EXP_{c,cc,t} + \sum_s CHA_{s,c,t} + \sum_{dsm} DSM_{c,t}^{inc} + CURT_{c,t} \\
 & + PTX_{pth,c,t} + PTX_{ptg,c,t} + PTX_STOR_{ev,c,t}^{CHA} + (1 - ff) * EV_{c,t} \\
 & - \sum_{tech} GEN_{tech,c,t} - \sum_{dsm} DSM_{dsm,c,t,tt}^{red} - DSM_{c,t}^{she} \quad \forall c \in C, t \in T \quad 5.6 \\
 & - \sum_{cc} IMP_{cc,c,t} - PTX_STOR_{ev,c,t}^{DIS}
 \end{aligned}$$

In equation (5.7) and (5.8), the export and import flows are restricted regarding the existing $cap_{c,cc}^{NTC}$ and new transfer capacity $CAP_{c,cc}^{NTC}$. Furthermore, the import and export capacities have to be equal.

$$EXP_{c,cc,t} \leq cap_{c,cc}^{NTC} + CAP_{c,cc}^{NTC} \quad \forall c, cc \in C, t \in T \quad 5.7$$

$$CAP_{c,cc}^{NTC} = CAP_{cc,c}^{NTC} \quad \forall c, cc \in C \quad 5.8$$

5.2.3 Constraints for the electricity sector

5.2.3.1 Dispatchable power plants

The electricity provision $GEN_{tech,c,t}$ by power plants and storage discharging is restricted by the model-endogenously determined maximal capacity of each technology $CAP_{tech,c}$. To reflect different flexibility characteristics of the power plants implying the ability to adjust the output to match the residual load, ramping up and down causes technology-specific costs, as introduced before. In equation (5.10), a load change of each power plant is defined as the difference between the level of generation in the current time step and the next time step.

$$GEN_{tech,c,t} \leq CAP_{tech,c} \quad \forall c \in C, t \in T, tech \in TE \quad 5.9$$

$$\begin{aligned}
 RAMP_{ramp,c,t}^{up} - RAMP_{ramp,c,t}^{down} \\
 = GEN_{ramp,c,t+1} - GEN_{ramp,c,t} \quad \forall c \in C, t \in T, ramp \in TE \quad 5.10
 \end{aligned}$$

For controllable RES, additional equations are required, to cope for technical particularities and assumed available potential. Firstly, for CSP plants, an average normalised hourly time series of solar radiation $norm_{c,t}^{solar}$ is derived for each country, based on the MERRA-2 weather data

of Chapter 3. Multiplied with the CSP capacity $CAP_{csp,c,t}$, the actual thermal energy flow $CSP_{csp,c,t}$ can be calculated (equation (5.11)). Electricity can be generated $GEN_{csp,c,t}$ considering an efficiency by using this thermal energy depending on the amount of energy charged $HECSP_{csp,c,t}^{CHA}$ or discharged $HECSP_{csp,c,t}^{DIS}$ in the heat storage of the CSP plant, as defined in equation (5.12). The corresponding storage restriction is shown in equation (5.13). Accordingly, the heat storage level $SL_{csp,c,t}^{csp}$ in one times step equals the level in the time step before (including storage losses), increased by storage charging and discharging. Furthermore, also the maximum storage level is restricted by the capacity installed CAP_c^{HECSP} (see equation (5.14)) as a result of the optimisation.

$$CSP_{csp,c,t} \leqslant CAP_{csp,c,t} * norm_{c,t}^{solar} \quad \forall c \in C, t \in T, csp \in TE \quad 5.11$$

$$CSP_{csp,c,t} = \frac{GEN_{csp,c,t}}{\eta_{csp}} + HECSP_{csp,c,t}^{CHA} - HECSP_{csp,c,t}^{DIS} \quad \forall c \in C, t \in T, csp \in TE \quad 5.12$$

$$SL_{csp,c,t}^{csp} = k * SL_{csp,c,t-1}^{csp} + HECSP_{csp,c,t}^{CHA} - HECSP_{csp,c,t}^{DIS} \quad \forall c \in C, t \in T, csp \in TE \quad 5.13$$

$$SL_{csp,c,t} \leqslant CAP_c^{HECSP} \quad \forall c \in C, t \in T, csp \in TE \quad 5.14$$

Since the RES expansion based on weather data is focused on fluctuating RES, further RES are included with additional restrictions for maximal generation or capacities based on literature data. This approach is implemented, to account for limited resources (in terms of potential and land) of the respective RES. While for run-of river and PSP maximal capacities $max_cap_{tech,c}$ are introduced to reflect limitations of installable capacities due to a lack of suitable locations (see data Chapter 5.1), reservoirs are further restricted regarding their maximum flh $flh_{reservoir \in tech,c}$ (see equation (5.15)). Furthermore, the use of biomass for electricity generation has an upper bound $maxGEN_c^{bio}$ (see equation (5.16)). In case of CSP and geothermal based electricity supply, maximum capacities are defined in equations (5.17) and (5.18).

$$\sum_{t, reservoir \in TE} GEN_{reservoir,c,t} \leqslant max_cap_{reservoir,c} * vlh_{reservoir,c} \quad \forall c \in C \quad 5.15$$

$$\sum_t GEN_{bio,c,t} \leqslant maxGEN_c^{bio} \quad \forall c \in C, bio \in TE \quad 5.16$$

$$CAP_{csp,c} \leqslant maxCAP_c^{csp} \quad \forall c \in C, csp \in TE \quad 5.17$$

$$CAP_{geo,c,t} \leq \max CAP_c^{geo} \quad \forall c \in C, geo \in TE \quad 5.18$$

5.2.3.2 Storages and demand-side-management processes

For storages, equations limiting storage capacity as well as charging and discharging power are required as well. Equation (5.19) controls the storage level $SL_{s,c,t}$ as well as the charging $CHA_{s,c,t}$ and discharging $GEN_{s,c,t}$ flows under consideration of respective efficiencies. In the model application, further equations ensure the same storage level at the beginning and the end of the modelled period. For each storage type s , an energy-to-power ratio²⁰ epr_s^{stor} is introduced. Depending from the installed storage power $CAP_{s,c}$, this ratio defines the corresponding storage capacity as upper bound of the storage level (equation (5.20)). Here storage types can be introduced with characteristically different energy-to-power ratios epr_s^{stor} , representing hourly, daily and seasonal storages. Additionally, similar to the discharging power, the maximum charging power is restricted by the storage capacity, as in equation (5.21).

$$SL_{s,c,t} = SL_{s,c,t-1} + CHA_{s,c,t} \cdot \eta_s^{cha} - \frac{GEN_{s,c,t}}{\eta_s^{dis}} \quad \forall c \in C, t \in T, s \in TE \quad 5.19$$

$$SL_{s,c,t} \leq CAP_{s,c} * epr_s^{stor} \quad \forall c \in C, t \in T, s \in TE \quad 5.20$$

$$CHA_{s,c,t} \leq CAP_{s,c} \quad \forall c \in C, t \in T, s \in TE \quad 5.21$$

For the mathematical formulation of DSM applications, the present work mainly applies the approach presented in Zerrahn & Schill (2015). Adjustments are made to include multiple countries and multiple processes with temperature- and thus time-dependent availabilities of DSM processes. In the equations (5.22) to (5.26), the restrictions for DSM processes to shift *shi* electricity are listed. Equation (5.22) defines the equalisation of load increases and reduction in a process-specific shifting time t_{dsm}^{shi} . $DSM_H_{dsm,c,t,tt}^{red}$ is load reduction, that accounts for load increase $DSM_{dsm,c,t}^{inc}$ in t , depending from t_{dsm}^{shi} . This balancing can take place either before, after, or both the load increase. For better readability, equation (5.23) assigns the sum of load reduction on hold $DSM_H_{dsm,c,t,tt}^{red}$ to actual load increase $DSM_{shi,c,t}^{red}$. Furthermore, the available capacity for load shifting is limited by the installed optimal capacity $CAP_{shi,c}$ multiplied with a

²⁰ Generally, energy storages can be characterised by two dimensions: the energy capacity (in MWh) as well as the power capacity or rating (in MW). The ratio between these parameters results in the energy-to-power ratio indicating the duration at which a storage can discharge at rated output.

normalised time series of DSM availability $norm_{shi,c,t}$ (equation 5.25). Additionally, a maximum number of activations per day is implemented, assigning a recovery time t_{shi}^{daylim} for each DSM process. Based on literature data, the maximal installable capacity of each process defines the upper bound for $CAP_{shi,c}$.

$$DSM_{shi,c,t}^{inc} = \sum_{tt=t-t_{shi}^{shi}}^{t+t_{shi}^{shi}} DSM_H_{shi,c,t,tt}^{red} \quad \forall c \in C, t \in T, shi \in DSM \quad 5.22$$

$$DSM_{shi,c,t}^{red} = \sum_{tt=t-t_{shi}^{shi}}^{t+t_{shi}^{shi}} DSM_H_{shi,c,t,tt}^{red} \quad \forall c \in C, t \in T, shi \in DSM \quad 5.23$$

$$DSM_{shi,c,t}^{inc} + DSM_{shi,c,t}^{red} \leqslant CAP_{shi,c} \cdot norm_{shi,c,t} \quad \forall c \in C, t \in T, shi \in DSM \quad 5.24$$

$$\sum_{tt=t}^{t+t_{shi}^{daylim}} DSM_{shi,c,tt}^{inc} \leqslant CAP_{shi,c} \cdot t_{shi}^{shi} \quad \forall c \in C, t \in T, shi \in DSM \quad 5.25$$

$$CAP_{shi,c} \leqslant max_{shi,c} \quad \forall c \in C, t \in T, shi \in DSM \quad 5.26$$

The DSM process for load shedding she , without the possibility to postpone and submit electricity demand to a later point in time, can be illustrated based on the equations (5.27) to (5.29). Similar to the shifting processes discussed before, a maximum number of activations per day is introduced t_{she}^{daylim} , restricting the amount of electricity that can be shedded, depending from the installed capacity $CAP_{she,c}$. This capacity is also restricted by a time-varying normalised time series $norm_{she,c,t}$, while the maximum capacity is bounded by $max_{she,c}$.

$$\sum_{tt=t}^{t+t_{she}^{daylim}} DSM_{she,c,tt} \leqslant CAP_{she,c} \quad \forall c \in C, t \in T, she \in DSM \quad 5.27$$

$$DSM_{she,c,t} \leqslant CAP_{she,c} \cdot norm_{she,c,t} \quad \forall c \in C, t \in T, she \in DSM \quad 5.28$$

$$CAP_{she,c} \leqslant max_{she,c} \quad \forall c \in C, t \in T, she \in DSM \quad 5.29$$

5.2.4 Constraints for the representation of sector coupling

To compare possible energy system benefits due to sector coupling, a benchmark is calculated in the NO scenario, with values for PtX related variables fixed to zero to exclude the electrification of the selected sectors. In contrast, the model formulation below presents the mathematical description of the constraints for the heating, the hydrogen and the passenger transport sector, allowing for scenario with low (LF) and high (HF) flexibility in sector coupling by introducing the flexibility factor ff . In general, besides the restrictions introduced below, the dispatch of the PtX technologies is not constrained by additional concepts of use, such as the solely use of surplus phases (as e.g. discussed in McKenna et al. (2018)). Thus, in the modelling perspective, the endogenous dispatch decision is mainly driven by the sector-specific energy demand, by the investment costs for the sector coupling technologies, by the value of the electricity consumed as well as by the opportunity costs for the alternative energy supply options. Regarding the latter aspect, for the competing technologies gas boiler, steam reforming and ICE based mobility model-endogenous investment decisions are neglected. As a simplification, assumptions on specific investments costs are combined with average full load hours for gas boiler and steam reformer as well as average driving distances for ICE cars to calculate the respective generation/provision costs (for further details see Section 5.3.2). Since the structure of the model-based representation of the three selected technologies is differently, in the following the sector-specific approaches are presented.

5.2.4.1 Constraints for the district heating sector

To allow for two flows, directly to satisfy the heat demand as well as indirectly by charging excess heat in storages, equation 5.31 and 5.32 define an allocation for both, the heat production of CHP plants $GEN_{chp,c,t}$ (with the CHP factor f^{chp} defining the share of heat produced by the cogeneration of heat and power) and heat pumps $PTX_{pth,c,t}$ (including a coefficient of performance η_{pth} for the transformation of electricity to heat). The role of ff is defined in equation 5.33, where it controls the lower bound for the amount of heat to be covered directly the heating demand as the share of total generation of the heat pumps. As a result, this formulation affects equation 5.32 and increases the potential of decoupling the heat production by charging the heat storages with a ff of 1. With these definition, the cogeneration of heat and power in CHP plants is not defined as sector coupling technology. Thus with an ff of 0, the storages can only be charged by CHP. Furthermore, in equation 5.34 exogenous hourly time series of temperature dependent district heating demand $dhe_{c,t}$ are used for each country, to formulate a time-dependent heat balance. The demand can be covered by CHP plants, heat pumps, heat storages $PTX_STOR_{pth,c,t}^{DIS}$ and gas boiler $BP_{c,t}^{GB}$. In equation (5.34), the corresponding

heat storage level $SL_{pth,c,t}^{PTX}$ is defined, taking heat inflows of heat pumps and CHP as well as outflows $PTX_STOR_{pth,c,t}^{DIS}$ into account. Furthermore, for the scenarios with enforced sector coupling a lower bound for the amount of heat provided by heat pumps is defined with sc in equation (5.36). Equations (5.37) to (5.39) restrict the heat pump capacity, the storage level as well as discharging power of the storage with the corresponding model-endogenous capacity variables. For the latter one, the heat pump capacity is utilized.

$$GEN_{chp,c,t} = (CHP_{chp,c,t}^d + CHP_{chp,c,t}^s) \cdot f^{chp} \quad \forall c \in C, t \in T, chp \in TE \quad 5.31$$

$$PTX_{pth,c,t} = \frac{(PTX_{pth,c,t}^d + PTX_{pth,c,t}^s)}{\eta_{pth}} \quad \forall c \in C, t \in T \quad 5.32$$

$$\frac{PTX_{pth,c,t}^d}{\eta_{pth}} \geq (1 - ff) \cdot PTX_{pth,c,t} \quad \forall c \in C, t \in T \quad 5.33$$

$$0 = dhe_{c,t} - \sum_{chp} CHP_{chp,c,t}^d - PTX_{pth,c,t}^d - PTX_STOR_{pth,c,t}^{DIS} - BP_{c,t}^{GB} \quad \forall c \in C, t \in T \quad 5.34$$

$$SL_{pth,c,t}^{PTX} = SL_{pth,c,t-1}^{PTX} + PTX_{pth,c,t}^s + \sum_{chp} CHP_{chp,c,t}^s - PTX_STOR_{pth,c,t}^{DIS} \quad \forall c \in C, t \in T \quad 5.35$$

$$\sum PTX_{pth,c,t} \cdot \eta_{pth} \geq sc \cdot \sum_t dhe_{c,t} \quad \forall c \in C \quad 5.36$$

$$PTX_{pth,c,t} \leq CAP_{pth,c}^{PTX} \quad \forall c \in C, t \in T \quad 5.37$$

$$SL_{pth,c,t}^{PTX} \leq CAP_{pth,c}^{PTX_STOR} \quad \forall c \in C, t \in T \quad 5.38$$

$$PTX_STOR_{pth,c,t}^{DIS} \leq CAP_{pth,c}^{PTX} \cdot \eta_{pth} \quad \forall c \in C, t \in T \quad 5.39$$

5.2.4.2 Constraints for the electrolyser-based hydrogen production

For the electrification of the industry's hydrogen demand with electrolyser, similar equations are applied as for PtH particularly regarding the allocation of the hydrogen flows (equation

5.40) and the definition of the flexibility factor (equation 5.41). However, since electrolyser are the only implemented PtG technologies, in equation (5.42) the hydrogen demand is only covered by direct hydrogen production $PTX_{ptg,c,t}$, discharging the hydrogen storages $SL_{ptg,c,t}^{PTX}$ and steam reforming $BP_{c,t}^{SR}$. Here, the hydrogen demand is assumed to be constant in each time step across a whole year and equally distributed for the total number of time steps T to meet the annual hydrogen need dhy_c . The hydrogen storage level equals the level of the time step before plus hydrogen in- and outflows $PTX_STOR_{ptg,c,t}^{DIS}$ (see equation 5.43). Equation (5.44) defines the lower bound for the hydrogen production based on electrolyser as share of the annual demand. Again, hydrogen production, storage level and storage discharging are limited by the corresponding installed capacity as in equations (5.45) to (5.47).

$$PTX_{ptg,c,t} = \frac{(PTX_{ptg,c,t}^d + PTX_{ptg,c,t}^s)}{\eta_{ptg}} \quad \forall c \in C, t \in T \quad 5.40$$

$$\frac{PTX_{ptg,c,t}^d}{\eta_{ptg}} \geq (1 - ff) \cdot PTX_{ptg,c,t} \quad \forall c \in C, t \in T \quad 5.41$$

$$0 = \frac{dhy_c}{T} - PTX_{ptg,c,t}^d - PTX_STOR_{ptg,c,t}^{DIS} - BP_{c,t}^{SR} \quad \forall c \in C, t \in T \quad 5.42$$

$$SL_{ptg,c,t}^{PTX} = SL_{ptg,c,t-1}^{PTX} + PTX_{ptg,c,t}^s - PTX_STOR_{ptg,c,t}^{DIS} \quad \forall c \in C, t \in T \quad 5.43$$

$$\sum_t PTX_{ptg,c,t} \cdot \eta_{ptg} \geq sc \cdot dhy_c \quad \forall c \in C \quad 5.44$$

$$PTX_{ptg,c,t} \leq CAP_{ptg,c}^{PTX} \quad \forall c \in C, t \in T \quad 5.45$$

$$SL_{c,t}^{HYS} \leq CAP_{ptg,c}^{PTX_STOR} \quad \forall c \in C, t \in T \quad 5.46$$

$$PTX_STOR_{ptg,c,t}^{DIS} \leq CAP_{ptg,c}^{PTX} \cdot \eta_{ptg} \quad \forall c \in C, t \in T \quad 5.47$$

5.2.4.3 Constraints for the private passenger transport sector

Compared with PtH and PtG, the implementation of EV in the model formulation differs stronger. The respective mathematical description partly relies on Schill et al. (2016). At first,

the EV charging profile is defined based on the normalised country-specific hourly charging profiles for a single car. Thus in equation (5.48), the multiplication with $CAP_{ev,c}^{PTX}$ (representing the total number of EV in each country) yields in the total hourly electricity demand for $EV_{c,t}$. By converting the energy demand of both, EV as well as the corresponding benchmark process BP_c^{ICE} , with respective efficiency, the resulting vehicle kilometre can be calculated. In equation (4.49), the sum has to be equal the overall mileage forming an annual balance. In the EV storage equation (4.50), representing the hourly state of charge of the EV connected to the grid, the charging profile $EV_{c,t}$ is a time-varying hourly reduction of the aggregated battery level $SL_{ev,c,t}^{PTX}$ due to consuming electricity while driving the EV. In the overall electricity balance (see equation (5.6)), the flexibility factor ff controls on the one hand inflexible EV to be immediately charged based on $(1 - ff) \cdot EV_{c,t}$. This affects vice versa the available BEV battery capacity in equation (4.50). On the other hand, the hourly electricity demand for charging and discharging the EV batteries is increasing or decreasing $SL_{ev,c,t}^{PTX}$ in equation (4.50) as well as simultaneously the overall electricity balance. However, the availability of the storage capacity as well as storage power is controlled by ff again, as formulated by equations (5.51) to (5.53). Thereby, the available upper bound of the storage capacity depends on the flexibility factor, the number of EV $CAP_{ev,c}^{PTX}$ as well as an assumed storage capacity per EV (equation 5.51). In equation (5.52) and (5.53), the charging and discharging of the EV batteries is again restricted by ff and the number of EV. Additionally, the availability of the EV is restricted by an hourly parking profile $norm_{c,t}^{ev,p}$, limiting the power available for the storage use. Thus, with $ff=0$, the EV are charged immediately as part of the overall electricity balance according to the charging profile. In this case, the storage of each EV is theoretically existing as well, but not accessible for the model optimisation, since all storage parameter are set to zero. As soon as ff is defined to be one, the EV batteries become available in the model formulation. Finally, in equation 5.54, the kilometres driven with EV are constraint by a share on total kilometres per country as a lower bound, representing the enforced sector coupling in the transport sector.

$$EV_{c,t} = CAP_{ev,c}^{PTX} \cdot norm_{c,t}^{ev,cha} \quad \forall c \in C, t \in T \quad 5.48$$

$$0 = ev^{km} - \frac{\sum_t EV_{c,t}}{\eta^{ev_km}} - \frac{BP_c^{ICE}}{\eta^{ice}} \quad \forall c \in C, t \in T \quad 5.49$$

$$SL_{ev,c,t}^{PTX} = SL_{ev,c,t-1}^{PTX} + PTX_STOR_{ev,c,t}^{CHA} \cdot \eta_{ev} - \frac{PTX_STOR_{ev,c,t}^{DIS}}{\eta_{ev}} - ff \cdot EV_{c,t} \quad \forall c \in C, t \in T \quad 5.50$$

$$SI_{ev,c,t}^{PTX} \leq ff \cdot CAP_{ev,c}^{PTX} \cdot ev^c \quad \forall c \in C, t \in T \quad 5.51$$

$$PTX_STOR_{ev,c,t}^{CHA} \leq ff \cdot CAP_{ev,c}^{PTX} \cdot ev^p \cdot norm_{c,t}^{ev,p} \quad \forall c \in C, t \in T \quad 5.52$$

$$PTX_STOR_{ev,c,t}^{DIS} \leq ff \cdot CAP_{ev,c}^{PTX} \cdot ev^p \cdot norm_{c,t}^{ev,p} \quad \forall c \in C, t \in T \quad 5.53$$

$$\frac{\sum_t EV_{c,t}}{\eta_{ev,km}} \geq sc \cdot ev^{km} \quad \forall c \in C \quad 5.54$$

5.3 Data input

The model formulation presented above requires a broad range of data to characterise the technologies with technical and economic data. Thereby, the expansion of these flexibility options is modelled endogenously. In contrast, the iRES capacities and generation time series, derived as a result of the model-based flexibility demand analysis, are exogenous input affecting the country-specific residual load in the energy balance. In the following, the data gathering and processing steps for the flexibility options in the electricity sector, including several power plant technologies, storages and DSM processes as well as NTC are described. Afterwards, the data requirements for implementing the PtX technologies are presented.

5.3.1 Electricity sector

Several power plants are included in the present work, implemented as aggregated technology types. For fossil-fuel based power plants the relevant technical parameter are the generation efficiency, the CO₂ emission factor and load change-related parameter (ramping cost of depreciation as well as ramping fuel demand), as listed in Table 5.2. Additionally, energy-policy induced maximum capacity restrictions are introduced for coal, lignite and nuclear power plants. For all but three (Czech Republic, Norway and Poland) of the 17 countries being members of the so-called Powering Past Coal Alliance (PPCA 2020) no installations in coal and lignite power plants are allowed. For Norway, this restriction is applied as well, since currently no coal capacities are installed. Furthermore, only the countries Czech Republic, France and Great Britain, currently building or planning new installations, are allowed to invest in nuclear power plants.

Table 5.2: Technical data for fossil fuel-based power plants (Data: Zöphel et al. 2019, Schröder et al. 2013)

	Generation Efficiency	CO ₂ Emission Factor	Ramping Cost Depreciation	Ramping Fuel Demand	Maximum Capacity Restriction
	[%]	[tCO ₂ /MWh _{th}]	[EUR/MW _{el}]	[MWh _{th} /MW]	
Gas OC*	0.39	0.550	10	3.5	
Gas CC**	0.61	0.330	10	3.5	
Gas CHP	0.36	0.330	10	3.5	
Coal	0.46	0.690	5	6.2	✓
Lignite	0.45	0.850	3	6.2	✓
Coal CHP	0.23	0.690	5	6.2	✓
Lignite CHP	0.23	0.850	3	6.2	✓
Nuclear	0.34	0.000	2	17.0	✓
Oil CC	0.50	0.330	10	4.0	

* Open Cycle Gas Turbine (OCGT), ** Closed Cycle Turbine (CCGT)

Table 5.3: Economic data for fossil fuel-based power plants (Data: Zöphel et al. 2019, NEP 2015, EA 2013, Bertsch et al. 2012, Fürsch et al. 2013, Schröder et al. 2013)

	Capital Cost	Fixed Cost	Variable Cost	Fuel Costs	Lifetime
	[kEUR/MW _{el}]	[kEUR/MW _{el}]	[kEUR/MW _{thel}]	[EUR/MW _{th}]	[a]
Gas OC*	400	15	3.00	33.70	25
Gas CC**	800	20	4.00	33.70	30
Gas CHP	1,050	20	4.00	33.70	30
Coal	1,300	25	6.00	10.40	45
Lignite	1,500	30	7.00	1.50	45
Coal CHP	1,700	25	6.00	10.40	45
Lignite CHP	1,900	30	7.00	1.50	45
Nuclear	6,000	12	5.00	3.24	60
Oil CC	800	6	4.00	86.20	25

* Open Cycle Turbine, ** Closed Cycle Turbine

For both, fossil fuel-based and renewable CHP, a CHP factor of 0.7, defining a fixed proportional relationship between electricity and heat production, is assumed. The production of heat and

power can be decoupled by heat storages. The heat supply thereby follows an hourly country-specific heat profile, introduced in Chapter 5.3.2. In Table 5.3, listing economic data for conventional power plants, extra costs (for extracting and distributing heat) for CHP are taken into account based on Fürsch et al. (2013), resulting in additional capital costs of 250 kEUR/MW_{el} for gas CHP and 400 kEUR/MW_{el} for coal and lignite CHP compared to power plants. Fuel costs are exogenous parameter and assumed to be independent from the actual demand. While assumptions on future fuel costs are derived based on BNetzA (2015), EA (2013) and Bertsch et al. (2012), the remaining costs parameters are relying on data found in Fürsch et al. (2013) and Schröder et al. (2013). To discount capital costs on annual basis, annuity factors including the lifetime and an interest rate of 8 % is assumed. Furthermore, emission specific costs are calculated, taking a CO₂-price of 80 EUR/tCO₂ into account. The technology and cost assumptions as well as exogenous expansion restrictions significantly influence the role of single technologies. While neglected in the present work, the Carbon Capture and Storage (CCS) technology plays varying roles in similar works (see also Zöphel et al. 2019). CCS is not included in the present work due uncertainties of this technology in the future energy system²¹. However, compared with the CCGT technology, CCGT power plants with CCS become cost optimal under the present assumptions with a CO₂ price of 96 EUR/tCO₂²², compared to 80 EUR/tCO₂.

The technical and economic data for controllable RES plus run-of-river (RoR) power plants, based on Gils et al. 2017, Schröder et al. 2013, Scholz 2012, can be found in Table 5.4 and Table 5.5. Thereby, maximum capacities are assumed, to take restrictions in generation potential and available area into account. The corresponding values for each country can be found in Table C.1 in Appendix C.1. Existing capacities for hydro power plants are included without causing capital costs, since the significant country-specific installation are assessed as favourable for the European energy transaction. According to ENTSO-E (2018), the total installed capacities for the observed region amount to around 85 GW for Reservoir and 49 GW for RoR power plants. While in contrast existing capacities for CSP and geothermal power plants are lower, biomass is implemented with an upper expansion potential existing capacities are neglected, since the role of biomass in the energy supply is rather uncertain (see e.g. Zöphel et al. 2019). For CSP

²¹ See for example Budinis et al. (2020) as well as Viebahn & Chappin (2018) for an overview on costs, potentials and barriers of the CCS technology.

²² This value is derived by equating the levelised cost of electricity for CCGT w/o and with CCS with values of Zöphel et al. (2019) and Schröder et al. (2013), assuming a carbon capture rate of 0.88, a power plant efficiency of 0.52, specific investment costs of 1,071 kEUR/MW and variable costs of 24,07 EUR/MWh for CCS plants, while further techno-economic parameter are similar to those of the CCGT power plants in Table 5.2 and 5.3.

power plants, heat storages are required, assuming the same techno-economic characteristics as introduced in Chapter 5.3.2.

Table 5.4: Technical data for RES (Data: Gils et al. 2017, Schröder et al. 2013)

	Generation Efficiency	Ramping Fuels	Ramp Cost Depreciation
	[%]	[MWh _{th} /MW]	[EUR/MW _{el}]
Reservoir	(1.00)	0.0	0
RoR	(1.00)	0.0	0
Biomass CHP	0.45	6.2	3
Geo	0.25	0.0	10
Geo CHP	0.25	0.0	10
CSP	0.37	0.0	10

Table 5.5: Economic data for controllable RES (Data: Gils et al. 2017, Schröder et al. 2013, Scholz 2012)

	Capital Cost	Fixed Cost	Variable Cost	Fuel Costs	Lifetime
	[kEUR/MW _{el}]	[kEUR/MW _{el}]	[kEUR/MWh _{el}]	[EUR/MWh _{th}]	[a]
Reservoir	(2000)	20	0.10	0.00	(55)
RoR	(3000)	60	0.10	0.00	(55)
Biomass CHP	2000	100	6.00	7.00	25
Geo	7600	80	23.30	0.00	25
Geo CHP	8000	80	23.30	0.00	25
CSP	3000	30	0.00	0.00	25

Similar to the controllable hydropower plants, PSP are included in the model analysis with existing capacities (in total 36 GW) as well as storage energy (13,477 GWh) based on ENTSO-E (2018) and JRC (2013). The high storage energy capacity mainly results from Norwegian PSP plants. Additionally, investments in three different generic storage types is allowed, represented by the techno-economic parameter presented in Table 5.6 and based on data of REFLEX 2019, FfE 2016 and Schill 2014. The storages differ in efficiencies and energy-to-power ratio (EPr) as well as corresponding cost assumptions to include a range of storage application potentials. Thereby, hourly storage (HOU) can be assessed as battery storages for short-term balancing with an energy-to-power ratio of 2. Daily storages (DAY) are suitable for electricity

shifting during a day, with characteristics similar to redox-flow batteries. Furthermore, seasonal storages allow for storing electricity over longer time frames at the expense of lower efficiencies. The variable costs depicted in Table 5.6, are dispatch costs without the model-endogenous electricity costs of charging the devices.

Table 5.6: Techno-economic data for electricity storages (Data: REFLEX 2019, FfE 2016, Schill 2014)

	Discharge Efficiency	Charge Efficiency	EPr	Variable Cost	Fixed Cost	Capital Costs	Lifetime
	[%]	[%]		[kEUR/MWh _{el}]	[kEUR/MW _{el}]	[kEUR/MW _{el}]	[a]
PSP	90%	89%	Exist.	1.0	16.00	(640)	(30)
HOU*	95%	98%	2	0.5	5.18	199	15
DAY**	90%	98%	10	0.5	22.02	752	15
SEA***	57%	75%	200	0.5	21.96	1098	40

*Hourly Storage, ** Daily Storage, *** Seasonal Storage

For the data input of the DSM applications three main steps are required to gather the respective parameter. Firstly, available maximum capacities for selected DSM processes have to be derived, forming the upper bound of DSM installations in the model analysis. Secondly, normalised time-series of process availability are applied to limit this potential on hourly basis. Thirdly, by introducing techno-economic characteristics, the dispatch of the DSM measures observed is further restricted.

Based on detailed European DSM potential estimations in Gils (2014), selected capacities are transferred for the present analysis. Thereby, the categorisation of DSM processes partly relies on Gils (2016). A table of the assignment of these processes to the selected main categories is given in Appendix C.1 (Table C.2). Compared to Gils (2014), the process distinction is less detailed to limit the computational time. Omitted processes are on the one side heating applications, which are examined as sector coupling technologies in the present work. On the other side, the household sector is neglected, due to data issues for the whole region observed. Additionally, it is assumed, that the willingness of households to participate in DSM is less economically rational and an aggregation to a significant potential requires a high coordination effort, compared to the other sectors (Müller & Möst 2018). However, the included processes give a good guidance of characteristics for DSM measures in the tertiary and industry sector. In total, the following three aggregated DSM processes for shifting and one process for shedding electricity demand are selected Gils (2016):

- Air conditioning and ventilation for shifting (ACVen)
- Cooling and water treatment (CoolW)
- Industry processes (IndShi)
- Industry processes (IndShe)

With air conditioning and ventilation, commercial and industrial air conditioning as well as ventilation and retail cooling are combined. Cooling and water treatment represents DSM potential in cooling industry and catering, cold stores as well as water supply and treatment. Furthermore, two processes combine applications of the industry for shifting (IndShi), aggregating the pulp, paper, cement, calcium carbide (CaC₂) and air separation industry as well as shedding (IndShe), including the aluminium, copper, zinc as well as steel and chlorine industry. The determined maximal potentials are illustrated in Figure 5.3. Accordingly, Germany and France show the highest value with almost 10 GW potential, followed by Italy and Spain with around 7 GW. In each country, air conditioning and ventilation (ACVen) contributes with the highest share within the DSM processes.

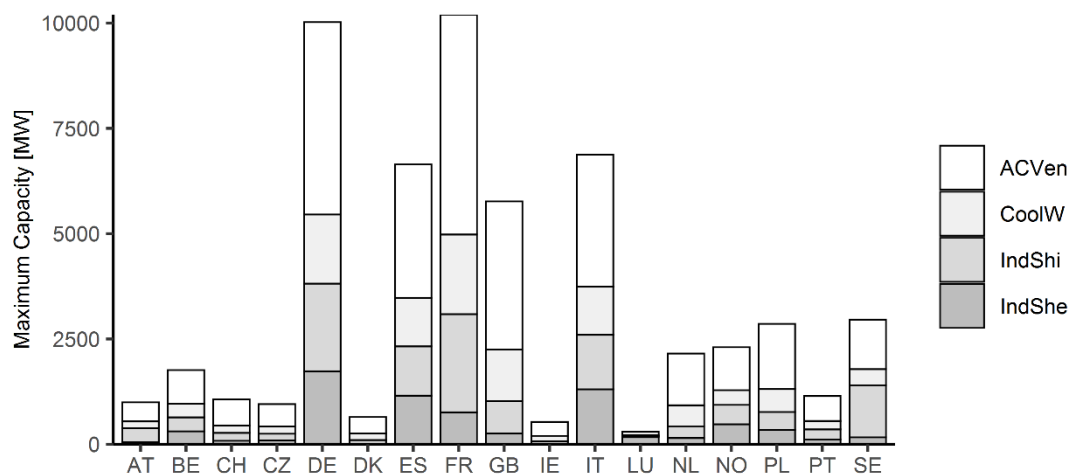


Figure 5.3: Maximum potentials of the selected DSM processes per country (Own illustration based on Gils (2016, 2014))

For the hourly availability of these processes, the temperature-sensitive applications air conditioning and ventilation as well as cooling and water treatment plus the industry shifting process are characterised by a time-dependent profiles, based on normalised time series of Müller (2019). Figure 5.4 shows an exemplary week for Germany for the different processes. The highest temperature sensitivity shows air conditioning and ventilation, while cooling and water treatment processes are also affected, but characterised by a higher inertia regarding temperature changes. For industry shifting process, the original production processes are reflected by valleys during the day and peaks during night as well as a generally higher

potential during weekends. In contrast the potential for shedding industry processes is constant at 100%. Country-specific differences of these availability curves are implemented for air conditioning and ventilation as well as cooling and water treatment based on adjustments regarding the average temperatures derived from the MERRA-2 dataset.

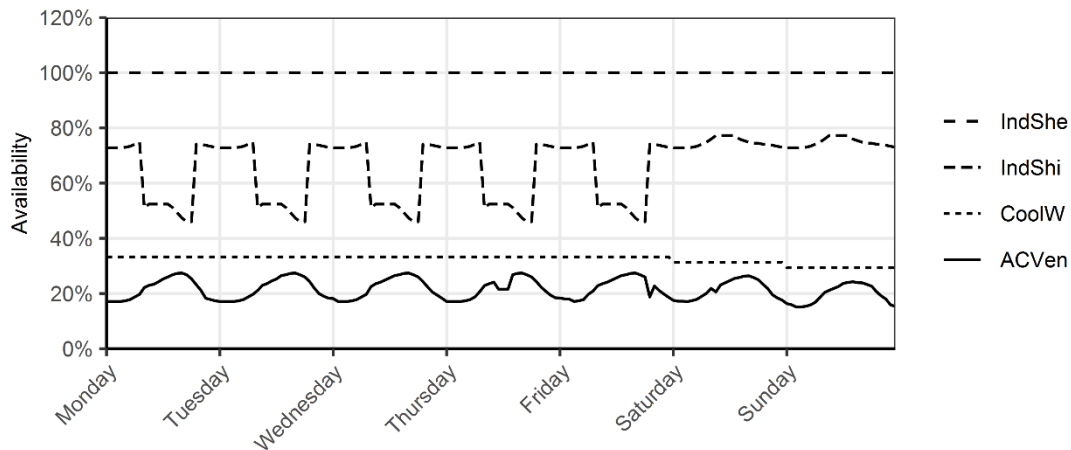


Figure 5.4: Availability of DSM processes in an exemplary summer week in Germany (Own illustration based on Müller 2019)

Finally, the different processes are characterised by technical data constraining maximum shifting time and maximum number of activation per day as well as cost data, as listed in Table 5.7. Thereby, it is assumed, that industry processes are already equipped with the ICT, therefore investments are already realised. In contrast, the higher opportunity costs for shifting and particularly for shedding these processes are reflected in higher variable (activation) costs, compared to air conditioning and ventilation as well as cooling and water treatment. Data input for the flexible electricity demand of sector coupling technologies (which also can be categorized as DSM applications) are discussed separately in the following chapter. Furthermore, regarding the categorisation of flexibility options, the three load shifting processes are within the category of technologies for providing shifting flexibility, while load shedding is assigned to the downward flexibility options.

Table 5.7: Techno-economic data of DSM processes (Data: Ladwig 2018, Gils 2016, 2014)

DSM process	DSM type	Maximum shifting time [h]	Maximum number of activations	Capital costs [EUR/MW _{el}]	Variable costs [EUR/MWh _{el}]
ACVen	shifting	2	4	10000	5
CoolW	shifting	6	8	5000	20
IndShi	shifting	48	24	0	150
IndShe	shedding		24	0	1000

A hybrid HVAC/HVDC is seen as a key feature in the future interconnected European electricity system (TYNDP 2018). In the present model, the NTC between two countries defines the maximum tradable electricity flow within one hour and is calculated model-endogenously as well. For the cost assumptions for NTC some simplifications are made. Expansions of NTC are allowed with distance-dependent costs of 500 EUR/MW/km as well as additional costs for converter stations of 75,000 EUR/MW (EWI 2011) assuming a combination between upgrading existing cross-border HVAC lines and the installation of new HVDC lines including converters. To transfer the distance dependent costs in EUR/MW, the connection between the centres of each country are applied, taking implicitly the country size into account as well as further grid expansion measures within each country. Grid constraints within a country are not explicitly modelled. Furthermore, an interest rate of 7 % and an amortization time of 40 years is assumed (Gils et al. 2017, EWI 2012). Existing capacities are included based on static values of the Mid-term Adequacy Forecast 2019 (ENTSO-E 2020). Table C.3 in Appendix C.1 gives an overview of the capacities included.

5.3.2 Sector coupling technologies

For PtX technologies and corresponding energy storages further data input is required, combining two steps each. Firstly, to quantify the enforced electrification of the three underlying energy end-use sectors, an annual energy demand has to be determined. Secondly, the hourly dispatch of the technologies has to be restricted, based on time series. In Figure 5.5 an overview on gathered data per country for the selected PtX options is given. For the dispatch of heat pumps, but also CHP, heat storages and gas boiler, the annual and hourly district heat demand for the tertiary and residential sector is taken into account and described at first below. Afterwards, the hydrogen demand for industry is estimated to define the amount of electricity required to be covered by electrolyser and hydrogen storages in the sector coupling scenarios.

Finally, BEV are characterised by three hourly profiles and the annual energy demand is derived based on mileages of passenger cars per country.

	Tertiary and residential district heat demand	Hydrogen demand for industry	Energy demand for passenger cars
Annual energy demand per country	<ul style="list-style-type: none"> Delivered energy for space and water heating Efficiency gains until 2050 	<ul style="list-style-type: none"> Demand for four processes Development until 2050 Distribution according to production capacities 	<ul style="list-style-type: none"> Average annual mileage per passenger car Vehicle stock Energy consumption of passenger cars
Hourly time series of energy demand per country	<ul style="list-style-type: none"> Based on gas standard load profiles Temperature time series Sigmoid coefficients and hourly heat profiles Distinction between tertiary and 	<ul style="list-style-type: none"> Assumption on constant hydrogen demand for each hour 	<ul style="list-style-type: none"> Two daily charging profiles per BEV Availability profile per BEV Distinction between weekdays and weekends

Figure 5.5: Overview on data requirements for PtX technologies (Own illustration)

The basis for the hourly country-specific heating demand is the assumed future development of the annual heat demand. In the present work, the assumptions are based on data on delivered energy for space and water heating in the European heat roadmap (Paardekooper et al. 2018) and the corresponding online data sets (HRE 2020). For the time horizon 2050, efficiency gains for space heating of 25 % and an increase in energy demand for water heating of 11 % are assumed, based on these sources. In Figure 5.6, the resulting district heating demand is displayed for the target year. The aggregation of space and water heating requirements for the tertiary and residential sector results in a total demand of more than 2,420 TWh_{th} in the observed region.

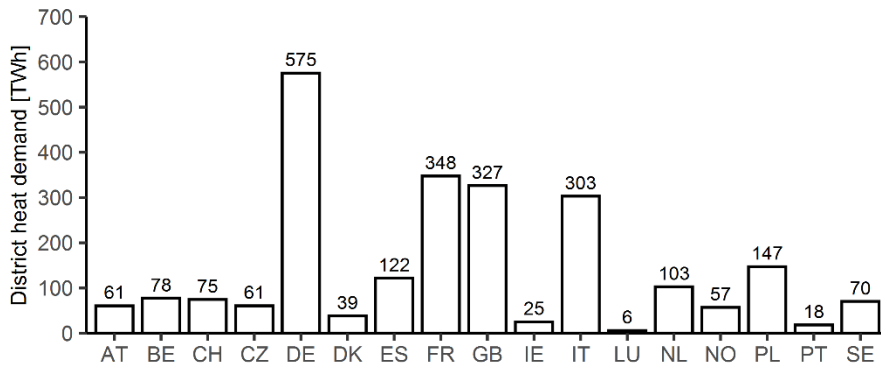


Figure 5.6: Annual district heat demand per country in the target year (Own illustration based on Paardekooper et al. 2018)

Furthermore, for the heat supply technologies CHP, PtH with heat pumps, heat storages as well as gas boilers, normalised hourly time series for the heating demand in each country are applied. To derive aggregated ambient temperature sensitive heat profiles for each country, the equations and data used in the present work is described in detail in Appendix C.2. Based on the gas standard load profile methodology of BDEW (2018) and BGW (2006), as for example also applied in Ruhnau et al. (2019), daily reference temperatures as weighted mean of the daily average ambient air temperature of the actual day are calculated. Thereby, MERRA-2 temperature data (2 m above ground) is applied and aggregated to average country-specific temperature time series. For the calculation of hourly heat load profiles, hourly demand factors as share of the daily heating demand, are multiplied with standardised sigmoid coefficients based on BDEW (2018). As a simplification, the same sigmoid coefficients are applied for each of the 17 countries. As a result, normalised country-specific district heat profile for an entire year can be derived. Finally, the normalised time series can be aggregated taking the yearly heat demand into account. In Figure 5.7, exemplary daily averages of the heat demand over the whole year in the countries Germany and France are displayed, reflecting differences in total heat demand and temperatures as well as structure of residential and tertiary sectors. Additionally, in both countries a base heat demand becomes obvious, resulting from a constant need for water heating.

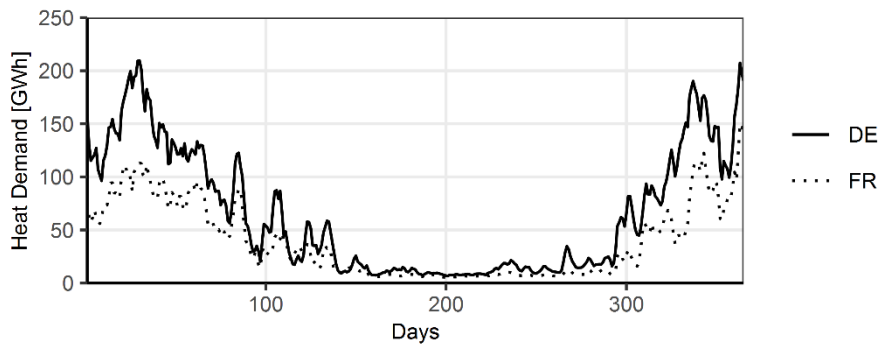


Figure 5.7: Exemplary time series of daily average heat demand in Germany and France for the target year (Own illustration)

For the time series regarding the hydrogen production for the industry, a constant value for each hour per country is assumed. In addition, the annual hydrogen demand defines the required capacities to meet this demand. According to Fraile et al. (2015), the highest hydrogen demand in the industry in the year 2013 occurred for producing ammonia (3.6 Mt), refinery products (2.1 Mt), other chemicals (0.7 Mt) and crude steel (0.4 Mt). Regarding the future development, a yearly growth in industries hydrogen demand of 3.5 % per year until the year 2030 is assumed based on Fraile et al. (2015). Assuming a yearly growth of 1.75 % for 2050 results in 12 Mt hydrogen demand for the European industry sector. To assign the total hydrogen demand to each country, data on European production capacities for ammonia (Egenhofer et al. 2014), refinery products (FoEE 2015) and crude steel WSA (2017) are gathered. Due to data issues, for processes aggregated as other chemicals, methanol production capacities are taken into account based on Burrige (2009). According to these data sources, the share of hydrogen production of the 17 countries observed in the present work at total EU-28 countries amounts to 73 % for ammonia, 43 % for methanol, 85 % for refinery products (including hydrogen production, hydrocracking and hydrotreating) and 90 % for crude steel production. Thus, in total, an amount of 9 Mt hydrogen is required in the region observed. The share of the four distinguished hydrogen processes on total hydrogen demand as well as the country-specific share of production capacity are used to assign total hydrogen demand per country. While in Table C.5 in Appendix C.1, this allocation is listed, the annual hydrogen demand per country is illustrated in Figure 5.8 with Germany, Netherlands and Poland accounting for more than half of the total demand (299 TWh).

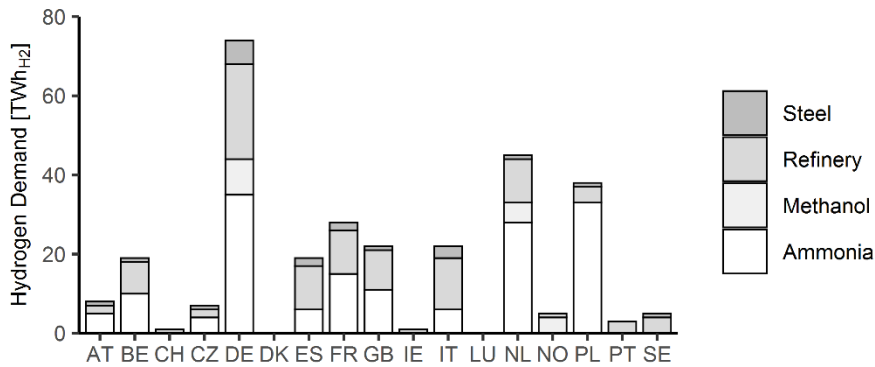


Figure 5.8: Hydrogen demand for industry per country in the target year (Own illustration)

For the calculation of the potential of BEV, both the annual mileage of passenger cars per country as well as time series limiting the accessibility and thus flexibility of BEV (storages) are required. Thereby, data issues necessitate a mapping of countries with no data to countries with information available based on Heinrichs (2013). For the annual mileage per country, average values per passenger car of the year 2015 can be found for the countries Germany, Austria, Spain, France, Italy, Netherlands and Great Britain based on the Odyssee Project (ADEME 2020). Together with data on the country-specific vehicle stock, based on ACEA (2019), total mileages can be determined, as listed in Table C.6 in Appendix C.1.

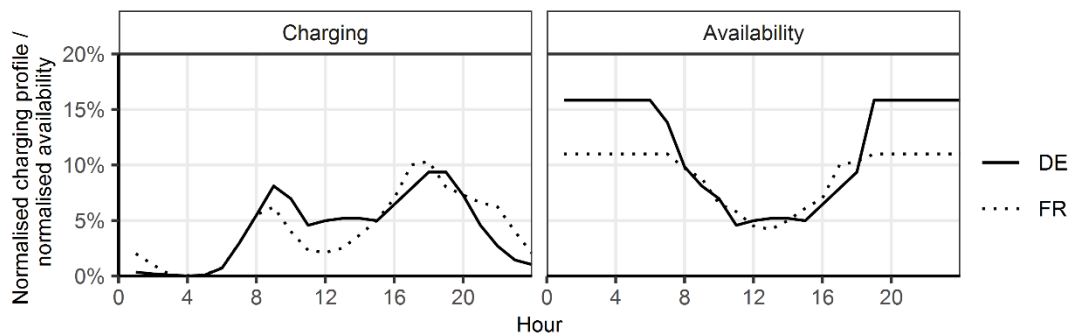


Figure 5.9: Exemplary normalised daily (immediately) charging profiles and availability profiles of BEV car fleet in Germany and France (Own illustration based on Heinrichs 2013)

Furthermore, regarding the energy consumption of single BEV, the average energy demand for passenger cars is 0.178 kWh/km for BEV and 0.458 kWh/km for ICE, based on Trost (2016). To distinguish the energy demand between weekdays and weekends, data on daily driving distance and travel time is gathered based on the European mobility survey (Pasaoglu et al. 2012). Multiplying the distance with the energy demand per car results in daily energy demand, which is later adjusted to the annual mileage, since more data for the 17 countries is available. Furthermore, two daily charging (immediately charging and late charging) profiles are derived

based on Heinrichs (2013)²³. The immediately charging profile defines the electricity demand time series for inflexible sector coupling with BEV ($ff=0$). Both charging profiles are used to define a third profile, the availability (or parking) profile, for BEV, limiting the available BEV storage and charging capacity in case it can be accessed in scenarios with more flexible sector coupling ($ff=1$). The calculation of the amount of BEV, available for charging and discharging measures is based on the maximum of both charging profiles and a projection of the peak charging demand into the night hours. As formulated in the model description (see equation (5.44)), the charging demand of the BEV has to be covered either way. The normalised profiles of Heinrichs (2013) are applied for the 17 countries in the present work, taking differences regarding weekdays and weekends as well as regarding the country-specific energy demands for passenger transport into account. Exemplary daily profiles, again for Germany and France, are illustrated in Figure 5.9. The charging profiles represent the energy demand for the BEV on hourly basis. Between the countries, the structural differences regarding driving patterns become obvious.

Additionally to the determination of annual and hourly energy demand for the three selected sectors, the techno-economic characteristics of the corresponding PtX technologies and energy storages are presented with varying units in Table 5.8 and Table 5.9. Data on heat pumps and electrolyser are based on REFLEX (2020) and Gulagi et al. (2017), while BEV are described relying on Ladwig (2018) and Trost (2016). Own assumptions were made regarding the EPr of the heat and hydrogen storages, allowing for comparably high energy amounts. Costs for batteries in BEV are already included in the capital costs for the car.

Table 5.8: Techno-economic data of PtX technologies (Data: REFLEX 2020, Ladwig 2018, Gulagi et al. 2017, Trost 2016)

	Capital Cost	Lifetime	Fixed Costs	Efficiency
Heat pump	300 kEUR/MW _{el}	40 [a]	5 kEUR/MW _{el}	4.00 [MWh _{el} /MWh _{th}]
Electrolyser	784 kEUR/MW _{el}	20 [a]	84 kEUR/MW _{el}	0.80 [MWh _{el} /MWh _{H2}]
BEV	38 kEUR/BEV	10 [a]	---	0.18 [kWh _{el} /km]

²³ In Heinrichs (2013), the charging curves are generated based on mobility studies, allowing for information about start- and end times of car uses as well as distances and parking locations in selected countries.

Table 5.9: Techno-economic data of energy storages for sector coupling (Data: REFLEX 2020, Ladwig 2018, Gulagi et al. 2017, Trost 2016)

	Capital Cost	Lifetime	EPr	Efficiency
Heat storage	9,209 EUR/MW _{th}	20 [a]	200	0.2 [%/h]
Hydrogen storage	5,000 EUR/MW _{H2}	40 [a]	200	0.1 [%/h]
BEV storage	---	---	11 kW/25 kWh*	1.78 [MWh _{el} /km]

Assuming a targeted sector coupling with a share of at least 50 % of electricity in the energy end-use sectors heating (by heat pumps), hydrogen for industry (by electrolyser) and passenger transport (by BEV) with the efficiencies introduced above, the original country-specific electricity demand is increased by up to 40 % in the Netherlands and Poland (see

Figure 5.10. Under these assumptions, the original cumulated electricity demand of 2709 TWh is increased in total at least by 303 TWh for heat provision, by 187 TWh for hydrogen production and by 272 TWh for BEV. Compared with the iRES surpluses in the FD scenarios (see Chapter 4.2, Table 4.1), the minimal additional electricity demand due to sector coupling (762 TWh) is corresponding to 161 % (High PV), 348 % (REF) and 1030 % (High Wind) of the scenario-specific surplus energy. However, electricity demand still has the highest share in total energy demand included in the present work, while an electricity demand increase due to sector coupling beyond 50 % of the energy end-use demand will be a model-endogenous results.

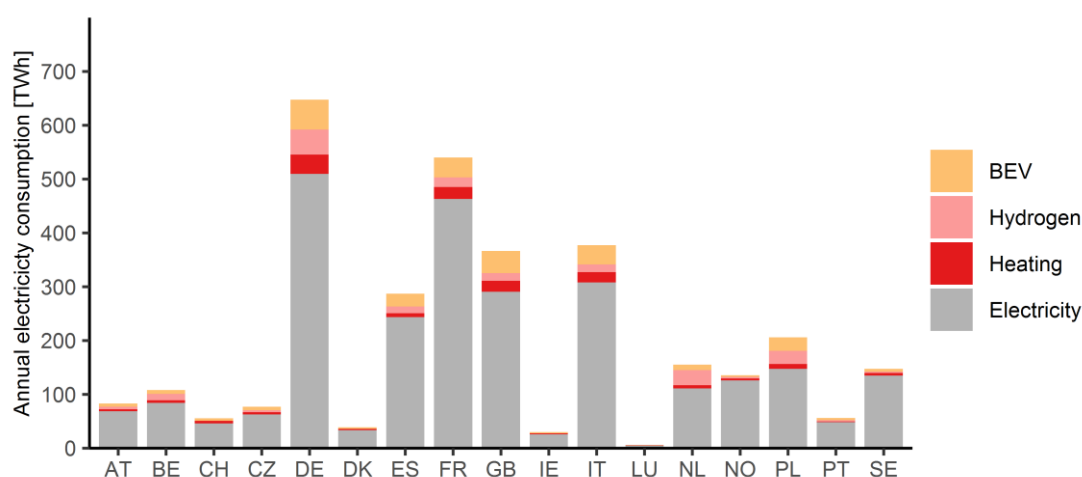


Figure 5.10: Annual electricity consumption including minimum additional electricity demand of the sector coupling technologies (Own illustration)

As mentioned before, the benchmark processes are included in the model with their respective generation costs to reflect the opportunity costs for the sector coupling technologies. These levelised costs are calculated as in Michaelis (2018) and similar to the concept of Levelized Costs of Electricity with the parameter listed in Table C.7 in Appendix C.1. Table C. Thereby, these costs consist of the annualised specific capital costs related to assumed full load hours (for gas boiler and steam reformer) and annual country-specific driving distances (for ICE cars) plus the variable costs including costs for fuels and CO₂ emissions. As a result, levelised costs of 56 EUR/MWh_{th} for gas boiler, of 79 EUR/MWh_{H2} for steam reformer and between 32 and 39 EUR/100 km for ICE based cars are calculated for the benchmark technologies. Finally, the levelised cost of the benchmark technologies can be calculated, resulting in 77 EUR/MWh_{th} for the gas boiler, 114 EUR/MWh_{th} for steam reformer as well as costs for ICE ranging between 0.50 and 0.60 EUR/km depending on the average driving distance.

5.4 Limitations of the modelling approach

The underlying assumptions in the present modelling approach are reflecting real world interactions in a simplified way. This concerns the key assumptions of an optimisation approach with perfect competition and perfect foresight in a central planner's perspective. The application of these models has been proven as suitable to fundamentally derive cost-based investment and dispatch decision in energy markets. However, the derived results should be interpreted taking the simplifications into account. A dispatch of all technologies involved solely based on price signals, as modelled in the present work, is a desired framework with regard to a market based flexibility provision. The value of price signals to reflect the need for flexibility is therefore also seen very high by the energy policy (see e.g. BMWi 2015). However, especially with rather small-scale technologies, like batteries, heat-pumps or BEV, a rational cost-minimisation based dispatch is less likely or at least requires convincing business models. This is especially true, when flexible technologies and PtX technologies (see for example BEV) are property of private households, where investment decisions are often driven by further aspect besides techno-economic ones. In addition, dispatch decisions are often based on comfort needs and inflexible retail electricity prices. Nevertheless, an increased electricity market driven dispatch of these technologies is likely (and therefore suitable for the present work), due to programs exploiting the flexibility potentials also on electricity consumer side, including the roll-out of smart meters and the aggregation of decentralised prosumers (BMWi 2015). A further aspect with regard to simplification in the presented model formulation concerns the level of detail of technologies implemented in the present model. While different flexibility options are included technology-specific, a further increase of detail to single plant or units enables more specific discussion of dispatch decisions. In addition, the regional resolution higher than on country-level offers

possibilities to assess local differences ideally when also taking national transmission and distribution electricity grids into account. This higher resolution may impact the optimal mix of flexibility options and leads to diverging synergy and competition effects. However, besides possible data issues, a higher detail significantly increases the computational effort. When interpreting the results, the large-scale perspective should be kept, while single technology owner's decisions or framework conditions for local flexibility accesses are excluded.

With similar influences on data gathering and computational effort, the regional and energy system related coverage can be seen as limitation. Taking further countries or regions as well as sectors of the energy system into account allows for the identification of additional potentials and interactions. Regarding the latter point, this concerns on the one hand the inclusion of additional parts of the energy end-use sectors. The focus of the present work on key technologies for sector coupling restricts a holistic analysis of potentials and challenges regarding the decarbonisation and/or electrification as well as flexibility provision in these sectors. On the other hand, by excluding further sub-markets in the energy system also the flexibility provision potential of single technologies might be under- or overestimated (see e.g. the role of storages in balancing markets).

The implemented greenfield approach is furthermore of high importance for the result interpretation. Although this may limit the transferability of the outcome to today's structures, the system-independent greenfield approach enables the isolation of interactions between flexibility demand and flexibility supply in an optimal electricity system. Additionally, since the examination of the system transformation is done in a long-term perspective, the structural changes for the present energy system in the presence of ambitious decarbonisation targets are assumed to be significant and only partly techno-economic driven. Policy incentive and funding programs will most likely further enforce the developments of low-carbon technologies. This means, the future technology mix will be very different from today's system, considering climate policy interventions and new boundary conditions (Schyska et al. 2020). While the validation of the ELTRAMOD model family shows good results in previous works, a calibration of a greenfield model to the existing power system is not convenient, since it is not the aim to reproduce historic system results. Nevertheless, besides the transparent inclusion and documentation of valid model input data, the application of scenarios and sensitivities further aims at increasing the overall transparency as well as traceability of the modelling results. Finally, the willingness and ability of all actors involved to participate in this energy system transformation is a main assumption, enabling the present techno-economic analysis. However, in this large-scale perspective the implementation on regional, national and international level requires further effort and research. However, the present modelling approach is seen as

valuable to give insights in optimal technology combinations, to shed light on required framework conditions and thus, to increase the required acceptance.

Taking the considerations above into account, the present choice of modelling framework is driven by the research questions, while the method and model applied is seen as suitable for further research with varying foci. In general, besides the aforementioned simplifications, the optimal outcomes most likely diver from real world observations due to reasons like market power and uncertainties. Generally, the results should be interpreted regarding the trade-offs and interactions between the research framework and the technologies included. Therefore, the present analysis is rather valuable to give benchmarks of optimal solution spaces whereas the future development pathways most likely are within this range.

6 Techno-economic analysis of optimal combinations of flexibility options

The two-dimensional scenario framework allows to investigate the effects of varying degrees of flexibility in the energy system on both, the demand and supply side. After applying a model for iRES expansion in 17 European countries and analysing the flexibility demand in scenarios with different Wind-PV ratios in Chapter 3 and 4, in the following, the impact on optimal flexibility provision is examined. For this model-based analysis, the contribution of the available technologies to integrate the iRES electricity is evaluated. This is done by applying the scenarios without and with sector coupling implemented in the adapted ELTRAMOD. With the objective to discuss optimal combinations of flexibility options, the present chapter aims to compare the mix of technologies with similar applications, on the one side within the flexibility demand (FD) scenarios (High PV, REF and High Wind) and on the other side, regarding the flexibility supply (FS) scenarios. The focus of the evaluation emphasising the impact of the flexibility demand on optimal investment and dispatch decisions for flexibility options is complemented by evaluations regarding the total system costs and CO₂-emissions. In a first step, an overview is given by presenting overall results on investment and dispatch decisions for the whole region observed. Therefore, in Chapter 6.1, the total original residual load²⁴ and the corresponding optimal energy system technology portfolio aggregated for the 17 countries are discussed.

²⁴ In the following, the original residual load is defined as the residual load, which can be derived by the difference of the system load (electricity demand as data input) and the iRES feed-in. Thus additional electricity demand due to sector coupling is not assigned to the original residual load.

Based on this overview, a more detailed analysis for relevant flexibility options is required. The results regarding the PtX technologies are discussed at first in Chapter 6.2. This improves the understanding of the results regarding storages and transmission capacity (see Chapter 6.2.3) as well as regarding power plant investments (see Chapter 6.2.2). Further flexibility options included in the present model-based analysis, namely curtailment, load shifting and load shedding, are present in Chapter 6.2.4. In general, country specific results are shown in the appendix, while a closer look is taken at relevant countries playing a crucial role within the overall flexibility provision in the scenario. The interplay within the optimised flexible technology portfolio on country level is further discussed in Chapter 6.3. Additionally to the technical analysis of the iRES integration, an economic evaluation compares the associated cost components, as presented in Chapter 6.4. This investigation is complemented by the analysis of corresponding CO₂-emissions in Chapter 6.5, allowing for the comparison of decarbonisation-related benefits of different approaches regarding the Wind-PV ratios as well as sector coupling. To gain a comprehensive overview and further increase the understanding of the interactions presented before, additional scenarios, focussing on the role of the iRES share as well as the share of electricity in the energy end-use sectors as well as selected sensitivities for relevant assumptions regarding the scenario framework are applied in Chapter 6.6 and 6.7, before summarising the results on the flexibility provision.

6.1 Aggregated results for the whole region observed

An overview about the flexibility provision in the scenarios High PV, REF and High Wind can be given in Figure 6.1, where the sorted residual load for the all 17 countries and the respective ordered hourly dispatch of different flexibility measures is illustrated. Note that the use of the transmission capacities for spatial flexibility are excluded, since with the aggregated results for the 17 countries the export-import flows are equalised. Without sector coupling (NO scenario) the original residual load (red line) is covered mainly by power plants (GEN) and electricity storages (STO) without significantly exceeding the positive peaks. The higher flexibility demand of High PV with higher positive and negative residual load peaks leads to larger amount of curtailed electricity (CUR) compared to the REF and High Wind scenario. Compared to the High PV scenario, electricity storages play a smaller role for flexibility provision in the latter two scenarios, since especially the surplus phases are smaller. With sector coupling in the LF and HF scenario, additional electricity demand for heat (PTH), hydrogen (PTG) and mobility (EV) increases the original residual duration curve. During most of the hours within the year observed, this leads to a higher demand for dispatchable electricity provision. Particularly in High PV a stronger use of surplus phases instead of curtailing iRES generation can be observed. In LF, this is mainly realised by an increase in electricity storage charging (compared to NO),

while in HF, the flexibilisation of the sector coupling allows for a more concentrated dispatch of the heat pumps, electrolyser and BEV. At the same time, curtailment can be reduced in each of the three FD scenarios, but still be observed in High PV. Since the amount of iRES surplus electricity is lower in High Wind, a change of the use of the hours with negative residual load is less obvious. However, the effect of an increase in flexibility of sector coupling from LF and HF can also be seen by comparing the dispatch of the PtX technologies during hours with very high positive residual loads. Particularly the charging of BEV is reduced in these times in all FD scenarios.

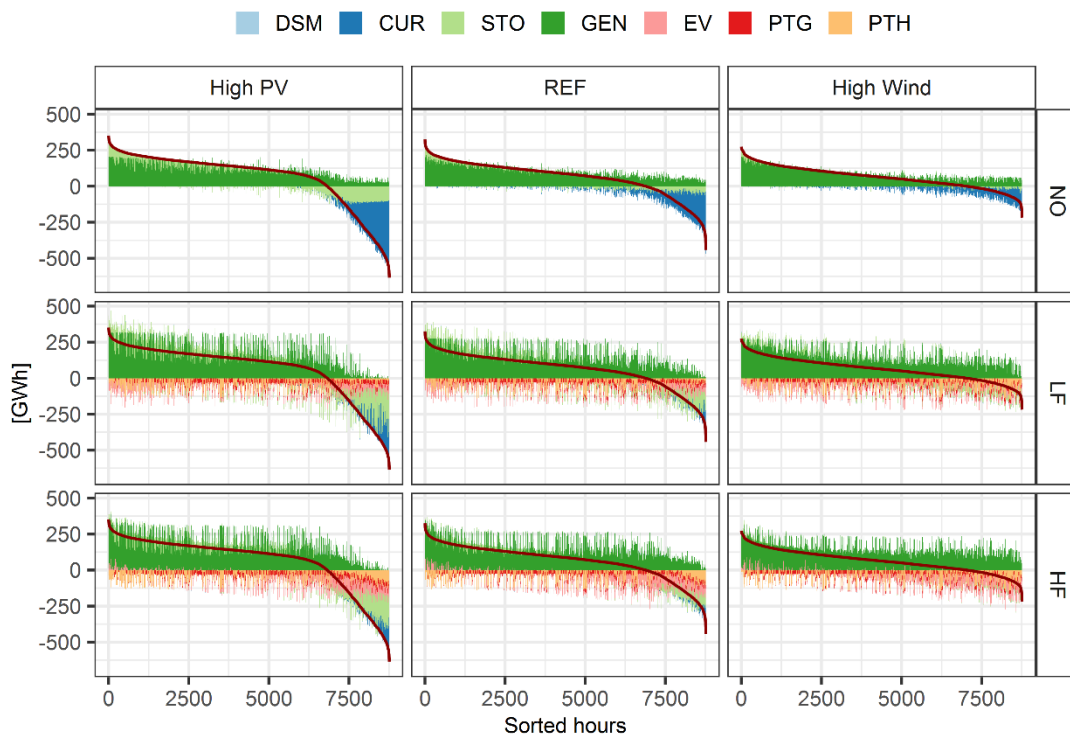


Figure 6.1: Sorted residual load and corresponding dispatch of flexibility options in the scenarios for the whole region observed (Own illustration)

When analysing the cumulated amount of electricity supplied and demanded separately for times with positive or negative residual load, the differences between the FD and FS scenarios become more obvious (see Figure 6.2). In times with overall positive residual load (pos), more dispatchable power plant generation is required in High PV to balance the lower availability of iRES capacities. Around 10 % of this higher deficit is covered by discharging the electricity storages. With sector coupling, Figure 6.2 further shows the increasing demand for electricity. Thus, by enforcing sector coupling as assumed in the LF and HF scenarios, between 61 % (High PV) to 80 % (High Wind) of additional electricity supply is required. In comparison, a higher flexibility in sector coupling (HF) allows for a similar reduction of additional electricity

generation by power plants or storages by 74 TWh (12 %) in High PV, by 60 TWh (10 %) in REF and 78 TWh (12 %) in High Wind compared to LF respectively. With sector coupling, the iRES surpluses (see neg in Figure 6.2) have a higher value and the amount of curtailment is reduced. While in the High Wind scenario and without sector coupling, in total 228 TWh of the iRES generation are curtailed, this value increases to 325 TWh (REF) and 359 TWh (High PV).

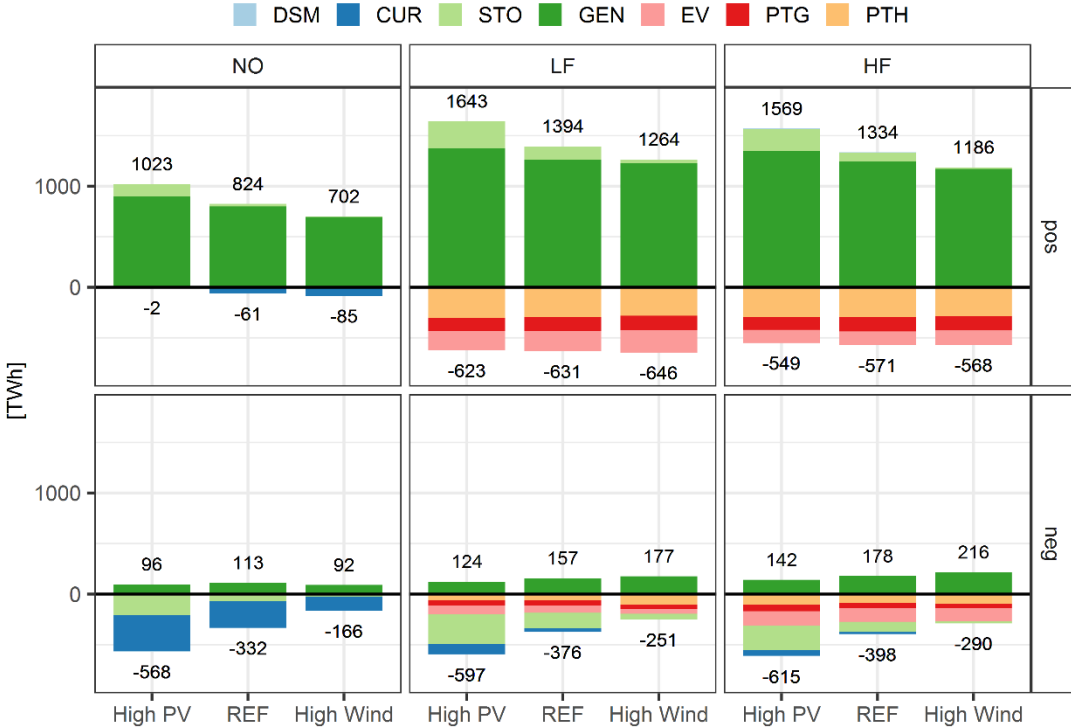


Figure 6.2: Composition of residual electricity demand and supply (without iRES) in times with positive (pos) and negative (neg) original residual load (Own illustration)

In contrast, curtailment of surplus electricity can only be completely avoided in the High Wind scenario with sector coupling. The amount of electricity consumed by PtX technologies during positive residual loads is more than twice as high compared to hours with iRES surplus electricity (negative residual load) in all FD scenarios. Particularly when looking at the HF scenario, this illustrates a limited exploitation of the sector coupling flexibility to shift electricity demand into iRES surplus phases. In LF, the electricity consumption by PtX technologies during negative residual loads is similar in High PV and REF (around 195 TWh) and slightly higher in High Wind (209 TWh), while additional electricity generation is required as well. The availability of energy storages for PtX technologies (HF scenario) enables a shift of the electricity demand to iRES surplus phases, mainly due to the shift of BEV charging and heat pump dispatch. Thereby, with a higher PV share in the iRES generation the amount of electricity

provided for sector coupling during times of iRES surplus is increasing up to 311 TWh in High PV.

An increase of temporal resolution on monthly level for the aggregated results shows differences in the temporal variability of electricity provision and consumption (including curtailment) between High PV, REF and High Wind (see Figure 6.3). Thereby, the dispatch of power plants and the electricity consumption of heat pumps is impacted most significantly, varying strongly between winter and summer month. In High PV these deviations are highest in all sector coupling scenarios. On the one side, this reflects the lower availability of PV plants requiring a larger dispatch of additional power plants. On the other side, as observed before, curtailment clearly reflects residual load surpluses during the year with high amounts in the summer month (up to 70 TWh in May) for the High PV scenario and increasing distributions across all month of the year with higher wind share. Higher seasonal variations can be observed in both scenarios with sector coupling, mainly driven by the electricity demand for PtH. The dispatch of the heat pumps is strongly connected with the seasonal heating demand and its peaks in the winter month. Further results regarding the dispatch of PtX technologies are introduced in the following. Flexibility options for temporal shifting like DSM and storages are less well observable. In general, this indicates a low seasonal shifting of these technologies and the flexibility provision is most likely realised in shorter time periods. This will be evaluated in the following chapters. The highest cumulated peak of storage charging occurs during the summer month (around 10 TWh in High PV without sector coupling), indicating a small seasonal shifting application. However, when analysing LF and HF, the flexibility of sector coupling does not significantly affect the flexibility provision in each FD scenario. This means, the potential of higher flexibility in sector coupling to seasonally balance the residual load is relatively low. Thus, the following analysis further increases the level of detail regarding the temporal resolution while focusing on single flexibility options.

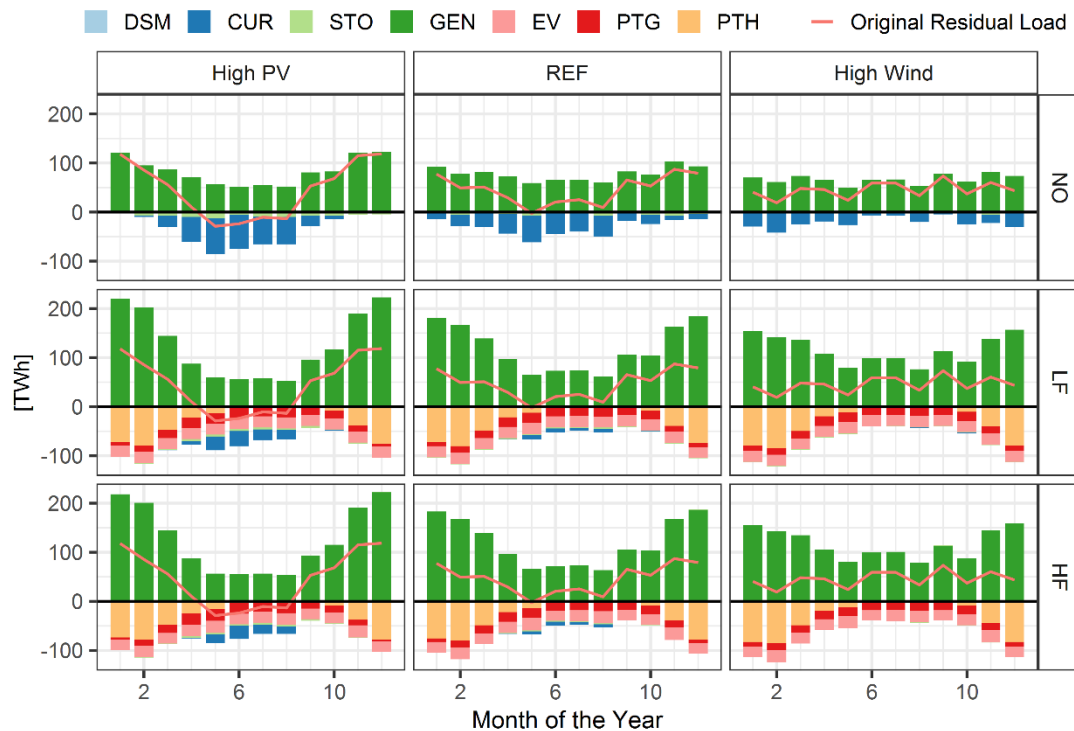


Figure 6.3: Sum of monthly dispatch of flexibility options (without iRES generation) to meet the residual load across all countries observed (Own illustration)

This overview emphasises major differences within the scenario framework. With the introduction of sector coupling, the electricity generation and demand is significantly changing. Thus, the investment in and dispatch of PtX technologies is analysed in detail at first. Thereby, the influence of a more flexible sector coupling by introducing energy storages is of particular interest. Afterwards, electricity storages are observed to evaluate the value of temporal shifting in the electricity sector within different flexibility demand (FD) and flexibility supply (FS) scenarios. Therefore, the role of different storage technologies as well as possible substitution effects due to the availability of further energy storages for the PtX technologies are analysed. Since also the spatial distribution of flexibility demand is expected to have a major influence on the technology mix, the contribution of electricity transmission capacities to flexibility provision is then discussed. To cover the positive residual loads in the countries, the power plant mix will be analysed finally in detail. Besides the capacities, the carbon intensity of the electricity generating technologies is of interest against the background of the scenario framework.

6.2 Detailed analysis of the role of different flexibility options

6.2.1 Evaluation of the role of sector coupling technologies

For the analysis of the technologies to provide upward flexibility multiple aspects have to be evaluated. The focus lies on the optimal capacity and dispatch decisions for heat pumps, electrolyser and BEV, while flexibility resulting from curtailing iRES generation is discussed in Chapter 6.2.4. For the PtX technologies, the analysis also includes results regarding the respective energy storages as well as the dispatch of the corresponding benchmark processes. Note that the model formulation introduces a minimum restriction for the electrification of the energy end-use sectors of 50 % for each of the PtX technologies (heat pumps, electrolyser and batter-electric vehicle (BEV)). Thus, the resulting electricity demand and required capacity are forced into the model results as minimum amounts.

6.2.1.1 Overall results on capacity and dispatch

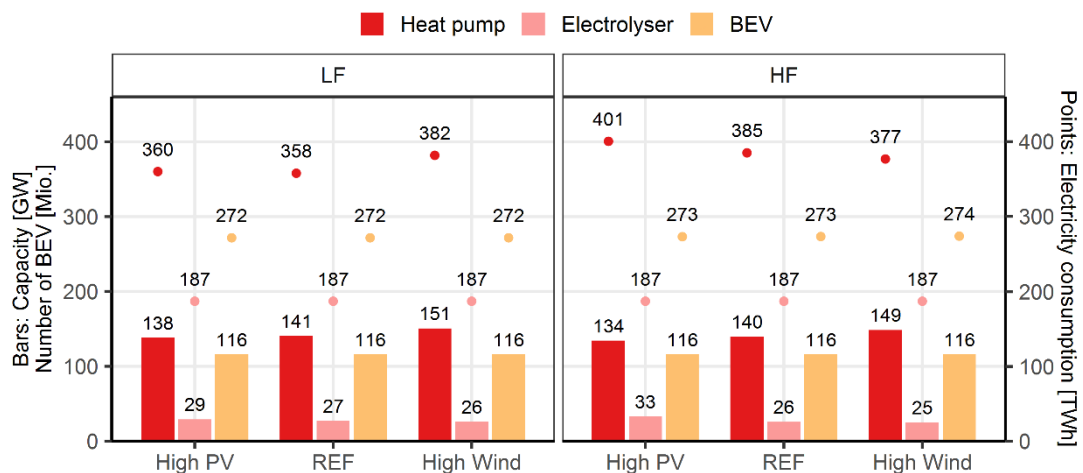


Figure 6.4: Optimal sector coupling capacities installed and dispatch across the whole region observed (Own illustration)

In Figure 6.4, the results for the total installed capacities (bars) of heat pumps, electrolyser and BEV are presented. Additionally, the cumulated electricity consumption (points) of these technologies is shown as well. Results on country level with similar trends can be found in Table D.1 to D.3 in Appendix D. Generally, the differences between the FD scenarios are rather small. When looking at power-to-heat, different impacts of the varying Wind-PV ratios as well as of the availability of heat storages can be observed. On the one side, the overall capacities for heat pumps are increasing in LF from 138 GW in High PV, to 141 GW in REF and 151 GW in High Wind. Thus, with higher wind-shares larger heat pump capacities are optimal. With heat

storages becoming available for the heat pumps (see HF scenario), decreasing values for heat pump installation in each of the three FD can be observed with the highest absolute capacity still in High Wind (149 GW). The heat storages enable the use of iRES surplus periods in times with low direct heating demand to be shifted into times with heating demand. This allows for a decrease of optimal capacity requirements for heat pumps. This heat shifting application will be discussed further in detail below. On the other side, with regard to the electricity consumed for PtH the overall results differ between the LF and HF scenario as well. While without heat storages, the higher wind shares tend to result in a larger heat pump dispatch, this trend is vice versa with heat storages available (HF scenario). Thus, with higher PV shares in total iRES generation, heat pumps are dispatched more and more constant with lower capacities when investments of heat storages are allowed. In addition, heat pumps are exceeding the 50 % (303 TWh) restriction resulting in 59 % (360 TWh) in High PV to 63 % (382 TWh) in High Wind as total share of electricity in the heat provision in the 17 countries observed. These amounts are further increased in the REF and High PV scenario when allowing for heat storages, with the highest total share of electricity for heat production in the latter scenario (66 %). In contrast, the total share of electrified heating demand is decreasing in the High Wind scenario compared to LF. In general, this means, the optimal share of electricity for heating is beyond the minimum restriction in the present analysis.

For electrolyser, different examination can be made. With low flexibility of sector coupling, the highest total electrolyser capacity is installed in High PV (29 GW) compared to a slightly lower optimal expansion of 27 GW in REF and of 26 GW in High Wind. In combination with hydrogen storages in HF, a reduction in electrolyser capacities can be observed for REF and High Wind, while in High PV the capacities are increasing by 14 %. For the provision of hydrogen in total 187 TWh of electricity are required, covering exactly 50 % of the total hydrogen demand of the industry. Thus, the dispatch of the electrolyser does not exceed the minimum restriction for the targeted sector coupling. This is still true for a higher flexibility of sector coupling with hydrogen storages.

When looking at BEV in Figure 6.4, the number of vehicles with 116 Mio. is not affected by the sector coupling approach. Also the minimum electricity demand implemented for passenger transport (272 TWh) by the model definition is constant across all scenarios observed. However, the higher value in HF reflects additional electricity demand due to efficiency losses of charging and discharging the BEV. Thus, the possibility to bi-directional charging of BEV is not incentivizing model-endogenous additional vehicles. The optimal share of electricity therefore has to be below the introduced 50 %. Calculations show, that with the present techno-economic parameter assumptions, a model-endogenous investment in BEV is not cost-optimal at all,

underlining the requirement for energy-political support or further adjustments of the framework conditions for the electrification of passenger transport.

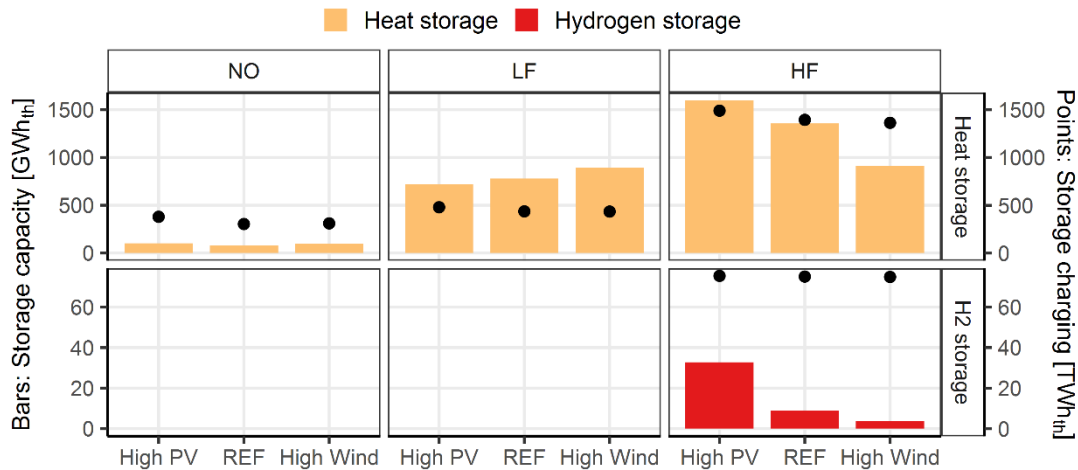


Figure 6.5: Total storage investments (bars) and sum of storage charging (points) across the whole region observed (Own illustration)

The possibility of model-endogenous investments in storage technologies (see results in Figure 6.5) in the HF scenario are drivers for the results discussed above. Heat storage capacities are also optimal in the scenario without sector coupling due to the CHP dispatch. In the model formulaion of the LF scenario, where heat pumps can only directly cover the time dependent heat demand, the optimal demand for heat storages is still increasing, again to increase the flexibility of the CHP plants. While the total installed capacity in the LF scenario is highest in the High Wind scenario, the application of heat pumps with heat storages (HF scenario) does not lead to a significant increase in storage capacities. In contrast, in High PV, the heat storage installations increase by 122 % to 1600 GWh_{th}. To a lesser extend, this effect can be observed as well for the REF scenario (1355 GWh_{th} heat storage capacity in HF). For the hydrogen production, where storages are only allowed in the HF scenario, the highest capacity cumulated for all 17 countries can be seen in High PV. Very high storage capacities are installed in Portugal, Spain and Italy, thus countries with high PV installations in this scenario. In contrast, in High Wind, the total storage capacity of 4 TWh_{th} is more evenly distributed across the region observed. However, the sum of storage charging is similar in all FD scenario, indicating a higher storage usage with higher wind shares.

The availability of energy storages enabling a flexibilisation of the sector coupling is influencing the full load hours of the PtX technologies (see Figure 6.6). For heat pumps, the total as well as country-specific results indicate a rather constant ratio in terms of full load hours of 2,500 h to 2,700 h (mean) regarding both Wind-PV ratio as well as flexibility of sector coupling. However,

particularly in HF, the median full load hours are highest in High PV, followed by REF and High Wind. For electrolyser without hydrogen storages, the median full load hours are increasing (more than 8000 h in single countries) with higher wind shares in the iRES generation, reflecting the lower total installed capacities in High Wind while the electricity demand is constant in all FD scenarios. While in REF and High Wind, the full load hours are increasing in HF, in High PV the median full load hours are reduced below 5,500 h with high flexibility in sector coupling. As mentioned above, also the full load hours (as ratio between the charged electricity and the EV's battery capacity) of the BEV are rather constant.

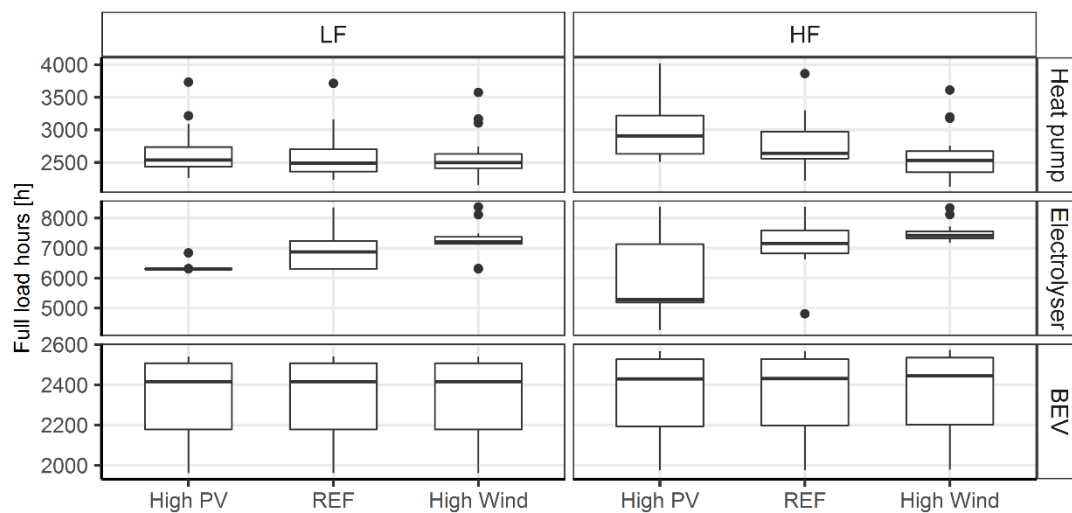


Figure 6.6: Boxplot of country-specific full load hours of heat pumps, electrolyser and BEV (Own illustration)

Although the mean and median results show a clear tendency, country-specific differences exist regarding the influence of sector-coupling flexibility on heat pumps and electrolyser. Figure 6.7 shows the relative change of full load hours in HF compared to LF as function of the PV share on total electricity demand per country. The colour of the points additionally reflects the change in capacity due to higher flexibility in sector coupling. In general, the country-specific relative changes of optimal capacity installations are higher for electrolyser (ranging from lower than -20 % in Norway and Sweden to +40 % in Portugal, Italy and Spain) compared to heat pumps. Thus, in countries with rather high wind installations a decrease of electrolyser capacity is optimal when hydrogen storages are available resulting in higher full load hours. In contrast, with PV as dominating iRES source, hydrogen storages allow for an increase in electrolyser capacity. For heat pumps a more significant increase in full load hours with higher PV shares on electricity demand can be observed.

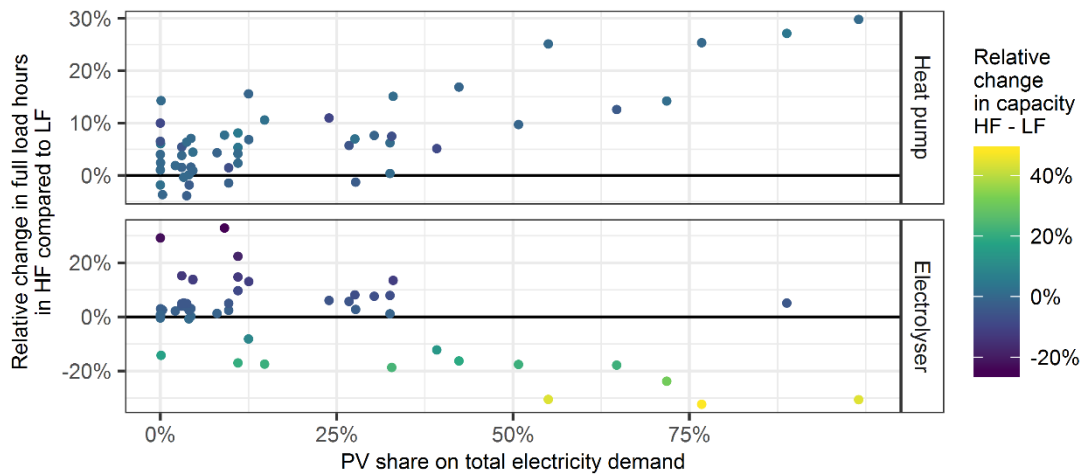


Figure 6.7: Country specific relative change of full load hours and capacity in HF compared to LF as function of the PV share on total electricity demand (Own illustration)

6.2.1.2 Temporal dispatch of sector coupling

To increase the understanding of the effects of additional electricity demand due to sector coupling, the monthly sum of the electricity consumption of all three PtX technologies across the whole region observed is displayed in Figure 6.8 for each of the FD scenarios. The distinction of the FS scenarios with low (LF) and high (HF) flexibility of sector coupling is illustrated with solid and dashed lines respectively. With the depicted additional electricity demand due to the assumed enforced sector coupling, the seasonal increase of the original residual load becomes obvious. The highest seasonal variation can be observed for heat pumps with peaks in winter month due to the heating demand, while in the summer month, heat pumps are dispatched very rarely particularly in the scenario without energy storages for the PtX technologies (LF). In High Wind, the seasonal fluctuation of electricity demand for PTH is highest, showing a maximum in January and February. This explains highest installed capacities as well as lower full load hours of heat pumps compared to the REF or High PV scenario. With increasing wind share, the higher amounts of iRES surpluses in the winter month are correlating with peak heating demand and higher heat pump capacities become optimal. Hydrogen production clearly shows a seasonal pattern as well with highest dispatch in summer month driven by PV surplus phases. Accordingly, in the High PV scenario, this effect is highest with a total monthly electricity demand of almost 20 TWh between April and August, while in January and December, the total consumption is reduced below 10 TWh. Thus, in this seasonal illustration, PtH and PtG are negatively correlating regarding the monthly dispatch. Compared to the heat

and hydrogen provision, the electricity consumption for BEV is rather constant due to the daily driving patterns demanding more than 20 TWh in each month. With energy storages increasing the flexibility of sector coupling, the effects are varying in the FD scenarios. In general, the seasonal impact is higher with increasing total share of PV in iRES generation. Heat pumps are additionally dispatched in the spring and summer month, particularly in the High PV scenario and to a lesser extend in REF, thus in times when the PV surplus amounts are increasing. This underlines the role of heat storages. Furthermore, while in High Wind in the HF scenario with hydrogen storages only small changes can be observed regarding the dispatch of electrolyser, the difference between peak and off-peak generation in this monthly illustration is highest in the High PV scenario. Additionally, the discharging and charging of BEV is more fluctuating during the year.

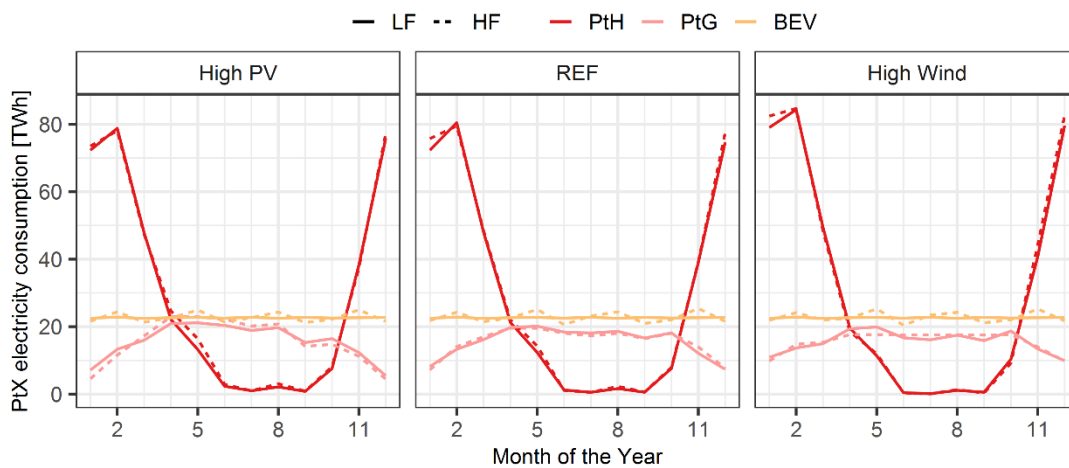


Figure 6.8: Monthly sums of electricity consumption of the sector coupling technologies across the whole region observed (Own illustration)

Further insights on the influence of the PtX technologies on the original residual load can be gained, when looking on the hourly sums with the similar approach as in the figures before. In Figure 6.9, this is done again for the High PV, REF and High Wind scenario displaying the hourly sums of PtX electricity consumption across the whole region observed. Without energy storages for sector coupling (solid lines for the LF scenario), the highest daily electricity demand results from the BEV in each FD scenario with in total almost 25 TWh at 7 p.m. reflecting the cumulated charging profiles in the 17 countries. In High PV, the hours with the highest heat pump dispatch (around 20 TWh) occur between 10 and 11 a.m. while during the night, the electricity consumption is lowest (10 TWh). With increasing wind share, the heat pump dispatch is shifted to earlier hours as a result of the relatively low original residual load during the night and the increasing heating demand in the morning. For the LF scenario, a similar but less

significant change in the hours with highest electricity demand can be observed for the hydrogen production with a peak of around 10 TWh during midday in the High PV (and to a lesser extend in REF) and during the early morning hours in the High Wind scenario. In general, in this daily perspective, both, the total dispatch of the heat pumps and electrolyser are correlating negatively with the BEV charging profiles. With only direct charging the BEV possible in the LF scenario, this electricity demand is the least flexible. In contrast, heat pumps have more freedom due to the possibility to supply heat with gas boiler and CHP. Thus, the optimal use of PtX technologies is applied to distribute the additional electricity demand of all three sector coupling technologies across the hours of the day.

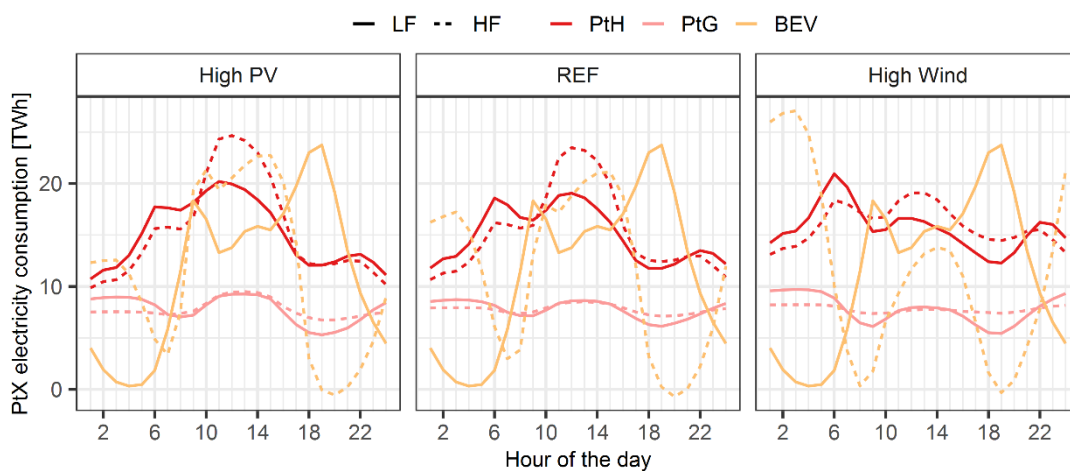


Figure 6.9: Hourly sums of electricity consumption of the sector coupling technologies across the whole region observed (Own illustration)

In contrast, the peak in electrolyser dispatch during the night hours is reduced when hydrogen storages become available (HF scenario) due to the competition of BEV charging during the night times. While the resulting hourly dispatch for PtG is more constant, the electricity provision for PtH and BEV is now more driven by the scenario-specific residual load. For the High PV and REF scenario, heat pumps are the PtX technologies with the highest electricity demand during the day. Furthermore, the optimal BEV charging profiles cause higher peaks during the midday hours in High PV (and to a lesser extend in REF), while in High Wind BEV are charged during the night. In a single car perspective this means a shift from a rather “charge immediately after the first day trip” strategy, to “charge later at home” as an optimal strategy in this wind dominated scenario. Additionally, the BEV’s discharge potential is most significantly used in the High PV scenario, where the total sum is negative between 7 and 9 p.m, thus providing electricity in these hours of the day. In general, the increase in electricity load due to sector coupling is also shifting the original residual load upwards and leading to lower

minimum peaks and higher maximum. With energy storages for sector coupling, this effect is weaker, since each of the selected sector coupling technologies further increases its electricity demand during low residual load phases and flattens the positive peaks in phases with high residual load. Thus, in contrast to the seasonal observations, the daily residual load smoothing potential of the three sector coupling technologies is exploited more excessively in each FD scenario, particularly regarding the BEV charging and discharging.

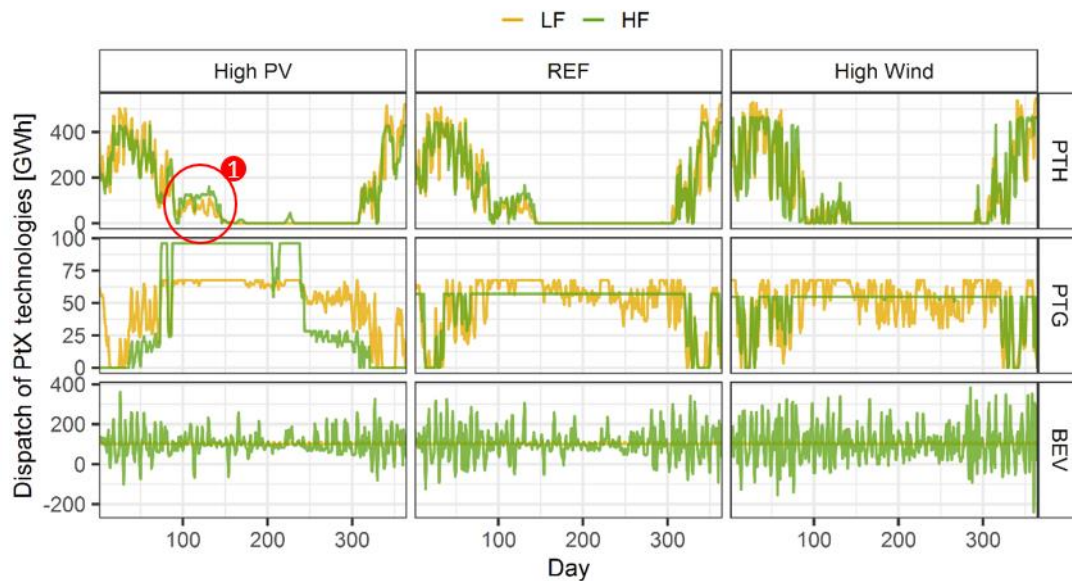


Figure 6.10: Exemplary daily dispatch of PtX technologies in France (Own illustration)

The described interactions regarding capacity, dispatch and the resulting full load as well as the effects regarding the temporal shift of dispatch can also be observed when analysing the dispatch of heat pumps, electrolyser and BEV on country level, as it is done exemplarily for France in Figure 6.10. While the majority of heat supply is required during winter, spring and autumn, the heat pumps are providing less heat during the summer month. When comparing LF and HF, the seasonal patterns are similar, however differences can be observed. In general, a flexibilisation with heat storages leads to greater short-term variations of heat pump dispatch (see also Table 6.1). Particularly during the spring times with increasing PV surpluses, this allows for additional heat supply exceeding the actual heat demand in the midday hours, while in the remaining hours there is no electricity consumption for the provision of heat (see mark 1). Figure 6.10 further reflects exemplarily for France, a more constant hydrogen production during the summer month due to the flexibilisation of sector coupling in all FD scenarios. However, this is due to varying reasons. Particularly in High PV, the electrolyser dispatch is significantly higher in HF compared to LF to benefit from surplus phases of the PV generation. With high PV capacities, this additionally enables to avoid the hydrogen supply by electrolyzers in the

winter month. This illustrates the overall decrease of full load hours due to an increase of optimal installed capacity in the High PV scenario. Since the winter months are characterised by high electricity demand for heat pumps (plus BEV charging), also in REF and High Wind, the resulting dispatch is more constant in summer.

Table 6.1: Standard deviation of the hourly dispatch of PtX technologies in France

[GW]	High PV		REF		High Wind	
	LF	HF	LF	HF	LF	HF
Heat pumps	6,1	6,7	6,2	6,8	6,7	6,8
Electrolyser	1,2	1,6	1,2	1,1	0,9	0,9
BEV	3,0	5,6	3,0	6,1	3,0	6,7

Finally, the charging and discharging (in HF) of the BEV in France can be seen as well in Figure 6.10. Additionally, the standard deviation of the hourly profiles can be seen in Table 6.1. While the charging profiles are fixed in the LF scenario, differences can be observed, when the storage capacities of the BEV become available²⁵. In this daily illustration hourly fluctuations of charging and discharging are smoothed. Particularly in summer month and with high PV shares, the charging and discharging peaks are high, since the midday surpluses are used to cover the transport demand as well as to balance residual load fluctuations by discharging at a later point in time. Nevertheless, the daily values show interesting insights. The BEV flexibility is more often used across days during winter month and with higher wind shares, to allow for a daily shifting application.

The results on PtX technologies represent additional electricity demand due to the enforced sector coupling assumed in the present work. PtX technologies increase total positive residual load peaks on seasonal (strong increases in winter month due to electrification of heating demand) and daily level (higher evening peaks mainly due to BEV charging). It was shown, that the availability of energy storages (heat storages, hydrogen storages as well as flexible use of the BEV batteries) allows for a more flexible dispatch of the sector coupling technologies. However, most of the dispatch adjustments are optimised to access iRES surplus phases on a daily basis. As a result, the flexibilisation of sector coupling in HF significantly changes the electricity consumption by sector coupling merely during the day. With higher PV shares this effect is most clearly caused by an increasing dispatch of PtX technologies during low residual

²⁵ It is important to note, that the results are based on optimal investment and dispatch decisions with perfect foresight. Additionally, a daily charging and discharging balance is neglected in the present work since a car fleet is represented rather than single cars.

load phases in the midday hours and by a decreasing electricity demand in high residual load phases in the evening hours. When looking at temporal and spatial shifting options in the electricity market, namely electricity storages and net-transfer-capacities (NTC) for electricity export/import, the influence on optimal capacity expansion and dispatch decisions are of interest. In the following, the flexibility provision for residual load balancing as well as electricity provision for sector coupling is evaluated.

6.2.2 Evaluation of the role of technologies for shifting flexibility in the electricity system

6.2.2.1 Electricity storages

With hourly (HOU), daily (DAY) and seasonal (SEA) as well as pumped hydro storage plants (PSP), four electricity storage types are included in the present model-based analysis. Thereby, the latter ones are included with their existing capacities of around 36 GW storage power and storage energy capacity of around 13,477 GWh and are restricted regarding further expansions. The results on optimal storage charging power (Figure 6.11) show, that in general very high amounts of additional storage capacity (mainly hourly storages with an energy-to-power ratio of 2 h) are installed in High PV, while decreasing installations can be observed with higher wind shares. This confirms similar findings in the literature as for example Gils et al. (2017). The additionally displayed cumulated discharged electricity is showing similar relations as well. In total, with around 100 GW in High PV, the hourly storage investments are exceeding those in the REF and High Wind scenario by 53 GW and by 94 GW respectively²⁶. As discussed in the overview in Chapter 6.1, hourly storages are discharged to provide electricity in times of positive residual load. When looking at the scenario without sector coupling (NO scenario), the storages are therefore also in competition with conventional power plants. Due to the day-night rhythm of iRES generation with higher PV shares, especially hourly storages have a value for shifting electricity from times with iRES surpluses to residual load deficits. Besides hourly storages seasonal storages (energy-to-power ratio of 200 h) have a high importance in the NO scenario to temporally balance iRES production and demand. The share of seasonal storages on total storage capacity is between 22 % (40 GW) in High PV, 25 % (41 GW) in REF and 26 % (15 GW) in High Wind. In each FD scenario, the highest seasonal storage investments occur in countries with a PV share lower than 50 %, particularly in France, Germany and Great Britain. On the one side, this reflects the wind share in the iRES generation, characterised by longer iRES

²⁶ See also Tables D.4 to D.6 in Appendix D listing country-specific results.

surplus and deficit duration phases. On the other side, although a strong seasonality can be observed for PV as well, the daily generation pattern is overlapping the seasonal demand for shifting flexibility in most rather PV dominated countries. This results in high hourly storage investments to shift the surplus of the midday peaks to the evening hours.

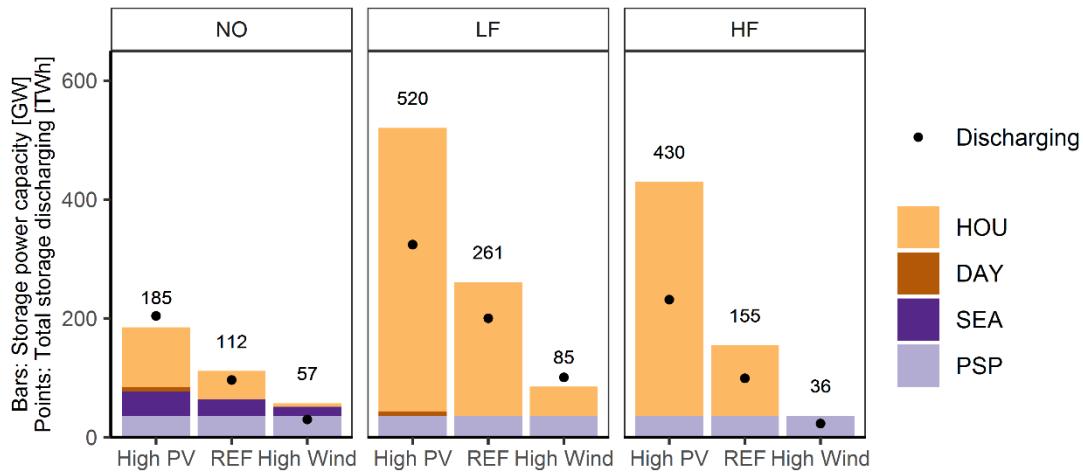


Figure 6.11: Total installed storage capacity across the whole region observed (Own illustration)

As it was discussed in the overview regarding the total residual load balancing in Chapter 6.1, with sector coupling storages gain in importance to further integrate iRES generation since iRES surplus electricity and the corresponding low marginal electricity costs are gaining in value with an enforced additional electricity demand. Compared to the NO scenario, in all sector coupling scenarios curtailment is reduced from up to 10 % to less than 1 % of total iRES generation (see Chapter 6.2.4 for further details on curtailment). Since new residual load peaks in winter caused by heat pumps are balanced mainly by additional generation capacity (see Chapter 6.2.3) as well as since the electricity demand for hydrogen production and BEV is more constant over the whole year, hourly storage capacity is of higher importance for a more short-term shifting flexibility provision. At the same time seasonal storages are substituted²⁷. While in High Wind, introducing sector coupling with low flexibility (LF) requires 49 % additional storage capacities, in REF and High PV a stronger increase by 133 % and 181 % respectively can be observed. In general, countries with highest surpluses due to high PV (Spain, Italy, Portugal) or high wind generation (Great Britain and Ireland) show strongest increase in storage installation from NO to LF. In comparison, high flexibility in sector coupling reduces total

²⁷ A part of the seasonal shifting demand is covered by PSP, especially in countries with high capacities like Norway, Spain and Portugal. See exemplary hourly storage level of these three countries in Figure D.2 in The Appendix D

storage demand for the electricity sector compared to LF across the whole region observed, since the PtX technologies are increasingly dispatched residual load driven and alternative energy storages become available. While in High Wind, almost no additional capacities besides PSP are required, also in REF and High PV reduction of 41 % and 17 % can be observed in HF compared to LF respectively. This only partly confirms earlier findings in literature (see e.g. Gils 2015) and underlines the importance of the Wind-PV ratio on the optimal storage expansion. Only in the High Wind scenario, a high flexibility in sector coupling allows for total storage capacity reductions compared to the NO scenario, while with higher PV shares, shifting flexibility in the electricity sector is still relevant.

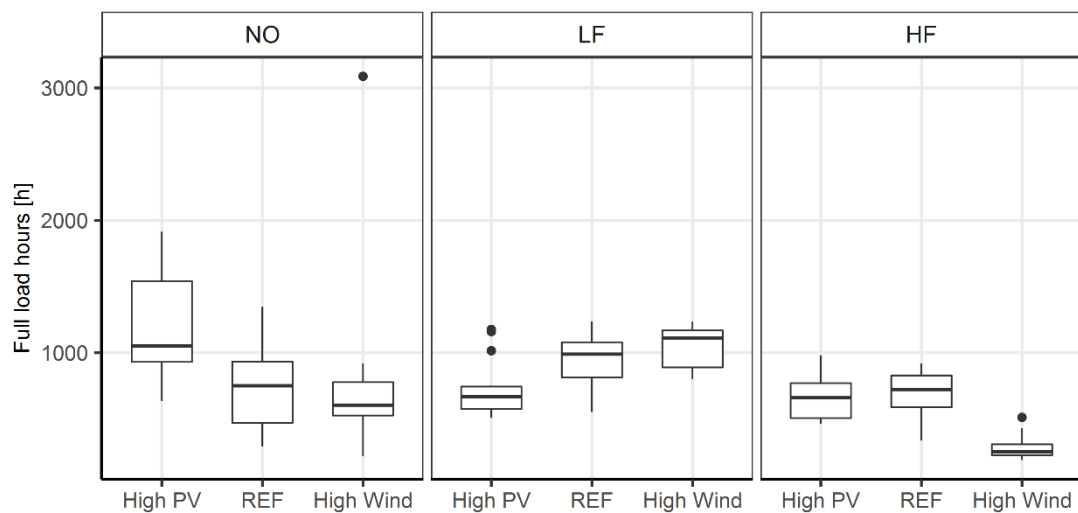


Figure 6.12: Boxplot of country-specific full load hours of the storage mix (Own illustration)

When comparing capacities with total amount of discharged electricity, the average full load hours of the electricity storage mix can be calculated. In Figure 6.12, boxplots of country-specific full load hours of the storage technology mix are displaying different impacts of Wind-PV ratios and sector coupling. Without sector coupling the High PV scenario shows the highest full load hours, reflecting the application of the electricity storages to provide daily balancing electricity. In contrast, the higher share of seasonal storages in REF and High Wind leads to less storage cycles. With the increasing role of hourly electricity storages when sector coupling is introduced, higher wind shares lead to an increase in full load hours in LF. In contrast, compared to NO, sector coupling decreases the utilisation of the storages in High PV. This indicates a capacity driven storage expansion (see also Figure 6.21 in Chapter 6.2.3). Thus, the high capacities of hourly storages are only required in single hours for surplus charging of the year resulting in low number of cycles. With the flexibilisation of sector coupling by energy storages (HF scenario), the significantly decreased value of electricity storages in the High Wind

scenario becomes obvious also with regard to the full load hours. Figure D.1 in Appendix D confirms, that the high increase of optimal storage installations in the High PV scenario is mainly caused by single countries particularly Italy and Portugal. In contrast, with increasing wind share, the influence of sector coupling more significantly results in reduced storage requirements.

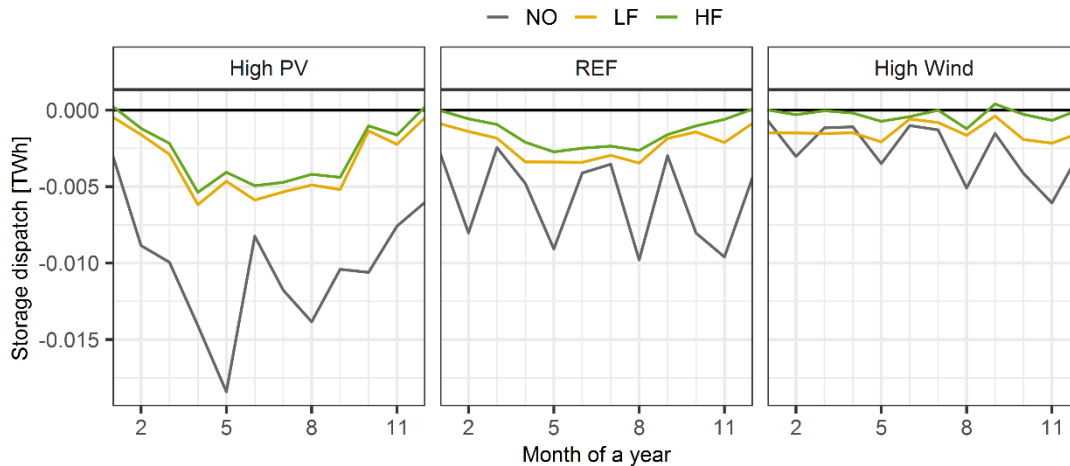


Figure 6.13: Monthly total sums of net charging across the whole region observed (Own illustration)

The illustration of monthly sums of net charging (aggregated for all storage types) shows an increasing seasonality with increasing PV shares. In Figure 6.13, the net charging is negative in most of the month, due to efficiency losses by charging and discharging (e.g. for seasonal storages with a roundtrip efficiency of 80 %). Particularly in the High PV scenario, the charged electricity is significantly higher than the discharging during the summer month. Without sector coupling, the higher capacities of seasonal storages further increase this seasonality. However, also in REF and High Wind monthly differences can be observed, indicating longer-term temporal shifting as well. With sector coupling (LF and HF scenario), the shorter-term flexibility provision becomes more relevant, resulting in smaller differences between the monthly charging and discharging sums, particularly with higher wind share in the FD scenarios. However, in High PV and REF, a shifting from the summer month to the winter month is still pronounced. As a result, in HF storages are mainly discharged during the January and December to additionally cover residual load as well as PtX electricity demand peaks. In contrast, in the High Wind scenario, this occurs more frequently across the year.

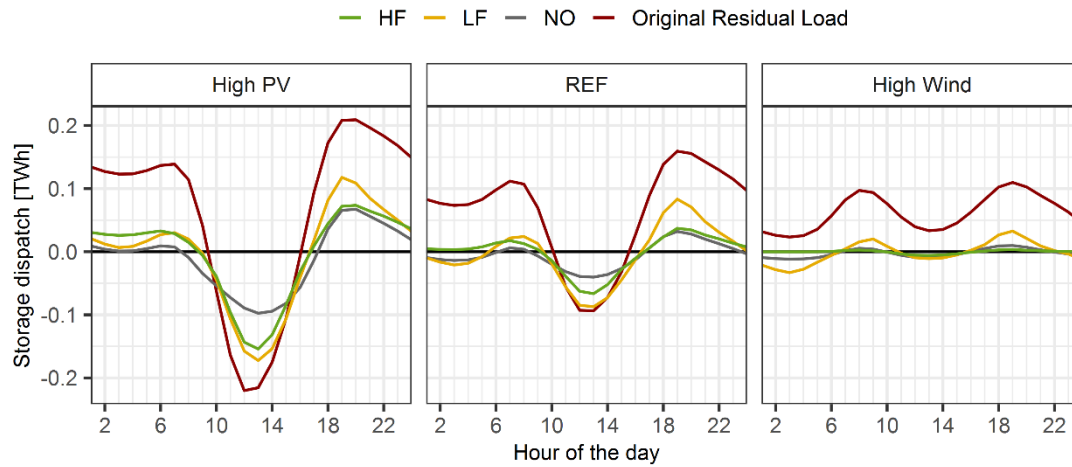


Figure 6.14: Hourly total sums of net charging across the whole region observed (Own illustration)

When looking at the hourly illustration of the net charging cumulated for all 17 countries (see Figure 6.14), the strong correlation of charging and discharging the storages with the residual load becomes obvious in all FD scenarios. However, in the High PV scenario, the effects of different sector coupling approaches can be seen most clearly. In the scenario without sector coupling, the iRES surplus phases are least used for storage charging. In addition, in the morning and evening hours with high PV generation ramps, storages are also charged, indicating also a value for balancing load changes for power plants. With low flexibility of sector coupling, charging and discharging is applied for both, balancing negative residual load phases as well as positive peaks during the day. However, particularly in the evening hours the high discharging activity is also caused by peak demand of PtX technologies mainly due to BEV charging. In contrast when storage become also available for the PtX technologies in HF, the surplus phases are still used extensively for storage charging (at lower overall installed capacity), while during iRES deficit phases storage discharging is less residual load driven. When again looking at High PV, particularly a more constant discharging during the evening and night hours becomes obvious. These interactions can further be emphasised in Chapter 6.3, where the interplay of the mix of flexibility options on country-level is discussed. Before, the results on electricity transmission capacity are presented in the following.

By analysing the optimal investments and dispatch decisions, a changing role of the electricity storages regarding their application to provide peak power capacity or surplus charging capacity becomes notable. This is illustrated in Figure 6.15. By illustrating the maximum charged and discharged electricity amount in a single hour in relation to the installed storage power capacity, the driver for the model-endogenous capacity expansion can be derived. Thus, with having an average ratio of -1.0 in High PV in each FS scenario, the maximum storage

capacity is clearly driven by the (surplus) charging requirements. In addition, in this scenario the maximum discharging capacity (positive ratio lower than 1.0) is never completely exploited especially when sector coupling is introduced. In contrast, with higher wind shares, this aspect is less obvious. Particularly in the High Wind scenario without sector coupling, the positive and negative ratios are vice versa, indicating an electricity storage expansion driven by electricity peak load requirements.

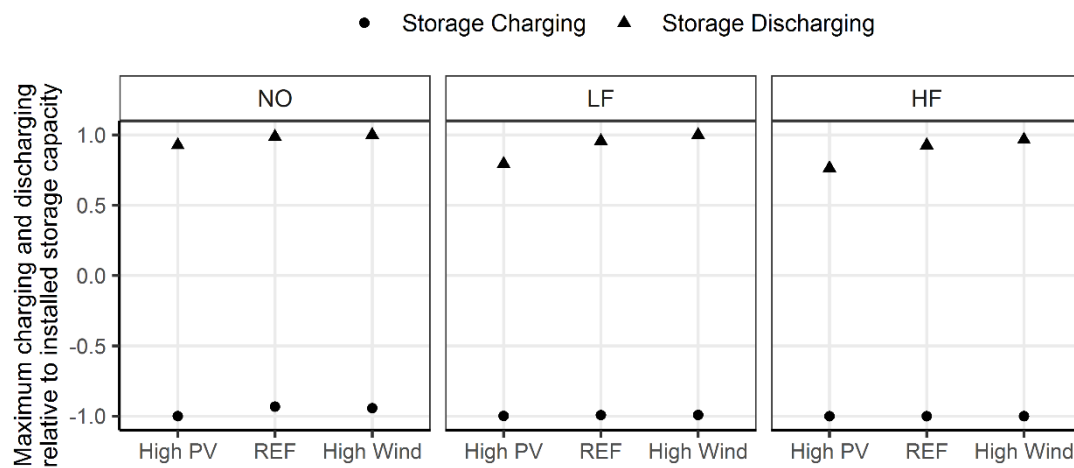


Figure 6.15: Mean country- and storage type-specific maximum electricity storage charging and discharging amount relative to the installed storage power capacity (Own illustration)

6.2.2.2 Electricity transmission capacity

In comparison with storages providing temporal shifting flexibility, the optimal capacity expansion for spatial shifting is less sensitive with regard to the FS scenarios. In Figure 6.16, the optimal expansion of the NTC (bars) between the 17 countries is illustrated. Additionally, the corresponding export flows (points) show the amount of exported (and imported) electricity in each FD and FS scenario. Without sector coupling, the lowest total transmission capacity is required in the REF scenario, followed by the High PV scenario and the High Wind scenario. Thereby, the optimal expansion is exceeding the existing capacity of 95 GW by 44 % in REF, 66 % in High PV and 74 % in High Wind. The NTC investments are correlating with the total export flows, which are highest in High Wind (461 TWh) and lowest in REF (439 TWh). The most significant effect of introducing sector coupling can be observed in the REF scenario. Compared to NO, the optimal capacities installed are increasing by 85 % in this scenario, while for High Wind and High PV these values are 25 % and 8 % respectively. In contrast, the optimal total NTC expansions in High PV are similar in the HF scenario compared to the NO scenario.

Compared to the scenarios with higher wind shares, the NTC expansion in the High PV scenario is least sensitive to the sector coupling approach. Similar observations can be found, when looking at the trade flows. While in the High PV scenario with sector coupling, the cumulated export-/import flows are increasing by 13 %/10 % (LF/HF) compared to no sector coupling, these values are higher for High Wind (30 %/27 %) and REF (40 %/36 %). To identify the drivers of the results, the regional distribution of NTC investments is analysed

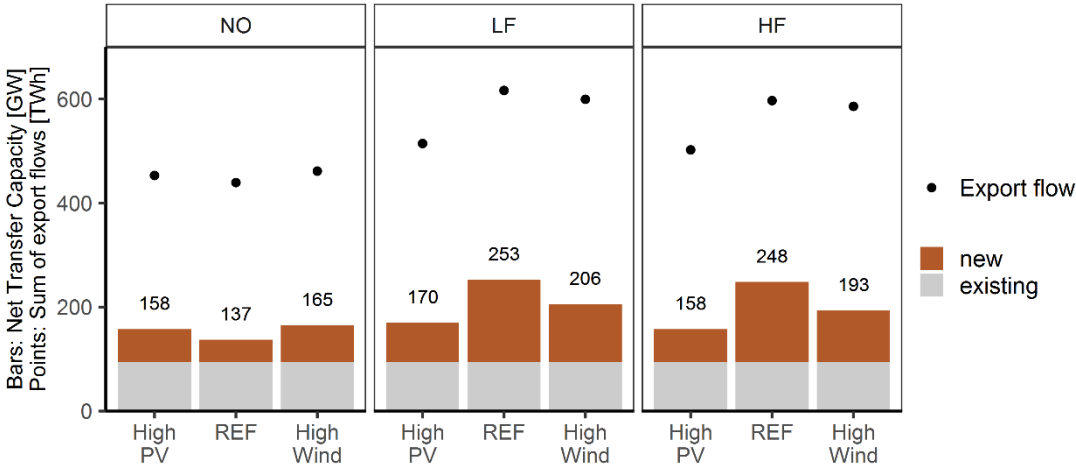


Figure 6.16: Optimal expansion of the electricity transmission grid and corresponding export flows across the whole region observed (Own illustration)

Figure D.3 in Appendix D shows, that the median optimal capacity investment per country is comparably constant in the FD scenarios with medians ranging between 2.8 and 3.6 GW per country. In contrast, high investments are rather outliers in most of the scenarios, reaching highest values in Austria, Germany and France (around 17 GW) in the REF scenario with sector coupling. To get an overview about the regional distribution of specific line expansions, Figure 6.17 depicts the NTC representation between the 17 countries included in the present work. Here, the line thickness represents the optimal capacity. Additionally, the colour of the countries reflects red shades for net importers (negative sum of export flows) and green shades for net exporters. In general, countries with relatively low total iRES shares are importing electricity originating from net exporters with rather high iRES shares. An exception can be found for the countries Austria, Switzerland and Sweden. These countries are net electricity exporters independently from iRES shares and scenarios, due to high hydro power plant capacities.

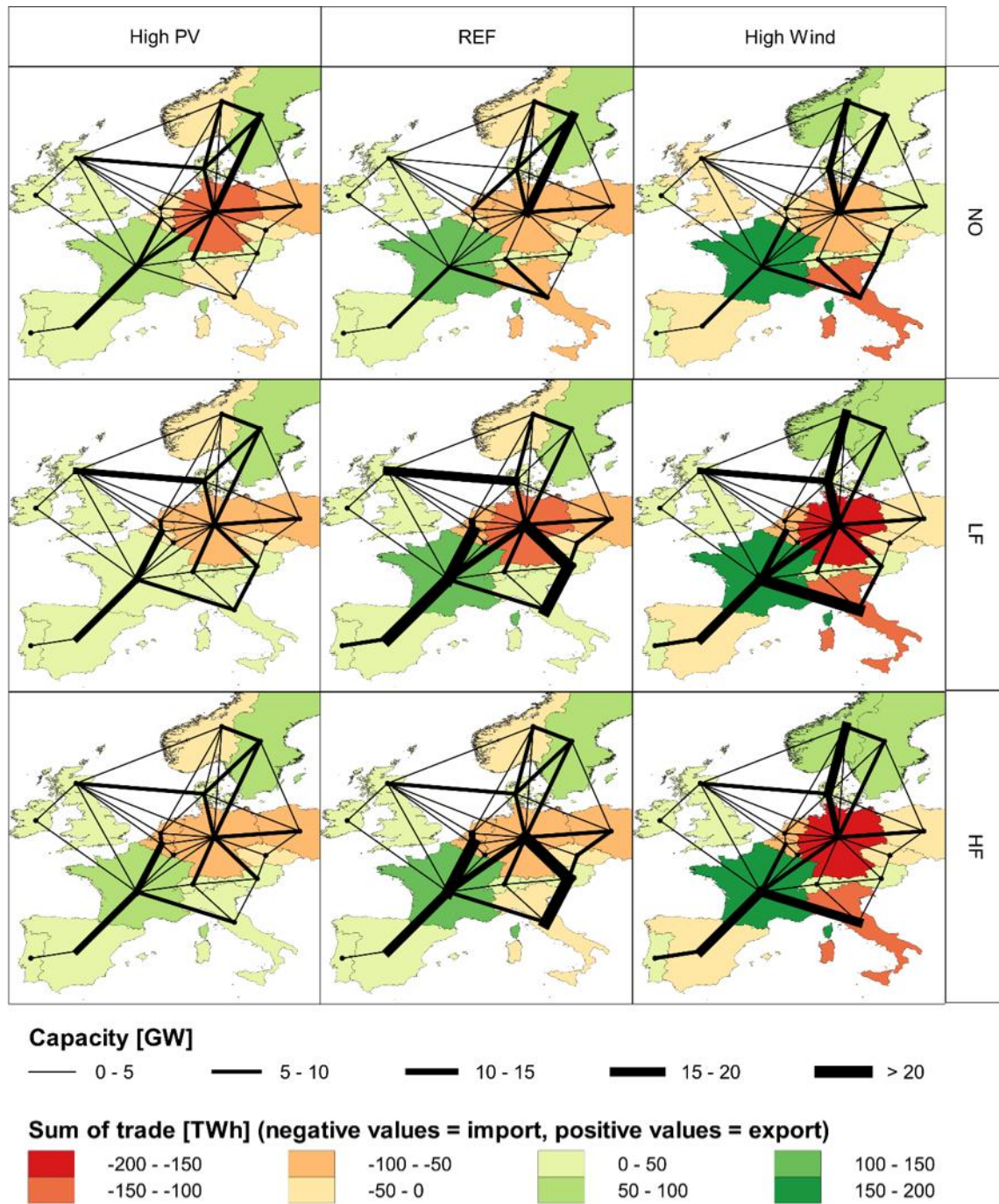


Figure 6.17: Scenario-specific maps of optimal NTC expansion and country-specific net export flows (Own illustration)

With higher PV capacities, particularly the countries in the south-west, west and north are providing electricity as net exporters. With higher wind shares across the whole region

observed, France increases its role as net exporter, since also here the wind installations are increasing and the total iRES electricity generation is highest within the 17 countries. In the High Wind scenario, most of the exported electricity is used to supply the southern countries with lower iRES shares and higher PV installations. Since without sector coupling high amounts of iRES electricity is curtailed and not shifted to later hours, the iRES deficit phases are (partly) covered by imports. With sector coupling in the High PV scenario, countries with high iRES surpluses, like Spain, France and Italy (with high PV capacities) but also Great Britain (with high Wind installations), are net exporters. Accordingly, the most significant increase in optimal NTC expansion can be observed in these countries. Particularly Italy (net importer in the NO scenario) is supplying PV surplus electricity to the neighbouring countries. Keeping the focus on Italy, the slight reduction of capacities between HF and LF reflects the more flexible PtX dispatch. Two influences decrease the optimal NTC investments when energy storages become available for sector coupling in the HF scenario. First, the PTX demand peaks are decreasing within the exporting and importing countries. Second, the domestic electricity provision for sector coupling can be improved, restricting the electricity amount to be transferred abroad. This generally explains the lower export flows when comparing LF and HF (see Figure 6.17). More extensive impacts of sector coupling on optimal NTC installations can be observed in the REF scenario. This is a result of the distribution of iRES installations within this scenario (see discussion in Chapter 4). The south-north connections as well as the west-east connections are expanded the most. Again Germany is the most import-dependent country. The strong NTC expansion between Great Britain and Denmark is mainly used to transfer surplus electricity from the first country through the second one to Germany (see also Appendix D Figure D.4 for the illustration of the hourly export/import flows for seven days in Great Britain and Denmark). The reduction of the NTC capacity in the HF scenario for this line can be explained again by a higher domestic electricity consumption. In High Wind, particularly France (with 189 TWh net export) and to a lesser extend Norway and Sweden are of high importance as net exporter. At the same time, Germany (with 162 TWh net import) and to a lesser extend Italy show highest values for importing electricity across all scenarios.

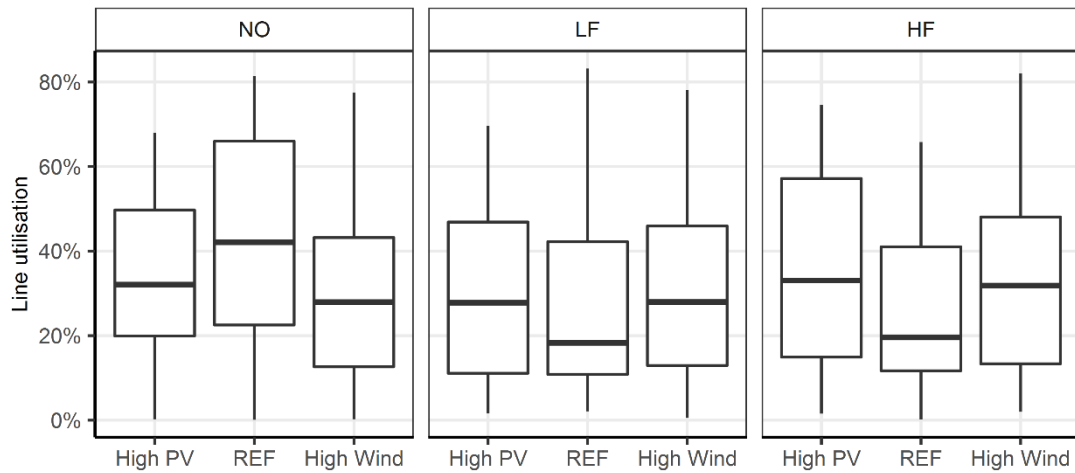


Figure 6.18: Boxplot of transmission line-specific utilisation rates (Own illustration)

The boxplot of line utilisation shows a similar pattern for the High PV and High Wind scenario (see Figure 6.18). Accordingly, the median utilisation of all connections is around 30 % without sector coupling. In comparison, this value slightly decreases in LF, while is rather similar in HF compared to NO. For the REF scenario, the lowest NTC expansion without sector coupling is accompanied by higher utilisation rates of more than 40 % for most of the 39 connections. The significant reduction of the line utilisation due to sector coupling emphasises, that the high NTC expansion is driven by export-import peak flows.

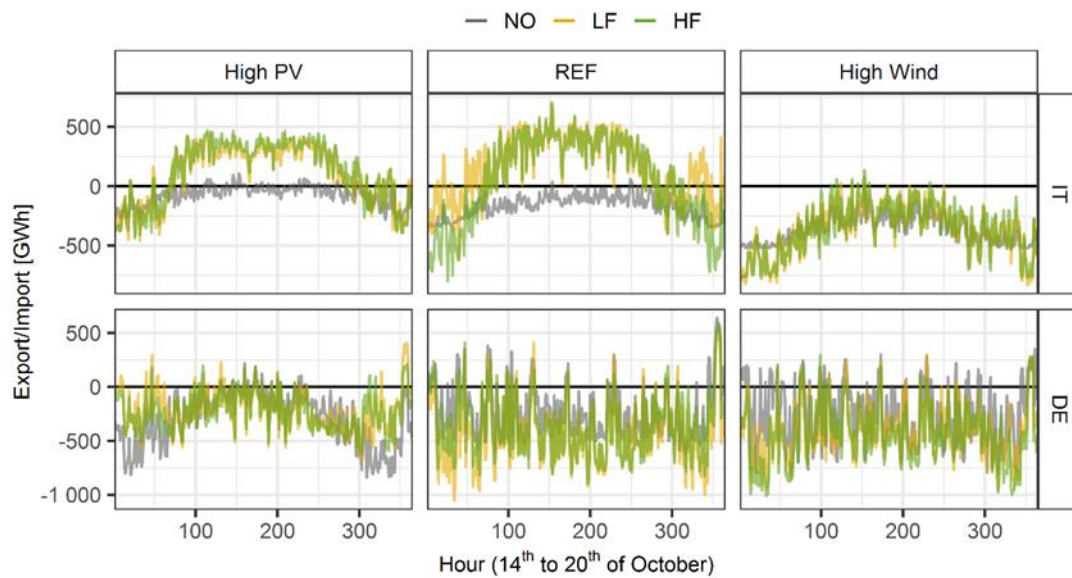


Figure 6.19: Daily export (positive values) and import (negative values) flows for selected countries (Own illustration)

Based on the observation of the optimal NTC expansion, Italy and Germany can be identified as countries highly sensitive with regard to the flexibility demand (FD) and flexibility supply (FS) scenario. In Italy, this is due to the highly varying iRES technology mix in the FD scenarios with very high PV capacities in High PV and REF. Germany is also characterised by differences in Wind-PV ratio of the countries iRES generation. Additionally, the original electricity demand as well as the additional demand due to sector coupling is particularly high. While in Italy without sector coupling, the import dependency increases with higher Wind-PV ratio across the whole region observed (see grey lines in Figure 6.19), reflecting the need to cover iRES deficit phases during times without solar radiation. However, with sector coupling, the summer months are characterised by significant export flows, due to the increased value of the PV surplus. This effect is higher in REF, since here, Italy has by far the highest PV share compared to the neighbouring countries. This aspect lowers the limitation of spatial balancing in the presence of high PV shares. For Germany, with a decreasing import-dependency in High PV due to sector coupling, the differences are caused mainly in the winter month. This is the time, when the additional power plant capacities are dispatched to meet both, the original as well as the PtX technology induced electricity demand. In contrast, in High Wind, Germany increases its import dependency in the presence of sector coupling, again mainly in the winter month. Here, the less correlating wind surpluses in neighbouring countries can be used to meet the respective electricity demand.

6.2.3 Evaluation of the role dispatchable power plants

6.2.3.1 Overall results on capacity and dispatch

The following evaluation of the results regarding dispatchable power plants is of high importance with regard to the interplay of different Wind-PV ratios and PtX technologies but also with regard to the storage technologies discussed before. With the assumed total iRES share of 80 % on the 17 countries' today's electricity demand, additional electricity generating technologies are required to cover the residual load. Further capacities become necessary to cover the additional electricity demand due to the enforced sector coupling. Besides investments and dispatch, the power plant mix is also highly relevant, due to the potentially resulting carbon emissions. Country-specific results are displayed in Table D.7 to D.9 in the Appendix D.

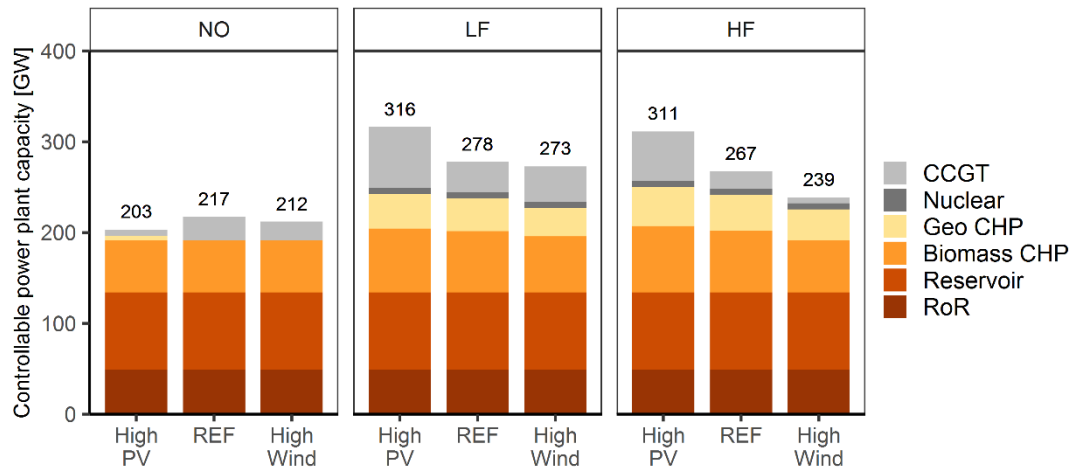


Figure 6.20: Total installed power plant capacities by technology (Own illustration)

In general, compared to iRES capacity with total installed capacities of 908 GW (High Wind), 1,128 GW (REF) and 1,385 GW (High Wind) across the whole region observed, the share of controllable capacities in the total power plant mix with a magnitude of 200 to 316 GW is relatively low (see Figure 6.20). Renewable energy sources are also the main source for controllable power plants. Besides hydro power plants, the biomass potentials, introduced with exogenous upper limits, are almost completely exploited across the 17 countries observed. Without sector coupling, additional capacities exceeding these renewable potentials are rather scarce, since investments in further flexibility options (mainly electricity storages) are more beneficial in the optimal system perspective. Note, that this is also driven by the assumed CO₂ prices of 80 EUR/tCO₂²⁸. In the NO scenario, the amount of investments is similar across all FD scenarios and rather independent from the Wind-PV ratio. Compared with the peak residual load (see Figure Figure 4.8 in Chapter 4), the share of secured power plant capacity is reduced from 76 % in the High Wind scenario and 66 % in REF to 59 % in High PV. This underlines the increasing role of electricity storages to provide secured capacity for the residual load with higher PV shares and without sector coupling. As expected before, sector coupling requires additional controllable power plant capacities. An increase can be observed in both, RES (geothermal and biomass) as well as conventional (nuclear and CCGT) technologies across the whole region observed. While in the High PV scenario, 56 % additional controllable capacity is installed in LF compared to the scenario without sector coupling, these values are lower in REF (28 %) and High Wind (29 %). Hence, with higher PV shares in the 17 countries, in total more additional power plant capacities, particularly CCGT technologies, are required to cover the

²⁸ In Chapter 6.7, a sensitivity analysis further sheds light on the impact of emission prices.

additional electricity demand due to sector coupling. This also indicates a changing role of the large storages capacities with higher PV shares to primarily provide balancing flexibility and to a lesser extend peak-power capacity when sector coupling is introduced. In addition, when energy storages allow for a more flexible dispatch of the PtX technologies (HF scenario), the observable overall reduction of dispatchable power plants is higher with higher wind shares in the FD scenarios. The investment in additional renewable-based CHP capacities again reflects the influence of CO₂ prices as well as the benefit of the cogeneration of heat and power. Although, specific investments in geothermal power plants are higher compared to gas capacities, the fuel and emission costs of the latter ones are increasing the total annual costs. For CHP, additionally gas boiler can be substituted in the heating sector, confirming the increase in heat storages also in LF. These model outcomes describe a significant change of the power plant mix compared to today (see Figure D.7 in Appendix D).

In the 17 countries observed, in total around 474 GW fossil-fuel based capacities are installed in today's power plant portfolio, thereof 158 GW CCGT and 114 GW nuclear capacities (ENTSO-E 2020). In present optimal power plants mix the two comparably low-carbon technologies are expanded by 42 % and 6 % compared to existing installations respectively. In contrast, in the optimal results for the future power plant mix no investments in coal (existing capacity 106 GW), lignite (existing capacity 40 GW), oil (existing capacities of 31 GW²⁹) or alternative gas technology (24 GW³⁰) power plant are observed. In addition, CSP plants are no option in the optimal power plant mix of the present model outcomes. Thus for lignite, coal, oil and CSP plants, this implies a lower cost competitiveness compared to alternatives within the present cost assumptions.

The analysis of absolute and relative change of dispatchable power plants due to sector coupling on country level reveals drivers for additional electricity generation requirements. The absolute increase in generation capacity is caused by single countries (Figure D.6 in Appendix D). In High PV this mainly results from Germany with an increase of around 45 GW in LF and HF respectively compared to NO. Generally, comparably strong increases can be observed in countries with a relatively low iRES share as well as a high increase in electricity demand due to sector coupling. When looking at the relative change of dispatchable power plant capacities due to sector coupling compared with the no sector coupling scenario, the increase is highest particularly in countries with a PV share below 50 %. The most significant change in all FD

²⁹ Aggregated for oil steam, OCOT and CCOT technologies

³⁰ Aggregated for gas steam and OCGT

scenarios (more than 200 % additional power plant capacities compared to the NO scenarios) can be observed in the countries Germany, Great Britain and Netherlands, thus countries with comparably high additional electricity demand due to sector coupling. While without sector coupling, these countries can secure power capacity at large shares by electricity trade (and electricity storages), additional power plant investments become optimal with sector coupling. As mentioned before, an exception to these rather wind-dominated countries can be found in Italy, with PV shares of almost 100 % in High PV and REF. The mean share of secured capacity on the country-specific peak electricity demand can be analysed in

Figure 6.21. Thereby, a distinction regarding secured capacity is made between controllable power plant capacities (see circles) as discussed in the present chapter as well as in addition electricity storage power capacities potentially also being able to be applied for peak power provision (see triangles). The lowest share of secured capacity on peak electricity demand can be found in the High Wind scenario, reflecting on the one side the higher availability of wind generation (decreasing the positive residual load) and on the other side the higher value of electricity export and import. In each FD scenario, sector coupling leads to higher investments in secured capacity also to cover the additional (peak) electricity demand. However, as observed before, this effect is strongest with higher PV shares in the iRES electricity generation. In addition, the increase in secured capacity with storages is also most significant in the High PV scenario. However, note, that the strong electricity storage expansion is mainly driven by the iRES surplus peaks in the High PV scenario and less driven by peak power provision requirements.

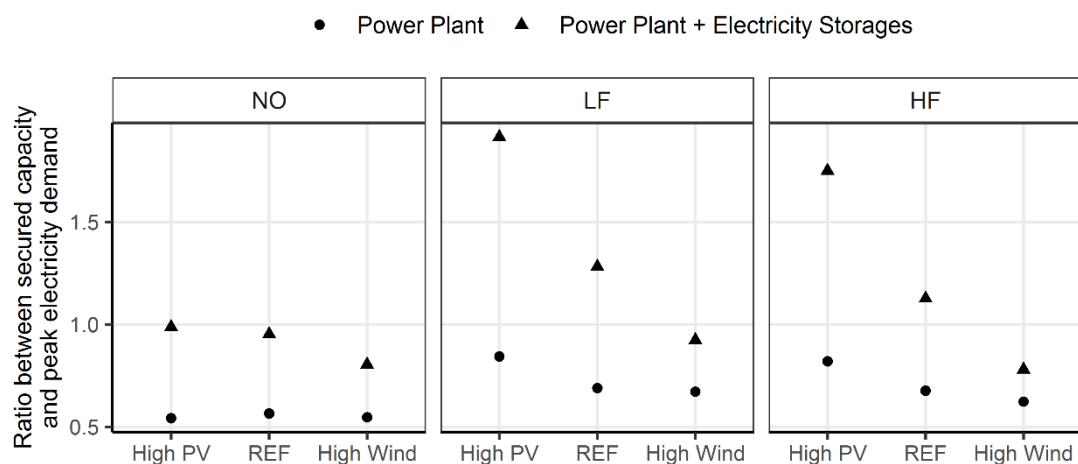


Figure 6.21: Mean of the country-specific ratios between secured capacity investments and peak electricity demand (Own illustration)

Besides the capacities, the dispatch of the power plants is influenced by the scenario framework as well. Without sector coupling the highest additional electricity generation is required in the High PV scenario (1066 TWh), followed by REF (962 TWh) and High Wind (807 TWh) resulting from the different pattern of the original residual load. Based on the lowest variable generation costs, this difference is mainly provided by additional hydropower generation (without PSP) leading to increasing shares in electricity generation with higher PV shares across the 17 countries observed (see Figure 6.22). In contrast, the amount of electricity generated in biomass power plants is rather constant with around 386 TWh due to the generation potential restriction, while the contribution of gas-fuelled power plants is low confirming their role as peak load power plants. Compared to the NO scenario, sector coupling without storages for the PtX technologies (LF) is causing an increase in electricity generation by 46 % in High PV, by 52 % in the REF scenario and 81 % in the High Wind scenario. Thus, with higher wind shares, the impact of an enforced sector coupling within the 17 countries is increasing with regard to the required electricity from dispatchable power plants. In each FD scenarios, the main share of this increase is provided by geothermal power plants with 250 to 290 TWh. Additionally, in High PV gas-fuelled power plants are increasing their output, while in REF and in High Wind, the electricity generation of hydropower plants becomes more important.

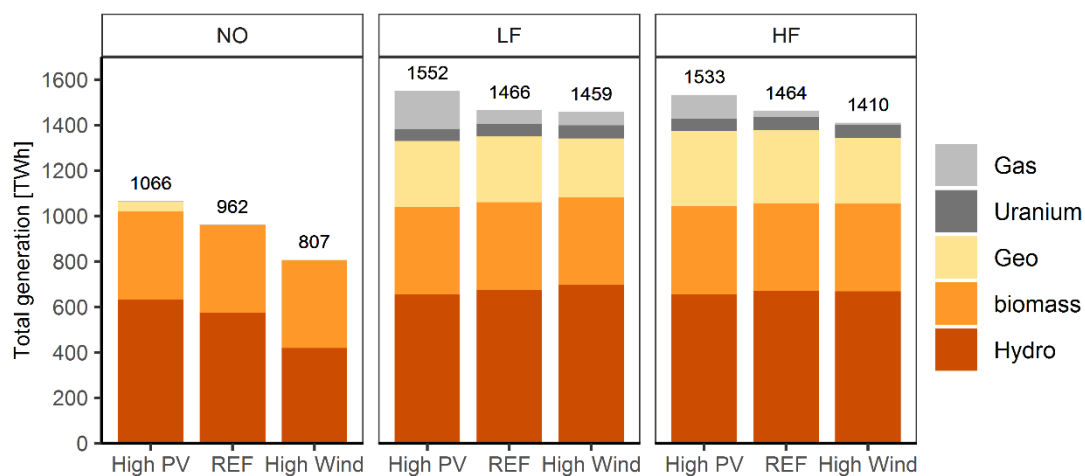


Figure 6.22: Total electricity generation of controllable power plants (Own illustration)

Thus, regarding the emission intensity of the total power plant mix, with higher PV shares more carbon-intensive (gas-) fired power plants are required to cover the electricity demand. This can also be observed with high flexibility in sector coupling, although particularly the generation of gas power plants can be substituted compared to the LF scenario. A flexibilisation of sector coupling (comparing HF with LF) has rather small effects on the electricity generation with the highest effect in High Wind (reduction by 3 %). Compared with the stronger overall capacity

reduction, this means the power plant mix is characterised by a higher utilisation rate in HF compared to LF.

Accordingly, Figure 6.23 illustrates the full load hours for the power plants distinguished by fuel-type in each country with boxplots. Since reservoir power plants are restricted by natural inflow restrictions, the resulting full load hours of around 2,500 h are similar, whereas run-of-river (RoR) power plants are influenced by the electricity demand in the FD and FS scenario. Without sector coupling, high full load hours of more than 7,000 h can be observed in most of the countries in High PV, while with higher wind shares these values are significantly lower on average. However, in the High Wind scenario with sector coupling the additional electricity demand is partly supplied by a higher utilisation of hydropower plant utilisation. For biomass and geothermal capacities, an increase in capacities due to sector coupling has been observed before. When looking at the full load hours, this change results in reduced full load hours for biomass CHP with a decrease from more than 8,000 h (NO) to less than 6,000 h (LF and HF) regarding the median values. At the same time, the additional geothermal capacities are achieving very high full load hours particularly in the High Wind scenario in all countries with actual installations. Thus, biomass power plants with higher marginal costs rather become peak (heating) load power plants, while geothermal capacities are dispatched more constantly at high full load hours.

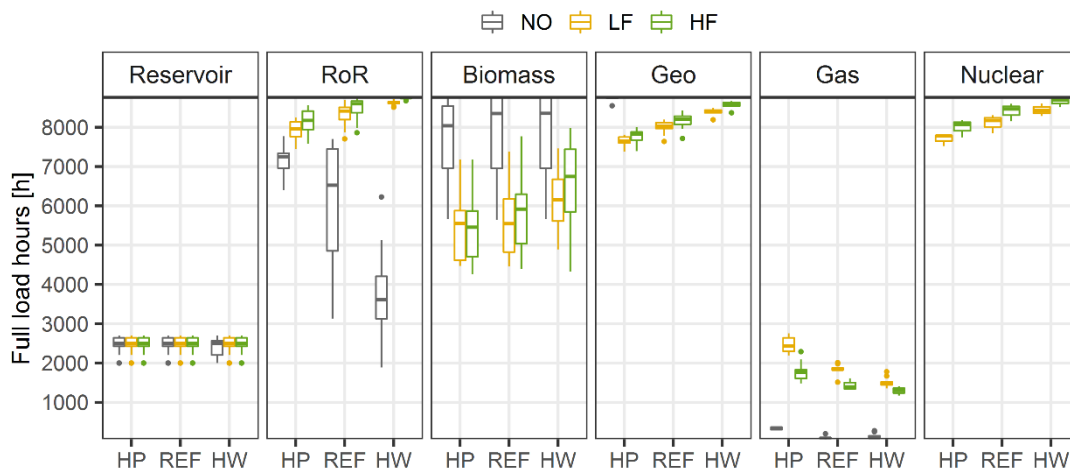


Figure 6.23: Boxplot of fuel-type specific full load hours in the 17 countries observed (Own illustration)

Furthermore, while without sector coupling, the gas power plants are dispatched as typical peak load capacities with low full load hours (below 400 h), the additional electricity demand in the LF and HF scenario does not only increase the required optimal capacities, but also the full load hours in the countries with respective optimal investments in this fuel-type. With higher PV share this effect is most significant. In contrast to LF, the utilisation of gas-fired power

plant is reduced with higher flexibility in sector coupling. Finally, in the three countries with nuclear power plants, the installed capacities and underlying cost structure (high investments and low variable costs), result in high full load hours. Both, a higher wind share as well as a higher flexibility in sector coupling increases the utilisation of these power plants, since the residual load is smoother.

6.2.3.2 Temporal dispatch of power plants

As illustrated in Figure 6.24 for the whole region observed, the total monthly electricity generation of the controllable power plants clearly follows the original residual load (dark red line). Thereby, without sector coupling (grey line) the generation is exceeding the residual load deficits mainly in the summer month. With sector coupling, an increase in total electricity generation can be observed following the seasonal residual load including electricity demand of PtX technologies. In High PV this increase is clearly occurring in the winter month, while in REF and more significantly in High Wind the additional generation is more evenly distributed across the year compared to the NO scenario. As discussed before, in High PV the dispatch of the electricity storages mainly occurs in the summer month to shift electricity from surplus phases to the deficit phases in a daily pattern substituting the power plant generation. Only small differences between LF and HF are notable.

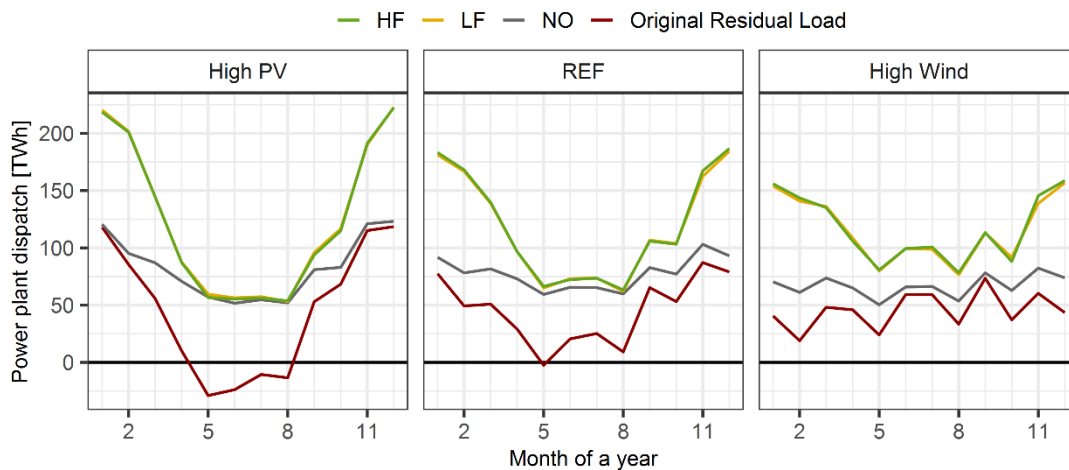


Figure 6.24: Monthly sum of electricity generation by controllable power plants for the whole region observed (Own illustration)

For the hourly sums of electricity generation by controllable power plants (see Figure 6.25), again greater differences regarding the FS scenarios can be observed. The electricity supply follows the original residual load. Without sector coupling, the correlation is highest in the High Wind scenario, while with higher PV shares, the power plants are running although high

amounts of iRES surplus energy occurs during the midday hours. At the same time, the residual load surplus peak in the evening hours are not entirely covered by dispatchable electricity generation, illustrating the influence of storages being discharged in the evening hours particularly in the summer month. Sector coupling increases the total electricity generation in each hour, while the pattern compared to the NO scenario stays rather similar. However, particularly in the High Wind scenario a smoothed power plant dispatch can be observed with higher flexibility in sector coupling. For each FD scenario, the difference between LF and HF clearly reflect the changes in overall power plant capacity demand as discussed before with the highest reductions observed in the High Wind scenario.

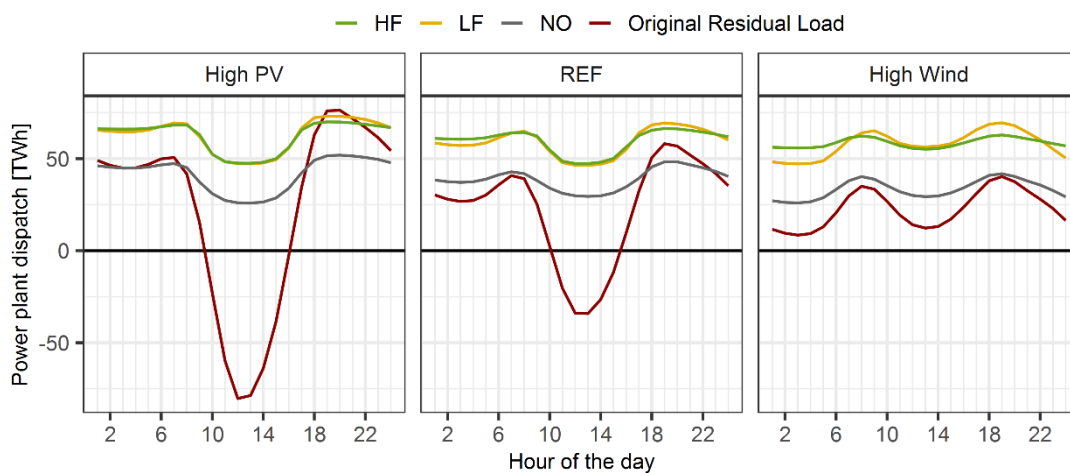


Figure 6.25: Hourly sum of electricity generation by controllable power plants for the whole region observed (Own illustration)

On country level, the dispatch of the power plants is clearly showing a seasonality, when looking at the hourly generation in Denmark, Italy and Poland (see Figure 6.26). These three countries are very well representing different impacts of Wind-PV share and sector coupling on optimal power plant dispatch. For Poland with increasing total iRES share as well as wind share from High PV to High Wind, the reduced power plant demand becomes obvious. Furthermore, the influence of additional flexibility options can be seen for Denmark and Italy. While Denmark has a constant iRES mix, the dispatch of power plants is strongly contrasting in the FD scenario. Particularly in the High Wind scenario, the maximum installed capacity is similar in LF and lower in HF compared to NO, indicating an increasing role of storages and electricity grids for flexibility provision. In Italy, with very high shares of PV generation in High PV and REF, the impact of different sector coupling approaches on the power plant dispatch is also varying significantly. While in High PV, the additional electricity demand is causing almost three times more electricity generation requirements in the winter days particularly in HF, in REF a

significant reduction of power plant dispatch with high flexibility in sector coupling compared to LF can be observed.

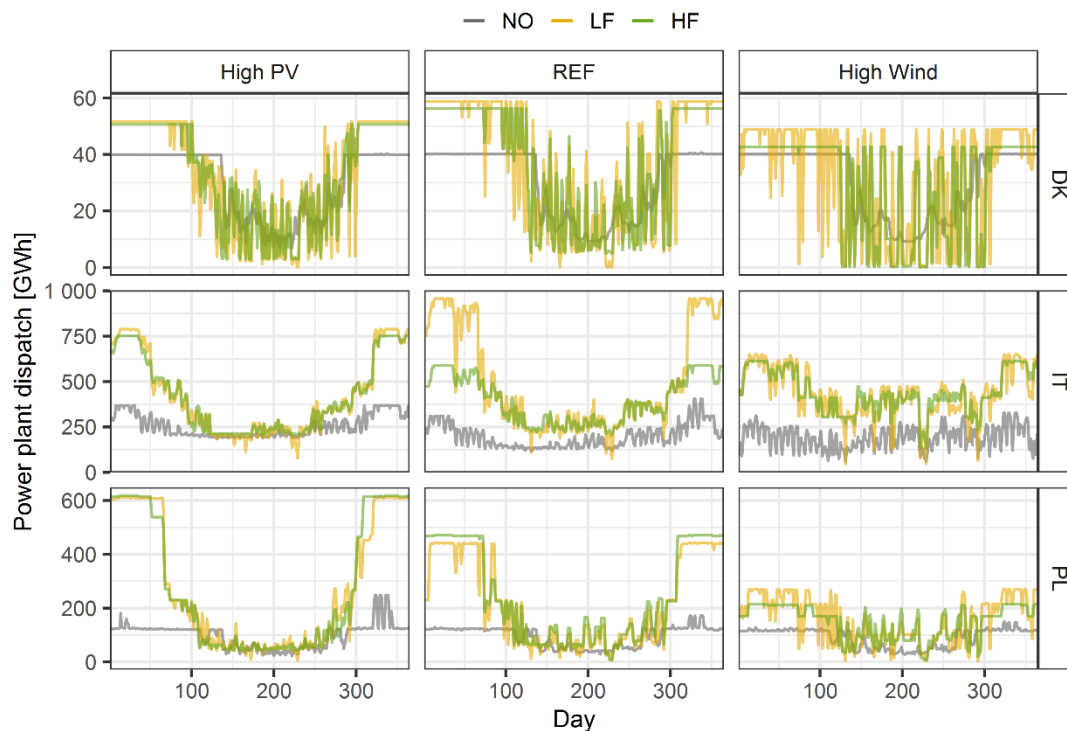


Figure 6.26: Daily dispatch of power plants in selected countries (Own illustration)

6.2.4 Analysis of further flexibility options

After analysing the effects of varying Wind-PV ratios as well as PtX technologies on the residual load and main flexibility options, the curtailment is of additional interest. As the discussion on aggregated results in Chapter 6.1 indicates, the amounts of curtailed iRES electricity increases with higher PV share, particularly in the summer month. It is important to note particularly regarding curtailment, that neglecting national grid congestions, thus assuming optimal grid expansion within single countries, the curtailed amounts are most likely underestimated. In the figure below, without sector coupling the curtailed iRES electricity of 359 TWh in High PV accounts for more than 16 % of total iRES generation, while the values are decreasing in REF (15 %) and High Wind (11 %). The low surplus amounts in High Wind enable the complete avoidance of curtailment when electricity demand is increasing due to sector coupling. This result reflects optimal outcomes in the system perspective. In real world energy system developments, a reduction of curtailment to zero can be expected to be less likely. For REF and High PV, the shares of curtailed electricity are significantly reduced in LF and HF as well. The highest amounts of iRES curtailment occur in countries with high PV shares, as depicted in

Figure D.8 Appendix D. In High PV and REF with curtailed electricity also in LF and HF, these results are still similar.

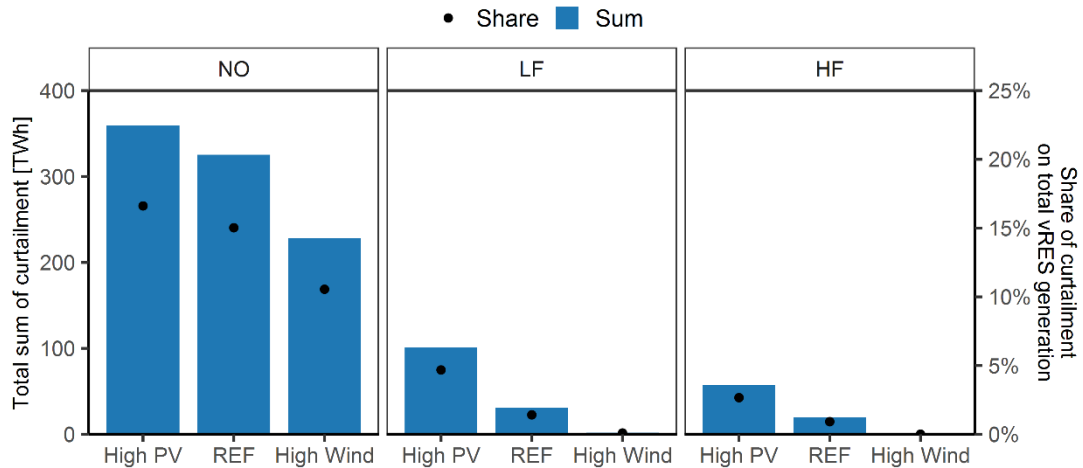


Figure 6.27: Overall amount of curtailment and share on total iRES generation across the whole region observed (Own illustration)

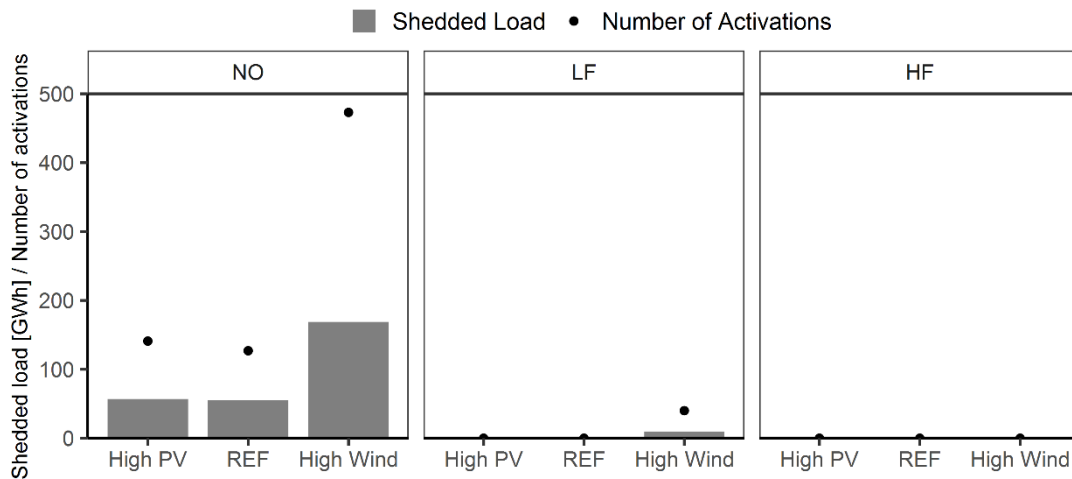


Figure 6.28: Total shedded load and corresponding number of activations (Own illustration)

For load shedding, as flexibility option providing downward flexibility, the amount of dumped electricity and corresponding activations observed are rather low compared to the application of the technologies discussed before (see

Figure 6.28). As the CAPEX are assumed to be zero, since already today, applications for load shedding in industry exist, the assumed potential is fully exploited in each FD scenario. However, the activation is limited by comparably high costs (1000 EUR/MWh). The highest amount of shedded load occurs in High Wind (0.168 TWh compared with 2636 TWh total

electricity), associated with the highest number of activations (473). In contrast, with sector coupling, the role of load shedding further decreases in each FD scenario.

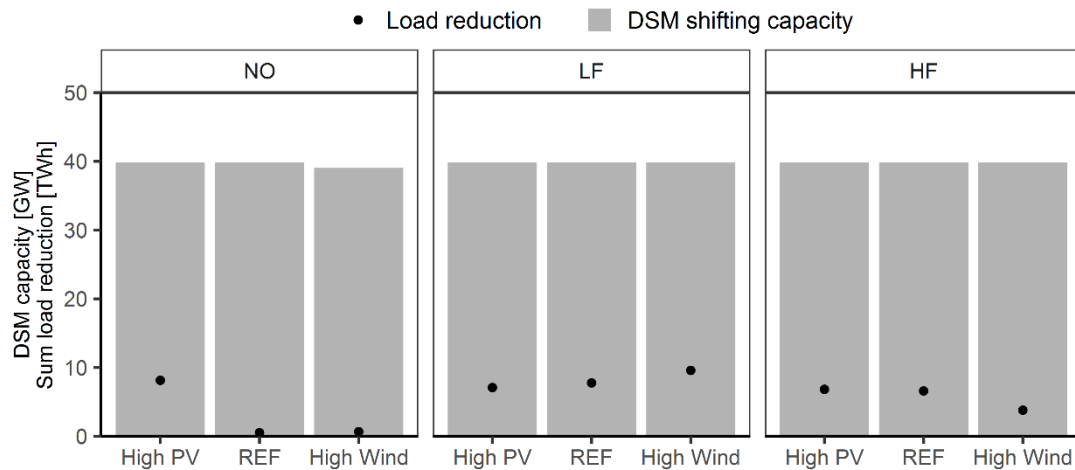


Figure 6.29: Optimal investments in DSM capacity and sum of load reduction (Own illustration)

Compared to load shedding, the activation costs of load shifting are assumed lower. Compared to other shifting flexibility options like storages, also the CAPEX of the identified potential is lower (between 0 and 10 kEUR/MW). This results again in the almost complete exploitation of the assumed potential of more than 39 GW (see Figure 6.29). Without sector coupling, the activation is significantly in the High PV scenario, with total shifted electricity of around 9 TWh. With sector coupling the shifted electricity is in a similar range with highest values in High Wind with low flexibility and in High PV with high flexibility in sector coupling. However, independent from the FD scenario, the average usage of the available DSM potential is highest in countries with high wind shares, like The Netherlands, Denmark and Ireland (see also Figure D.9 in Appendix D). Thus, the fluctuations of the wind generation are stronger balanced by load shifting, while the high demand for electricity storages with higher PV shares substitutes the DSM measures.

6.3 Interplay of flexibility options on country level

After discussing relevant aspects of flexibility provision of technologies within the flexibility categories, the final perspective on optimal combination of flexibility options is given in the following by analysing the interplay of flexibility options on country level. This is done on the one hand, by observing the pairwise correlation between the country-specific dispatch of the flexibility options. On the other hand, selected countries and selected days are presented, depicting the hourly interplay of the flexibility options included.

To underline differences of technology dispatch both the correlation with the residual load as well as with the increased electricity demand resulting from sector coupling are analysed. Thereby the focus is on the flexibility options, electricity generation by power plants (GEN), storages (STO), export (EXP) as well as the PtX technologies itself. In Figure 6.30, the mean country-specific pairwise correlation coefficients between the hourly time series are illustrated. For the balancing of the residual load (RL) without sector coupling, the relevant flexibility options have different roles. While in High PV, storages are most clearly following the residual load on average, with increasing wind share in the iRES generation storages (and power plants) are less residual load driven. In contrast, the electricity exchange between the countries is gaining in importance³¹. With sector coupling, the average correlation coefficients are rather constant for storages and electricity generation. The influence of the Wind-PV ratio in the FD scenarios on residual load-driven electricity trade flows is increasing with the highest average coefficient in High Wind above 0.6. In contrast, the inflexible PtX dispatch is not oriented on the residual load, since the underlying profiles have to be met. This changes when storages are available for the sector coupling technologies. Here, the PtX technologies can adjust the electricity consumptions driven by available residual load surpluses. The remaining flexibility options show a rather constant average correlation coefficient in HF compared to LF. For the balancing of the additional flexibility demand of the PtX technologies in LF (see lower row in Figure 6.30), the power plants show the highest coefficients, while shifting flexibility is less driven by sector coupling. The dispatch changes, when energy storages allow for a more flexible PtX approach. Instead of power plants, the storages are charged and discharged in correlation with the electricity demand resulting from sector coupling, while the power plants are run more constantly. In comparison, export and import flows occur rather independently from the PtX dispatch. With higher wind shares, grids are often sufficient to export regional surplus electricity. In these countries, NTC and storages are in competition regarding the shifting application. However, in countries with high PV shares, storages and export are used synergistically. That means, storages are used to charge surplus during the day, while the discharged energy is used partly to supply the countries demand including PTX and to export remaining electricity. This effect is strengthened with rather uneven distributed iRES as seen in the REF scenario.

³¹ The average correlation coefficient is negative since positive residual load is often met by imports (negative exports)

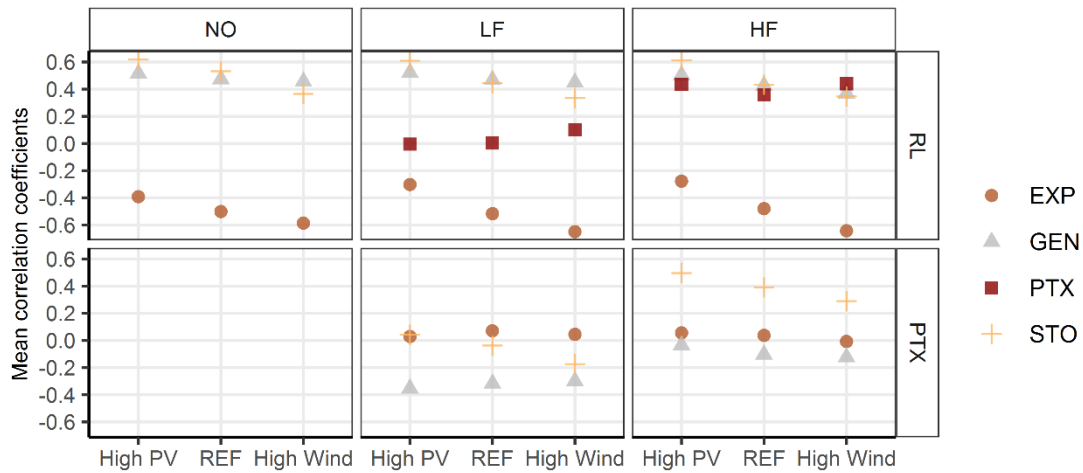


Figure 6.30: Mean of pairwise correlation between country-specific dispatch of flexibility options and residual load time series (Own illustration)

As an example, three summer days for Italy as well as three autumn days for Great Britain are compared. For both countries, the respective days are selected since they include the day with the highest iRES surplus. In Italy (see Figure 6.31), this leads to PV induced surplus peaks of 150 GW in High PV. While the majority of the corresponding surplus energy is curtailed without sector coupling, an increased need for storages to absorb the concentrated PV surplus for the electrification of the selected energy end-use sectors can be noted. As observed before, in LF the highest storages charging occurs after the iRES feed-in peak to allow for higher discharging in the evening hours, since the energy-to-power ratio is limited. Particularly in the High PV and REF scenario, it becomes obvious that the storage discharging in the evening hours is used to cover the positive residual load plus BEV charging. In addition, the NTC are used to export discharged storage electricity (see mark 1 in Figure 6.31). As explained before, the synergies between storages and NTC to charge short-term surplus peaks and discharge at lower rates for export in the evening is notable particularly in the REF scenario with low flexibility in sector coupling. In HF, the storages are used more excessively during the midday PV-peak generation. In addition, the PtX technologies and the respective energy storages enable a shift of electricity consumption to the surplus phases reducing the evening discharge activity of the electricity storages (see mark 2). The latter aspect can also be seen in the High Wind scenario for Italy. Thereby, the increased flexibility of BEV charging in HF substitutes the storages. In High PV and REF, the dispatch of heat pumps enabled by heat storages with high flexibility in sector coupling is illustrating the value of the surplus energy, also for heat generation in the summer month. This competition with regard to the surplus phases is an additional factor reducing the optimal storage capacity expansion in HF compared to LF. Furthermore, with high flexibility in sector the domestic electricity provision for sector coupling is increased in all 17

countries, restricting the electricity amount to be transferred abroad. For net exporting countries, this results in lower total export flows and at the same time less import for countries with lower iRES share. In these countries, additional power plants have to substitute the imported electricity (as for example in Germany).

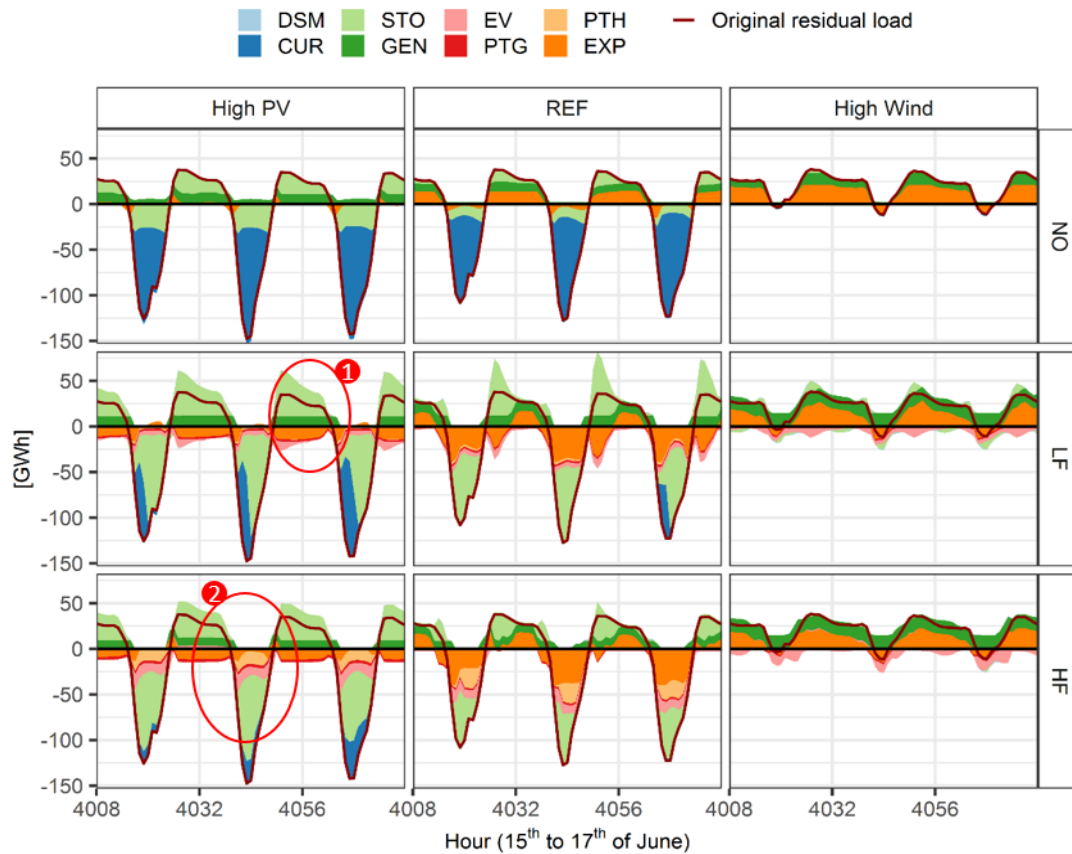


Figure 6.31: Exemplary week in Italy illustrating the dispatch of flexibility options (Own illustration)

With higher wind generation, the surplus balancing and allocation is done directly by exporting without storing the surplus energy, since the hourly surplus peaks are lower. This can be seen for Great Britain and exemplary autumn days in October (see Figure 6.32 with different y-scale compared to Italy). Without sector coupling, the slightly higher PV share in High PV results in storages to become optimal, while with higher wind shares curtailment and export-import are mostly balancing the residual load in these three days with high wind-feed-in (compare mark 1 and 2 in Figure 6.32). With sector coupling, the role of NTC is increased and curtailment can be strongly reduced as discussed before. Especially, the surplus period of more than 24 h on 3rd and 4th October as well as additional electricity generation is spatially shifted at large parts (see mark 3). In LF, storages are used less compared to Italy, but still dispatched for peak charging and discharging. With high flexibility in sector coupling, the BEV storages are excessively used

to balance the iRES surplus phases (see mark 4). Due to the heat demand in the autumn time, the dispatch of heat pumps is less flexible, while import peaks are used for BEV charging in HF.

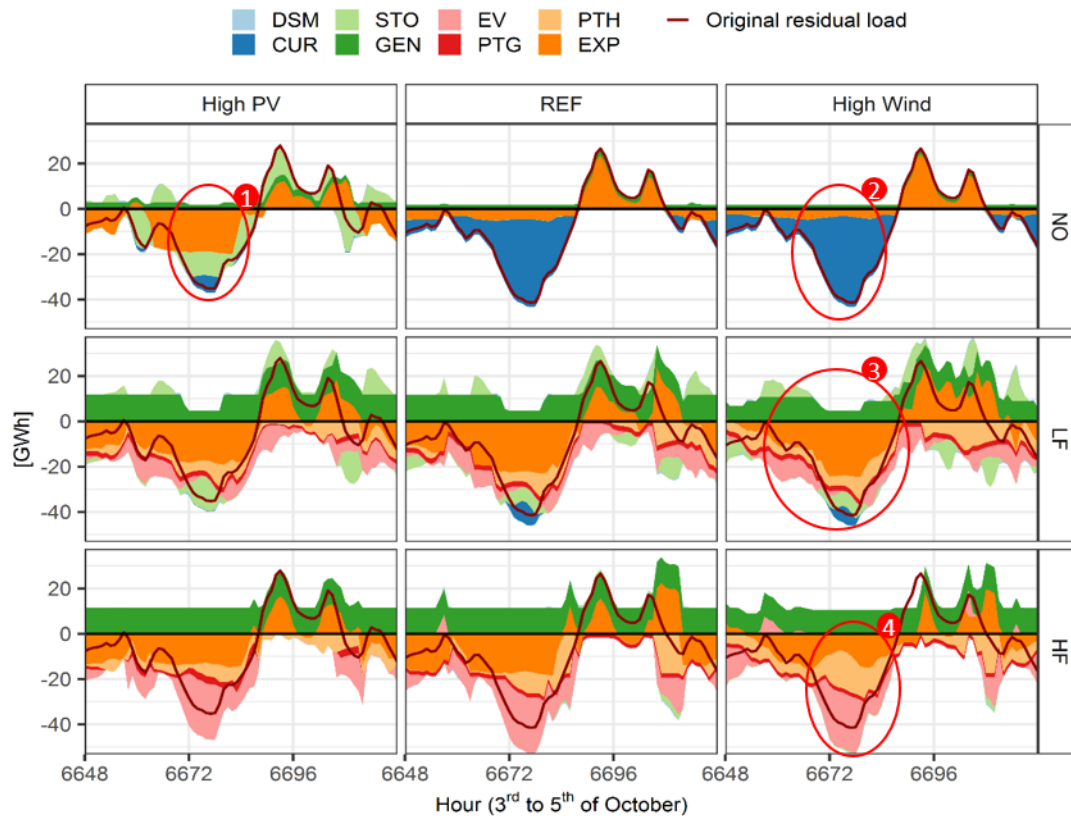


Figure 6.32: Exemplary week in Great Britain illustrating the dispatch of flexibility options (Own illustration)

These exemplary days underline the complex interactions between the flexibility options within single countries, additionally influenced by the interconnection with neighbouring countries. The flexibility demand resulting from various combinations of iRES share and Wind-PV ratios as well as sector coupling result in different optimal combinations of flexible technologies within the 17 countries observed. With the system cost minimisation approach, applied in the present model-based analysis, the result is based on techno-economic investment and dispatch decisions. With the following analysis of total system costs, the resulting outcomes can further be compared.

6.4 Total system costs evaluation

The total costs summarise the results regarding the CAPEX and the OPEX of the technologies involved. As presented above, the corresponding capacities and costs are strongly influenced

by the assumption of an enforced sector coupling. To cope for this aspect, the costs including sector coupling are discussed and illustrated separately. The total costs of the electricity system are entirely an endogenously result of the optimisation in the greenfield approach.

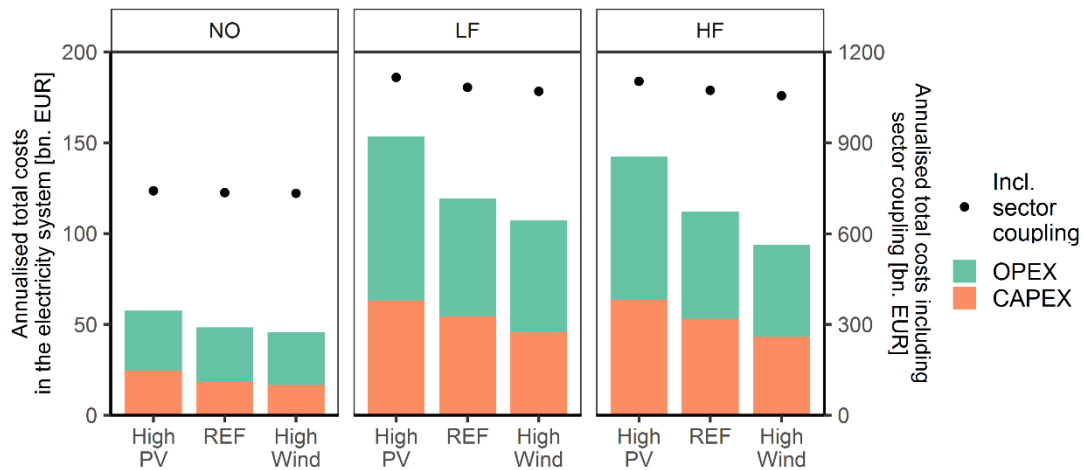


Figure 6.33: Annualised system costs in the electricity system and comparison with total costs including sector coupling (Own illustration)

While in the following, the CAPEX for the capacity investments are annualised, the OPEX, composed of fixed and variable costs as well as fuel, emission, ramping and load shifting cost are aggregated for the 17 countries and the years observed. In total, the system costs of the electricity system are higher with higher PV share across the region observed (see Figure 6.33). Without sector coupling, the costs account for 58 bn. EUR in High PV, exceeding those of the REF scenario (48 bn. EUR) and of the High Wind scenario (46 bn. EUR). With sector coupling, the total costs in the electricity sector increase significantly in each FD scenario. In LF and High PV this increase is highest with 167 %, compared to REF (146 %) and High Wind (134 %), due to the comparably high investment and dispatch requirements mainly caused by the additional power plant technologies (see Figure D.10 in Appendix D). This cost increase in the electricity system due to sector coupling is also driven by the additional electricity demand of the PtX technologies. In contrast, when energy storages are available for sector coupling (HF scenario), the total costs in the electricity system compared to LF are decreasing in each FD scenario. Compared to the CAPEX and OPEX associated with sector coupling (investments in heat pumps, electrolyser and BEV including the respective storages plus the dispatch costs for the

benchmark processes³² (gas boiler, steam reformer and ICE) are higher by magnitudes of up to 15 times compared to the costs of the electricity system.

A closer look at the OPEX shows the increase in variable and emission costs in the electricity system due to the electrification of the selected energy end-use sectors (see Figure 6.34). Thereby, compared to the scenario without sector coupling, the increase is again highest in the High PV scenario. Due to the comparably high dispatch costs of the benchmark processes, an electrification of the sectors allows for high total OPEX reduction of around 50 % from 717 bn. EUR to lowest values of 350 bn. EUR per year in High Wind and HF.

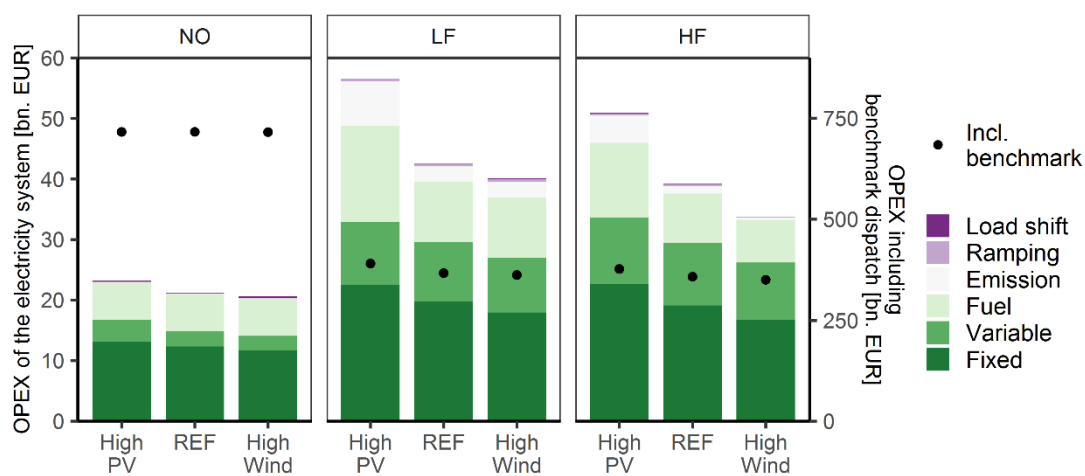


Figure 6.34: OPEX in the electricity system and total OPEX including sector-specific benchmark technologies (Own illustration)

Combining both, the expenditures for iRES as well as for flexibility options (non-iRES expenditures), the specific total system costs can be calculated. Table 6.2, summarises the overall values. Thereby, the annualised costs for the iRES expansion are low compared to the costs associated with the flexibility provision. Again, it is important to note, that the cost increase in each FD scenario due to sector coupling includes capacities and electricity generation to meet the demand of the PtX technologies. In general, the higher electricity generation required to cover the residual load deficits with increasing PV shares is resulting higher annual costs. As a result, the highest specific costs can be observed in the High PV scenario. While without sector coupling, the range is between 16 and 18 EUR/MWh, the cost increase with sector coupling. However, with a higher flexibility of sector coupling, the specific costs can be reduced by up to

³² In the costs analysis, the fuel and emission costs for the benchmark processes are.

15 % in High Wind compared to low flexibility. In general, the resulting costs are comparable with today's costs (iea 2015).

Table 6.2: Overview of system costs and resulting specific costs in the electricity system

	Unit	FS scenario	High PV	REF	High Wind
Annualised CAPEX for iRES expansion	[Mio. EUR]	-	82	82	85
Annualised non-iRES CAPEX + OPEX of electricity system*	[Mio. EUR]	NO	57,517	48,380	45,821
		LF	153,456	119,348	107,282
		HF	142,364	112,180	93,782
iRES generation	[TWh]	-	2,162	2,162	2,162
Non-iRES electricity generation	[TWh]	NO	1,010	914	795
		LF	1,505	1,417	1,400
		HF	1,491	1,422	1,387
Specific total system costs	[EUR/MWh]	NO	18	16	16
		LF	42	33	30
		HF	39	31	26

*without costs caused by investment in and dispatch of PtX technologies and the benchmark processes

In Figure 6.35, the specific-costs for each country are illustrated as function of the corresponding PV share on the electricity demand. Without sector coupling the costs range between 5 and 39 EUR/MWh. The cost increase due to sector coupling is varying within the countries. The highest increase in LF compared to NO can be observed in countries with high additional electricity demand (e.g. Germany and the Netherlands) or high storages investments (e.g. Italy). In contrast, as observed before, in HF the specific costs are decreasing, with highest effects in the same countries named before. Besides very high PV shares (as in Italy) as an exception, the relation between specific costs and PV share on the electricity demand is showing a tendency of higher costs with lower Wind-PV ratio. Thus, in the scenario with high PV expansion, especially the countries with low PV potential and comparably low PV installations are facing the highest specific costs, when sector coupling is enforced into the system. As seen before, this is mainly due to higher additional power plant capacities and dispatch to cover the increase in electricity demand by sector coupling.

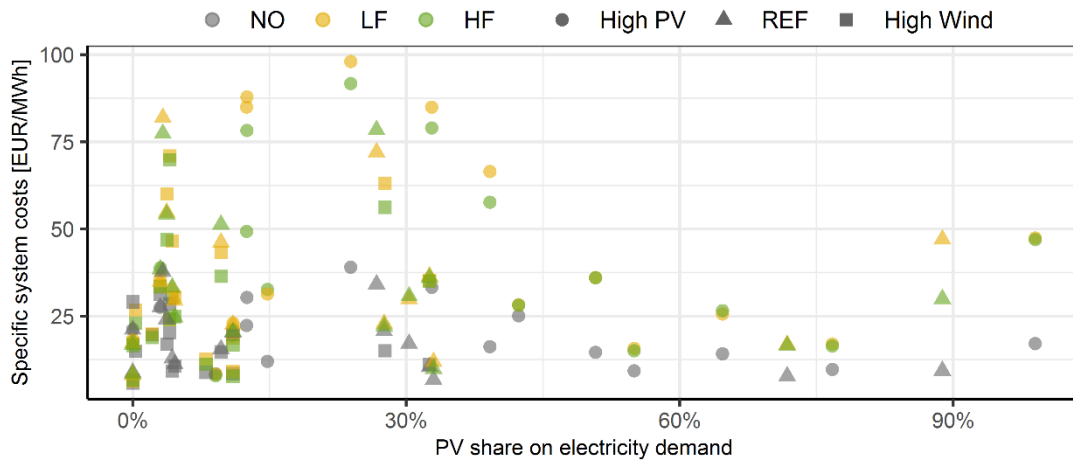


Figure 6.35: Specific system costs per country and scenario as function of the PV share on the electricity demand (Own illustration)

6.5 Comparison of CO₂-emissions

Of high importance are furthermore the resulting CO₂-emissions within the FD and FS scenarios. Due to the interacting energy sectors, different sources and sinks for emissions are included. To allocate the emissions to the analysed sectors, the approach as depicted in Figure 6.36 is applied. Time series of hourly specific emissions in the power sector for each country are derived by dividing the hourly emissions by the hourly amount of electricity generated including iRES. Thereby, the emissions caused by CHP are allocated to the heating and electricity sector based on the CHP ratio. The country-specific time series of emission factors are then used to calculate the emissions in the energy end-use sectors for heat, hydrogen and mobility provision by hourly summing up the emissions resulting from the use of the benchmark processes (gas boiler, steam reformer and ICE) as well as the electricity used by the PtX technologies multiplied with the hourly emission factors. The specific emissions of the electricity sector itself are defined by multiplying the residual load with the time series of the specific emission factors.

As a result, sector specific emission can be compared, as done in Figure 6.37. For most of the scenario combinations, the highest emissions occur in the scenario without sector coupling with a maximum total value of 1,108 Mt CO₂ emissions in the High Wind scenario. The difference between the Wind-PV scenarios is mainly resulting from the optimal CHP dispatch replacing the gas boiler usage. Without sector coupling, the emissions of the electricity sector are close to zero, since almost no fossil-fuel based electricity is required. In contrast, the included energy demand of the heating sector is causing the highest emissions of more than 600 Mio. t CO₂ in each flexibility demand (FD) scenario.

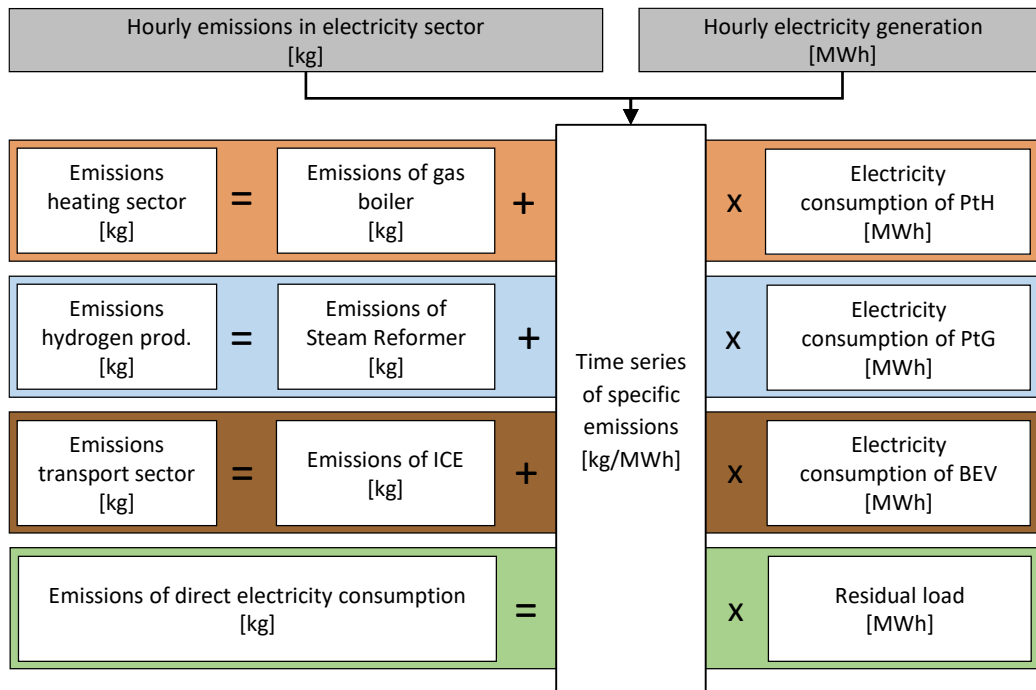


Figure 6.36: Calculation of sector specific emissions (Own illustration)

With sector coupling but without available energy storages for the PtX technologies (LF), the further energy demand sectors can reduce their emissions. Since in the heating sector the electrification by heat pumps substitutes more than 50 % of the gas boiler dispatch, the achievable emission reduction is exceeding 50 % compared to the NO scenario although the electricity mix is characterised with specific emissions. The stronger expansion of gas-based power plants with sector coupling results in an increase of emissions allocated to the electricity sector. Thereby, in High PV these power plants are dispatched the most due to the high residual load resulting in the strongest increase of emissions in the electricity sector for this scenario. In contrast, the total emissions in the REF and High Wind scenario can be reduced by 46 % and 42 % to 603 and 644 Mt CO₂ respectively. With higher flexibility in sector coupling, the CO₂-emission reduction compared to NO is highest in each FD scenario. In total, the High Wind scenario shows the lowest values with 321 Mt CO₂. While High Wind and REF show highest sector specific emissions in the transport sector (around 155 Mt CO₂), the electricity sector still contributes most to total emissions in High PV. Cumulating the emissions solely for the hydrogen, transport and heating sector, the total values range between 267 and 314 Mt CO₂. This underlines the importance of further emission reductions also in the electricity sector and the importance of additional alternatives (see also the discussion in Chapter 5.3.1 about CCS becoming cost competitive with a CO₂ price of 96 EUR/tCO₂). Compared with the implemented CO₂-price of 80 EUR/tCO₂, this emphasises the potential of the energy-policy instrument of

CO₂-emission pricing to further decrease the emissions in the energy system. A sensitivity analysis in Chapter 6.7 evaluates a stronger CO₂-price increase on the results.

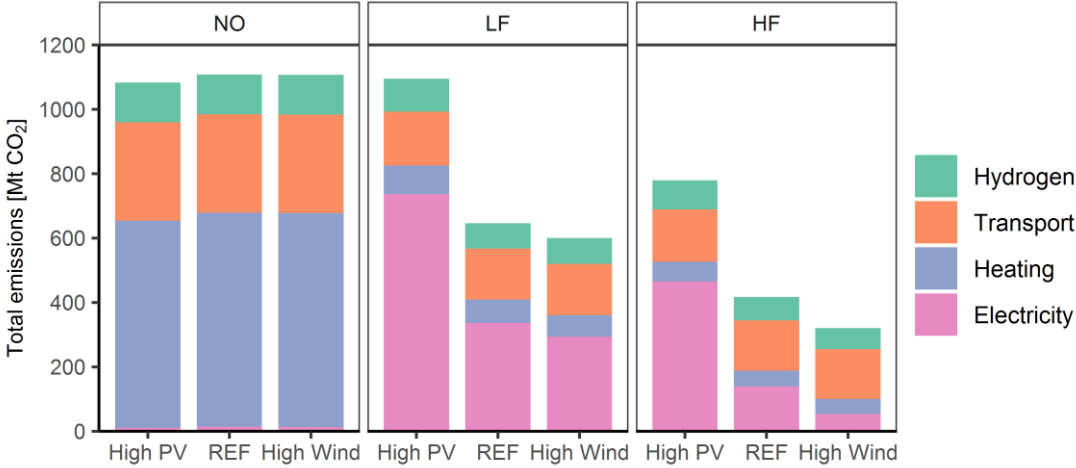


Figure 6.37: Total sector-specific emissions (Own illustration)

The presented values can be compared with the reference values for emission reduction strategies in Europe of the year 1990³³. Table 6.3 gives an overview about the sector specific contributions and compares them with the result for the HF scenario in the present work. Compared with the 1990 value for the 17 countries of 2,177 Mt CO₂ in the sectors electricity and heating, road transport as well as refining, iron and steel and chemicals, the emissions in the HF scenario with the lowest CO₂ emissions in the present work are reduced by 64 % (High PV) to 85 %. Thereby, the role of the electricity sector is crucial to achieve significantly lower reductions compared to the year 1990.

³³ Based on the GHG emission inventory (GHGEI) of the European Environment Agency (EEA 2019), the emissions of the selected parts of energy end-use sectors implemented in the present work can be estimated. However, since the categories in the inventory are difficult to be assigned exactly to the sectors included in the present work, the values are meant to give an orientation for the assessment of the emission reduction potential of the result presented before.

Table 6.3: Comparison of resulting CO₂ emissions in the HF scenario with values of the year 1990 (Data: EEA 2019 and own results)

	Category GHGEI	GHGEI number	Emissions 1990 [Mt CO ₂]	High PV [Mt CO ₂]		REF [Mt CO ₂]		High Wind [Mt CO ₂]	
Electricity	Electricity and heating	1.A.1.a	1174	465	-55 %	140	-84 %	54	-91 %
Heating				61		49		47	
Transport	Road Transport	1.A.3.b	652	162	-75 %	157	-76 %	155	-76 %
Hydrogen	Refining	1.A.1.b	101	90	-74 %	72	-79 %	66	-81 %
	Iron and Steel	1.A.2.a	162						
	Chemicals	1.A.2.c	88						
Total			2,177	780	-64 %	417	-81 %	321	-85 %

Figure 6.38 illustrates the specific emissions per country as function of the PV share on the electricity demand. Note that here, the total amount of emissions within the system borders of the present work including sector coupling and the respective benchmark process are included. With sector coupling (in the LF and HF scenarios) a major part of countries with a PV share below 40 % is having specific emissions of more than 0.2 t CO₂/MWh_{th}. Furthermore, Figure 6.38 confirms a high emission reduction potential in the heating sector due to sector coupling rather equally distributed across the countries observed. Similar outcomes but with lower reductions of the specific emissions can be seen for the transport sector. In contrast, while most of the countries can reduce their specific emission for hydrogen production by almost 50 %, some countries show a significantly higher specific emission. Besides Italy, this is also true for Switzerland and Czech Republic, indicating a higher correlation of gas-fuelled electricity generation and electrolyser dispatch compared to the remaining countries.

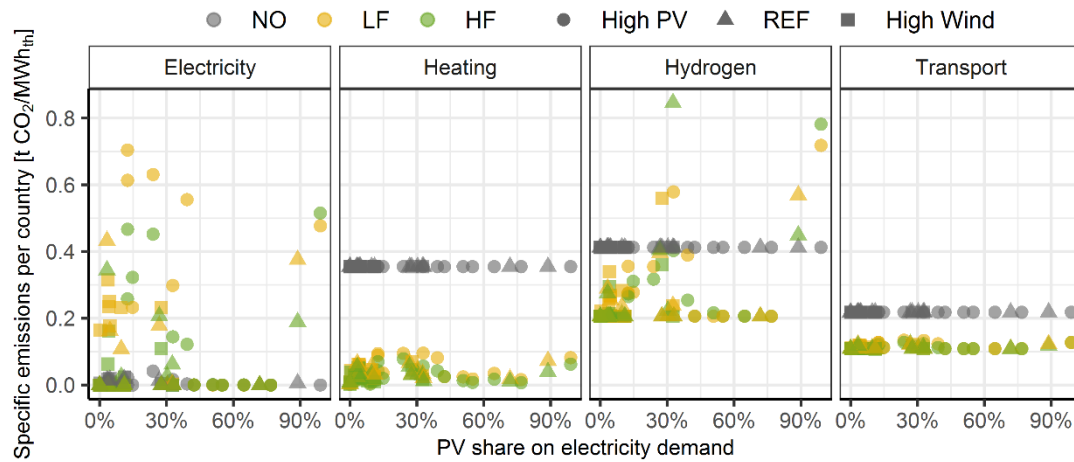


Figure 6.38: Specific emissions per country and sector as function of the PV share on electricity demand (Own illustration)

6.6 Additional scenarios

With the iRES share as well as the minimum share for the electrification of the energy end-use sectors heating, industry and transport, two crucial assumptions are introduced as framework conditions for the future energy system. Since these restrictions can be assessed to have high impact on the results, two additional scenarios are calculated using the same model formulation. The scenario results presented above are named *original results* in the following to distinguish them from the additional scenario outcomes presented below. On the one hand, with the additional scenario *iRES+*, an accelerated iRES expansion compared to the 80 % scenarios evaluated before is assumed. With this stronger expansion, the required iRES capacities are increased to potentially cover the total electricity demand including the electricity demand resulting from a 50 % electrification of the energy sector included. Details will be introduced in Chapter 6.6.1. On the other hand, higher ambitions in sector coupling are analysed in the scenario *PtX+*, analysing a 75 % minimum share of electricity provided in the energy end-use sectors by PtX technologies. Hence, this additional scenario sheds light on the impact of an accelerated sector coupling, compared to the original results. The outcomes are presented in Chapter 6.6.2. In general, the result analysis is more condensed, since relevant interactions are emphasised above. Main differences are shown and discussed regarding the total costs, the emissions and the sector coupling aggregated for the 17 countries observed, while further details are given in the appendix.

6.6.1 Increase of total iRES share in the observed region

As mentioned above, the *iRES+* scenario reflects an accelerated iRES expansion across the region observed. Therefore, the iRES expansion model of Chapter 3 is used to derive three scenarios with different Wind-PV ratios and a total iRES electricity generation of 3,471 TWh (compared to 2,162 TWh in the original scenario). This electricity amount is equal to 128 % of the original electricity demand in the 17 countries. The additional electricity is theoretically sufficient to cover 50 % of the energy demand of the sectors included by electrification. A further important adjustment for the iRES expansion model is the increase of the maximum iRES share per country to 150 % (compared to 110 % in the original scenario), allowing to further exceed the country-specific original electricity demand. These additional iRES capacities are influencing the residual load parameter including the maximum and minimum residual load as well as the cumulated and time-dependent surplus phases. Table D.10 in Appendix D summarizes the observed in the *iRES+* scenario. In addition, country-specific generation and capacities for the *iRES+* scenarios can be found in the Tables D.11 and D.12 in Appendix C.

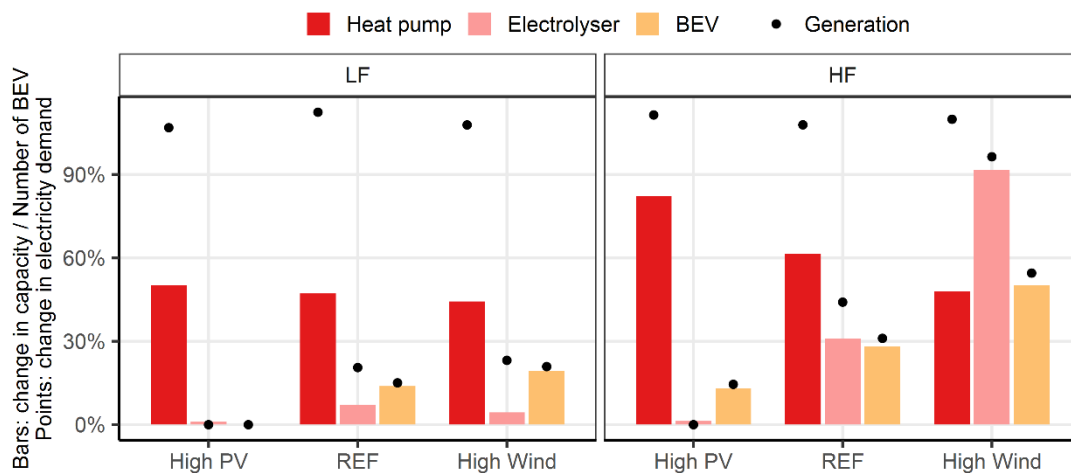


Figure 6.39: Percentage change of PtX capacities and electricity demand in *iRES+* compared to original results (Own illustration)

For the sector coupling technologies the minimum restriction still sets a lower bound of 50 % for the share of electricity to be used in the heating, the transport as well as the industry sector. The increase of the iRES generation in *iRES+* and the resulting surpluses have significant effects on sector coupling. Figure 6.39 depicts the percentage change of optimal capacity investments (bars) and electricity demand (points) in the *iRES+* scenario compared to the original FD and FS scenarios. With regard to the capacities, the heat pump installations are increasing most in the High PV scenario. Additional capacities are optimal also for electrolyser and for BEV with a higher total iRES share in the region observed. An exception can be found for High PV with low

flexibility in sector coupling. However, in general, the observed effect is higher when energy storages are available for sector coupling and increasing with higher Wind-PV ratios. With regard to the electrification, in most of the FD scenario, the increase in electricity consumption of the PtX technologies is higher compared to the corresponding capacities expansion, indicating higher full load hours. Around 100 % of the heating demand are covered by electricity as an optimal model-endogenous result for the HF scenario. Compared with the original results with an electricity share of 50 % on total energy demand for the hydrogen sector and BEV, the higher iRES share results in optimal values of 98 % for the hydrogen production and of 77 % for the private passenger transport in the High Wind scenario with flexible sector coupling. The results indicate, that the more frequent surplus periods in the High Wind scenario are beneficial for an optimal PtX expansion, resulting in the highest total share of electrification in the selected sectors. In general, the higher impact of the *iRES+* scenario on the electrification of the selected energy end-use sectors in the High Wind scenario underlines the value of iRES surplus energy for an optimal sector coupling. While in High PV, these surpluses are already existing also with lower iRES share, the more constant electricity generation of wind power plants requires higher iRES shares to increase the surplus energy amount. However, the lower seasonality of the wind-based generation is beneficial also for the sector coupling, since less balancing is required.

The results for the investment and dispatch decisions of the PtX technologies are interacting with the flexibility options in the electricity system (see Figure D.11 to D.13 in Appendix D). With regard to electricity storages, most countries significantly reduce their storage needs in the NO scenario due to lower peak load requirements, while with higher wind shares, seasonal storages become more relevant to balance the larger surplus phases. In contrast, in High PV hourly storages are still most relevant. When energy storages are also available for the PtX technologies (HF scenario), strong reductions of the hourly storage demand in most of the countries can be observed. In total, the storage capacity in HF is reduced by 30 % and 70 % in High PV and REF compared to the original results, while in High Wind there are still no additional storage requirements beyond PSP. Thus with an increase in iRES shares in an energy system with flexible sector coupling, the role of electricity storages is reduced. The two main reasons are the generally lower residual load as well as the higher temporal shifting activity of the energy storages in the energy end-use sectors. In contrast, the spatial balancing by transmission capacity is gaining in importance with a higher iRES share compared to the original results, to distribute the higher iRES surpluses for sector coupling. Conventional power plant technologies fuelled by gas and nuclear energy are reduced significantly with sector coupling.

With the changes of capacities for power plants storages and NTC, the CAPEX in the electricity system are decreasing in total by up to 38 bn. EUR in REF with flexible sector coupling (see Figure D.14 in Appendix D). Also the OPEX in the electricity system are decreasing due to savings in fixed and variable O&M costs as well as emissions and fuel costs. In addition, the cost savings including the sector coupling related OPEX are higher, since the fuel and emission costs of the benchmark processes can be reduced significantly.

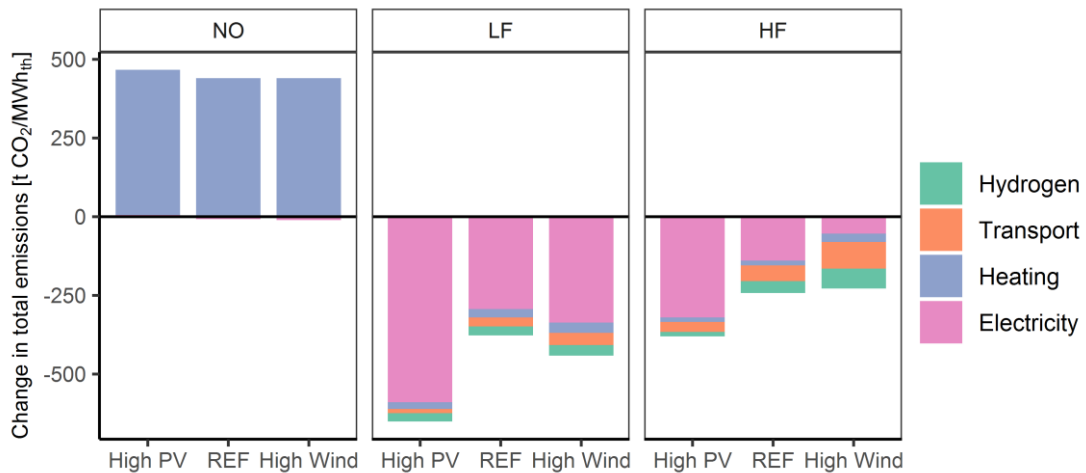


Figure 6.40: Absolute change of CO₂ emissions in *iRES+* compared to original results (Own illustration)

Finally, the discussion of the *iRES+* scenario can be summarised by analysing the CO₂ emissions resulting from the optimal dispatch of the flexibility options (see Figure 6.40). Without sector coupling, a reduction of CHP capacities (due to the decrease of base-load capacity requirements) causes a higher dispatch of gas boiler resulting in higher emissions in the heating sector. In contrast, with sector coupling particularly the emissions allocated to the electricity sector are decreasing, since more *iRES* electricity can be integrated into the energy system and CO₂ emitting fuels are substituted. Starting from the highest amount of CO₂-emissions in LF and HF, in the High PV scenario the emission reduction is strongest. Nevertheless, only in REF and High Wind, the electricity sector is carbon-free. Nevertheless, based on the results a stronger increase of *iRES* capacities beyond 80 % is highly recommendable in terms of a reduced demand for capital intensive flexibility options like hourly storages and carbon intensive power plants.

6.6.2 Higher share of electricity in the energy demand sectors

In the second additional scenario, *PtX+*, the impact of a faster deployment of sector coupling compared to the original scenarios is analysed. Thus instead of setting the lower limit of electrification in each of the selected sectors to 50 %, this value is increased to 75 %. As a result, at least 1,143 TWh additional electricity demand has to be provided by the electricity system

(see Table 6.4). For the following analysis, the differences compared to the original results are analysed solely for the LF and HF scenario, since the assumed variation is only affecting the sector coupling scenarios.

Table 6.4: Overview of differences regarding electricity demand due to sector coupling in *PtX+* compared the original scenarios

		Original scenario	<i>PtX+</i>
iRES surplus of cumulated residual load (High PV REF High Wind)	[TWh]	473 219 74	
Electricity demand for heating demand*	[TWh]	303	455
Electricity demand for hydrogen production*	[TWh]	187	281
Electricity demand for passenger transport*	[TWh]	272	408
Total	[TWh]	762	1,143

* Minimum based on model formulation for minimal share of electricity in respective sector

Similar to the analysis before, in a first step, the influence on capacities and electricity consumption of the PtX technologies are discussed. In Figure 6.41, a higher increase in generation compared to capacity can be observed, indicating higher full load hours of the PtX technologies compared to original results to meet the higher electricity demand and avoid additional capital intensive investments in capacity. In absolute terms, in *PtX+* a flexibilisation of the sector coupling has negligible impact on the capacities installed (less than 1 % change between LF and HF in each FD scenario). 50 % additional BEV are required to cover the increased minimum electricity share. Regarding the share of electricity for heating and hydrogen, the 75 % minimum restriction is not exceeded in *PtX+*. Thus in each FD and FS scenario, the consumed electricity is meeting the minimum value of 1,143 TWh and a further electrification beyond the 75 % restriction is not optimal. This indicates, that the framework conditions enabling a flexibilisation of electrolysers (in general a high iRES share as well as higher surpluses in summer as discussed before) are less beneficial due to the higher electricity demand.

The enforced increase of electricity demand influences the remaining flexibility options (see Figure D.15 to D.17 in Appendix D). Especially due to the higher share of electricity for the heating demand, a switch from CHP to gas-fuelled power plant can be observed in both scenarios with low and high flexibility in sector coupling. In general, with higher Wind-PV ratio the percentage increase of power plant capacities is stronger (up to 24 % in High Wind compared to maximum 15 % in High PV). The identified interrelation of a higher PV share leading to an increasing role of hourly storages is further strengthened in LF. Similar

interactions are true for the electricity storage reducing effect when heat storages and hydrogen storages as well as bi-directional charging of the BEV become available. Furthermore, with regard to the NTC expansion especially in High PV, the NTC requirements can be reduced in both flexibility supply (FS) scenarios compared to the original results.

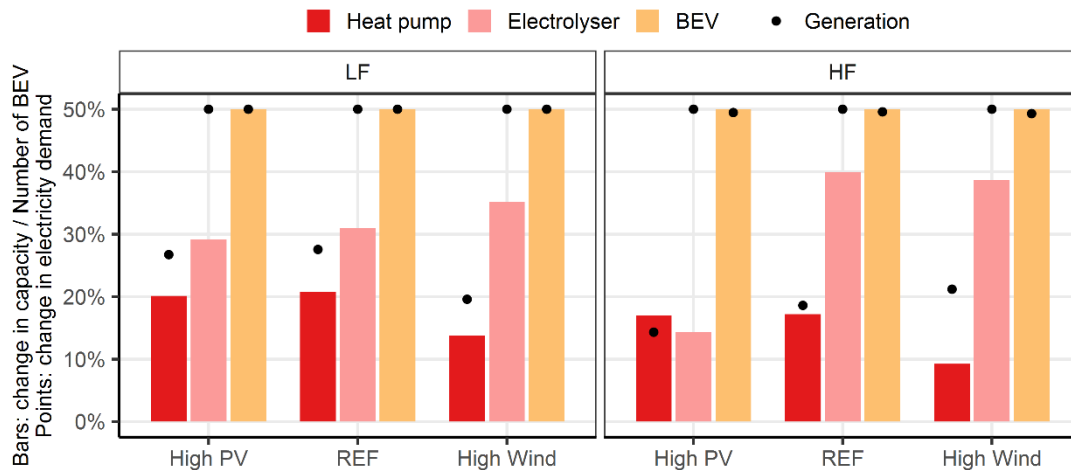


Figure 6.41: Percentage change of PtX capacities and electricity demand in *PtX+* compared to original results (Own illustration)

In LF, the reduced investments in CHP plants lower the CAPEX in *PtX+* compared to the original results (see Figure D.18 in Appendix D). In High PV this effect is highest, also overlapping the increased costs for electricity storages. The coverage of the additional electricity demand mainly by gas-fuelled power plants increases the OPEX as well as emissions. The accompanied increase in fuel and emission costs is generally higher in LF. However, again when including the costs caused by the benchmark technologies, the cost savings are significantly higher (around 150 bn. EUR) compared to both the OPEX in the electricity system as well as the original results.

Nevertheless, the comparison of the emissions in the sectors in comparison with the original results shows strong increases mainly in the electricity sector by more than 1,300 Mt. CO₂ (High PV) to more than 1,600 Mt. CO₂ (REF) in LF compared to the original results (see Figure 6.42). Thereby, the higher specific emissions of the electricity also used for the sector coupling are overlapping the emission reductions resulting from the benchmark process substitution.

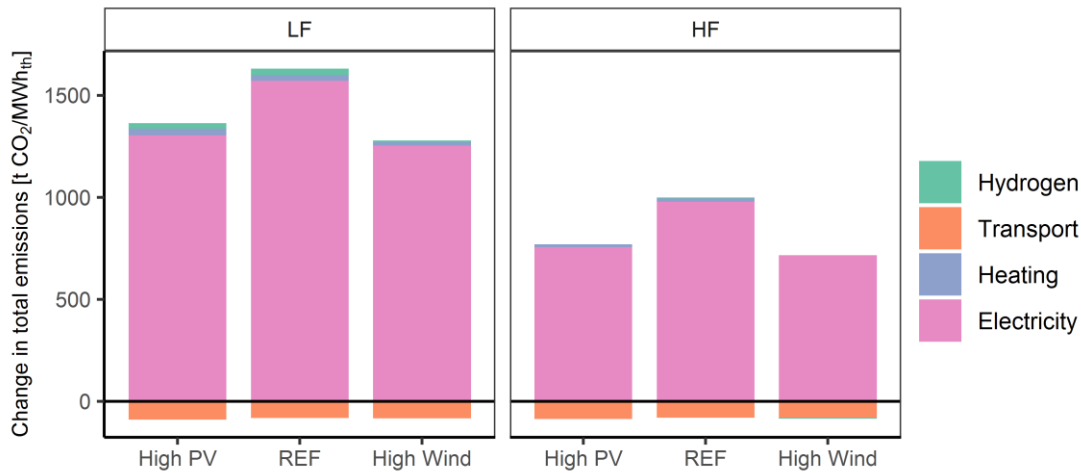


Figure 6.42: Absolute change of CO₂ emissions in PtX+ compared to original results (Own illustration)

6.7 Sensitivities for selected input assumptions

Furthermore, the presented results are additionally discussed with regard to selected assumptions. Three sensitivities are applied to increase the understanding of influences on the optimal combination of flexibility options within the present modelling framework. On the one hand two cost parameter assumptions are sensitised, namely the capital costs of PtX technologies as well as of electricity storages. On the other side, a main energy-policy instrument, the pricing of CO₂-emissions is further assessed. For better clarity, the focus is on the High PV and High Wind scenario. The aim of this analysis is to examine the effects on optimal capacity investments for the most important flexible technologies as well as the resulting emissions.

Reduced PtX capital costs

Since sector coupling is targeted for emission reduction, learning effects due to technological improvements and gains in application experience are likeable. Therefore, in the following sensitivity a further decrease of CAPEX related costs for the PtX technologies heat pumps, electrolyser and BEV as well as the corresponding energy storages by up to 50 % compared to the data input assumed before is applied. For these sector coupling technologies, a reduction in specific investment costs is directly influencing the competition with the benchmark processes.

In Figure 6.43, the reduction of PtX costs shows the highest influence on BEV in both sector coupling approaches. With a price reduction of 20 %, thus 30,400 instead of 38,000 EUR/car, BEV completely replace ICE as an optimal model-endogenous result under the assumptions made. Heat pumps show a higher effect for the High PV scenario, however are less sensitive to capital cost reductions. In contrast, the optimal total capacities for electrolyser are only affected with

higher flexibility in sector coupling, mainly in the High PV scenario. Again, this underlines the competition about the surplus phases. With hydrogen storages, a CAPEX reduction results in lower investments in electrolyser, since the flexibility of the additional BEV is preferably used for the electricity demand in the transport sector. However, with cost reductions exceeding 40 %, electrolyser installations also increase in HF, reflecting a break-even point, where the CAPEX reductions are higher compared to the electricity costs. The sector coupling approach also decides about the influence of PtX CAPEX reductions on investments in electricity storage capacities. While a less flexible sector coupling requires additional storages to meet the increased electricity demand peaks, in HF the BEV and the available energy storages for the PtX technologies also replace storages, mainly in High PV. Due to the low absolute storage installation in High Wind, rather small changes result in higher relative sensitivity results. In general, the additional electricity demand is covered by further power plant investments including gas technologies.

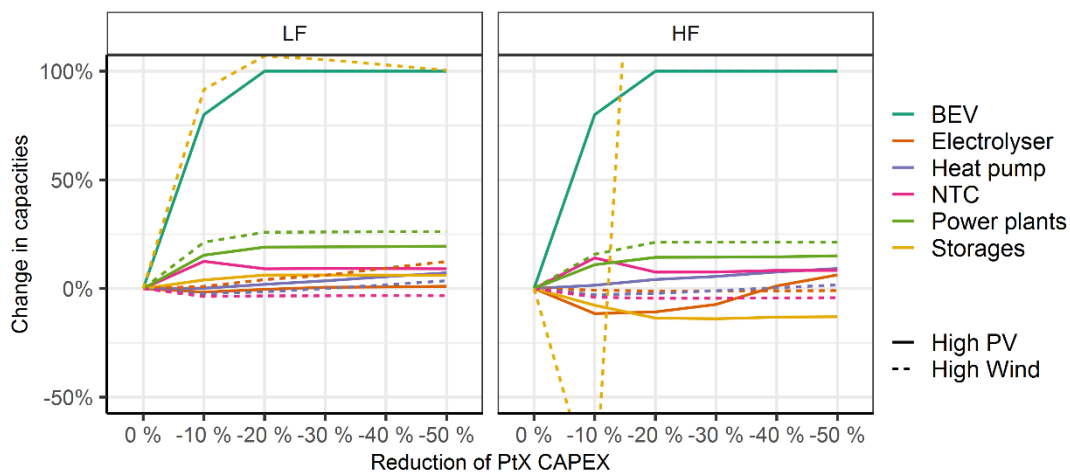


Figure 6.43: Change of installed capacities of flexibility options in the sensitivity with lower CAPEX for sector coupling technologies (Own illustration)

The emissions in the sector are reflecting the results on optimal capacity investments (see Figure 6.44). With the higher shares of BEV up to 100 %, the corresponding emissions can be reduced significantly. At the same time, mainly the electricity sector shows higher emissions, since the increases in PtX capacities requires also gas-fuelled power plants. The highest relative increases compared to the original results can be seen in the High Wind scenario with values of more than 100 %. However, the higher absolute values in High PV cause the strongest absolute increase in both the LF as well as the HF scenario.

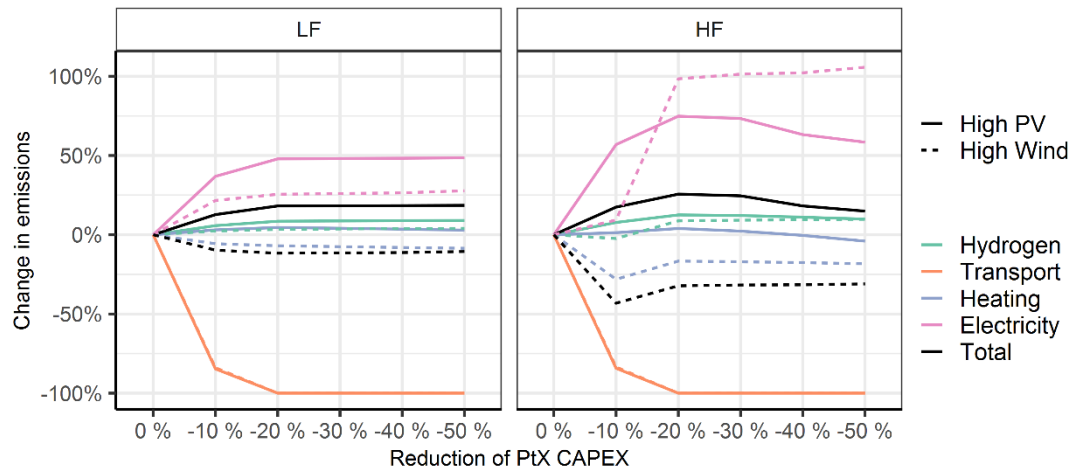


Figure 6.44: Sector-specific changes in emissions in the sensitivity with lower CAPEX for sector coupling technologies (Own illustration)

The aforementioned more cost-beneficial use of iRES surpluses by BEV in HF and the resulting replacement of hydrogen production in these times can be confirmed, when looking at the total emissions of the hydrogen provision with an increase by around 10 % in both FD scenarios. In the High PV scenario, the emissions resulting from the heating sector are only slightly influenced by reduced capital costs for the PtX technologies. In contrast, in the High Wind scenario a cost reduction leads to lower emissions by up to 25 % compared to the original data input. Since the highest shares on total emissions can be found in the electricity and heating sector, the discussed sensitivities result in an increase of total emissions due to lower CAPEX of the sector coupling technologies in High PV, while a decrease can be observed in the High Wind scenario.

Reduced electricity storage capital costs

A further sensitivity is applied to shed light on the impact on costs reductions for electricity storages, thus the flexibility option strongly influenced by the scenario framework as presented before. To improve the understanding of the role of electricity storages, a sensitivity of further capital cost reductions by up to 50 % compared to the original cost assumptions is applied for each of the implemented electricity storage technologies.

These cost reductions further increase the optimal electricity storage investments in the High PV and more significantly in the High Wind scenario independently from the sector coupling approach (see Figure 6.45). In the latter scenario, a reduction of electricity storage related CAPEX by 50 % causes an increases of storage capacities compared to the original scenario by more than 100 % and up to 400 % in HF. The cost reduction for all storage types particularly increases the installations of hourly storages in High PV. In contrast, in High Wind additional

seasonal storages are optimal. Thus a further costs decline causes a stronger difference of storage technology combinations reflecting more clearly the differences in the flexibility demand with varying Wind-PV ratios.

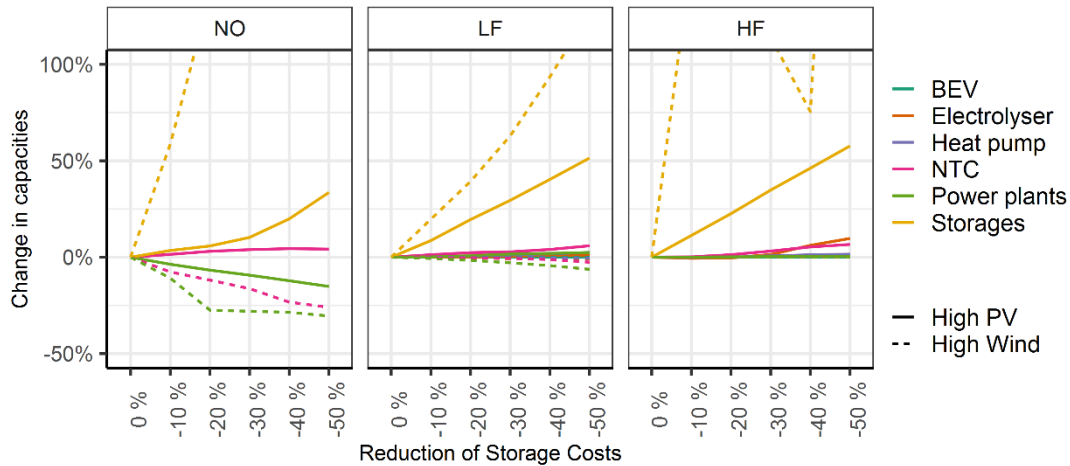


Figure 6.45: Change of installed capacities of flexibility options in the sensitivity with lower CAPEX for electricity storages (Own illustration)

However, the effects on further flexibility options are rather small. Without sector coupling, a decreasing influence on power plant capacities (mainly gas-fuelled) can be observed illustrating the replacement of generation capacities for peak load provision by electricity storages. In addition, for the High Wind scenario additional temporal shifting flexibility lowers the demand for spatial balancing. With sector coupling, lower storage costs slightly increase the optimal electrolyser and heat pump capacity in High PV. The lower storage costs enable a further charging of PV surpluses also to provide electricity for heat pumps. This leads to a reduction of CHP requirements and improves the competitiveness of additional gas-fuelled power plants. This effect is stronger with flexible sector coupling.

The already low emissions in the electricity sector without sector coupling are further reduced with lower storage cost, but with a low effect on total emissions (see Figure 6.46). In contrast, the differences of the effects on power plant investments with sector coupling result in an increase of total emissions in High PV by up to 13 % in HF, while for High Wind a further reduction can be observed.

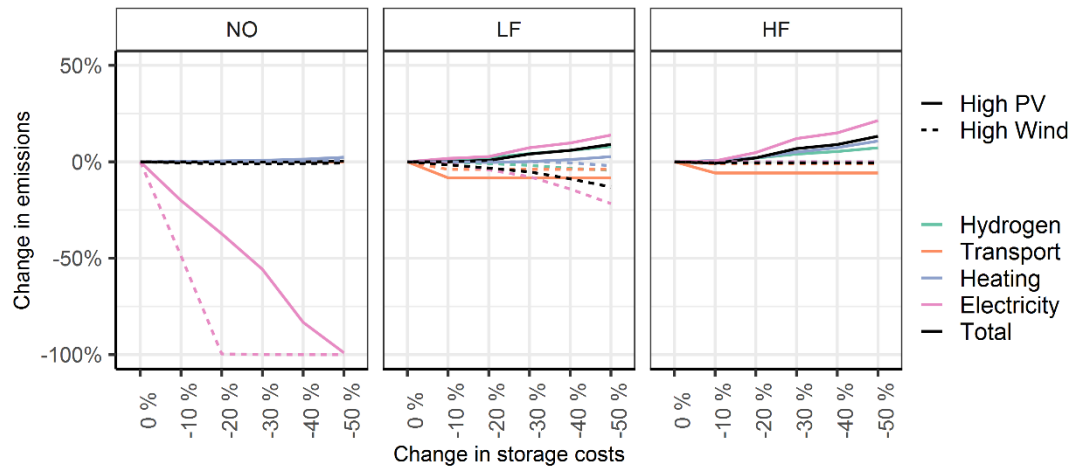


Figure 6.46: Sector-specific changes in emissions in the sensitivity with lower CAPEX for electricity storages (Own illustration)

Higher CO₂-prices

On the one hand, CO₂-prices directly influence the dispatch of technologies providing and demanding energy. This concerns the power plant mix affecting the emissions in the electricity sector as well as those in the selected energy-demand sector due to both, the electricity consumption and the use of benchmark fuels. On the other side, further flexibility options are indirectly affected due to shifts in optimal combinations of flexible technologies. Thus, the impact of this sensitivity analysis is expected to have cross-sectoral influences. The analysis can give a hint on the emission reducing effect of higher CO₂-prices within the present modelling framework under otherwise constant assumptions. In the following, the model calculations are done with a stepwise increase of the CO₂-prices up to 180 EUR/tCO₂ for the High PV and High Wind scenario. This highest value is often discussed as required compensate for environmental costs caused by one tonne of CO₂ (UBA 2019).

Without sector coupling, a CO₂-price increase has different effects on the mix of flexibility options in High PV and High Wind (see Figure 6.47). In both scenarios, gas-fuelled power plants are replaced (but not completely substituted), due to the increase in emission related costs. At the same time renewable CHP capacities are increased significantly, also since the heat supply with gas boiler as benchmark process is more cost-intensive. This effect is stronger in the High PV scenario, where the increasing share of CHP with higher CO₂-prices also substitutes electricity storages for peak load provision. With a very high price of 180 EUR/tCO₂, this storage replacement results in an increase in CCGT capacities in High PV. Thus, to reduce emission-related costs in the heating sector, emission increases in the electricity sector are more beneficial. In contrast, in the High Wind scenario, the reduction of carbon intensive power plants and

increase of CHP also requires additional (mainly daily and seasonal) storages with CO₂-prices above 80 EUR/tCO₂ and below 180 EUR/tCO₂. Furthermore, the increasing country-specific domestic electricity production with higher CO₂-prices due to the combined heat and power generation reduces the need for transnational electricity transmission by more than 20 % in High PV and a high CO₂-price of 180 EUR/tCO₂.

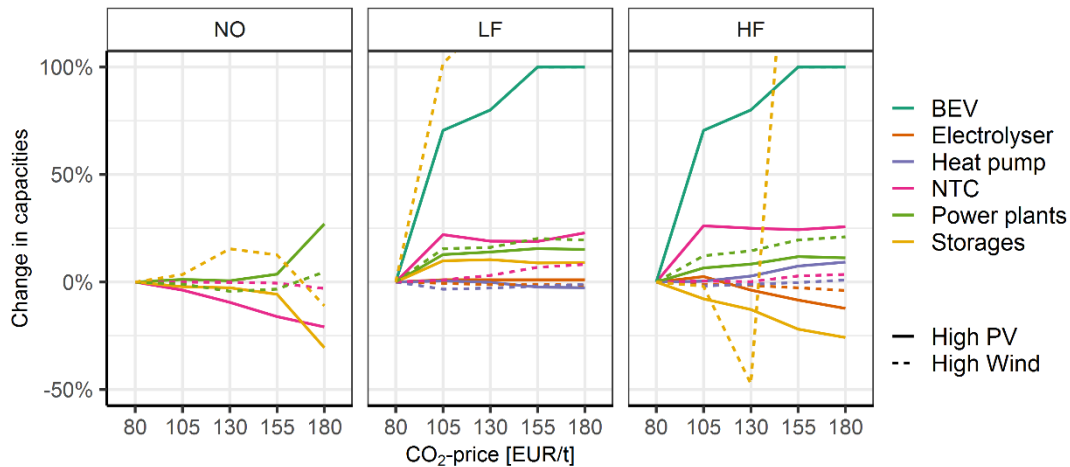


Figure 6.47: Change of installed capacities of flexibility options in the sensitivity with higher CO₂-prices (Own illustration)

With sector coupling, a higher CO₂-price significantly increases optimal investments in BEV. Compared to 80 EUR/tCO₂, a price increase of 25 EUR/tCO₂ already results in almost 75 % more BEV in both FD scenarios and independently from the availability of energy storages. However, without flexibility in sector coupling, a CO₂-price increase causes a slight decrease of the installed capacity of the remaining PtX technologies. Here, the interplay between the levelised costs of the benchmark processes and the PtX technologies affects most strongly the BEV and ICE, while the cost differences between the respective benchmark processes for heat pumps and electrolyser are less impacted. The additional electricity demand for BEV requires additional storages and power plant capacities. Particularly in High Wind, the role of storages is increasing with higher CO₂-prices and sector coupling by up to 150 % (LF) and 300 % (HF) compared to a CO₂-price of 80 EUR/tCO₂. In contrast, in High PV storages are less relevant, while NTC become more important with total capacity increases of around 25 % since the value of the spatially distributed PV surplus energy becomes increasingly important.

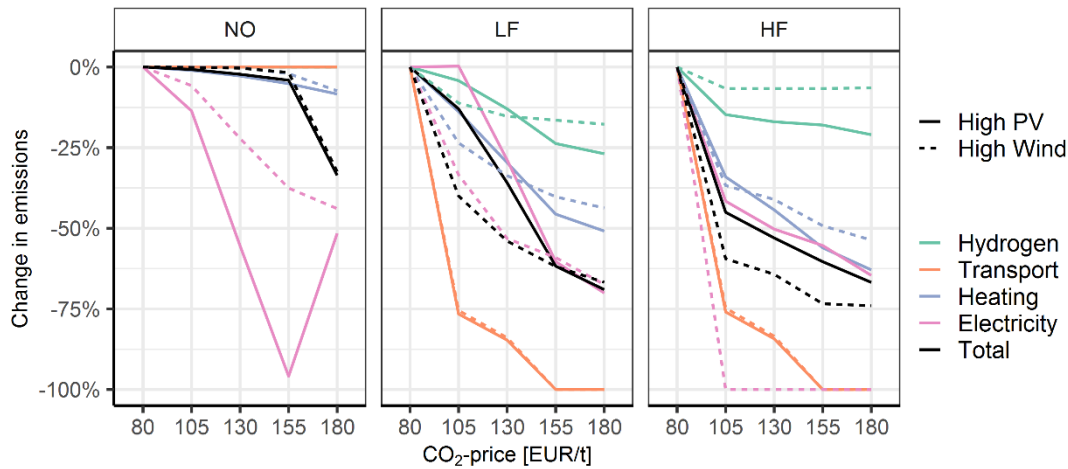


Figure 6.48: Sector-specific changes in emissions in the sensitivity with higher CO₂-prices (Own illustration)

In each FD and FS scenario, an increase in CO₂-prices results in emission reductions in each energy demand sector (see Figure 6.48). In the present modelling framework and without sector coupling, this price increase effects most significantly the electricity sector but also the heating sector due to additional substitutions of gas boiler by (renewable) CHP. With sector coupling, the increase in competition of BEV compared to ICE due to higher CO₂-prices allows for emission reductions in the transport sector compared to a CO₂-price of 80 EUR/tCO₂ by almost 100 % with prices above 155 EUR/tCO₂ in both FD scenarios. The second highest decreasing effect can be observed for the electricity sector, while the hydrogen sector shows the lowest sensitivity to higher CO₂-prices in the High PV as well as the High Wind scenario. However, although the total capacities (and dispatch) of heat pumps and particularly of electrolyser are less sensitive to a CO₂-price increase, the achievable emission reduction indicate a further adjustment of dispatch decisions to times with less emission-intensive electricity supply (mainly surplus phases) and a higher substitution of benchmark processes. This effect is stronger in High PV due to the higher amount of surplus energy resulting in stronger relative emission reductions in the heating and hydrogen provision. While in LF the total relative emission reductions due to higher CO₂-prices are similar in High PV and High Wind, with higher flexibility in sector coupling, this total decrease is more sensitive in the wind-dominated scenario. In High Wind, a flexible sector coupling allows for a complete decarbonisation of the electricity sector as well, resulting in total emission reduction of up to 75 % with a CO₂-price of 180 EUR/t compared to 80 EUR/tCO₂.

7 Conclusion

In the following the outcomes of analysis in the present work are summarised and discussed with regard to the overall research questions introduced in Chapter 1. Furthermore, a critical appraisal takes up limitations of the present work, while reflections on further research potentials shows possibilities to build up on the methods and insights gained in the present work. Finally, the conclusions are used to derive recommendations.

7.1 Summary and research questions

Within the present work, three research fields regarding the future transformation of a multinational European energy system were addressed to identify interactions between flexibility demand and flexibility supply. The first research field provides insights into the interactions between different Wind-PV ratios in the iRES generation and the resulting flexibility needs based on fundamental considerations of generation characteristics and available potentials across 17 countries in central-western Europe. Therefore, weather- and GIS-data based wind onshore and PV potentials were derived in Chapter 3 and optimal iRES expansion scenarios were evaluated in Chapter 4. To analyse influences on the flexibility requirements, three scenarios each with high total iRES shares but varying Wind-PV ratios are applied in a iRES expansion model. This model is developed to cope for geographically highly resolved weather data, for limitations of iRES potentials due to land-use restrictions as well as for energy-policy constraints of wind and PV expansion. Although the model was developed to derive different iRES expansion scenarios and the corresponding outcomes are based on a cost-minimisation, the influence of non-cost related factors is represented as well. The present model formulation introduces possibilities to include additional restrictions like a dispersion of land-use for iRES capacities to cope for possible future techno-economic as well as socio-ecologic challenges. These constraints are limiting the solution space and increasing the costs of the

optimal solution as it is most likely in the future iRES expansion pathways. As a result, scenario-specific residual loads with varying flexibility demands were assessed. The analysis confirms the high potential of iRES in Europe with generation potentials for PV and wind exceeding the today's electricity demand by magnitudes. In addition, high shares of these potentials can be assessed with (future) LCOE ranging between 10 and 30 EUR/MWh. Thus, these energy sources are competitive with fossil fuels, in particular when assuming further increasing costs for the latter ones due to emission reduction efforts. The focus on the generation characteristics of PV and wind as well as the differently distributed potentials allows to answer the question of the first research field, *how do varying Wind-PV ratios in the iRES electricity generation influence the flexibility needs of a transnational European energy system?* The present analysis emphasises the importance, of taking the Wind-PV ratio for the assessment of future iRES expansion pathways into account, especially when analysing the underlying integration challenges. The availability of the iRES, their temporal generation pattern as well as the simultaneity of iRES feed-in are the most important characteristics of iRES electricity generation in Europe. A higher or lower Wind-PV ratio leads to very different residual loads to be balanced across the 17 countries observed. Due to the daily and seasonal generation characteristics of PV strongly correlating across larger geographical areas, a higher PV share in iRES generation increases crucial parameters of the flexibility demand. Accordingly, a lower Wind-PV ratio leads to a higher range between maximum and minimum residual load peaks during a year as well as to higher total surplus energy amounts. In a time-dependent perspective, especially the iRES surplus phases are clearly different with shorter but higher surplus phases with higher PV shares compared to longer periods with less energy content in the scenario with high wind shares. Summarising, mainly due to the higher seasonal balancing challenges, a higher share of PV based electricity generation increases the iRES integration efforts in terms of required flexible capacity and energy in an electricity system perspective.

In a second research field, the options to provide flexibility for the balancing of the flexibility demand were introduced as well as mathematically implemented in ELTRAMOD. Therefore, the existing electricity market model was adjusted to represent multiple flexible technologies with different application potentials for upward, downward and shifting flexibility provision. In a greenfield approach, the model represents a suitable approach for the techno-economic evaluation of optimal combinations of flexibility options with different flexibility demand at reasonable computational effort. Within research field two and the question of *are different Wind-PV ratios in a transnational European energy system and the resulting flexibility demand influencing the optimal provision of flexibility in the electricity market?*, the analysis shows a significant impact on flexibility provision and changing roles of flexible technologies. Table 7.1 summarises the

findings against the background of an increasing wind share in the iRES generation mix. In a purely electricity market perspective without sector coupling, the smaller range of positive and negative residual load with higher Wind-PV ratio requires less iRES integration effort compared to higher PV shares. Thus, in total less flexible capacities are required in the High Wind scenario compared to High PV. Thereby, mainly the value of electricity storages changes significantly with increasing PV shares. While without sector coupling, the optimal power plant mix is rather similar with different Wind-PV ratios, electricity storages maintain increasing shares of peak load supply by discharging surplus electricity. With higher PV shares especially hourly storages are highly relevant. Furthermore, without sector coupling the transnational electricity transmission requirements are strongly influenced by the distribution of iRES generation within the FD scenarios. Without sector coupling, the total system costs are similar and the resulting CO₂-emissions show very low remaining emissions in the electricity sector, since the majority of capacities are renewable based. In contrast, the implemented benchmark processes covering the energy demand in the heating, the hydrogen and the transport sector cause comparably high emissions.

With research field three the emerging developments of sector coupling to facilitate the decarbonisation of further energy end-use sectors is included in the model-based analysis. Thereby, an enforced sector coupling is assumed introducing additional electricity demand driven by energy-policy programs. With heat pumps for space heating, electrolyser for hydrogen production and BEV for private passenger transport PtX technologies are selected, representing sector technologies with a most likely expansion in the mid- to long-term perspective. For the selected PtX technologies, adequate model representations were developed and two different sector coupling approaches were introduced by ex- and including the access to energy storages to answer the research question three, *how does sector coupling influence the optimal flexibility provision in the European electricity market?* The mix of flexibility options is differing more significantly due to the impact of additional electricity demand profiles correlating differently with the available iRES generation. Summarising the outcome, the additional electricity demand exogenously introduced into the energy system requires additional electricity generation capacities independently from the Wind-PV ratio. Within the present modelling framework, gas-fuelled power plants for peak load provision become optimal with a stronger impact with higher PV shares, since the seasonal PV generation results in higher deficits in the winter month with characteristically high electricity demand. The provision of peak load capacity by a fossil-fuel technology is generally influencing the resulting emissions. Based on the assumptions on available controllable RES potential further electricity generation technologies are carbon-free. Furthermore, also the value of temporal shifting is

increasing with sector coupling. In particular, hourly storages are not only highly sensitive to the Wind-PV ratio, but in addition strongly impacted by sector coupling. In both dimensions, a higher PV share is increasing the value for short-term shifting.

Table 7.1: Summary of main results for the mix of flexibility options

	Impact of increasing wind share		
	NO	LF	HF
Electricity storages	<ul style="list-style-type: none"> Decreasing capacity investments for hourly electricity storages for short-term shifting flexibility 		
	<ul style="list-style-type: none"> Decreasing role of storages for balancing application (surplus charging) 		
	<ul style="list-style-type: none"> Decreasing storage dispatch 		
	<ul style="list-style-type: none"> Increasing share of seasonal storages in storage mix 	<ul style="list-style-type: none"> No investments in seasonal storages 	
	<ul style="list-style-type: none"> Decreasing full load hours 	<ul style="list-style-type: none"> Increasing full load hours 	<ul style="list-style-type: none"> Indifferent
Electricity trade	<ul style="list-style-type: none"> Country-specific NTC expansion strongly driven by iRES share on electricity demand 		
	<ul style="list-style-type: none"> Rather similar total capacity investments and trade flows 	<ul style="list-style-type: none"> Tendency to higher total capacities and higher total trade flows 	
		<ul style="list-style-type: none"> Country-specific NTC expansion strongly driven by additional electricity demand due to sector coupling 	
Dispatchable power plants	<ul style="list-style-type: none"> High share of RES based dispatchable power plants 		
	<ul style="list-style-type: none"> Decreasing share of secured capacity on electricity demand peak 		
	<ul style="list-style-type: none"> Rather similar total capacity investments 	<ul style="list-style-type: none"> Decreasing total capacity investments 	
	<ul style="list-style-type: none"> Decreasing dispatchable generation 	<ul style="list-style-type: none"> Rather similar total generation 	<ul style="list-style-type: none"> Decreasing dispatchable generation
		<ul style="list-style-type: none"> Decreasing amount of gas-based (peak) electricity generation Increasing seasonality of electricity generation due to sector coupling 	
Heat pumps	<ul style="list-style-type: none"> Increasing total capacity installations 		
	<ul style="list-style-type: none"> Significant shift of daily dispatch independently from wind share 		
	<ul style="list-style-type: none"> Increasing dispatch 	<ul style="list-style-type: none"> Decreasing dispatch 	
	<ul style="list-style-type: none"> Similar full load hours 	<ul style="list-style-type: none"> Decreasing full load hours 	
		<ul style="list-style-type: none"> Decreasing heat storage investments 	
Electrolyser	<ul style="list-style-type: none"> Decreasing total capacity installations 		
	<ul style="list-style-type: none"> Constant dispatch 		
	<ul style="list-style-type: none"> Significant shift of daily dispatch independently from wind share 		
	<ul style="list-style-type: none"> Increasing full load hours 		
		<ul style="list-style-type: none"> Decreasing heat storage investments 	
Battery-electric vehicle	<ul style="list-style-type: none"> Constant number of BEV and electricity demand 		
	<ul style="list-style-type: none"> Significant shift of daily dispatch independently from wind share 		

The results show, that including sector coupling in model-based analysis of the future energy system is crucial to properly evaluate the storage requirements. In contrast, curtailment can be reduced significantly with sector coupling, since iRES surplus periods are extensively shifted to other locations or later points in time. In general, a higher flexibility in sector coupling slightly decreases the demand for flexibility options in the electricity sector, but is far from making them dispensable. Nevertheless, the expansion of or access to energy storages in the end-use sector rather effects the optimal PtX capacities but changes the dispatch of the respective technologies. The observed shift in daily electricity consumption also improves the iRES integration.

7.2 Limitations and further research

While the uncertainty of the future energy system development pathway increases with larger time horizon, the model-based analysis is influenced by the today's perspective and expectations of the future. This has to be taken into account when modelling and discussing the long-term energy system transformation. Due to multiple energy policy interventions significant changes in the energy infrastructure have already been established and can be further expected in the future. This not only affects energy-policy framework conditions but also the actual techno-economic situation of single technologies. The targeted iRES expansion serves well as an example for a policy driven deployment of technologies, despite liberalised electricity markets. By applying a greenfield approach, possible restrictions of the existing energy system are neglected in the present work. While this enables the analysis of real optima under the assumptions made in a techno-economical system perspective, the transferability of the results to today's structures as well as the assessment of implications for the implementation challenges is limited. However, gained insights regarding the interactions between flexibility demand and flexibility supply resulting from different Wind-PV ratios are valuable for the assessment of the system transformation, since the infrastructure for high iRES shares as well as for sector coupling has to be expanded significantly. This is true in a European perspective with different status quo in terms of energy system transformation as well as on a more regional level where iRES integration challenges can also be affected by local wind and PV resources. Thus, the model-based analysis of future energy systems provides valuable insights regarding optimal technology combinations to show techno-economic benchmark solutions for the desired energy system transformation. The insights can form the basis for discussions of interactions between flexibility demand and flexibility provision within the energy policy triangle including security of supply, sustainability and competitiveness and should be accompanied by interdisciplinary research on technical, economic, social and ecological implications is crucial. In addition to solely cost-effective solutions, the energy policy ambition and societies ability to implement the required technologies are most likely of high importance as well. The interdisciplinary

technology impact assessment should therefore be applied to broaden the perspective of the interactions of energy system transformation with additional influencing factors e.g. on ecological and societal level. Methodological approaches are diverse and range for example from scenario development techniques (see e.g. Pruditsch and Zöphel 2017) to complex model couplings (see e.g. Xu et al. 2020). With regard to the analysis of future iRES expansion pathways, the focus was on wind onshore and PV potentials driven by current cost data and emerging challenges regarding the land-use. However, the role of wind offshore has to be assessed in detail. With regard to the flexibility demand, the more constant electricity generation at high availability can be expected to be beneficial integration cost reductions. Similarly, the potential of controllable RES based power plants needs to be further assessed to validly derive recommendations regarding their future contribution to provide secured electricity generation capacity. The iRES expansion model developed over the course of the present work can form the basis for further research to include the aforementioned topics. In addition, the implemented policy restriction can be applied to emphasise the potential of cooperation between the European countries for the energy system transformation. Different levels of coordination can be used to assess the impact of the resulting flexibility demand on the flexibility provision. With this aspect, the intended separation of iRES expansion and optimal flexibility provision can be seen as further limitation. While in the present work, this approach was selected to show the effects of an energy policy driven iRES expansion independently from the electricity market integration, in the future, a market driven expansion as well as electricity generation is likely. For further research, a closed optimisation of iRES and flexibility option investments can increase the understanding of optimal pathways. As a result, insights could be gained with regard to optimal combinations of supply and demand technologies taking available potentials and generation characteristics into account.

In general, the energy system modelling approach enables the analysis of a broad range of research questions relevant for the energy system transformation. However, assumed techno-economic data is open to debate and should be updated for any future consideration. The data uncertainty can be further decreased by applying additional sensitivity analysis. The transparent model and data presentation allows on the one hand for individual discussions. On the other hand, this transparency can form the starting point for either reduce the complexity, to focus on single technologies or to increase the interaction potentials of the presented modelling framework. Both options are valuable and should always be interpreted within the underlying assumptions. Although, the analysis of single flexibility options in system perspective while neglecting further technologies is most likely overestimating the value of the respective technology, a more isolated analysis of selected flexibility options still increases the

understanding of relevant interactions. In contrast, an increase in modelling complexity is required to broaden the analysis on iRES integration. Particularly the extension of the geographical scope as well as the inclusion of additional energy demand sectors and underlying technologies are examples for further research potential based on the present work. While the former one offers possibilities to access further iRES as well as balancing potentials e.g. in the south-east of Europe, the latter one enables the analysis of further synergies and competitions between the energy sectors. Thereby, a precondition for an increase in modelling technologies are sufficient computational capacities.

Finally, the role of energy-policy instruments particularly with regard to the pricing of CO₂ emissions should be analysed in future research. The actual CO₂-price derivation due to the trade of emission certificates under an emission cap are neglected in the present work by explicitly setting a CO₂-price. For further research, the examination of the influence of a limited emission budget on interactions between cross-sectoral flexibility options help to assess the effectiveness of policy interventions. In addition, the value of sector-specific approaches can be observed.

7.3 Implications and recommendations resulting from the insights

Based on the greenfield optimisation approach in a central planner's system perspective, the implications regarding the results require general preconditions.

- *A significant and rapid RES expansion* is required for the targeted energy system decarbonisation. This is crucial independently from the flexibility demand scenarios and in cross-national joint European perspective. Along with an underlying European integration process, the acceptance of this energy-policy across multiple stakeholder has to be ensured.
- *The European interconnected energy market* is of high importance to allow for the observed balancing effects. This again requires a common European energy policy and a high willingness to cooperate between the respective countries with varying energy-political preconditions and ambitions. For infrastructure investments, adequate energy policy framework conditions are a precondition to allow for a market based substitution of fossil fuels.
- *The market design* to enable a free access to energy markets for flexibility provision also originating from small-scale units is crucial. For flexibility provision, a fair competition between available technologies is required. Thereby, within the current wholesale market design as energy-only-market, high shares of renewable energies probably lead to a higher frequency of times with marginal costs and electricity prices close to zero.

To efficiently provide flexibility, price signals reflecting the need for flexibility and setting incentives for price-based dispatch decisions as well as investments for flexibility options are required. This also includes the demand side participating with potentials for DSM and flexibility sources due to sector coupling.

The discussion about a reasonable set-up for the iRES expansion in multiple countries within Europe emphasised the range of challenges to be addressed, if a coordinated energy system transformation is based on PV and wind capacities. The analysis shows, that possible restrictions regarding an optimal exploitation of iRES potentials (as implemented in the present work due to limited coordinated European iRES expansion, limitation of iRES expansion density, technology diversity or land-use restrictions) are increasing the costs of wind and PV expansion. However, with regard to the systems flexibility demand, a distributed iRES extension reduces extreme national (or regional) flexibility requirements, thus distributes potential iRES integration costs. Nevertheless, this coordinated expansion requires international, national and local governance. On the one side, challenges arise due to barriers concerning national energy-policy sovereignty and the requirements to combine heterogeneous interests into a common ambitious energy system transformation strategy across the European countries. On the other side, rather local hurdles like public acceptance resulting from land-use issues of the iRES expansion have to be decreased. As mentioned before, the future development of the energy system transformation is most likely driven by multiple stakeholder interests beyond techno-economic criteria. Within this discussion, the centrality or decentrality of the transformation is often in the focus, since this aspect also includes questions of public acceptance and approval. In a system perspective, a mixture of both approaches is rather likely. However, the participation potential, directly affecting public acceptance is assessed to be higher in a decentral energy system (ESYS 2020). Decentral characteristics are usually described by, besides others, higher shares of PV, particularly rooftop-PV, while in a more central system large (onshore and offshore) wind farms are more relevant³⁴. The flexibility demand (FD) scenarios in the present work directly give hints on optimal flexibility provision in a rather PV or wind dominated system. Thus, the public preferences can be discussed, while taking possible implications for optimal combinations of flexibility options derived in the present work into account.

A pathway into a rather wind-dominated energy system should be accompanied by rather central cross-sectoral infrastructure expansions to connect spatially dispersed locations of electricity production and energy consumptions. At the same time, the coordination of iRES

³⁴ A detailed overview on different decentral and central aspects can be found in ESYS (2020).

integration on national but also international level via wholesale markets has to be ensured. Depending on future cost reductions, the sensitivity analysis also shows potential for temporal balancing particularly with seasonal storages. In contrast, the flexibility provision in a PV-dominated scenario indicates a crucial role of hourly storages, already becoming increasingly relevant today in PV-Battery systems. In an electricity system perspective, the high seasonality of PV electricity generation requires comparably high capacity investments (especially for surplus charging power) leading to low full load for electricity storages (as well selected power plants). This optimal result might be less beneficial for single plant owners needing sufficient times of dispatch to refinance their investment. Again, price signals are of high importance to secure investment incentives. Since the High PV scenario shows high similarities with the optimal flexibility provision in a decentral energy system, another perspective on a iRES expansion pathway strongly based on PV is a rather decentral approach including decentral sector coupling accompanied with battery storages. In case of a higher PV share in Europe, energy system planners should take higher (battery) storage requirements into account. Access to these potentials also on household level for system and grid stability are of high value for flexibility provision. In addition, the realisation of sector coupling in a more decentral approach can further increase the approval as well as unlock flexibility potential on the local and household level. For both, the iRES expansion as well as the stronger sector coupling suitable incentives and regulatory framework conditions for private individuals have to be developed. Furthermore and independently from the overall Wind-PV ratio, grid expansions are required in each FD and FS scenario emphasising the importance of spatial balancing in a European energy system with high shares of iRES. The results show, that the west-east as well north-south connections are most likely becoming increasingly relevant to enable the access to high wind potentials in the west as well as the high PV potentials in the south of Europe.

Due to sector coupling, emissions in the selected energy end-use sectors can be reduced significantly. Thereby, the role of the electricity sector for back-up capacity provision is crucial. While back-up electricity generating capacity is required with and without sector coupling, the underlying power plant mix is significantly influencing the total emission reduction. Although the present work shows, that available RES potentials can meet high shares of the additional secured power and energy demand, peak load power plants and storages are needed to meet peak load requirements particularly with higher PV shares. Taking these aspects into account, on the one side, the exploitation of further RES capacities is of high importance. On the other hand, for conventional plant technologies, existing or future gas-fuelled power plants have to be retrofitted or installed with respective measures to avoid an increase in emissions due to sector coupling. CCS technologies might therefore be relevant. Therefore, measures to increase

the CO₂-emission costs are advised to increase the cost-benefit of relevant options. The sensitivity analysis showed, that an increase in CO₂-prices enables a further total emission reduction. Thereby, particularly the transport and the electricity sector are very sensitive to emission prices.

The analysis emphasised the high value of energy storages in the energy end-use sectors, since a more flexible electricity demand allows for the substitutions of flexibility options in the electricity system and enables lower system costs as well as additional emission reductions. Particularly the flexibility of BEV can significantly contribute to iRES integration. This effect can be observed independently from the overall Wind-PV ratio. In general, the expansion of PtX technologies has to be realised together with setting incentives to invest in or to access for relevant energy storages. Assuming a higher decentrality of iRES generation and integration with a lower overall Wind-PV ratio, these incentives should accordingly also increasingly address private households and possible barriers. As seen in the modelling results, only single PtX technologies are expanded beyond the targeted share of electricity in the energy demand sectors. To further increase the electrification of the energy demand sectors market-driven (and not enforced as assumed in the present work), the additional scenarios as well as sensitivities showed two options. One the one side, a higher iRES share across the region observed enables a higher electricity demand from the selected sectors and an overall CO₂-emission reduction effect. On the other side, also cost reductions of PtX technologies increase the electrification and enable a market driven deployment of the considered technologies. BEV are especially highly sensitive to changing framework conditions influencing the cost-benefit in comparison to ICE. However, the additional scenarios and sensitivities show, that an accelerated sector coupling also due to strong energy-policy promotion and/or strong cost reductions should be incentivised carefully, since the additional flexibility demand for the electricity system might lead to increase in emissions. As mentioned before, a faster exploitation of European iRES potentials is therefore recommended since it improves both, the electrification of further energy end-use sectors as well as overall emission reductions.

Bibliography

- Agency for Ecological Transition (ADEME) (2020). Change in distance travelled by car. Online (Access date: 22th of April 2019) <https://www.odyssee-mure.eu/publications/efficiency-by-sector/transport/distance-travelled-by-car.html>
- Agora Energiewende (2017): Flexibility in thermal power plants – With a focus on existing coal-fired power plants. Study on behalf of Agora Energiewende, Berlin, 2014.
- Agora (2014). Power-to-Heat zur Integration von ansonsten abgeregeltem Strom aus Erneuerbaren Energien. Study on behalf of Agora Energiewende, Berlin, 2014.
- Alizadeh, M. I., Parsa Moghaddam, M., Amjady, N., Siano, P., & Sheikh-El-Eslami, M. K. (2016). Flexibility in future power systems with high renewable penetration: A review. *Renewable and Sustainable Energy Reviews*, 57, 1186–1193. <https://doi.org/10.1016/j.rser.2015.12.200>
- Alshehri, F., Suárez, V. G., Rueda Torres, J. L., Perilla, A., & van der Meijden, M. A. M. M. (2019). Modelling and evaluation of PEM hydrogen technologies for frequency ancillary services in future multi-energy sustainable power systems. *Heliyon*, 5(4). <https://doi.org/10.1016/j.heliyon.2019.e01396>
- Auer, H., & Haas, R. (2016). On integrating large shares of variable renewables into the electricity system. *Energy*, 115, 1592–1601. <https://doi.org/10.1016/j.energy.2016.05.067>
- Bataille, C., Jaccard, M., Nyboer, J., & Rivers, N. (2006). Towards general equilibrium in a technology-rich model with empirically estimated behavioral parameters. *Energy Journal*, 27(SPEC. ISS. OCT.), 98–112. <https://doi.org/10.5547/ISSN0195-6574-EJ-VolSI2006-NoSI2-5>
- Bauknecht, D., Heinemann, C., Koch, M., Ritter, D., Harthan, R., Sachs, A., Vogel, M., Tröster, E., & Langanke, S. (2016). *Systematischer Vergleich von Flexibilitäts- und Speicheroptionen im deutschen Stromsystem zur Integration von erneuerbaren Energien und Analyse entsprechender Rahmenbedingungen*. <https://doi.org/10.13140/RG.2.2.10951.50087>
- Bauknecht, D., Heinemann, C., Koch, M., Ritter, D., Harthan, R., Tröster, E., & Langanke, S. (2014). Entwicklung des Flexibilitätsbedarfs im Stromsystem und der Beitrag verschiedener Flexibilitätsoptionen. *Energiewirtschaftliche Tagesfragen*, 64(11), 52–55.
- Beaudin, M., Zareipour, H., Schellenberglobe, A., & Rosehart, W. (2010). Energy storage for mitigating the variability of renewable electricity sources: An updated review. *Energy for Sustainable Development*, 14(4), 302–314. <https://doi.org/10.1016/j.esd.2010.09.007>

-
- Bechberger, M., Körner, S., Reiche, D. (2003). Erfolgsbedingungen von Instrumenten zur Förderung Erneuerbarer Energien im Strommarkt. *Study on behalf of Bundesverbandes Erneuerbare Energie (BEE)*. January, 2003.
- Belderbos, A., Virag, A., D'haeseleer, W., & Delarue, E. (2017). Considerations on the need for electricity storage requirements: Power versus energy. *Energy Conversion and Management*, 143, 137–149. <https://doi.org/10.1016/j.enconman.2017.03.074>
- Bertram, R.; Primova, R. (Eds.) *Energy Atlas 2018: Facts and Figures About Renewables in Europe*; Heinrich Böll Foundation, FOEE, EREF, GEF: Luxembourg, 2018
- Bertsch, J., Growitsch, C., Lorenczik, S., & Nagl, S. (2012). Flexibility options in European electricity markets in high RES-E scenarios. *Study on behalf of the International Energy Agency (IEA)*. October, 2012.
- Bertsch, J., Growitsch, C., Lorenczik, S., & Nagl, S. (2016). Flexibility in Europe's power sector- An additional requirement or an automatic complement? *Energy Economics*, 53, 118–131. <https://doi.org/10.1016/j.eneco.2014.10.022>
- Bloess, A., Schill, W. P., & Zerrahn, A. (2018). Power-to-heat for renewable energy integration: A review of technologies, modeling approaches, and flexibility potentials. *Applied Energy*, 212, 1611–1626. <https://doi.org/10.1016/j.apenergy.2017.12.073>
- Bogdanov, D., Farfan, J., Sadovskaia, K., Aghahosseini, A., Child, M., Gulagi, A., Oyewo, A. S., de Souza Noel Simas Barbosa, L., & Breyer, C. (2019). Radical transformation pathway towards sustainable electricity via evolutionary steps. *Nature Communications*, 10(1), 1–16. <https://doi.org/10.1038/s41467-019-08855-1>
- Bosch, J., Staffell, I., & Hawkes, A. D. (2017). Temporally-explicit and spatially-resolved global onshore wind energy potentials. *Energy*, 131, 207–217. <https://doi.org/10.1016/j.energy.2017.05.052>
- Bosilovich, M. G., R. Lucchesi, and M. Suarez, 2016: MERRA-2: File Specification. GMAO Office Note No. 9 (Version 1.1), 73 pp, available from http://gmao.gsfc.nasa.gov/pubs/office_notes.
- Breitschopf B, Winkler J (2019). The EU 2030 Renewable Energy Vision - Can it be more Ambitious?. *Adv Environ Stud* 3(1):164-178.
- Bremen, L. Von, Greiner, M., Knorr, K., Hoffmann, C., Bofinger, S., & Lange, B. (2008). *A full Renewable Power Supply Scenario for Europe : The Weather determines Storage and Transport. March 2018*.
- Brijs, T., Stiphout, A. Van, Siddiqui, S., & Belmans, R. (2017). Sustainable Energy , Grids and Networks Evaluating the role of electricity storage by considering short-term operation in long-term planning. *Sustainable Energy, Grids and Networks*, 10, 104–117. <https://doi.org/10.1016/j.segan.2017.04.002>

- Brouwer, A. S., van den Broek, M., Seebregts, A., & Faaij, A. (2015). Operational flexibility and economics of power plants in future low-carbon power systems. *Applied Energy*, 156, 107–128. <https://doi.org/10.1016/j.apenergy.2015.06.065>
- Brown, T., Kies, A., & Greiner, M. (2018). Synergies of sector coupling and transmission extension in a cost-optimised, highly renewable European energy system. *Energy*, 160, 720–739. <https://doi.org/10.1016/j.energy.2018.06.222>
- Brunner, C., Deac, G., Braun, S., & Zöphel, C. (2020). The future need for flexibility and the impact of fluctuating renewable power generation. *Renewable Energy*, 149. <https://doi.org/10.1016/j.renene.2019.10.128>
- Brunner, Christoph, & Müller, T. (2015). Kostenvergleich von unterschiedlichen Optionen zur Flexibilisierung des Energiesystems. *ET. Energiewirtschaftliche Tagesfragen*, 65 (Nov. 2016), 55–60.
- Budinis, S., Krevor, S., Dowell, N. Mac, Brandon, N., & Hawkes, A. (2018). An assessment of CCS costs, barriers and potential. *Energy Strategy Reviews*, 22(May), 61–81. <https://doi.org/10.1016/j.esr.2018.08.003>
- Bundesministerium für Wirtschaft und Energie (BMWi) (2020). Die Nationale Wasserstoffstrategie. Berlin, 2020.
- Bundesministerium für Wirtschaft und Energie (BMWi) (2015). An electricity market for Germany's energy transition. Berlin, 2015.
- Bundesnetzagentur (BNetzA) (2015). Netzentwicklungsplan Strom 2025, Version 2015, 2. Entwurf. Berlin 2015.
- Bundesverband der Energie- und Wasserwirtschaft e.V. (BDEW) (2018): Abwicklung von Standardlastprofilen Gas. Leitfaden. Berlin 2018.
- Bundesverband der deutschen Gas- und Wasserwirtschaft (BGW) (2006). Anwendung von Standardlastprofilen zur Belieferung nichtleistungsgemessener Kunden. Praxisinformation P 2006 / 8.
- Burridge (2009). European chemical profile: Methanol. Online (Access Date: 11th of March 2019): <https://www.icis.com/explore/resources/news/2009/11/16/9263011/european-chemical-profile-methanol/>.
- Caglayan, D. G., Ryberg, D. S., Heinrichs, H., Linßen, J., Stolten, D., & Robinius, M. (2019). The techno-economic potential of offshore wind energy with optimized future turbine designs in Europe. *Applied Energy*, 255(September), 113794. <https://doi.org/10.1016/j.apenergy.2019.113794>
- Cebulla, F., & Fichter, T. (2017). Merit order or unit-commitment : How does thermal power plant modeling affect storage demand in energy system models ? *Renewable Energy*, 105, 117–132. <https://doi.org/10.1016/j.renene.2016.12.043>

-
- Cebulla, Felix. (2017). Storage demand in highly renewable energy scenarios for Europe : The influence of methodology and data assumptions in model-based assessments. *Disseration*. University of Stuttgart, 2017.
- Child, M., & Breyer, C. (2016). Vision and initial feasibility analysis of a recarbonised Finnish energy system for 2050. *Renewable and Sustainable Energy Reviews*, 66(December), 517–536. <https://doi.org/10.1016/j.rser.2016.07.001>
- Child, M., Kemfert, C., Bogdanov, D., & Breyer, C. (2019). Flexible electricity generation, grid exchange and storage for the transition to a 100% renewable energy system in Europe. *Renewable Energy*, 139, 80–101. <https://doi.org/10.1016/j.renene.2019.02.077>
- Connolly, D., Lund, H., & Mathiesen, B. V. (2016). Smart Energy Europe: The technical and economic impact of one potential 100% renewable energy scenario for the European Union. In *Renewable and Sustainable Energy Reviews* (Vol. 60, pp. 1634–1653). <https://doi.org/10.1016/j.rser.2016.02.025>
- Copernicus (CLC) (2012). Corine Landcover dataset. Online (Access date: 27th of November 2019): <https://land.copernicus.eu/pan-european/corine-land-cover/clc-2012>.
- Del Río, P. (2005). A European-wide harmonised tradable green certificate scheme for renewable electricity: is it really so beneficial? *Energy Policy*, Vol. 33 (10), pp. 1239 – 1250. DOI: 10.1016/j.enpol.2003.11.019.
- Denholm, P., & Hand, M. (2011). Grid flexibility and storage required to achieve very high penetration of variable renewable electricity. *Energy Policy*, 39(3), 1817–1830. <https://doi.org/10.1016/j.enpol.2011.01.019>
- Duwe, M., Velten, E.K., Evans, N. et al. (2019). Planning For Net Zero: Assessing the Draft National Energy and Climate Plans. Report on behalf of the European Commission.
- Edenhofer, O., Madrugá, R. P., Sokona, Y., Seyboth, K., Matschoss, P., Kadner, S., Zwickel, T., Eickemeier, P., Hansen, G., Schlömer, S., & von Stechow, C. (IPCC) (2011). Renewable energy sources and climate change mitigation: Special report of the intergovernmental panel on climate change. *Renewable Energy Sources and Climate Change Mitigation: Special Report of the Intergovernmental Panel on Climate Change*. <https://doi.org/10.1017/CBO9781139151153>
- Egenhofer, C., Schrefler, L. et al. (2014). Study on Composition and Drivers of Energy Prices and Costs in Energy Intensive Industries: The Case of the Chemical Industry – Ammonia. Final report. Brussels 2014.
- Eller, D. (2015). Integration erneuerbarer Energien mit Power-to-Heat in Deutschland. Springer, Wiesbaden. DOI 10.1007/978-3-658-10561-7.
- EMHIRES (2020). EMHIRES datasets for wind and solar power generation. Online (Access date 9th of January 2020): <https://setis.ec.europa.eu/EMHIRES-datasets>.

- Enercon (2015). Enercon Product Catalogue. Aurich 2015
- Energiesysteme der Zukunft (ESYS) (2020). Zentrale und dezentrale Elemente im Energiesystem. München, 2020.
- Energy Analysis (EA) (2013). Analysis of biomass prices - Future Danish Prices for Straw, Wood Chips and Wood Pellets. Final report. Copenhagen, 2013.
- ENTSO-E (2020). Mid-term Adequacy Forecast. *ENTSO-E Reports 2020 Committee*. Brussels, 2020.
- ENTSO-E (2018). Connecting Europe : Electricity. *ENTSO-E Reports 2018 Committee*. Brussels, 2018.
- ENTSO-E (2015). Scenario Outlook & Adequacy Forecast. Brussels, 2015.
- Eurek, K., Sullivan, P., Gleason, M., Hettinger, D., Heimiller, D., & Lopez, A. (2017). An improved global wind resource estimate for integrated assessment models. *Energy Economics*, 64, 552–567. <https://doi.org/10.1016/j.eneco.2016.11.015>
- European Automobile Manufacturers' Association (ACEA) (2019). Vehicles in use Europe 2019. Report. Brussels, 2019.
- European Climate Foundation (ECF) (2010). Roadmap 2050. Project Report. Brussels.
- European Commission (EC) (2019a). The European Green Deal. *COM(2019) 640*. Brussels
- European Commission (EC) (2019b). Renewable Energy Progress Report. *COM(2019) 225*. Brussels
- European Commission (EC) (2019). A Clean Planet for all - A European strategic long-term vision for a prosperous, modern, competitive and climate neutral economy. *COM(2018) 773*. Brussels
- European Commission (EC) (2014). A policy framework for climate and energy in the period from 2020 to 2030. *COM(2014) 15*. Brussels
- European Commission (EC) (2011). Energy Roadmap 2050. *COM(2011) 885*. Brussels
- European Commission (EC) (2007). An Energy Policy For Europe. *COM(2007)*. Brussels
- European Environment Agency (EEA) (2017). Renewable energy in Europe – 2017 Update. Recent growth and knock-on effects. EEA Report, No 23/2017.
- European Parliamentary Research Service (EPRS) (2019). Energy storage and sector coupling - Towards an integrated, decarbonised energy system. Briefing of European Parliament. Brussels, 2019.
- European Union (EU) (2020). Long-term low greenhouse gas emission development strategy of the European Union and its Member States. *European Council Conclusions*. Brussels.

-
- European Union (EU) (2019). Factsheet on Internal Energy Market. *European Council Conclusions*. Brussels. Online (Access Date: 27th of February 2020): <https://www.europarl.europa.eu/factsheets/en/sheet/45/internal-energy-market>.
- European Union (EU) (2019). Rules for the internal market in electricity. Directive 96/92/EC of the European Parliament.
- Eurostat (2019). Database on Energy. Online at (Access date: 12th of November 2019): <https://ec.europa.eu/eurostat/data/database>.
- Fiukowski, J., Wernitz, C., & Gaudchau, E. (2016). Metastudie Potenziale Erneuerbarer Energien in Ostdeutschland.
- Fleiter, T., Steinbach, J., Ragwitz, M., Arens, M., Aydemir, A., Elsland, R., Frassine, C., Herbst, A., & Hirzel, S. (2016). Mapping and analyses of the current and future (2020-2030) heating/cooling fuel deployment (fossil/renewables). *Work Package 2: Assessment of the Technologies for the Year 2012, September 2016*. <https://doi.org/10.13140/RG.2.2.29193.75361>
- Fraille, D., Lanoix, J.-C., Maio, P., Rangel, A., & Torres, A. (2015). Overview of the market segmentation for hydrogen across potential customers groups, based on key application areas. *CertifHy, 1*, 1–32. <https://doi.org/10.1155/2013/789705>
- Fraunhofer ISE (2018). Levelized Cost of Electricity Renewable Energy Technologies. Freiburg, 2018.
- Fraunhofer ISI (2017). Optionen der Sektorkopplung in verschiedenen Dekarbonisierungsszenarien. Presentation at: Ökonomische Grundsatzfragen der Sektorkopplung: Technisches Systemdesign und Governance, 22.03.2018, Berlin
- Fraunhofer IWES (2015): The European Power System in 2030: Flexibility Challenges and Integration Benefits. An Analysis with a Focus on the Pentalateral Energy Forum Region. Analysis on behalf of Agora Energiewende.
- Friends of the Earth Europe et al. (FFoE) (2015). Assessment of the European Refining Sector's Capability to Process Unconventional, Heavy Crude Oils. Maryland, 2015.
- Fürsch, M., Hagspiel, S., Jagemann, C., Nagl, S., Lindenberger, D., & Tröster, E. (2013). The role of grid extensions in a cost-efficient transformation of the European electricity system until 2050. *Applied Energy, 104*(12), 642–652. <https://doi.org/10.1016/j.apenergy.2012.11.050>
- Gaetani, M., Huld, T., Vignati, E., Monforti-Ferrario, F., Dosio, A., & Raes, F. (2014). The near future availability of photovoltaic energy in Europe and Africa in climate-aerosol modeling experiments. *Renewable and Sustainable Energy Reviews, 38*, 706–716. <https://doi.org/10.1016/j.rser.2014.07.041>
- GE (2014). GE product catalogue - Die GE 2.75-120 Windenergieanlage. Salzbergen, Germany.

- Gils, H. C. (2014). Assessment of the theoretical demand response potential in Europe. *Energy*, 67, 1–18. <https://doi.org/10.1016/j.energy.2014.02.019>
- Gils, H. C. (2016). Economic potential for future demand response in Germany - Modeling approach and case study. *Applied Energy*, 162, 401–415. <https://doi.org/10.1016/j.apenergy.2015.10.083>
- Gils, H. C., Scholz, Y., Pregger, T., Luca de Tena, D., & Heide, D. (2017). Integrated modelling of variable renewable energy-based power supply in Europe. *Energy*, 123, 173–188. <https://doi.org/10.1016/j.energy.2017.01.115>
- Gonzalez Aparicio, I., Huld, T., Careri, F., Monforti, F., & Zucker, A. (2017). EMHIRE dataset Part II : Solar power generation. In *European Meteorological derived High resolution RES generation time series for present and future scenarios*. <https://doi.org/10.2760/044693>
- Gonzalez Aparicio, I., Zucker, A., Careri, F., Monforti, F., Huld, T., & Badger, J. (2016). EMHIRE dataset Part I: Wind power generation. In *European Meteorological derived High resolution RES generation time series for present and future scenarios*. <https://doi.org/10.2790/831549>
- Götz, M., Lefebvre, J., Mörs, F., McDaniel Koch, A., Graf, F., Bajohr, S., Reimert, R., & Kolb, T. (2016). Renewable Power-to-Gas: A technological and economic review. *Renewable Energy*, 85, 1371–1390. <https://doi.org/10.1016/j.renene.2015.07.066>
- Gulagi, A., Bogdanov, D., & Breyer, C. (2017). The Demand for Storage Technologies in Energy Transition Pathways Towards 100% Renewable Energy for India. *Energy Procedia*, 135(March), 37–50. <https://doi.org/10.1016/j.egypro.2017.09.485>
- Gimeno-Gutiérrez, M., Lacal-Arántegui, R. (2013). Assessment of the European potential for pumped hydropower energy storage. Study for Joint Research Centre.
- Heating Roadmap (HRE) (2020). HRE4 summary tables and figures. Online data access (Access date: 17th of June 2019): <https://heatroadmap.eu/roadmaps/>.
- Heide, D., von Bremen, L., Greiner, M., Hoffmann, C., Speckmann, M., & Bofinger, S. (2010). Seasonal optimal mix of wind and solar power in a future, highly renewable Europe. *Renewable Energy*, 35(11), 2483–2489. <https://doi.org/10.1016/j.renene.2010.03.012>
- Heinrichs, H. (2013). Analyse der langfristigen Auswirkungen von Elektromobilität auf das deutsche Energiesystem im europäischen Energieverbund. *Dissertation*. KIT Scientific Publishing. DOI: 10.5445/KSP/1000037111. Karlsruhe Institute for Technology, 2014.
- Hidalgo González, I., Quoilin, S., Zucker, A., & European Commission. Joint Research Centre. Institute for Energy and Transport. (2014). Dispa-SET 2.0 : unit commitment and power dispatch model : description, formulation, and implementation. Publications Office.
- Hillberg, E., & Oleinikova, I. (2019). Flexibility needs in the future power system. *Discussion paper*. April, 48. <https://doi.org/10.13140/RG.2.2.22580.71047>

-
- Hinz, F. (2017). Voltage Stability and Reactive Power Provision in a Decentralizing Energy System. *Dissertation*. Schriften des Lehrstuhls für Energiewirtschaft, TU Dresden.
- Hirth, L., & Ziegenhagen, I. (2015). Balancing power and variable renewables: Three links. *Renewable and Sustainable Energy Reviews*, 50, 1035–1051. <https://doi.org/10.1016/j.rser.2015.04.180>
- Hobbie, H., Schmidt, M., & Möst, D. (2019). Windfall profits in the power sector during phase III of the EU ETS: Interplay and effects of renewables and carbon prices. *Journal of Cleaner Production*, 240. <https://doi.org/10.1016/j.jclepro.2019.118066>
- Höltinger, S., Salak, B., Schauppenlehner, T., Scherhauser, P., & Schmidt, J. (2016). Austria's wind energy potential – A participatory modeling approach to assess socio-political and market acceptance. *Energy Policy*, 98(2016), 49–61. <https://doi.org/10.1016/j.enpol.2016.08.010>
- Holttinen, H., Miettinen, J., & Sillanpää, S. (2013). Wind power forecasting accuracy and uncertainty in Finland. *VTT Technical Research Centre of Finland*. <http://www.vtt.fi/publications/index.jsp>
- Hu, J., Morais, H., Sousa, T., & Lind, M. (2016). Electric vehicle fleet management in smart grids: A review of services, optimization and control aspects. *Renewable and Sustainable Energy Reviews*, 56(51877078), 1207–1226. <https://doi.org/10.1016/j.rser.2015.12.014>
- Huber, M. (2017). Flexibility in power systems - requirements , modeling , and evaluation. *Dissertation*. TU München, 2017.
- Huber, M., Dimkova, D., & Hamacher, T. (2014). Integration of wind and solar power in Europe: Assessment of flexibility requirements. *Energy*, 69, 236–246. <https://doi.org/10.1016/j.energy.2014.02.109>
- Huld, T., Gottschalg, R., Beyer, H. G., & Topič, M. (2010). Mapping the performance of PV modules, effects of module type and data averaging. *Solar Energy*, 84(2), 324–338. <https://doi.org/10.1016/j.solener.2009.12.002>
- Hummon, M., Denholm, P., Margolis, R. (2012). Impact of photovoltaic orientation on its relative economic value in wholesale energy markets. *Prog. Photovolt: Res. Appl.* (2012). DOI: 10.1002/pip.2198
- Hydrogen Council (HC) (2020). Path to hydrogen competitiveness - A cost perspective. Study. <https://hydrogencouncil.com/en/path-to-hydrogen-competitiveness-a-cost-perspective/>
- IEA Wind (2020). Data Viewer. Online Access date 16th of November 2019): <https://community.ieawind.org/task26/dataviewer>
- International Institute for Sustainability Analysis and Strategy IINAS (2017). Selected results from GEMIS 4.95: Electricity generation. Excel file online (access date: 18th of September 2019): http://iinas.org/tl_files/iinas/downloads/GEMIS/2017_GEMIS-results.xlsx.

- International Electrotechnical Commission (IEC) (2019). Standard: DIN EN IEC 61400-1 VDE 0127-1:2019-12, Part 1. VDE, Berlin, 2019.
- International Energy Agency (iea) (2015). Projected Costs of Generating Electricity. Paris 2015
- International Energy Agency (iea) (2008). Empowering variable renewables: options for Flexible Electricity Systems. Paris 2009.
- IRENA (2020). Renewable capacity statistics 2020. International Renewable Energy Agency (IRENA), Abu Dhabi.
- Jaccard, M. (2005). Hybrid Energy-Economy Models and Endogenous Technological Change. In R. Loulou, J. P. Waaub, & G. Zaccour (Eds.), *Energy and Environment*. Springer, Boston, MA. https://doi.org/https://doi.org/10.1007/0-387-25352-1_4
- Jacobson, M. Z., Delucchi, M. A., Cameron, M. A., & Mathiesen, B. V. (2018). Matching demand with supply at low cost in 139 countries among 20 world regions with 100% intermittent wind, water, and sunlight (WWS) for all purposes. *Renewable Energy*, 123, 236–248. <https://doi.org/10.1016/j.renene.2018.02.009>
- Jamil, B., Siddiqui, A. T., & Akhtar, N. (2016). Estimation of solar radiation and optimum tilt angles for south-facing surfaces in Humid Subtropical Climatic Region of India. *Engineering Science and Technology, an International Journal*, 19(4), 1826–1835. <https://doi.org/10.1016/j.jestch.2016.10.004>
- Jansen, M., Staffell, I., Kitzing, L., Quoilin, S., Wiggelinkhuizen, E., Bulder, B., Riepin, I., & Müsgens, F. (2020). Offshore wind competitiveness in mature markets without subsidy. *Nature Energy*, 5(8), 614–622. <https://doi.org/10.1038/s41560-020-0661-2>
- Kasten, P., & Hacker, F. (2014). DEFINE: Development of an Evaluation Framework for the Introduction of Electromobility - Two electromobility scenarios for Germany: Market development and their impact on CO₂ emissions of passenger cars in DEFINE. <https://www.ihs.ac.at/projects/define/files/DEFINE-Oeko-english-version.pdf>
- Kavvadias, K., J.P., J.-N., & Thomassen, G. (2019). *Decarbonising the EU heating sector*. <https://doi.org/10.2760/943257>
- Knopf, B., Bakken, B., Carrara, S., Kanudia, A., Keppo, I. et al. (2013). Transforming the European Energy System: Member States' Prospects within the EU Framework. *Climate Change Economics*, 2013, 4, pp.1340005/1-26. DOI:10.1142/S2010007813400058.
- Koch, M., Bauknecht, D., Heinemann, C., Ritter, D., Vogel, M., & Tröster, E. (2015). Modell based analysis of grid-development within the European grid and options providing flexibility within the German electricity system from 2020 to 2050. *Zeitschrift Für Energiewirtschaft*, 39(1), 1–17. <https://doi.org/10.1007/s12398-015-0147-2>
- Ladwig, T. (2018). Demand Side Management in Deutschland zur Systemintegration erneuerbarer Energien. *Disseration*. TU Dresden, 2018.

-
- Lantz, E., Roberts, O., Nunemaker, J., Demeo, E., Dykes, K., & Scott, G. (2019). Increasing wind turbine tower heights: opportunities and challenges. *Technical report NREL/TP-5000-73629*.
- Lindberg, K. B., Seljom, P., Madsen, H., Fischer, D., & Korpås, M. (2019). Long-term electricity load forecasting: Current and future trends. *Utilities Policy*, 58(May), 102–119. <https://doi.org/10.1016/j.jup.2019.04.001>
- Luca de Tena, D., & Pregger, T. (2018). Impact of electric vehicles on a future renewable energy-based power system in Europe with a focus on Germany. *International Journal of Energy Research*, 42(8), 2670–2685. <https://doi.org/10.1002/er.4056>
- Lund, H., Østergaard, P. A., Connolly, D., & Mathiesen, B. V. (2017). Smart energy and smart energy systems. *Energy*, 137, 556–565. <https://doi.org/10.1016/j.energy.2017.05.123>
- Lund, P. D. (2011). Boosting new renewable technologies towards grid parity - Economic and policy aspects. *Renewable Energy*, 36(11), 2776–2784. <https://doi.org/10.1016/j.renene.2011.04.025>
- Lund, P. D., Lindgren, J., Mikkola, J., & Salpakari, J. (2015). Review of energy system flexibility measures to enable high levels of variable renewable electricity. *Renewable and Sustainable Energy Reviews*, 45, 785–807. <https://doi.org/10.1016/j.rser.2015.01.057>
- Lund, Peter D., Skytte, K., Bolwig, S., Bolkesjö, T. F., Bergaentzle, C., Gunkel, P. A., Kirkerud, J. G., Klitkou, A., Koduvere, H., Gravelsins, A., Blumberga, D., & Söder, L. (2019). Pathway analysis of a zero-emission transition in the Nordic-Baltic region. *Energies*, 12(17), 1–20. <https://doi.org/10.3390/en12173337>
- Ma, J., Silva, V., Belhomme, R., Kirschen, D. S., Ochoa, L. F. (2012). Evaluating and Planning Flexibility in Sustainable Power Systems. *IEEE Transactions on Sustainable Energy*, vol. 4, no. 1, pp. 200-209, Jan. 2013, doi: 10.1109/TSTE.2012.2212471.
- Martino, A., Fiorello, D., Heitel, S., & Jochem, P. (2019). Transport trends in the context of future energy scenarios. *Policy Brief for REFLEX project*.
- Mathiesen, B. V., Lund, H., Connolly, D., Wenzel, H., Ostergaard, P. A., Möller, B., Nielsen, S., Ridjan, I., KarnOe, P., Sperling, K., & Hvelplund, F. K. (2015). Smart Energy Systems for coherent 100% renewable energy and transport solutions. In *Applied Energy* (Vol. 145, pp. 139–154). <https://doi.org/10.1016/j.apenergy.2015.01.075>
- Matthes, F. C., Flachsbarth, F., Loreck, C., Hermann, H., Falkenberg, H., & Cook, V. (2018). Zukunft Stromsystem II - Regionalisierung der erneuerbaren Stromerzeugung. <https://www.oeko.de/fileadmin/oekodoc/Stromsystem-II-Regionalisierung-der-erneuerbaren-Stromerzeugung.pdf>

- McKenna, R. C., Bchini, Q., Weinand, J. M., Michaelis, J., König, S., Köppel, W., & Fichtner, W. (2018). The future role of Power-to-Gas in the energy transition: Regional and local techno-economic analyses in Baden-Württemberg. *Applied Energy*, 212(September 2017), 386–400. <https://doi.org/10.1016/j.apenergy.2017.12.017>
- McKenna, R., Hollnaicher, S., Ostman, P., & Fichtner, W. (2015). Cost-potentials for large onshore wind turbines in Europe. *Energy*, 83, 217–229. <https://doi.org/10.1016/j.energy.2015.02.016>
- Ministerial Council on Renewable Energy, Hydrogen and Related Issues (METI) (2017). Basic Hydrogen Strategy. Tokyo, 2017.
- Michaelis, J. (2018). Modellgestützte Wirtschaftlichkeitsbewertung von Betriebskonzepten für Elektrolyseure in einem Energiesystem mit hohen Anteilen erneuerbarer Energien. *Dissertation*. TU Dresden, 2018.
- Michaelis, J., Muller, T., Reiter, U., Fermi, F., Wyrwa, A., Chen, Y. K., Zöphel, C., Kronthaler, N., & Elsland, R. (2017). Comparison of the techno-economic characteristics of different flexibility options in the European energy system. *International Conference on the European Energy Market, EEM*. <https://doi.org/10.1109/EEM.2017.7981983>
- Michalski, J., Poltrum, M., & Bünger, U. (2019). The role of renewable fuel supply in the transport sector in a future decarbonized energy system. *International Journal of Hydrogen Energy*, 44(25), 12554–12565. <https://doi.org/10.1016/j.ijhydene.2018.10.110>
- Möst, D., Schreiber, S., Herbst, A., Jakob, M., Martino, A., Poganietz, W-R. (edt.) (2021). The Future European Energy System. Springer International Publishing; 2021; Available from: <http://dx.doi.org/10.1007/978-3-030-60914-6>
- Möst, D., Hinz, F., Schmidt, M., Zöphel, C. (2015). Kurzgutachten zur regionalen Ungleichverteilung der Netznutzungsentgelte - Bestandsaufnahme und pragmatische Lösungsansätze. Schriftenreihe des Lehrstuhls für Energiewirtschaft, 8. URL: <http://nbn-resolving.de/urn:nbn:de:bsz:14-qucosa-184452> .
- Müller, T., & Möst, D. (2018). Demand Response Potential : Available when Needed ? *Energy Policy*, 115(December 2017), 181–198. <https://doi.org/10.1016/j.enpol.2017.12.025>
- NASA (2020). Nasa Earth Science Data. Online (Access date 8th of April 2019): <https://urs.earthdata.nasa.gov/>.
- Nitsch, J., Pregger, T., Scholz, Y., Naegler, T., Heide, D., Luca De Tena, D., Trieb, F., Nienhaus, K., Gerhardt, N., Trost, T., Von Oehsen, A., Schwinn, R., Pape, C., Hahn, H., Wickert, M., Sterner, M., & Wenzel, B. (2012). Long-term scenarios and strategies for the deployment of renewable energies in Germany in view of European and global developments. *Summary of the final report*.

-
- Ntanos, S., Kyriakopoulos, G., Chalikias, M., Arabatzis, G., & Skordoulis, M. (2018). Public perceptions and willingness to pay for renewable energy: A case study from Greece. *Sustainability (Switzerland)*, 10(3). <https://doi.org/10.3390/su10030687>
- Obeidat, F. (2018). A comprehensive review of future photovoltaic systems. *Solar Energy*, 163(July 2017), 545–551. <https://doi.org/10.1016/j.solener.2018.01.050>
- Oei, P.-Y., Hainsch, K., Löffler, K., von Hirschhausen, C. R., Holz, F., & Kemfert, C. (2019). A new climate for Europe: 2030 climate targets must be more ambitious. *DIW Weekly Report*, 9(40/41), 365–372.
- Olauson, J., & Bergkvist, M. (2016). Correlation between wind power generation in the European countries. *Energy*, 114, 663–670. <https://doi.org/10.1016/j.energy.2016.08.036>
- OPeNDAP (2020). Open-source Project for a Network Data Access Protocol – MERRA 2 Data. Online (Access date 7th of April 2019): <https://goldsmr4.gesdisc.eosdis.nasa.gov/opensdap/hyrax/MERRA2/>.
- Paardekooper, S., Lund, R. S., Mathiesen, B. V., Chang, M., Petersen, U. R., Grundahl, L., Persson, U. et al. (2018). Heat Roadmap Europe 4 : Quantifying the Impact of Low-Carbon Heating and Cooling Roadmaps. Deliverable 6.5.
- Palizban, O., & Kauhaniemi, K. (2016). Energy storage systems in modern grids—Matrix of technologies and applications. *Journal of Energy Storage*, 6(2015), 248–259. <https://doi.org/10.1016/j.est.2016.02.001>
- Papaefthymiou, G., & Dragoon, K. (2016). Towards 100% renewable energy systems: Uncapping power system flexibility. *Energy Policy*, 92, 69–82. <https://doi.org/10.1016/j.enpol.2016.01.025>
- Papaefthymiou, G., Grave, K., Dragoon, K. (2014). Flexibility Options in Energy Systems. Project Report for Ecofys.
- Pape, C., Gerhardt, N., Härtel, P., Scholz, A., Schwinn, R., & Drees, T. et al. (2014). Bestimmung des Speicherbedarfs in Deutschland im europäischen Kontext und Ableitung von technisch-ökonomischen sowie rechtlichen Handlungsempfehlungen für die Speicherförderung. *Final Report*.
- Pasaoglu, G., Fiorello, D., Martino, A., Scarcella, G., Alemanno, A., Zubaryeva, A., & Thiel, C. (2012). Driving and parking patterns of European car drivers - a mobility survey. *European Commission JRC Scientific and Policy Reports*. <https://doi.org/10.2790/7028>
- Paulus, M., & Borggreffe, F. (2011). The potential of demand-side management in energy-intensive industries for electricity markets in Germany. *Applied Energy*, 88(2), 432–441. <https://doi.org/10.1016/j.apenergy.2010.03.017>
- Pfenninger, S.; Staffell, I. (2020). Renewables Ninja. Online (Access date: 8th of April 2019): <https://www.renewables.ninja/>.

- Pfenninger, S., & Staffell, I. (2016). Long-term patterns of European PV output using 30 years of validated hourly reanalysis and satellite data. *Energy*, *114*, 1251–1265. <https://doi.org/10.1016/j.energy.2016.08.060>
- Posma, J., Lampropoulos, I., Schram, W., & van Sark, W. (2019). Provision of ancillary services from an aggregated portfolio of residential heat pumps on the Dutch Frequency Containment Reserve market. *Applied Sciences (Switzerland)*, *9*(3), 1–16. <https://doi.org/10.3390/app9030590>
- Powering Past Coal Alliance (PPCA) (2020): Members. Online (Access date: 30th of July 2019): <https://poweringpastcoal.org/about/members>.
- Pruditsch, N. (2017). The Conditions of Successful Renewable Energy Governance. Exploring Qualitative Comparative Analysis (QCA) in Energy Policy Research. *Energy Procedia*, *118*, 21–27. <https://doi.org/10.1016/j.egypro.2017.07.004>
- Pruditsch, N., & Zöphel, C. (2017). Szenarien für ein europäisches Energiesystem (Scenarios for a European energy system). *Uwf UmweltWirtschaftsForum*, *25*(1–2), 81–90. <https://doi.org/10.1007/s00550-017-0443-x>
- Reindl, D. T., Beckman, W. A., & Duffie, J. A. (1990). Evaluation of hourly tilted surface radiation models. *Solar Energy*, *45*(1), 9–17. [https://doi.org/10.1016/0038-092X\(90\)90061-G](https://doi.org/10.1016/0038-092X(90)90061-G)
- Renn, O., & Marshall, J. P. (2016). Coal, nuclear and renewable energy policies in Germany: From the 1950s to the “Energiewende.” *Energy Policy*, *99*, 224–232. <https://doi.org/10.1016/j.enpol.2016.05.004>
- Richardson, D. B. (2013). Electric vehicles and the electric grid: A review of modeling approaches, Impacts, and renewable energy integration. *Renewable and Sustainable Energy Reviews*, *19*, 247–254. <https://doi.org/10.1016/j.rser.2012.11.042>
- Ringkjøb, H., Haugan, P. M., Solbrekke, I. M., Zürich, E. T. H., & Pfenninger, S. (2018). A review of modelling tools for energy and electricity systems with large shares of variable renewables. *Renewable and Sustainable Energy Reviews*, *96*(July), 440–459. <https://doi.org/10.1016/j.rser.2018.08.002>
- Rinne, E., Holttinen, H., Kiviluoma, J., & Rissanen, S. (2018). Effects of turbine technology and land use on wind power resource potential. *Nature Energy*, *3*(6), 494–500. <https://doi.org/10.1038/s41560-018-0137-9>
- Rodríguez, R. A., Becker, S., Andresen, G. B., Heide, D., & Greiner, M. (2014). Transmission needs across a fully renewable European power system. *Renewable Energy*, *63*, 467–476. <https://doi.org/10.1016/j.renene.2013.10.005>
- Ruhnau, O., Hirth, L., & Praktiknjo, A. (2019). Time series of heat demand and heat pump efficiency for energy system modeling. *Scientific Data*, *6*(1), 189. <https://doi.org/10.1038/s41597-019-0199-y>

-
- Ryberg, D. S., Caglayan, D. G., Schmitt, S., Linßen, J., Stolten, D., & Robinius, M. (2019). The future of European onshore wind energy potential: Detailed distribution and simulation of advanced turbine designs. *Energy*, *182*, 1222–1238. <https://doi.org/10.1016/j.energy.2019.06.052>
- Salm, S., Hille, S. L., & Wüstenhagen, R. (2016). What are retail investors' risk-return preferences towards renewable energy projects? A choice experiment in Germany. *Energy Policy*, *97*, 310–320. <https://doi.org/10.1016/j.enpol.2016.07.042>
- Sarabi, S., Davigny, A., Courtecuisse, V., Riffonneau, Y., & Robyns, B. (2016). Potential of vehicle-to-grid ancillary services considering the uncertainties in plug-in electric vehicle availability and service/localization limitations in distribution grids. *Applied Energy*, *171*, 523–540. <https://doi.org/10.1016/j.apenergy.2016.03.064>
- Schaber, K., Steinke, F., Mühlich, P., & Hamacher, T. (2012). Parametric study of variable renewable energy integration in Europe: Advantages and costs of transmission grid extensions. *Energy Policy*, *42*, 498–508. <https://doi.org/10.1016/j.enpol.2011.12.016>
- Schellong, W. (2016). *Analyse und Optimierung von Energieverbundsystemen*. Springer, Berlin Heidelberg, 2016. DOI: 10.1007/978-3-662-49463-9.
- Schill, W.P. (2019). Power-to-X: so wenig wie nötig, nicht so viel wie möglich. DIW Kommentar. Berlin, 2019.
- Schill, W.P., & Zerrahn, A. (2017). Long-run power storage requirements for high shares of renewables: Results and sensitivities. *Renewable and Sustainable Energy Reviews*, September 2016, 1–16. <https://doi.org/10.1016/j.rser.2017.05.205>
- Schill, W.P., Gerbaulet, C. (2015). Power system impacts of electric vehicles in Germany: Charging with coal or renewables? *Applied Energy* *156*, 185-196. <https://doi.org/10.1016/j.apenergy.2015.07.012>
- Schill, W. P. (2014). Residual load, renewable surplus generation and storage requirements in Germany. *Energy Policy*, *73*, 65–79. <https://doi.org/10.1016/j.enpol.2014.05.032>
- Schlachtberger, D. P., Brown, T., Schramm, S., & Greiner, M. (2017). The benefits of cooperation in a highly renewable European electricity network. *Energy*, *134*, 469–481. <https://doi.org/10.1016/j.energy.2017.06.004>
- Scholz, Y. (2012). Renewable energy based electricity supply at low costs. *Dissertation*. University of Stuttgart, 2012.
- Schröder A., Kunz F., Meiss J., u.a. (2013): Current and Prospective Costs of Electricity Generation until 2050. *DIW data documentation*, 2013.
- Schyska, B. U., Kies, A., Schlott, M., von Bremen, L., & Medjroubi, W. (2020). The Sensitivity of Power System Expansion Models. *Submitted to Applied Physics*. <http://arxiv.org/abs/2007.09956>

- Schubert, K.J.D. (2016). Bewertung von Szenarien für Energiesysteme: Potenziale, Grenzen und Akzeptanz. *Dissertation*, TU Dresden, 2016.
- Sensfuß, F., Ragwitz, M., Genoese, M. (2007). The Merit-order effect: A detailed analysis of the price effect of renewable electricity generation on spot market prices in Germany. Working Paper Sustainability and Innovation No. S 7/2007.
- Shafiee, S., & Topal, E. (2009). When will fossil fuel reserves be diminished? *Energy Policy*, 37(1), 181–189. <https://doi.org/10.1016/j.enpol.2008.08.016>
- Staffell, I., Scamman, D., Velazquez Abad, A., Balcombe, P., Dodds, P. E., Ekins, P., Shah, N., & Ward, K. R. (2019). The role of hydrogen and fuel cells in the global energy system. *Energy and Environmental Science*, 12(2), 463–491. <https://doi.org/10.1039/c8ee01157e>
- Staffell, I., & Green, R. (2014). How does wind farm performance decline with age? *Renewable Energy*, 66, 775–786. <https://doi.org/10.1016/j.renene.2013.10.041>
- Staffell, I., & Pfenninger, S. (2016). Using bias-corrected reanalysis to simulate current and future wind power output. *Energy*, 114, 1224–1239. <https://doi.org/10.1016/j.energy.2016.08.068>
- Steffen, B., Hischier, D., & Schmidt, T. S. (2018). Historical and projected improvements in net energy performance of power generation technologies. *Energy and Environmental Science*, 11(12), 3524–3530. <https://doi.org/10.1039/c8ee01231h>
- Steinke, F., Wolfrum, P., & Hoffmann, C. (2013). Grid vs. storage in a 100% renewable Europe. *Renewable Energy*, 50, 826–832. <https://doi.org/10.1016/j.renene.2012.07.044>
- Sterchele, P., Kersten, K., Palzer, A., Hentschel, J., & Henning, H. M. (2020). Assessment of flexible electric vehicle charging in a sector coupling energy system model – Modelling approach and case study. *Applied Energy*, 258(November), 114101. <https://doi.org/10.1016/j.apenergy.2019.114101>
- Stetter, D. (2012). Enhancement of the REMix energy system model: Global renewable energy potentials, optimized power plant siting and scenario validation. *Dissertation*. <https://doi.org/http://dx.doi.org/10.18419/opus-6855>
- Stoft, Steven (2002): *Power System Economics – Designing Markets for Electricity*; New York; Wiley.
- Šúri, M.; Huld, T.; Dunlop, E.; Hofierka, J. (2007). Solar Resource Modelling in Energy Applications. In: Peckham, R.J.; Jordan, G. (Eds.) (2007). *Digital Terrain Modelling – Development and Applications in a Policy Support Environment*. Springer, Berlin Heidelberg, 2007.

-
- Thien, T., Chen, H., Moos, M., Wolf, P., Cai, Z., Alvarez, R., Moser, A., Sauer, D. U., Bussar, C., & Leuthold, M. (2014). Optimal Allocation and Capacity of Energy Storage Systems in a Future European Power System with 100% Renewable Energy Generation. *Energy Procedia*, 46, 40–47. <https://doi.org/10.1016/j.egypro.2014.01.156>
- Troen, I., & Lundtang Petersen, E. (1989). European wind atlas. [http://orbit.dtu.dk/en/publications/european-wind-atlas\(335e86f2-6d21-4191-8304-0b0a105089be\).html](http://orbit.dtu.dk/en/publications/european-wind-atlas(335e86f2-6d21-4191-8304-0b0a105089be).html)
- Trost, T. (2016). Erneuerbare Mobilität im motorisierten Individualverkehr. *Dissertation*, University of Leipzig, 2016.
- Troy, N., Denny, E., O'Malley, M. (2010). Base-load cycling on a system with significant wind penetration. *IEEE Transactions on Power Systems*, Vol. 25, No. 2 (1 May 2010), pp. 1088-1097.
- Turconi, R., Boldrin, A., & Astrup, T. (2013). Life cycle assessment (LCA) of electricity generation technologies: Overview, comparability and limitations. *Renewable and Sustainable Energy Reviews*, 28, 555–565. <https://doi.org/10.1016/j.rser.2013.08.013>
- UN Climate Summit 2020: 2020 climate progress tracker tool. Online (Access date: 05th of June 2020): <https://unclimatesummit.org/trackerhome/trackercountries/>.
- UNCCD & IRENA (2017). Energy and Land Use – Global Land Outlook. *Working Paper*.
- United Nations Framework Convention on Climate Change (UNFCCC) (2020). Paris Agreement - Status of Ratification, Online (Date of access: 5th of July 2020): <https://unfccc.int/process/the-paris-agreement/status-of-ratification>
- United Nations Framework Convention on Climate Change (UNFCCC) (1998). Kyoto Protocol to The United Nations Framework Convention on Climate Change
- Umweltbundesamt (UBA) (2020). Erneuerbare Energien in Deutschland - Daten zur Entwicklung im Jahr 2019.
- U.S. Geological Survey (USGS) (1996). Global 30 Arc-Second Elevation (GTOPO30). Online (Date of Access: 12th of March 2019): <https://earthexplorer.usgs.gov/>.
- Unteutsch, M. (2014). Who benefits from cooperation? A numerical analysis of redistribution effects resulting from cooperation in European. *EWI Working Paper*, No 14/02.
- van der Wiel, K., Stoop, L. P., van Zuijlen, B. R. H., Blackport, R., van den Broek, M. A., & Selten, F. M. (2019). Meteorological conditions leading to extreme low variable renewable energy production and extreme high energy shortfall. *Renewable and Sustainable Energy Reviews*, 111(May), 261–275. <https://doi.org/10.1016/j.rser.2019.04.065>
- Van Nuffel, L., Gorenstein Dedecca, J., Smit, T., & Rademaekers, K. (2018). Sector coupling: how can it be enhanced in the EU to foster grid stability and decarbonise? *Study on behalf of the ITRE committee*.

- Vartiainen, E., Masson, G., Breyer, C., Moser, D., & Román Medina, E. (2020). Impact of weighted average cost of capital, capital expenditure, and other parameters on future utility-scale PV levelised cost of electricity. *Progress in Photovoltaics: Research and Applications*, 28(6), 439–453. <https://doi.org/10.1002/pip.3189>
- Verzijlbergh, R. A., De Vries, L. J., Dijkema, G. P. J., & Herder, P. M. (2017). Institutional challenges caused by the integration of renewable energy sources in the European electricity sector. *Renewable and Sustainable Energy Reviews*, 75(November 2015), 660–667. <https://doi.org/10.1016/j.rser.2016.11.039>
- Viebahn, P., & Chappin, E. J. L. (2018). Scrutinising the gap between the expected and actual deployment of carbon capture and storage - A bibliometric analysis. In *Energies* (Vol. 11, Issue 9). <https://doi.org/10.3390/en11092319>
- von Selasinsky, A. (2016). The Integration of Renewables in Continuous Intraday Markets for Electricity. *Dissertation*. Schriften des Lehrstuhls für Energiewirtschaft, TU Dresden, 2016.
- Wappelhorst, S., Hall, D., Nicholas, M., Lutsey, N. (2020). Analyzing Policies to Grow - The Electric Vehicle Market in European Cities. White paper for International Council on Clean Transportation.
- Weitemeyer, S., Kleinhans, D., Vogt, T., & Agert, C. (2015). Integration of Renewable Energy Sources in future power systems: The role of storage. *Renewable Energy*, 75, 14–20. <https://doi.org/10.1016/j.renene.2014.09.028>
- Wolsink, M. (2018). Social acceptance revisited: gaps, questionable trends, and an auspicious perspective. *Energy Research and Social Science*, 46(July), 287–295. <https://doi.org/10.1016/j.erss.2018.07.034>
- World Database on Protected Areas (WDPA) (2014). World Database on Protected Areas. Online (Date of Access: 12th of March 2019): <https://www.protectedplanet.net/>.
- World Forum Offshore Wind (WFO) (2019). Global Offshore Wind Report 2019. Singapur, 2019.
- World Steel Association (WSA) (2017). Steel Statistical Yearbook 2017. Brussels 2017.
- Xu, L., Fuss, M., Poganietz, W.-R., Jochem, P., Schreiber, S., Zoephel, C., & Brown, N. (2020). An Environmental Assessment Framework for Energy System Analysis (EAFESA): The method and its application to the European energy system transformation. *Journal of Cleaner Production*, 243. <https://doi.org/10.1016/j.jclepro.2019.118614>
- Zappa, W., Junginger, M., & van den Broek, M. (2019). Is a 100% renewable European power system feasible by 2050? *Applied Energy*, 233–234(August 2018), 1027–1050. <https://doi.org/10.1016/j.apenergy.2018.08.109>

-
- Zappa, W., & van den Broek, M. (2018). Analysing the potential of integrating wind and solar power in Europe using spatial optimisation under various scenarios. *Renewable and Sustainable Energy Reviews*, 94(August), 1192–1216. <https://doi.org/10.1016/j.rser.2018.05.071>
- Zerrahn, A., & Schill, W. (2017). Long-run power storage requirements for high shares of renewables : review and a new model. *Renewable and Sustainable Energy Reviews*, 79(November 2016), 1518–1534. <https://doi.org/10.1016/j.rser.2016.11.098>
- Zerrahn, A., & Schill, W. P. (2015). On the representation of demand-side management in power system models. *Energy*, 84, 840–845. <https://doi.org/10.1016/j.energy.2015.03.037>
- Zhao, P., Wang, J., & Dai, Y. (2015). Capacity allocation of a hybrid energy storage system for power system peak shaving at high wind power penetration level. *Renewable Energy*, 75, 541–549. <https://doi.org/10.1016/j.renene.2014.10.040>
- Zoellner, J., Schweizer-Ries, P., & Wemheuer, C. (2008). Public acceptance of renewable energies: Results from case studies in Germany. *Energy Policy*, 36(11), 4136–4141. <https://doi.org/10.1016/j.enpol.2008.06.026>
- Zöphel, C., Schreiber, S., Herbst, A., Klingler, A.-L., Manz, P., Heitel, S., Fermi, F., Wyrwa, A., Raczynski, M., Reiter, U., & Möst, D. (2019). Report on cost optimal energy technology portfolios for system flexibility in the sectors heat, electricity and mobility. http://reflex-project.eu/wp-content/uploads/2020/02/D4.3_Report_on_cost_optimal_energy_technology_portfolios.pdf
- Zöphel, C., & Möst, D. (2017). The value of energy storages under uncertain CO₂-prices and renewable shares. *International Conference on the European Energy Market, EEM*. <https://doi.org/10.1109/EEM.2017.7981973>
- Zöphel, C., Schreiber, S., Müller, T., Möst, D. (2018). Which Flexibility Options Facilitate the Integration of Intermittent Renewable Energy Sources in Electricity Systems?. *Curr Sustainable Renewable Energy Rep* 5, 37–44 (2018). <https://doi.org/10.1007/s40518-018-0092-x>
- Zöphel, C., Müller, T. (2016). Flexibilitätsoptionen am Strommarkt - Eine Analyse zu Hemmnissen und Erlösmöglichkeiten. In: Institut für Elektrizitätswirtschaft und Energieinnovation (Eds.): Tagungsband des 14. Symposium Energieinnovation: Energie für unser Europa. Graz.

Appendix

A Literature on model-based analysis of flexibility demand and provision

Table A.1 Overview of literature discussing flexibility requirements and provision (Own compilation)

		Flexibility Requirement				Flexibility Provision		
		Region	Share of iRES	Wind-PV share	Analysis flexibility needs	Model specification	Flexibility options	Sector coupling
1	Denholm & Hand (2011)	Texas	80 %	✓	✓	• Simulation	• Storage	---
2	Heide et al. (2011)	Europe	100 % (WD)	✓	✓	• Time series analysis	• Storage	---
3	Huber et al. (2014)	Europe	10 – 70 % (WD)	✓	✓	• ---	---	---
4	Cebulla & Fichtner (2017)	Case study	40 % / 60 %	✓	---	• LP/MILP • Investment • Dispatch	• Power plants • Storage	---
5	Child et al. (2019)	Europe	Up to 100 % (ME)	---	---	• LP • Investment • Dispatch	• Power plants • Storage • NTC • DSM • (PtX)	---
6	Brijs et al. (2017)	BE	0 – 50 %	---	---	• MIP • Greenfield • Investment • Dispatch	• Power plants • Storage	---
7	Zerrahn und Schill (2017)	DE	60 – 100 % (ME)	---	---	• LP • Greenfield	• Power plants • Storage • DSM	---
8	Gils et al. (2017)	Europe	0 – 120 % (WD,WE)	✓	(✓)	• LP • Greenfield • Investment • Dispatch	• Power plants • Storage • NTC • DSM	---
9	Schlachtberger et al. (2017)	Europe	CO ₂ -Reduction target	✓		• LP • Greenfield • Dispatch	• Power plants • Storage • NTC	---
10	Steinke et al. (2013)	Europe	100 % (WD)	✓	(✓)	• LP • Dispatch	• Storage	---
11	Weitemeyer et al. (2015)	Europe	0 – 100 %	✓	(✓)	• LP • Dispatch	• Storage	---

Table A.1 (Continuation)

		Region	Flexibility Requirement			Flexibility Provision		
			Share of iRES	Wind-PV share	Analysis flexibility needs	Model specification	Flexibility options	Sector coupling
12	Koch et al. (2015)	DE Europe	37 – 86 %	---	---	<ul style="list-style-type: none"> • MILP • Dispatch 	<ul style="list-style-type: none"> • Power plants • Storage • NTC • DSM • PtX 	<ul style="list-style-type: none"> • Heating • Transport • Electrolysis
13	Matthiesen et al. (2015)	DK (Case study)	100 %	---	---	<ul style="list-style-type: none"> • Simulation 	<ul style="list-style-type: none"> • Power plants • Storage • PtX 	<ul style="list-style-type: none"> • Heating • Transport • Electrolysis
14	Brown et al. (2018)	Europe	CO ₂ -Reduction target (ME, WD)	---	---	<ul style="list-style-type: none"> • LP • Investment • Dispatch 	<ul style="list-style-type: none"> • Power plants • Storage • NTC • PtX 	<ul style="list-style-type: none"> • Heating • Transport • Electrolysis
15	Connolly et al. (2016)	Europe	0 – 100 % Linear scaling	---	---	<ul style="list-style-type: none"> • Simulation 	<ul style="list-style-type: none"> • Power plants • Storage • PtX 	<ul style="list-style-type: none"> • Heating • Transport • Electrolysis

WD – Weather Data, ME – Model Endogenous, LP – Linear Problem, MILP – Mixed Integer Linear Problem, PP – Power Plants

B Additional calculations and results for the iRES expansion model

B.1 Derivation of wind onshore generation time series

For the calculation, three data sets of the MERRA-2 data are necessary. For step 1, the "single-level diagnostics" data set (see dataset GMAO in (Bosilovich 2016)) contains the wind data (in m/s) at 50 m altitude in the east (dataset U50M) and in the north (dataset V50M) direction. These vectorial wind speeds are then combined by vector addition. Since different wind turbines are used for different wind conditions, the wind speeds of the raster points are first averaged over the year, then categorized into wind classes and finally assigned to three different turbine types. Based on the wind classes (IEC 2019), 88 % of the 1,481 raster can be categorised to wind class III and 12 % to wind class II. As mentioned before, very high-yielding locations with mean wind speeds of over 10 m/s are not found onshore in the observed area.

In step 2, the derived wind speeds are logarithmically scaled up for future wind turbine heights, taking the roughness of the earth surface into account. To include this, time series of the roughness lengths are gathered, which are called via the "Surface Flux Diagnostics" data set (Z0M) (see Bosilovich 2016).

In step 3, the wind speeds are converted into power generation time series based on the power curves of the two reference turbines. These reference curves can be divided into four phases. While in the first phase the wind speed is too low for the cut-in speed of the turbine (no power output), in the third phase, the nominal capacity of the wind power plant is kept constant to avoid damage to the turbine limited by phase four, in which the wind speed is too high, and the electricity generation is cut-off. During the second phase wind power output increases in third power in proportion to wind speed w :

$$P^{Wind} = \frac{1}{2} \cdot \rho \cdot c_P \cdot A_R \cdot w^3$$

While the air density ρ is assumed to be constant (1.225 kg/m³) and the coefficient of power c_P can be derived from the manufactures data, the rotor diameter will also be scaled based on the discussion of future trends.

Within step 3, the power curves are further processed based on Staffell and Pfenninger (2016). At first, the power curve's original discrete resolution of 1 m/s is increased to 0.001 m/s by applying a cubic spline interpolation. This enables a more detailed relation between wind speeds and power output. To derive an aggregated power curve of a wind farm instead of a single turbine, the power curves were further smoothed using a Gaussian filter with mean zero

and a standard deviation related to the wind speed as in Staffel and Pfenninger (2016). In Figure , the resulting power curves for the IEC III and II wind farms are normalized as ratio of hourly power output to nameplate capacity.

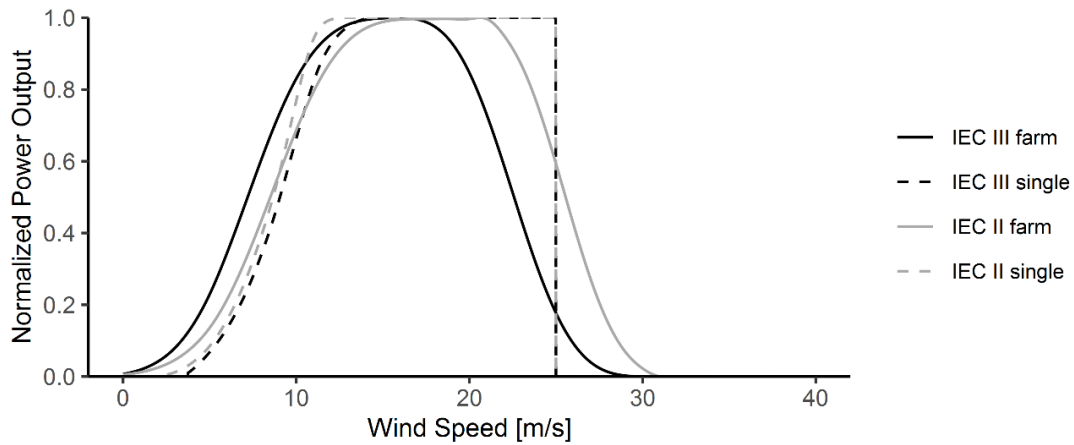


Figure B.1: Original manufactures (dotted lines) and smoothed (solid lines) power curves of the two reference farms (Enercon 2015, GE 2014)

Finally, the wind power generation time series for each raster are derived based on these power curves, the time series of wind speeds as well as the nominal capacity of the two reference wind turbines including technological progress.

B.2 Derivation of PV time series

The solar radiation data is based on the "Radiation Diagnostics" data set in MERRA-2, from which the hourly horizontal global radiation (dataset SWGDN) and the extra-terrestrial radiation (dataset SWTDN) are extracted according to the procedure in Figure 3.1. By applying the ratio of global and extra-terrestrial radiation, the relative global radiation (also called the Clearness Index) can be calculated, which is used to determine the direct and diffuse share of global radiation according to Reindl et al. (1990). In addition, the hourly surface temperature (T2M) from the "single-level diagnostics" dataset is used in step 3.

In step 2, the horizontal direct and diffuse radiations is converted to the inclined module surface of the PV systems according to Jamil et al. (2016). The direct sunlight on an inclined surface is influenced by the solar altitude, the solar azimuth, the module inclination and the module orientation. First, the solar altitude and the solar azimuth are calculated based on the hourly position of the sun depending on the geographical coordinates, the time, the date and the season. The sun declination and the hour angle define the position specification of the sun in an imaginary celestial sphere (in the so-called rotating equatorial coordinate system). With these two parameter the position of the sun can be assigned from the rotating to the stationary equatorial coordinate system. While the sun declination describes the elevation angle of the sun related to the latitude, the hour angle defines the deviation from the so-called vernal or spring equinox regarding the longitude. As a result, the sun altitude or elevation angle (i.e. the angle between sun's position from the point of observation and the horizontal line) and the solar azimuth (i.e. the western or eastern degree of longitude deviation) for each coordinate point can be calculated (Jamil et al. 2016). Afterwards, the angle of incidence on the inclined plane α is derived, by using the following formula where h is the sun's height, t is the module inclination, a_p is the module azimuth, and a_s is the solar azimuth (Pfenninger & Staffell 2016):

$$\alpha = \arccos\left(\sin(h) \cdot \cos(t) + \cos(h) \cdot \sin(t) + \cos(a_p - a_s)\right)$$

For Europe, the optimal module inclination lies between 30° - 40°. Therefore, an angle of 35 ° is assumed in the following. Furthermore, the literature describes an optimal module orientation and thus an optimal module azimuth facing to the equator, i.e. to the south for the northern hemisphere (Schellong, 2016 and Šúri et al., 2007). In reality, this orientation is often not possible or desirable due to structural or constructional restrictions, but also due to considerations regarding the optimisation of self-consumption. A deviating module azimuth can lead to a different feed-in characteristic of the PV system (Hummon et al. 2012) and accordingly influence the need for flexibility locally. However, since these interactions are not part of the study in the present work, a uniform module azimuth angle of 0 ° (i.e., south orientation) is assumed.

With α and the sun's position parameter as well as the MERRA-2 data, the direct and diffused radiation in the inclined plane ($I_{dir,g}$ and $I_{diff,g}$) results from the horizontal global radiation ($I_{dir,h}$ and $I_{diff,h}$) as shown in the formulas below, where the surface albedo a is set to 0.3 according to Pfenninger & Staffell (2016). The direct and diffuse radiation on the PV modules are then added to the global radiation on the inclined plane.

$$I_{dir,g} = \frac{I_{dir,h} \cdot \cos(\alpha)}{\cos\left(\frac{\pi}{2} - \alpha_s\right)}$$

$$I_{diff,g} = I_{diff,h} \cdot \frac{1 + \cos(t)}{2} + a \cdot (I_{dir,h} + I_{diff,h}) \cdot \frac{1 - \cos(t)}{2}$$

In step 3, the hourly time series of the global radiation obtained for each raster are transformed into normalised PV generation time series. As in Huld et al. (2010), in addition to the global radiation the previously derived temperature time series as well as a reference plant under standard test conditions (STC - reference radiation 1000 W/m², reference temperature 25 °C) are included to get PV generation time series based on global radiation using the following equation:

$$P(I, T_{mod}) = P_{STC} \cdot \frac{I}{I_{STC}} \cdot \mu_{rel}(I', T')$$

where the power output P depends from the module temperature T_{mod} and the in-plane irradiance ($I = I_{dir,g} + I_{diff,g}$). For the calculation of the relative efficiency μ_{rel} , I' and T' are normalized to STC conditions and fitted to describe the relation of module efficiency and ambient temperature as well as irradiation using the coefficients as applied in Huld et al. (2010).

B.3 Additional data and results of the iRES expansion

Table B.1: Studies included with varying Wind-PV ratio

Source	iRES generation [TWh]			Wind-PV ratio	
	PV	Wind onshore	Wind offshore		
ENTSO-E (2018) (DG 2040)		1104	1214	0	0,52
Heide et al. (2010)					0,55
Thien et al. (2014)		1422	2024	0	0,59
ECF (2010)		19	15	15	0,61
ENTSO-E (2018) (GCA 2040)		859	1509	0	0,64
ENTSO-E (2015)		850	1500	0	0,64
Knopf (2013)		19	35	0	0,65
Steinke (2013)					0,65
REFLEX (2019) (decentral)		787	1319	422	0,69
Capros et al. (2016)		429	980	0	0,70
ENTSO-E (2018) (ST 2040)		496	1162	0	0,70
REFLEX (2019) (central)		529	1344	165	0,74
Nitsch et al. (2012)		200	589	0	0,75
Fürsch (2013)		600	2000	0	0,77
Scholz et al. (2014)		369	757	560	0,78
Fraunhofer ISI (2017)		559	2209	0	0,80
Fraunhofer IWES (2015)		169	448	323	0,82
Schaber (2012)		93	282	163	0,83
Pellinger et al. (2016)		186	654	348	0,84
Bertsch et al., 2012		300	1900	0	0,86
Eurelectric (2011)		3	20	0	0,87

Table B.2: iRES generation in the FD scenarios per iRES technology type and country

[TWh]	High PV			REF			High Wind		
	PV	Wind onshore	Wind offshore	PV	Wind onshore	Wind offshore	PV	Wind onshore	Wind offshore
AT	44.4	6.9	0.0	20.8	6.9	0.0	2.8	25.0	0.0
BE	10.5	25.3	5.7	3.6	36.7	5.7	3.6	36.7	5.7
CH	23.3	2.6	0.0	15.0	1.7	0.0	15.0	1.7	0.0
CZ	20.6	2.3	0.0	16.8	6.1	0.0	2.6	20.4	0.0
DE	199.8	142.8	23.7	49.4	293.2	23.7	49.4	293.2	23.7
DK	1.0	28.9	6.8	1.0	28.9	6.8	1.0	28.9	6.8
ES	133.9	133.9	0.0	80.3	187.4	0.0	19.6	176.1	0.0
FR	196.2	196.2	0.0	127.8	331.8	0.0	9.8	458.8	41.2
GB	42.9	245.6	31.0	13.4	275.2	31.0	13.4	275.2	31.0
IE	2.8	25.5	0.0	2.8	25.5	0.0	2.8	25.5	0.0
IT	305.2	20.4	13.5	273.8	20.4	10.0	85.3	20.4	10.6
LU	0.0	0.0	0.0	0.0	0.0	0.0	0.0	0.0	0.0
NL	13.9	35.0	3.5	4.1	44.8	3.5	4.1	58.8	3.5
NO	11.4	29.7	0.0	0.0	37.1	4.1	0.0	124.6	13.8
PL	35.3	26.9	1.5	4.9	57.3	1.5	0.5	145.9	15.8
PT	37.4	16.2	0.0	35.0	18.6	0.0	5.4	48.2	0.0
SE	0.0	44.3	14.8	0.0	38.4	20.7	0.0	32.5	26.6

Table B.3: Installed capacities in the FD scenarios per iRES technology type and country

[GW]	High PV			REF			High Wind		
	PV	Wind onshore	Wind offshore	PV	Wind onshore	Wind offshore	PV	Wind onshore	Wind offshore
AT	42.18	3.34	0.00	19.77	3.34	0.00	2.64	12.00	0.00
BE	10.69	9.03	1.70	3.71	13.12	1.70	3.71	13.12	1.70
CH	21.50	1.97	0.00	13.79	1.26	0.00	13.79	1.26	0.00
CZ	20.55	0.89	0.00	16.76	2.37	0.00	2.56	7.92	0.00
DE	201.64	58.07	7.03	49.83	119.22	7.03	49.83	119.22	7.03
DK	1.12	8.27	1.87	1.12	8.27	1.87	1.12	8.27	1.87
ES	105.83	49.98	0.00	63.50	69.97	0.00	15.46	65.72	0.00
FR	179.89	72.72	0.00	117.18	122.95	0.00	9.01	169.97	12.32
GB	47.39	75.77	13.90	14.78	84.89	13.90	14.78	84.89	13.90
IE	3.11	7.60	0.00	3.11	7.60	0.00	3.11	7.60	0.00
IT	258.69	10.58	4.02	232.10	10.58	2.98	72.40	10.58	3.16
LU	5.13	0.55	0.00	1.53	0.16	0.00	1.53	0.16	0.00
NL	14.54	12.37	1.05	4.33	15.80	1.05	4.33	20.73	1.05
NO	15.00	11.19	0.00	0.00	13.95	1.13	0.00	46.90	3.78
PL	36.98	9.78	0.45	5.11	20.83	0.45	0.47	53.05	4.68
PT	29.66	5.64	0.00	27.74	6.48	0.00	4.25	16.79	0.00
SE	0.00	19.81	4.04	0.00	17.17	5.65	0.00	14.52	7.27

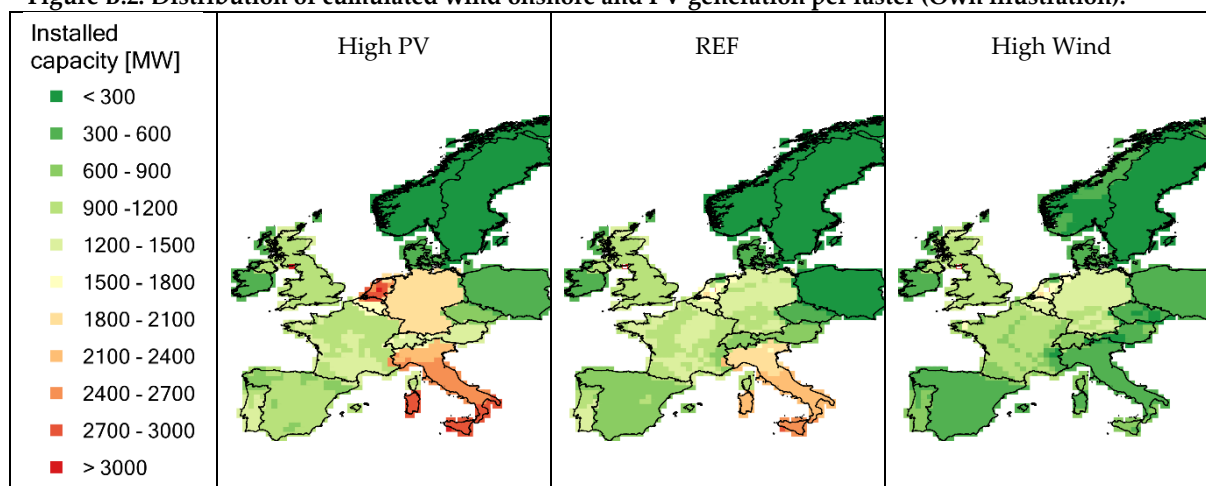
Figure B.2: Distribution of cumulated wind onshore and PV generation per raster (Own illustration).

Table B.4: Normalisation procedure for regression analysis

	Variable	Description
Independent	iRES share	Share of iRES generation on total electricity demand
	PV-share	Share of PV generation on total iRES generation
Dependent	Maximum residual load	Share of maximum residual load on maximum electricity demand
	Minimum residual load	Share of minimum residual load on maximum electricity demand
	Surplus hours	Cumulated hours with iRES surplus normalised to 8760 h
	Surplus energy	Share of cumulated iRES surplus energy on total iRES generation
	Mean and maximum residual load gradients	Share of gradients on installed iRES capacity
	Mean and maximum surplus and deficit phase duration	Not normalised
	Mean and maximum surplus and deficit phase energy	Share of surplus or deficit phase energy on total surplus energy

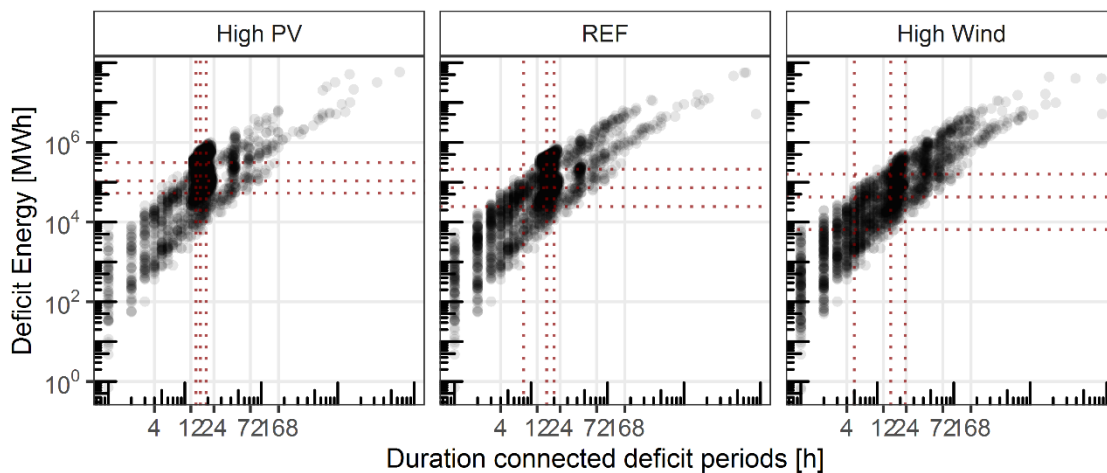


Figure B.3: Energy amount and duration of connected deficit periods (Own illustration)

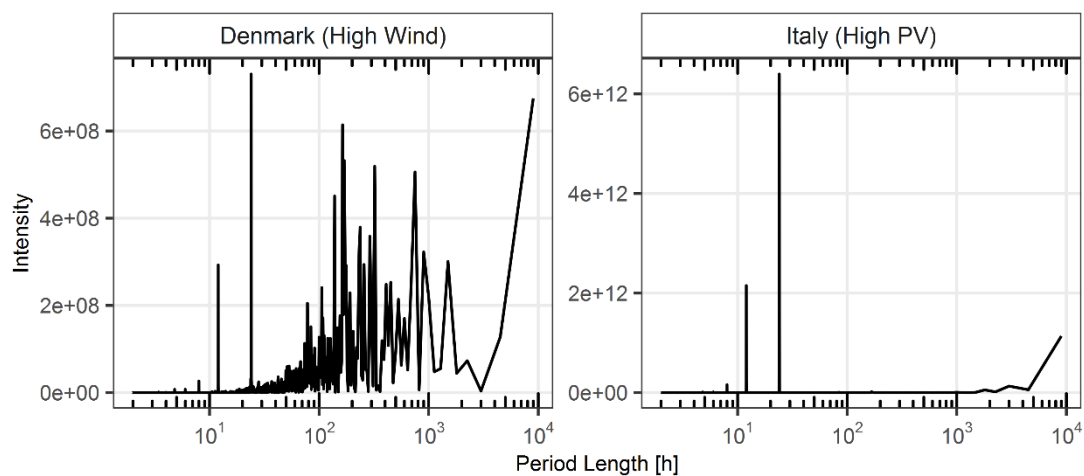


Figure B.4: Exemplary periodogram for Denmark (High Wind) and Italy (High PV) (Own illustration)

Table B.5: Investments in iRES per country and scenario

[bn. EUR]	High PV	REF	High Wind
AT	25	13	17
BE	20	22	22
CH	12	8	8
CZ	11	11	11
DE	189	184	184
DK	15	15	15
ES	109	117	92
FR	175	206	241
GB	10	10	10
IE	141	126	51
IT	2	1	1
LU	21	19	24
NL	21	20	68
NO	33	30	77
PL	20	21	23
PT	34	34	34
SE	123	118	118

B.4 Impact of selected model equations on the optimal iRES expansion

The results on optimal iRES expansions presented in Chapter 4 are based on a iRES expansion model developed in Chapter 3. In general, the outcomes are highly sensitive with regard to the constraints, in particular restricting the iRES expansion in the countries. As an important feature, the distribution of the iRES capacities across the region observed (see equations 3.12 and 3.13) as well as within single countries (see equations 3.15) is restricted, to consider possible energy political challenges based on the land-use of PV and wind onshore. To emphasise the impact of these constraints, two relaxations of the iRES expansion model are introduced, named in the following as S-RAST and S-ALL. The outcomes aim to underline the requirements for the model adjustments, since the resulting flexibility need as well as expansion costs might be underestimated, when neglecting the effects of distributing the iRES capacities. Table B.6 gives an overview of the sensitivities. For S-RAST the model as presented in Chapter 3 is applied without restricting the raster concentration, thus equation (3.15) are excluded. In S-ALL, the country-wise restriction for minimum and maximum iRES shares (equations (3.13) and (3.15)) are additionally omitted. In both sensitivities, the equations constraining the available area per raster as well as introducing existing iRES capacities are still applied. In the following, the analysis focuses on installed capacities and generation as well as cost-related parameter.

Table B.6: Description of sensitivity analysis

	Original Results	Relaxation	
		S-RAST	S-ALL
Excluded equations of iRES model		(3.15)	(3.12), (3.13), (3.15)
Description	Model is applied as presented in Chapter 3	Model is applied as presented in Chapter 3, but <u>without</u> restricting raster concentration	Model is applied as presented in Chapter 3, but <u>without</u> restricting raster concentration <u>and</u> <u>without</u> minimum and maximum iRES shares

Without restricting the distribution of iRES capacities, the optimal solution of the expansion model potentially can install more capacities at locations with better conditions for PV or wind onshore power plants. In Figure B.5, the resulting change in total iRES capacities compared to the results in Chapter 4.1 Figure 4.1 can be displayed. In S-RAST with no restrictions for the raster concentration the total iRES capacities reduce by 6 % in all scenarios with the highest absolute decrease in the High PV scenario. Without implementing an enforced distribution of

the capacities, less than 20 % of the number of raster (1,482) are used for iRES installations in each scenario and sensitivity. In the sensitivity with an additional omission of the maximum and minimum iRES share per country, the required capacities can be further reduced in total. However, in High Wind, PV installations are displaced to locations with worse conditions by wind onshore turbines with higher specific costs (see further explanation below). Additionally, the distribution of wind onshore technologies in regions with higher full load hours further lowers the optimality of wind offshore installations and leads to comparably high offshore capacity reductions.

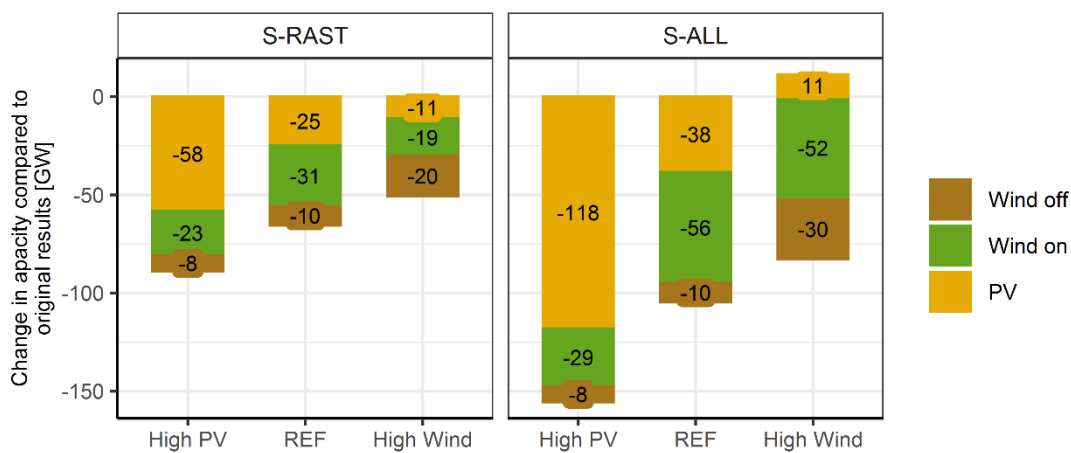


Figure B.5: Change in iRES capacities compared to the original results for both relaxations (S-RAST – no limitation of iRES capacity raster concentration, S-ALL – similar to S-RAST as well as no minimum and maximum iRES shares) (Own illustration)

In general, since the availability improves with access to locations with higher iRES potentials, the resulting decrease in capacities leads to less extreme flexibility needs, when analysing the total residual load aggregated for all the countries observed. As an example, for the High PV scenario the minimal aggregated residual load decreases in S-ALL by more than 8 %. Particularly the missing restriction of maximum iRES shares per country in the S-ALL sensitivity results in significant shifts of the distribution of PV and wind generation (see Figure B.6), with country-specific iRES share of more than 800 % in Ireland and Portugal. Thus, while the overall iRES expansion requirements can be reduced, due to the exploitation of optimal locations, the resulting flexibility demand in single countries increases significantly compared to the original results. When comparing the sorted residual loads for Ireland and Portugal in Figure B.7, the influence of these extreme iRES share become obvious. In both countries, the iRES surpluses are increasing significantly. In Portugal, a iRES share of 875 % results in a very steep negative residual load curve with a minimum peak almost six times as high compared to the original results. With a high wind share, as it is the case of Denmark (iRES

share = 839 %), the effects are even more extreme. As an example, the surplus energy increases from around 7 TWh (Original) to 190 TWh (S-All) corresponding to 97 % of the country's total iRES generation.

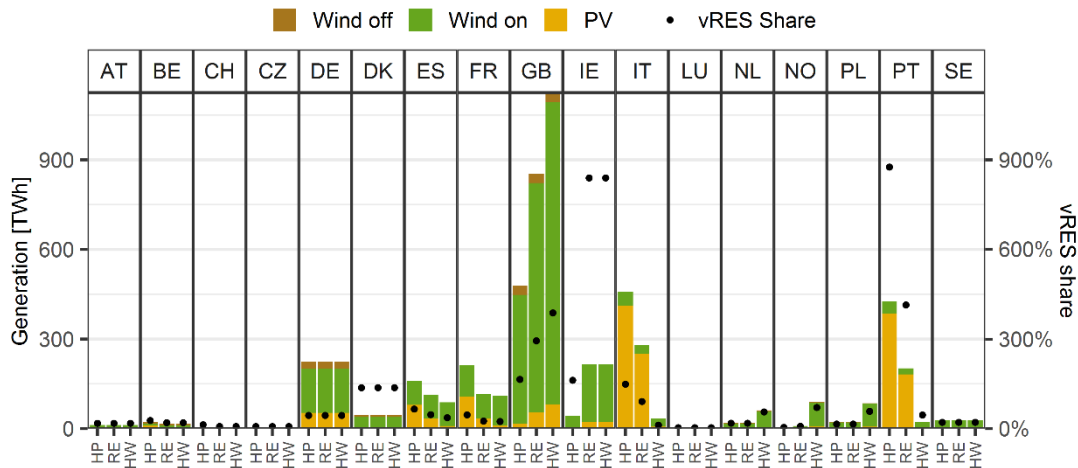


Figure B.6: Scenario-specific distribution of iRES generation without constraining maximum and minimum iRES share per country (S-ALL) (Own illustration)

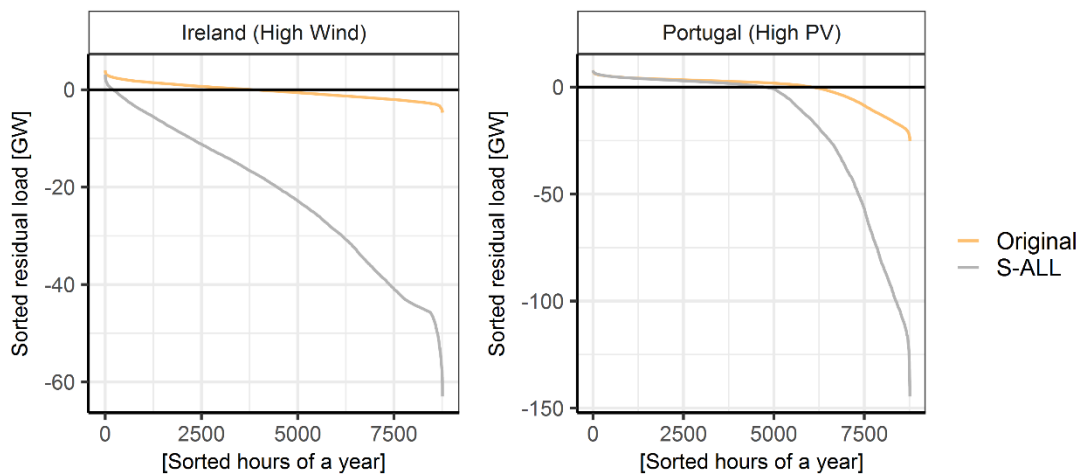


Figure B.7: Comparison of sorted residual load for Denmark and Portugal with and without selected model restrictions (Own illustration)

Table B.7 shows the influence of the two sensitivities on total costs and LCOE of iRES installations. With regard to the total costs of iRES expansion, a relaxation of capacity distribution restrictions decreases these costs by more than 20 % in each scenario. Thereby, particularly the geographical concentration of PV and wind onshore plants within one country has a high impact, as it is shown for the S-RAST. An additional removal of the maximum and

minimum iRES share, as in S-ALL, further decreases the total costs by up to one third in High Wind compared to the original results. Since with increasing wind share in the scenarios, the share of more cost-intensive technologies is increasing, an unrestricted distribution of iRES capacities has the most significant influence in the High Wind scenario in both relaxations.

Table B.7: Sensitivity analysis for selected model equations and impact on total costs and LCOE

	Scenarios [Unit]	Original Results	S-RAST	S-ALL
Total iRES investments	High PV/REF/High Wind [bn EUR]	961 / 953 / 994	748 / 711 / 733	722 / 687 / 669
Relative change to original results	High PV/REF/High Wind [%]		-22 / -25 / -26	-25 / -28 / -33
Weighted average LCOE of PV	High PV/REF/High Wind [EUR/MWh]	54 / 51 / 53	47 / 45 / 46	40 / 42 / 56
Relative change to original results (PV)	High PV/REF/High Wind [%]		-12 / -11 / -13	-26 / -18 / 4
Weighted average LCOE of Wind onshore	High PV/REF/High Wind [EUR/MWh]	24 / 24 / 25	14 / 14 / 15	14 / 13 / 13
Relative change to original results (Wind onshore)	High PV/REF/High Wind [%]		-41 / -42 / -39	-40 / -46 / -47

In Figure B.8 and B.9, the resulting cost-potential curves are illustrated for the two sensitivities. For both, the LCOE of PV and wind onshore, the weighted average of LCOE (LCOE of each raster times the share of realised generation on total generation in the same raster) is decreasing by up to 47 % in most of the scenarios and sensitivities. Again, the LCOE of wind onshore show the highest sensitivity. An exception can be found again for the LCOE of PV in the High Wind scenario (S-ALL). With the highest share of wind and limited available area for iRES capacities in each raster, placing wind onshore capacities in raster with high wind potentials is optimal, at the expense of PV capacities although the PV capacities are replaced at locations with higher LCOE. However, the impact on the total costs as discussed before shows the overall decrease of costs.

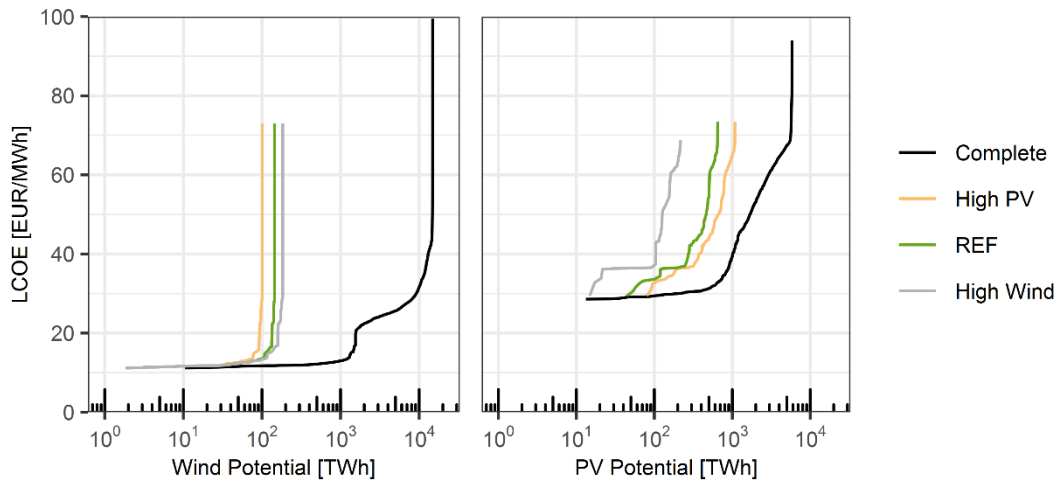


Figure B.8: Costs-potential curves without restriction of the raster density (S-RAST) (Own illustration)

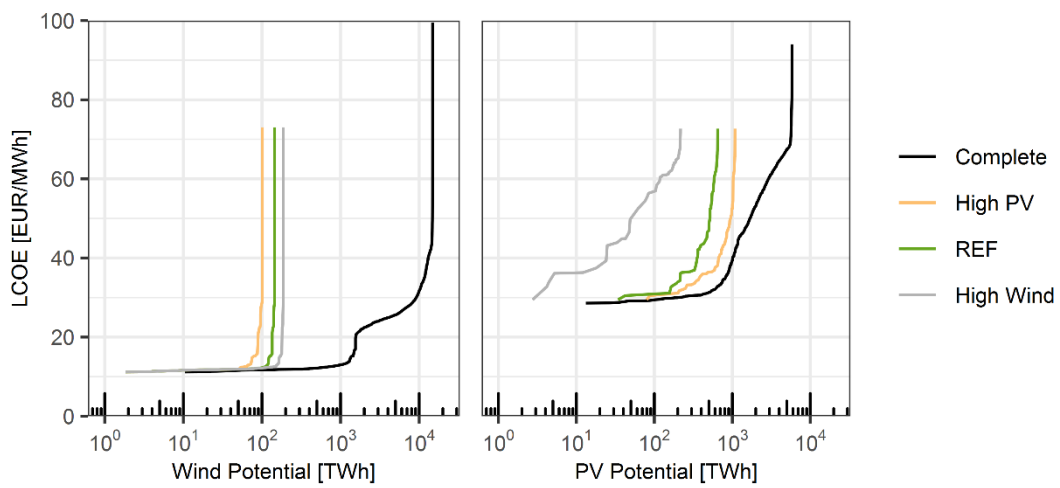


Figure B.9: cost-potential curve without restriction of the raster density as well as maximum and minimum iRES share(S-ALL) (Own illustration)

C Additional data input for the investment and dispatch model

C.1 Additional data

Table C.1: Capacity and Generation Restrictions for controllable RES (Data: Gils et al. 2017, Scholz 2012)

	Maximal installable capacity					Maximal Generation	
	PSP	Reservoir	Run-of-River	Geothermal	Geothermal CHP	CSP	Biomass
	[MW _{el}]					[TWh/a]	
AT	4.503	7.205	5.241	300	1.400	0	13
BE	1.308	0	113	100	900	0	4
CH	1.384	8.073	3.768	600	2.000	0	3
CZ	1.147	612	444	400	2.400	0	11
DE	6.390	584	2.003	9.400	20.000	0	68
DK	0	0	9	600	1.600	0	11
ES	2.667	13.231	3.153	8.400	4.100	76000	21
FR	4.263	13.514	7.641	29.000	18.000	6900	135
GB	2.828	0	989	1.300	4.700	0	17
IE	292	0	216	0	100	0	6
IT	7.543	4.888	5.764	5.000	9.200	38000	20
LU	1.096	17	15	0	100	0	1
NL	0	0	37	600	2.900	0	5
NO	1.336	30.164	0	0	0	0	2
PL	1.413	167	378	3.900	14.600	0	31
PT	240	2.157	2.562	0	0	120	5
SE	0	4.701	16.552	0	0	0	33

Table C.2: Assignment of DSM processes (Data: Gils 2016, Gils 2014)

DSM processes used in the present work	Assigned process of Gils (2014)
Air conditioning and ventilation (shifting)	<ul style="list-style-type: none">• Industrial Ventilation• Cooling Retailing• Commercial Ventilation• Commercial AC
Water and Cooling (shifting)	<ul style="list-style-type: none">• Cold Storages• Cooling Hotels/Restaurants• Water Supply• Water Treatment
Industry processes (shifting)	<ul style="list-style-type: none">• Pulp• Paper• Recycling Paper• Cement• Calcium Carbide• Air Separation
Industry processes (shedding)	<ul style="list-style-type: none">• Cement• Calcium Carbide• Air Separation• Steel

Table C.3: Existing static NTC values for the model region of 2019 (Data: ENTSO-E 2020)

Countries		NTC [MW]	Countries		NTC [MW]
AT	CH	1200	DE	PL	5650
AT	CZ	900	DE	SE	0
AT	DE	4900	DK	PL	1700
AT	IT	380	DK	SE	3400
BE	DE	1000	DK	GB	3000
BE	FR	1300	DK	NL	4600
BE	GB	2400	DK	NO	1100
BE	LU	2880	ES	FR	4200
BE	NL	300	ES	PT	1640
CH	DE	4000	FR	GB	4200
CH	FR	1300	FR	IE	1200
CH	IT	3750	FR	IT	2000
CZ	DE	2100	FR	LU	4100
CZ	PL	600	GB	IE	150
DE	DK	6500	GB	NL	400
DE	FR	3000	GB	NO	450
DE	LU	800	NL	NO	350
DE	NL	1000	NO	SE	5850
DE	NO	1300	PL	SE	300

Table C.4: Total and share of heating demand in the residential and tertiary sector (Data: HRE 2018)

	Share of residential (tertiary) heating demand in total heating demand	Demand for space and water heating in residential and tertiary sector
	[%]	[MWh _{th}]
AT	26 % (74 %)	60,672,280
BE	22 % (78 %)	77,657,299
CH	26 % (74 %)	74,709,230
CZ	31 % (69 %)	60,791,659
DE	28 % (72 %)	575,080,545
DK	35 % (65 %)	38,510,940
ES	53 % (47 %)	128,851,536
FR	21 % (79 %)	347,548,150
GB	38 % (62 %)	326,532,459
IE	29 % (71 %)	25,343,605
IT	32 % (68 %)	303,127,832
LU	14 % (86 %)	6,144,956
NL	22 % (78 %)	102,882,127
NO	25 % (75 %)	57,167,755
PL	28 % (72 %)	147,314,703
PT	48 % (52 %)	18,395,722
SE	25 % (75 %)	70,441,204

Table C.5: Data table on hydrogen demand in the countries observed

		Ammonia	Methanol	Refinery Products	Crude Steel	Sum
Source		Egenhofer et al. (2014)	Burridge (2009)	FoEE (2015)	WSA (2017)	
Total production capacity in Europe		22 [kt/a]	9 [kt/a]	14,769 [kbbbl/a]	164,144 [Mt/a]	
Total share of 17 countries	[%]	73 %	43 %	85 %	90 %	
Share of process on total hydrogen demand in 2050 (12 Mt)	[Mt]	4.6	0.5	3.2	0.7	8.97
AT	[Mt]	0.15	0.00	0.05	0.03	0.24
BE	[Mt]	0.31	0.00	0.23	0.03	0.58
CH	[Mt]	0.00	0.00	0.02	0.01	0.02
CZ	[Mt]	0.11	0.00	0.06	0.02	0.19
DE	[Mt]	1.06	0.26	0.72	0.19	2.22
DK	[Mt]	0.00	0.00	0.01	0.00	0.01
ES	[Mt]	0.19	0.00	0.33	0.06	0.58
FR	[Mt]	0.46	0.00	0.33	0.06	0.85
GB	[Mt]	0.34	0.00	0.31	0.03	0.68
IE	[Mt]	0.00	0.00	0.02	0.00	0.02
IT	[Mt]	0.19	0.00	0.39	0.10	0.68
LU	[Mt]	0.00	0.00	0.00	0.01	0.01
NL	[Mt]	0.84	0.14	0.34	0.03	1.35
NO	[Mt]	0.00	0.12	0.03	0.00	0.15
PL	[Mt]	0.99	0.01	0.13	0.04	1.18
PT	[Mt]	0.00	0.00	0.08	0.01	0.09
SE	[Mt]	0.00	0.00	0.11	0.02	0.13

Table C.6: Data input for BEV (Data: ADEME 2020, ACEA 2019, Heinrichs 2013)

	Annual driving distance	Passenger car stock	Total mileage of passenger cars	Annual energy demand	Daily energy demand (weekday)	Daily energy demand (weekend)
	[km/pc*]	[Mio]	[Mio km]	[MWh/pc*]	[kWh/pc*]	[kWh/pc*]
AT	14283	4.7	67,130	2.539	6.957	6.957
BE	14292	5.5	78,603	2.541	6.961	6.961
CH	11031	4.4	48,536	1.961	5.224	5.746
CZ	14106	4.9	69,116	2.508	6.870	6.870
DE	14106	44.4	626,284	2.508	6.870	6.870
DK	14106	2.3	32,442	2.508	6.868	6.868
ES	12253	22.0	269,555	2.178	5.734	6.554
FR	13268	31.8	421,922	2.359	6.299	6.872
GB	14292	32.6	465,902	2.541	6.961	6.961
IE	14292	1.9	27,153	2.541	6.961	6.961
IT	11031	37.0	408,147	1.961	5.224	5.746
LU	11031	0.37	4,081	1.961	5.224	5.746
NL	13593	8.2	111,458	2.416	6.615	6.615
NO	13268	2.5	33,170	2.359	6.299	6.872
PL	14106	20.0	282,110	2.508	6.870	6.870
PT	11031	4.5	49,639	1.961	5.224	5.746
SE	13268	4.6	61,032	2.359	6.297	6.870

Table C.7: Parameter for calculating the levelised costs of the benchmark processes (Data: Michaelis 2018, Ladwig 2018, Gulagi et al. 2017, Trost 2016)

	Capital Cost	Lifetime	Efficiency	Fuel costs	CO ₂ Emission Factor	Assumed full load hour / driving distance
Gas Boiler	160 [kEUR/MW _{el}]	40 [a]	0.93	33.70 [EUR/MWh _{th}]	0.200 [tco ₂ /MWh _{th}]	4,500 [h]
Steam Reformer	400 [kEUR/MW _{H2}]	30 [a]	0.80	33.70 [EUR/MWh _{th}]	0.285 [tco ₂ /MWh _{th}]	4,500 [h]
ICE	21 [kEUR/BEV]	10 [a]		0.1068 [EUR/km]	100.00 [g/km]	Country-specific [km]

C.2 Derivation of heating profiles

Steps for derivation of heat profiles for space and water heating in the residential and tertiary sector:

1. Average temperature time series for each country based on MERRA-2 dataset
2. Calculation of daily reference temperature of day d and country c :

$$T_{d,c}^{ref} = \frac{T_{d,c} + 0.5 \cdot T_{d-1,c} + 0.25 \cdot T_{d-2,c} + 0.125 \cdot T_{d-3,c}}{1 + 0.5 + 0.25 + 0.125}$$

3. Calculation of daily demand factors with sigmoid function based on BDEW (2018):
 - Profile: HMF for multi-family house for residential heating demand
 - Profile: GHA for tertiary sector for tertiary heating demand

$$f(T) = \left[\frac{A}{1 + \left(\frac{B}{T - T_0} \right)^c} + D \right] + [max] \left\{ \begin{array}{l} m_H \cdot T_0 + b_H \\ m_W \cdot T_0 + b_{HW} \end{array} \right\}$$

4. Calculation of hourly demand factors with daily load profiles based on BGW (2006):
 - Profile multi-family house (class 3) for residential heating demand
 - Profile for tertiary sector (Germany) with distinction in weekdays for tertiary heating demand
5. Aggregation of hourly country-specific time series for heating demand
 - Residential and tertiary heating potentials weighted regarding share of heating and tertiary demand of residential sector on total demand (based on Paardekooper et al. 2018)
 - Normalised time series with regard to total annual heating demand per country

D Additional results for the investment and dispatch model

Table D.1: Installed capacity of heat pumps in the FD scenarios

	High PV			REF			High Wind		
	LF [MW]	HF [MW]	Difference [%]	LF [MW]	HF [MW]	Difference [%]	LF [MW]	HF [MW]	Difference [%]
AT	2895	2936	1%	3098	2981	-4%	3392	3291	-3%
BE	4844	4828	0%	5080	4904	-3%	5140	4971	-3%
CH	4134	4290	4%	4233	4298	2%	4510	4280	-5%
CZ	3224	3156	-2%	3359	3182	-5%	3917	3767	-4%
DE	31631	31053	-2%	34651	31442	-9%	36444	35153	-4%
DK	1900	1992	5%	1950	1986	2%	2163	2072	-4%
ES	7898	8303	5%	8105	8353	3%	8683	8036	-7%
FR	21700	17798	-18%	21713	18384	-15%	22725	19282	-15%
GB	17800	17651	-1%	17839	17466	-2%	18320	17335	-5%
IE	1091	1096	0%	1146	1147	0%	1233	1120	-9%
IT	18286	17582	-4%	18354	18141	-1%	19235	17936	-7%
LU	338	333	-1%	362	336	-7%	378	364	-4%
NL	5773	5751	0%	6064	5958	-2%	6718	6442	-4%
NO	3317	3493	5%	3328	3422	3%	3590	3664	2%
PL	7953	7749	-3%	8539	7810	-9%	9684	9085	-6%
PT	994	994	0%	1033	1014	-2%	1117	1113	0%
SE	3491	3844	10%	3665	3842	5%	4067	3570	-12%
Sum	137272	132848		142518	134664		151314	141481	

Table D.2: Installed capacity of electrolyser in the FD scenarios

	High PV			REF			High Wind		
	LF [MW]	HF [MW]	Difference [%]	LF [MW]	HF [MW]	Difference [%]	LF [MW]	HF [MW]	Difference [%]
AT	778	1106	42%	778	644	-17%	642	646	1%
BE	1921	1625	-15%	1921	1573	-18%	1921	1579	-18%
CH	73	106	44%	73	62	-16%	73	59	-19%
CZ	636	577	-9%	636	526	-17%	636	540	-15%
DE	7325	6279	-14%	6658	6011	-10%	7325	6035	-18%
DK	35	31	-12%	35	28	-19%	35	29	-18%
ES	1920	2810	46%	1920	2764	44%	1920	1500	-22%
FR	2818	4010	42%	2818	2378	-16%	2818	2283	-19%
GB	2249	3286	46%	2249	1813	-19%	2249	1751	-22%
IE	53	46	-13%	53	45	-15%	53	43	-19%
IT	2235	3406	52%	2235	2901	30%	1913	1833	-4%
LU	32	26	-18%	27	26	-3%	26	26	-2%
NL	4447	3680	-17%	3811	3647	-4%	3849	3611	-6%
NO	495	394	-21%	401	390	-3%	496	383	-23%
PL	3549	3241	-9%	3306	3121	-6%	3694	3288	-11%
PT	310	468	51%	310	528	71%	310	243	-21%
SE	421	339	-20%	421	334	-21%	421	326	-23%
Sum	29298	31427		27652	26790		28380	24176	

Table D.3: Installed BEV

	Constant in High PV, REF and High Winds
	Constant in LF and HF
	[1000]
AT	2,350
BE	2,750
CH	2,200
CZ	2,450
DE	22,200
DK	1,150
ES	11,000
FR	15,900
GB	16,300
IE	950
IT	18,500
LU	185
NL	4,100
NO	1,250
PL	10,000
PT	2,250
SE	2,300
Sum	115,835

Table D.4: Installed electricity storage capacity in the NO scenario

[GW]	HOU			DAY			SEA			PSP			
Country	HP	REF	HW	HP	REF	HW	HP	REF	HW	HP	REF	HW	
AT	0	0	0	0	0	0	0	0	0	0	5	5	5
BE	0	1	0	0	0	0	0	1	0	0	1	1	1
CH	0	0	0	0	0	0	0	0	0	0	1	1	1
CZ	1	1	0	0	0	0	0	1	1	0	1	1	1
DE	5	0	0	0	0	0	0	9	5	0	6	6	6
DK	0	0	0	0	0	0	0	0	0	0	0	0	0
ES	27	4	2	0	0	0	0	0	0	0	3	3	3
FR	16	0	0	0	0	0	0	8	0	0	4	4	4
GB	3	12	1	0	0	0	0	13	9	9	3	3	3
IE	1	1	0	0	0	0	0	1	0	0	0	0	0
IT	31	18	3	7	0	0	5	4	2	8	8	8	8
LU	0	0	0	0	0	0	0	0	0	0	1	1	1
NL	2	7	0	0	0	0	0	2	4	3	0	0	0
NO	0	0	0	0	0	0	0	0	0	0	1	1	1
PL	6	3	0	0	0	0	0	1	4	0	1	1	1
PT	6	0	0	0	0	0	0	0	0	0	0	0	0
SE	1	0	0	0	0	0	0	0	0	0	0	0	0
Total	100	48	6	7	0	0	0	41	28	15	36	36	36

Table D.5: Installed electricity storage capacity in the LF scenario

[GW]	HOU			DAY			SEA			PSP			
Country	HP	REF	HW	HP	REF	HW	HP	REF	HW	HP	REF	HW	
AT	15	0	0	0	0	0	0	0	0	0	5	5	5
BE	0	0	0	0	0	0	0	0	0	0	1	1	1
CH	13	0	0	0	0	0	0	0	0	0	1	1	1
CZ	5	0	0	0	0	0	0	0	0	0	1	1	1
DE	46	0	0	0	0	0	0	0	0	0	6	6	6
DK	0	0	0	0	0	0	0	0	0	0	0	0	0
ES	85	39	9	0	0	0	0	0	0	0	3	3	3
FR	85	20	4	0	0	0	0	0	0	0	4	4	4
GB	24	7	16	0	0	0	0	0	0	0	3	3	3
IE	2	2	2	0	0	0	0	0	0	0	0	0	0
IT	173	132	7	6	0	0	0	0	0	0	8	8	8
LU	0	0	0	0	0	0	0	0	0	0	1	1	1
NL	0	0	2	0	0	0	0	0	0	0	0	0	0
NO	2	0	0	0	0	0	0	0	0	0	1	1	1
PL	5	0	6	0	0	0	0	0	0	0	1	1	1
PT	17	24	3	2	0	0	0	0	0	0	0	0	0
SE	5	0	0	0	0	0	0	0	0	0	0	0	0
Total	477	225	49	8	0	0	0	0	0	0	36	36	36

Table D.6: Installed electricity storage capacity in the HF scenario

[GW]	HOU			DAY			SEA			PSP			
Country	HP	REF	HW	HP	REF	HW	HP	REF	HW	HP	REF	HW	
AT	13	0	0	0	0	0	0	0	0	0	5	5	5
BE	0	0	0	0	0	0	0	0	0	0	1	1	1
CH	11	0	0	0	0	0	0	0	0	0	1	1	1
CZ	2	0	0	0	0	0	0	0	0	0	1	1	1
DE	26	0	0	0	0	0	0	0	0	0	6	6	6
DK	0	0	0	0	0	0	0	0	0	0	0	0	0
ES	78	18	0	0	0	0	0	0	0	0	3	3	3
FR	65	0	0	0	0	0	0	0	0	0	4	4	4
GB	0	0	0	0	0	0	0	0	0	0	3	3	3
IE	0	0	0	0	0	0	0	0	0	0	0	0	0
IT	176	77	0	0	0	0	0	0	0	0	8	8	8
LU	0	0	0	0	0	0	0	0	0	0	1	1	1
NL	0	0	0	0	0	0	0	0	0	0	0	0	0
NO	0	0	0	0	0	0	0	0	0	0	1	1	1
PL	0	0	0	0	0	0	0	0	0	0	1	1	1
PT	23	24	0	0	0	0	0	0	0	0	0	0	0
SE	0	0	0	0	0	0	0	0	0	0	0	0	0
Total	394	119	0	0	0	0	0	0	0	0	36	36	36

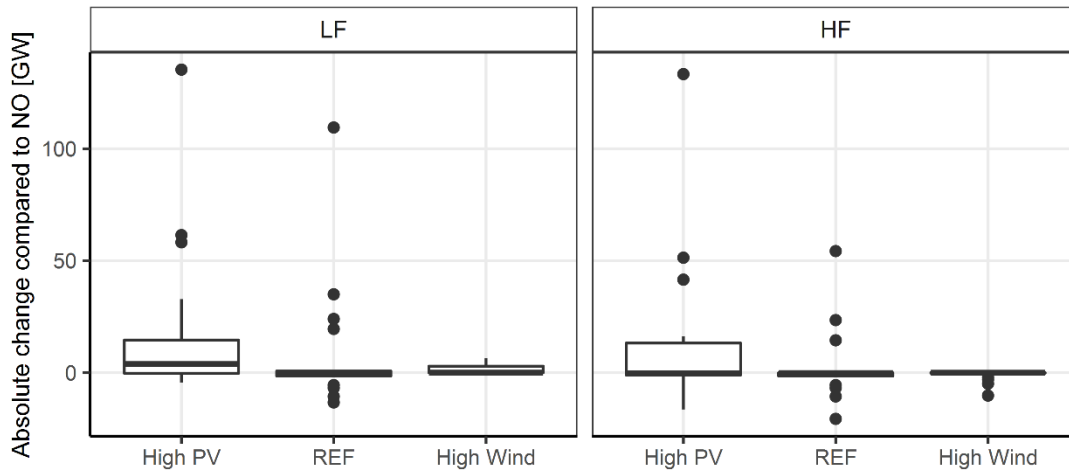


Figure D.1: Boxplots of absolute change in storage capacities in LF and HF compared to NO (Own illustration)

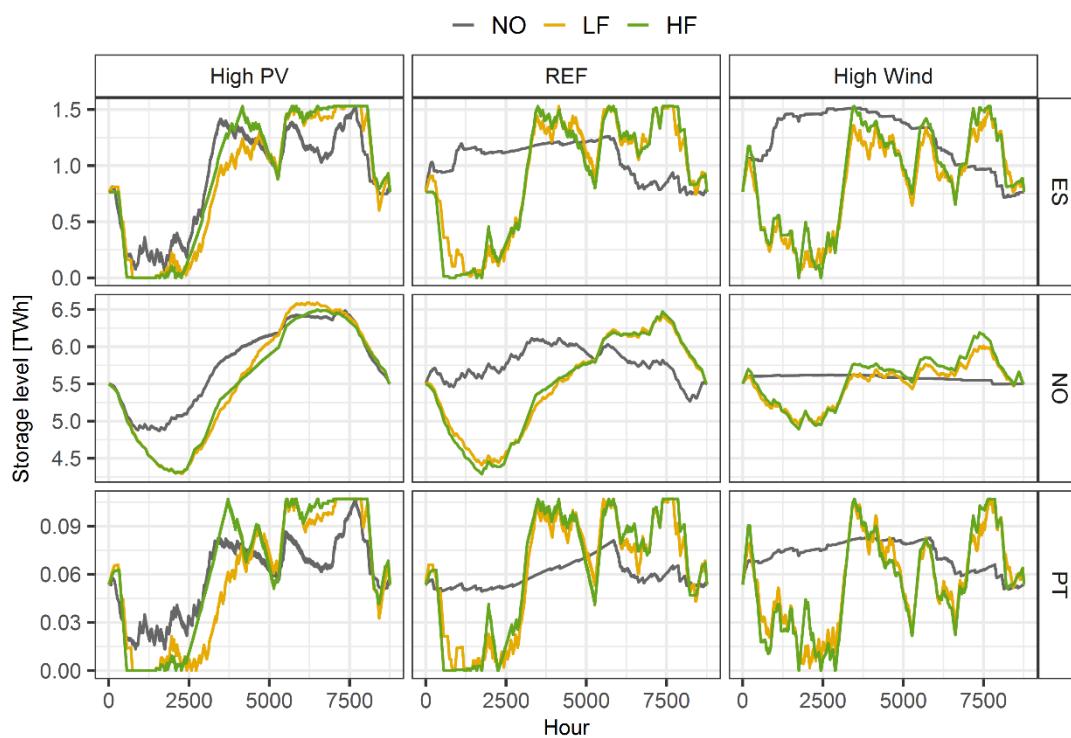


Figure D.2: Hourly storages level of PSP in three selected countries (Own illustration)

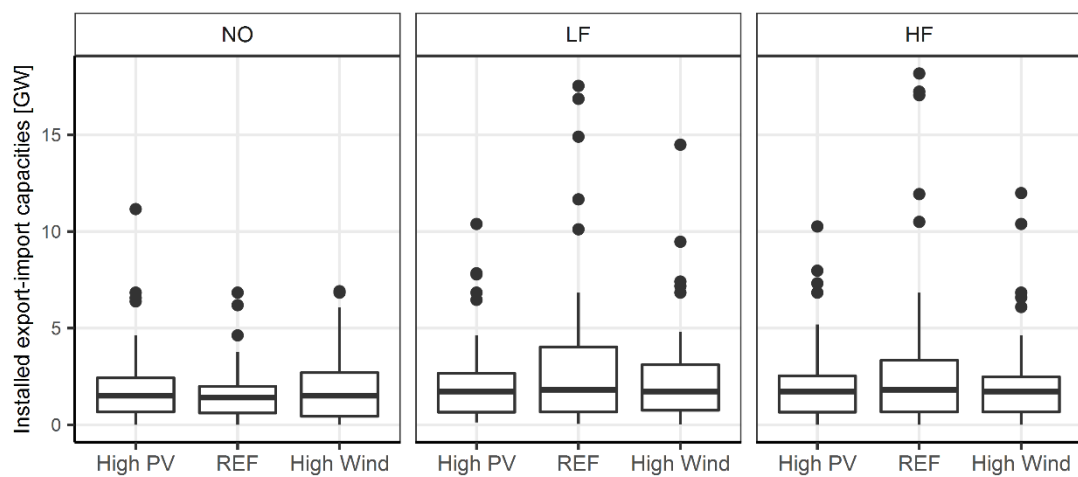


Figure D.3: Boxplot of country-specific NTC investments (Own illustration)

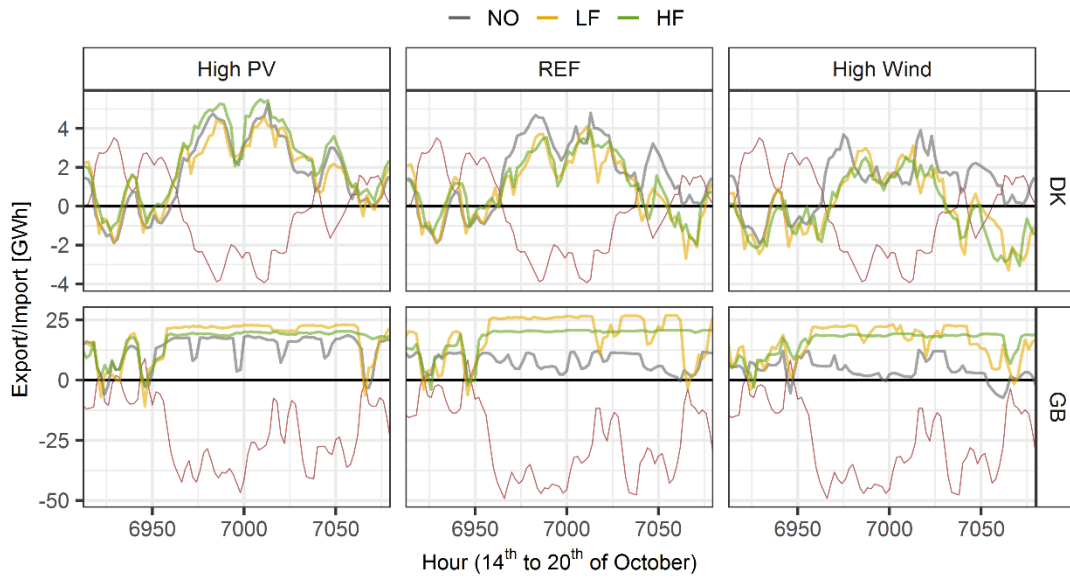


Figure D.4: Exemplary import and export flows for Denmark and Great Britain (Own illustration)

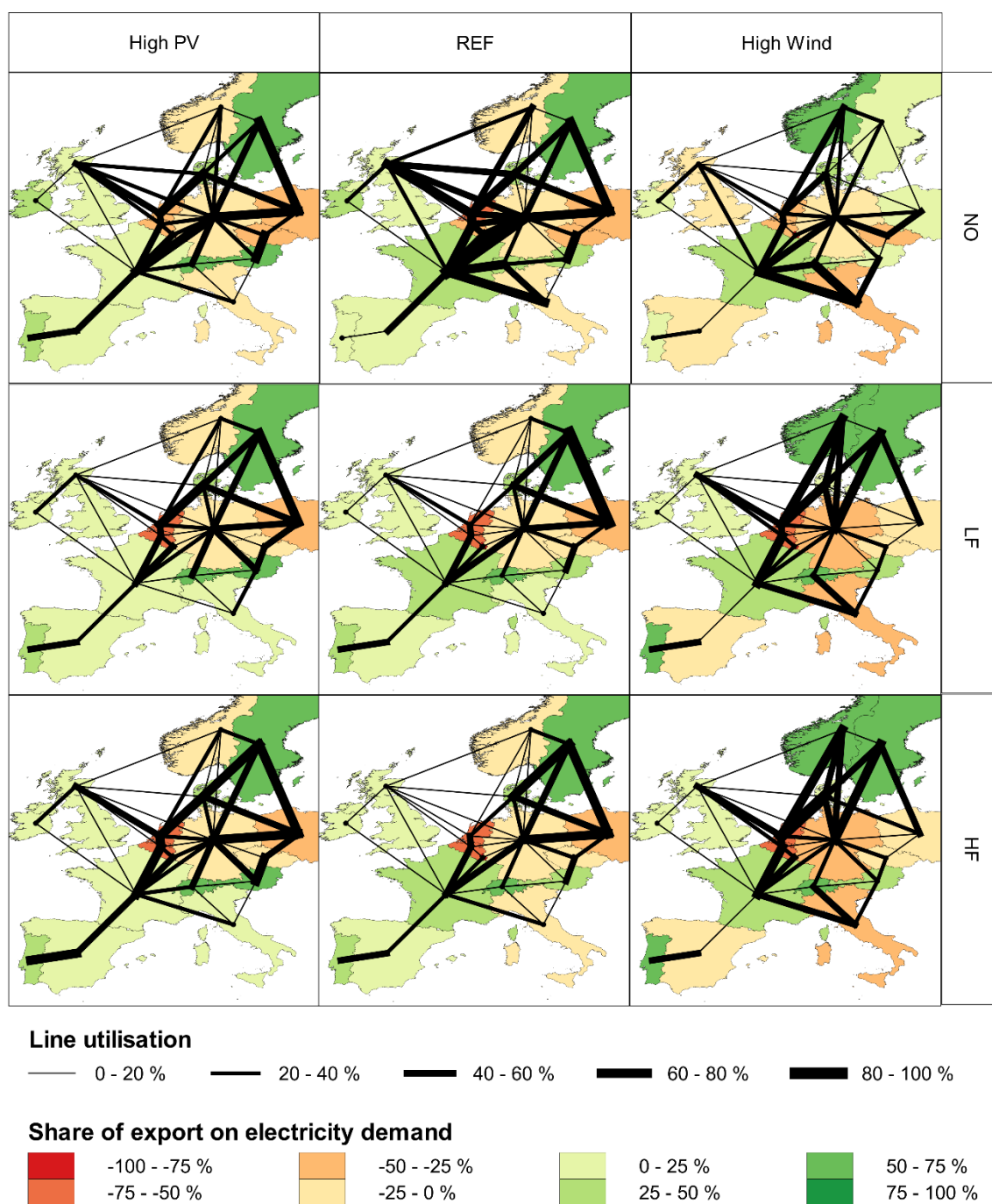


Figure D.5: Geographical presentation of transmission line utilisation and share of export on each country's electricity demand (Own illustration)

Table D.7: Installed power plant capacity in the NO scenario

[GW]	CCGT			Nuclear			Biomass CHP			Geo CHP			Reservoir			RoR		
Country	HP	REF	HW	HP	REF	HW	HP	REF	HW	HP	REF	HW	HP	REF	HW	HP	REF	HW
AT	0	0	0	0	0	0	2	2	2	0	0	0	7	7	7	5	5	5
BE	0	2	0	0	0	0	1	1	1	0	0	0	0	0	0	0	0	0
CH	0	0	0	0	0	0	0	0	0	0	0	0	8	8	8	4	4	4
CZ	1	2	0	0	0	0	2	2	2	0	0	0	1	1	1	0	0	0
DE	1	3	3	0	0	0	8	8	8	0	0	0	1	1	1	2	2	2
DK	0	0	0	0	0	0	2	2	2	0	0	0	0	0	0	0	0	0
ES	0	0	0	0	0	0	2	2	2	0	0	0	13	13	13	3	3	3
FR	0	0	0	0	0	0	24	24	24	0	0	0	14	14	14	8	8	8
GB	0	10	10	0	0	0	2	2	2	1	0	0	0	0	0	1	1	1
IE	0	2	1	0	0	0	1	1	1	0	0	0	0	0	0	0	0	0
IT	0	2	1	0	0	0	2	2	2	2	0	0	5	5	5	6	6	6
LU	0	0	0	0	0	0	0	0	0	0	0	0	0	0	0	0	0	0
NL	1	3	4	0	0	0	1	1	1	1	0	0	0	0	0	0	0	0
NO	0	0	0	0	0	0	0	0	0	0	0	0	30	30	30	0	0	0
PL	4	3	1	0	0	0	5	5	5	0	0	0	0	0	0	0	0	0
PT	0	0	0	0	0	0	1	1	1	0	0	0	2	2	2	3	3	3
SE	0	0	0	0	0	0	6	6	6	0	0	0	5	5	5	17	17	17
Total	7	26	21	0	0	0	57	57	57	5	0	0	85	85	85	49	49	49

Table D.8: Installed power plant capacity in the LF scenario

[GW]	CCGT			Nuclear			Biomass CHP			Geo CHP			Reservoir			RoR		
Country	HP	REF	HW	HP	REF	HW	HP	REF	HW	HP	REF	HW	HP	REF	HW	HP	REF	HW
AT	0	0	0	0	0	0	3	3	2	1	1	1	7	7	7	5	5	5
BE	7	0	3	0	0	0	1	1	1	1	1	1	0	0	0	0	0	0
CH	0	0	0	0	0	0	1	1	1	2	2	2	8	8	8	4	4	4
CZ	2	1	2	2	2	2	2	2	2	1	1	1	1	1	1	0	0	0
DE	23	4	13	0	0	0	15	14	12	15	13	9	1	1	1	2	2	2
DK	0	0	0	0	0	0	2	2	2	1	0	0	0	0	0	0	0	0
ES	0	0	0	0	0	0	3	3	3	0	0	0	13	13	13	3	3	3
FR	0	0	0	2	2	2	23	22	20	0	0	0	14	14	14	8	8	8
GB	4	4	5	3	3	3	3	3	3	5	5	5	0	0	0	1	1	1
IE	0	0	0	0	0	0	1	1	1	0	0	0	0	0	0	0	0	0
IT	14	17	9	0	0	0	4	4	4	5	5	9	5	5	5	6	6	6
LU	0	0	0	0	0	0	0	0	0	0	0	0	0	0	0	0	0	0
NL	6	0	5	0	0	0	1	1	1	3	3	3	0	0	0	0	0	0
NO	0	0	0	0	0	0	0	0	0	0	0	0	30	30	30	0	0	0
PL	11	7	2	0	0	0	5	5	5	4	4	1	0	0	0	0	0	0
PT	0	0	0	0	0	0	1	1	1	0	0	0	2	2	2	3	3	3
SE	0	0	0	0	0	0	5	4	4	0	0	0	5	5	5	17	17	17
Total	67	33	39	7	7	7	70	68	62	38	36	31	85	85	85	49	49	49

Table D.9: Installed power plant capacity in the HF scenario

[GW] Country	CCGT			Nuclear			Biomass CHP			Geo CHP			Reservoir			RoR		
	HP	REF	HW	HP	REF	HW	HP	REF	HW	HP	REF	HW	HP	REF	HW	HP	REF	HW
AT	0	0	0	0	0	0	3	2	2	1	1	1	7	7	7	5	5	5
BE	2	0	0	0	0	0	1	1	1	1	1	1	0	0	0	0	0	0
CH	0	0	0	0	0	0	1	1	1	2	2	2	8	8	8	4	4	4
CZ	1	2	1	2	2	2	2	2	2	2	2	2	1	1	1	0	0	0
DE	6	1	0	0	0	0	16	15	11	20	18	10	1	1	1	2	2	2
DK	0	0	0	0	0	0	2	2	1	1	1	0	0	0	0	0	0	0
ES	0	0	0	0	0	0	3	3	3	0	0	0	13	13	13	3	3	3
FR	0	0	0	2	2	2	25	22	18	0	0	0	14	14	14	8	8	8
GB	9	0	0	3	3	3	3	3	3	5	5	5	0	0	0	1	1	1
IE	0	0	0	0	0	0	1	1	1	0	0	0	0	0	0	0	0	0
IT	19	9	4	0	0	0	4	4	5	3	3	9	5	5	5	6	6	6
LU	1	0	0	0	0	0	0	0	0	0	0	0	0	0	0	0	0	0
NL	5	0	1	0	0	0	1	1	1	3	3	3	0	0	0	0	0	0
NO	0	0	0	0	0	0	0	0	0	0	0	0	30	30	30	0	0	0
PL	11	7	0	0	0	0	6	5	4	5	4	1	0	0	0	0	0	0
PT	0	0	0	0	0	0	1	1	1	0	0	0	2	2	2	3	3	3
SE	0	0	0	0	0	0	5	4	4	0	0	0	5	5	5	17	17	17
Total	55	19	6	7	7	7	73	68	58	43	39	34	85	85	85	49	49	49

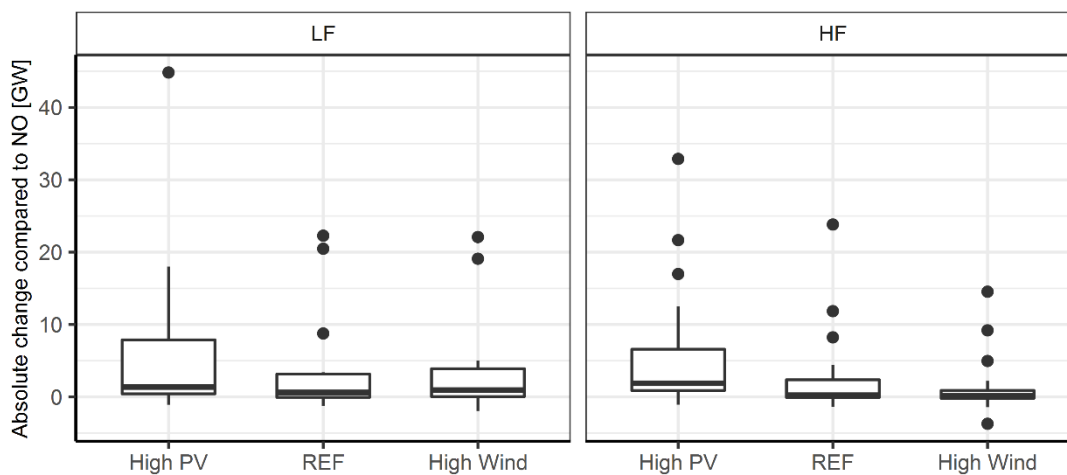


Figure D.6: Boxplot of country-specific increase in power plants capacities compared to the NO scenario (Own illustration)

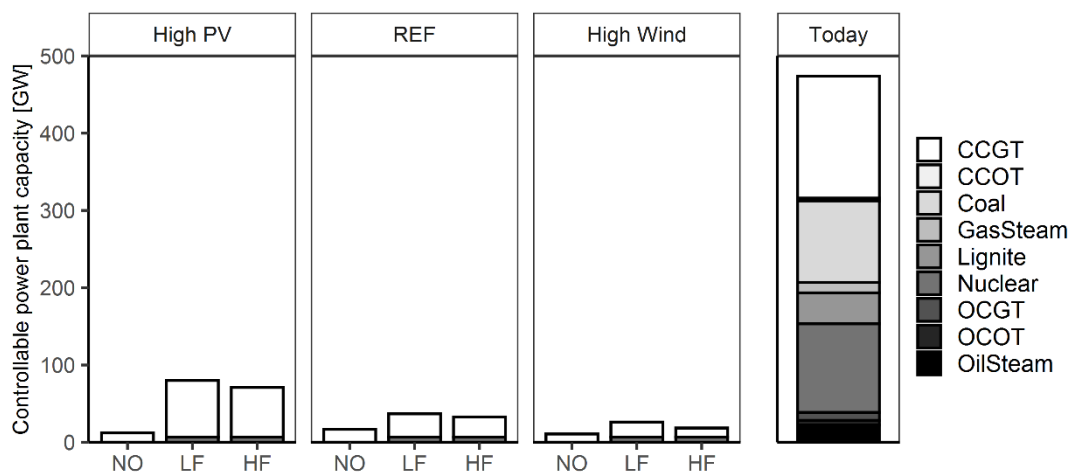


Figure D.7: Comparison of optimal expansion of power plants by technology with existing capacities

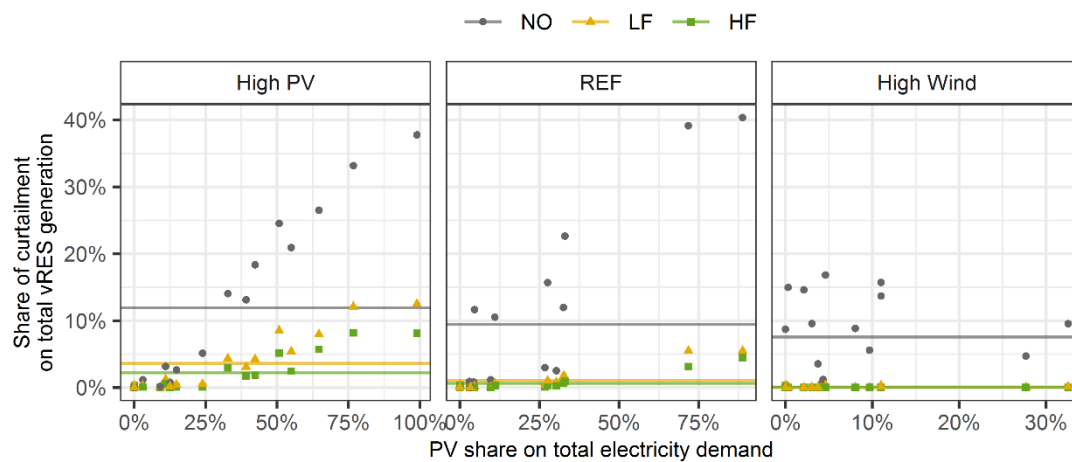


Figure D.8: Country-specific share of curtailment on total iRES generation as function of the PV share on total electricity demand (Own illustration)

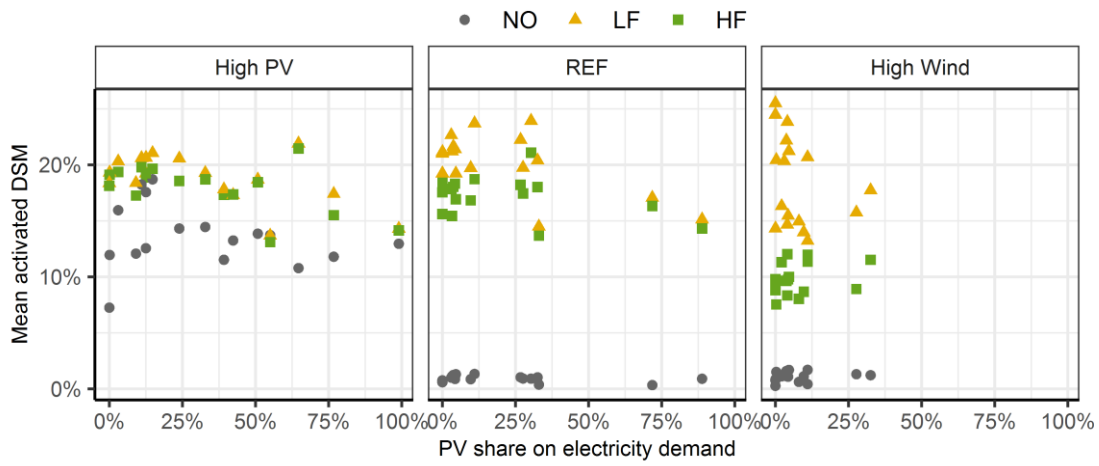


Figure D.9: Average activated DSM measures per country normalised to capacities installed as function of the PV share on the electricity demand (Own illustration)

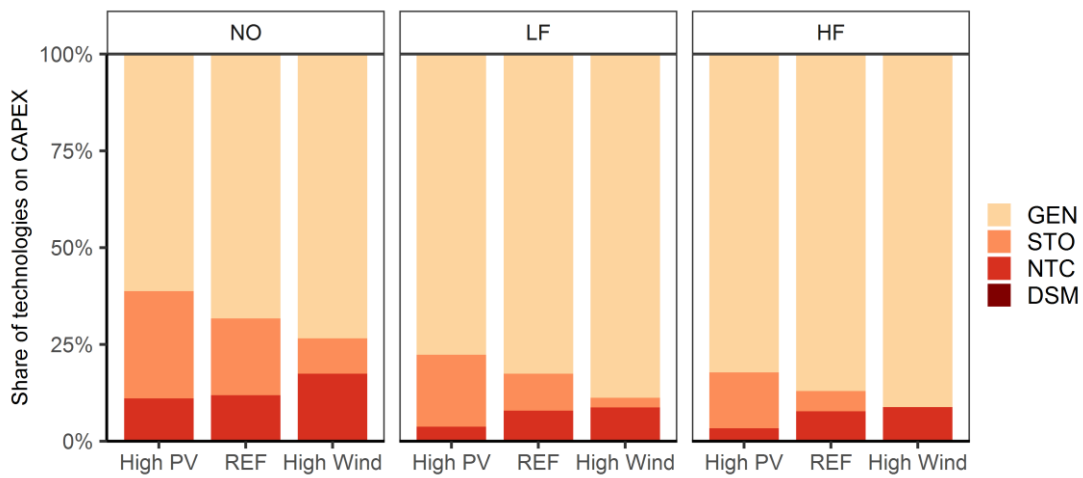


Figure D.10: share of technology-specific CAPEX on total CAPEX (Own illustration)

Table D.10: Scenario-specific residual load parameter cumulated for the whole region observed in the *iRES+* scenario

		High PV	REF	High Wind
Total iRES generation	[TWh]	3,471	3,471	3,471
iRES deficits of cumulated residual load	[TWh]	532	251	152
iRES surplus of cumulated residual load	[TWh]	1134	853	760
Share of deficits on total iRES generation	[%]	15%	7%	4%
Share of surplus on total iRES generation	[%]	33%	25%	22%
Maximum cumulated residual load	[GW]	306	262	213
Minimum cumulated residual load	[GW]	-1116	-815	-520
Numbers of hours with cumulated iRES surplus		3195	5051	6285

Table D.11: iRES generation for the additional scenario *iRES+* in the FD scenarios per iRES technology type and country

[TWh]	High PV			REF			High Wind		
	PV	Wind onshore	Wind offshore	PV	Wind onshore	Wind offshore	PV	Wind onshore	Wind offshore
AT	89	10	0	38	7	0	18	10	0
BE	17	36	6	7	36	6	4	43	6
CH	56	6	0	23	3	0	15	2	0
CZ	42	5	0	17	5	0	9	85	0
DE	237	143	24	80	421	24	49	688	27
DK	1	42	7	1	42	7	1	42	7
ES	183	183	0	110	256	0	37	329	0
FR	348	348	0	209	487	0	70	626	0
GB	95	310	31	13	391	31	13	391	31
IE	4	35	0	4	35	0	4	35	0
IT	416	20	26	405	20	25	99	20	0
LU	0	0	0	0	0	0	0	0	0
NL	28	53	4	4	59	4	4	104	7
NO	11	141	4	0	170	19	0	170	19
PL	69	151	1	21	199	1	0	199	22
PT	57	16	0	57	16	0	7	66	0
SE	0	44	15	0	38	21	0	33	27
Total	1653	1542	117	989	2186	136	330	2842	145

Table D.12: Installed capacities for the additional scenario *iRES+* in the FD scenarios per *iRES* technology type and country

[GW]	High PV			REF			High Wind		
	PV	Wind onshore	Wind offshore	PV	Wind onshore	Wind offshore	PV	Wind onshore	Wind offshore
AT	85	5	0	36	3	0	17	5	0
BE	17	13	2	7	13	2	4	15	2
CH	51	5	0	22	2	0	14	1	0
CZ	42	2	0	17	2	0	9	33	0
DE	239	58	7	80	171	7	50	280	8
DK	1	12	2	1	12	2	1	12	2
ES	144	68	0	87	95	0	29	123	0
FR	319	129	0	191	180	0	64	232	0
GB	105	96	14	15	121	14	15	121	14
IE	4	10	0	4	10	0	4	10	0
IT	352	11	8	343	11	7	84	11	0
LU	7	1	0	7	1	0	2	0	0
NL	29	19	1	4	21	1	4	37	2
NO	15	53	1	0	64	5	0	64	5
PL	72	55	0	22	72	0	0	72	6
PT	45	6	0	45	6	0	6	23	0
SE	0	20	4	0	17	6	0	15	7
Total	1529	560	39	882	802	44	302	1053	47

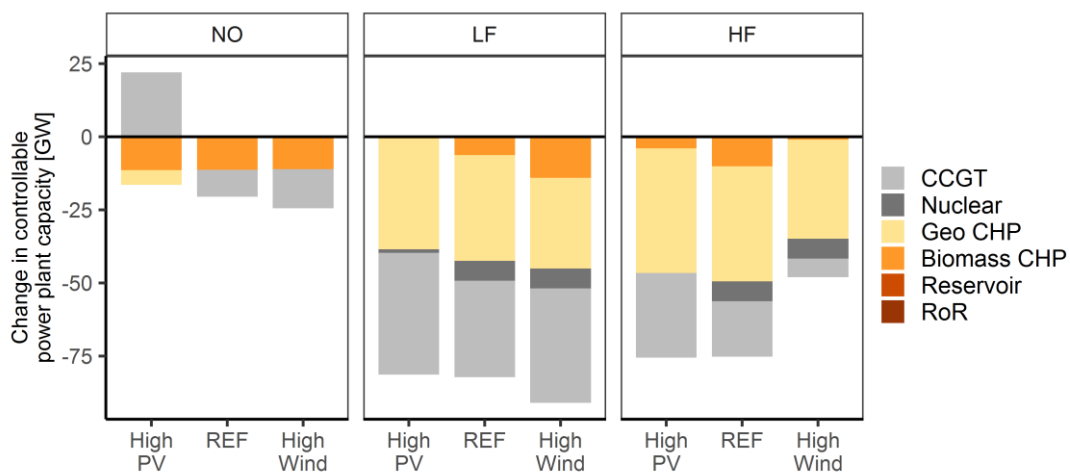


Figure D.11: Absolute change in controllable power plant capacity in *iRES+* compared to the original results (Own illustration)

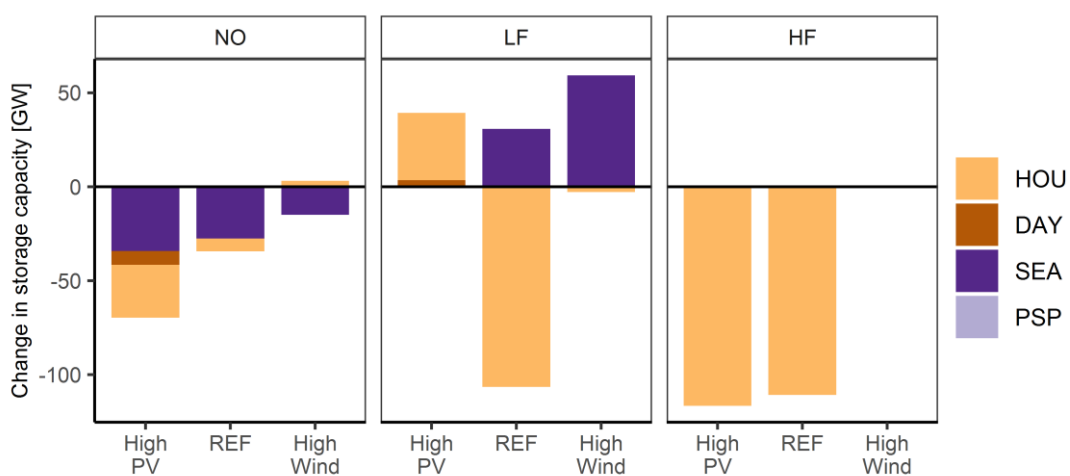


Figure D.12: Absolute change in electricity storage capacity in *iRES+* compared to the original results (Own illustration)

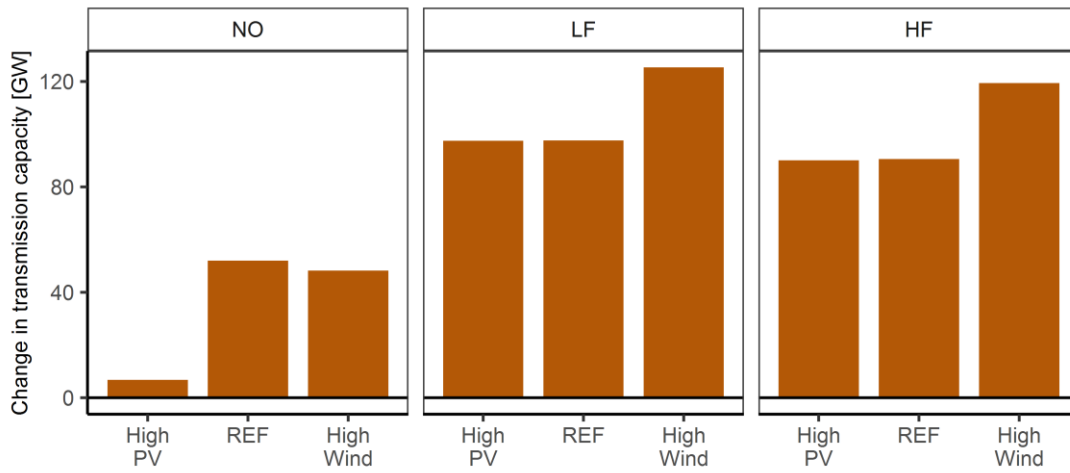


Figure D.13: Absolute change in NTC in *iRES+* compared to the original results (Own illustration)

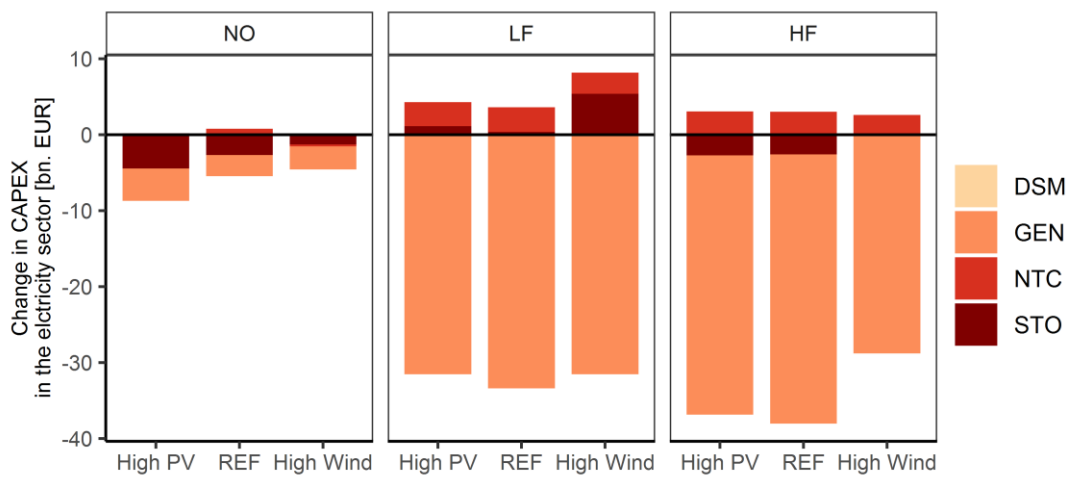


Figure D.14: Absolute change in CAPEX in *iRES+* compared to the original results (Own illustration)

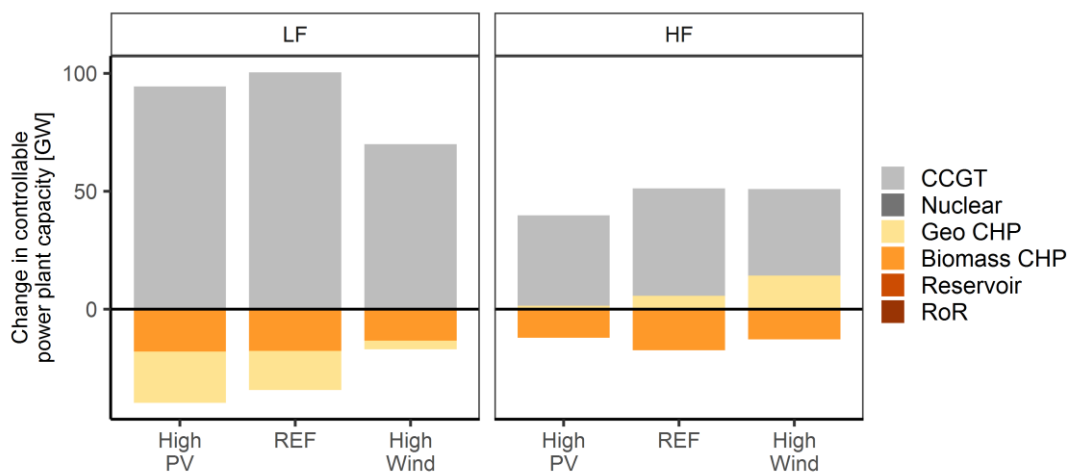


Figure D.15: Absolute change in controllable power plant capacity in *PtX+* compared to the original results (Own illustration)

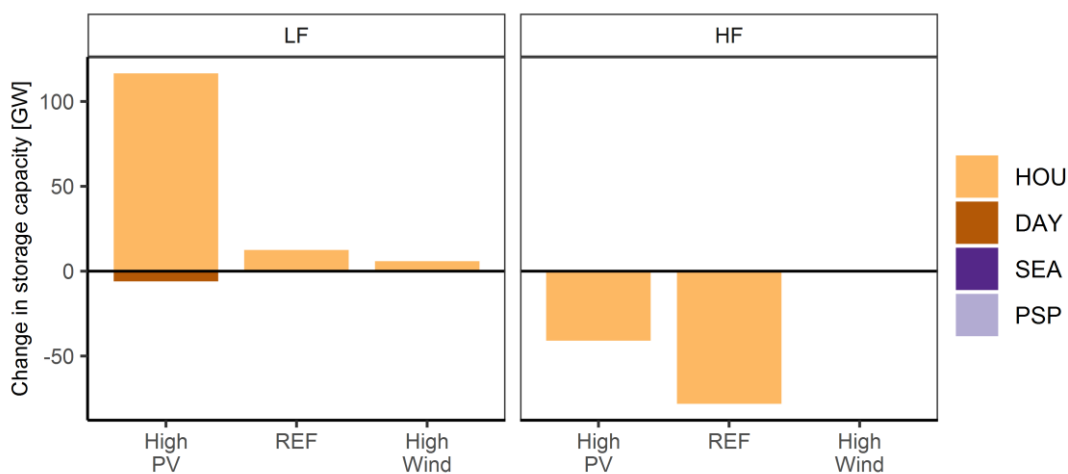


Figure D.16: Absolute change in electricity storage capacity in *PtX+* compared to the original results (Own illustration)

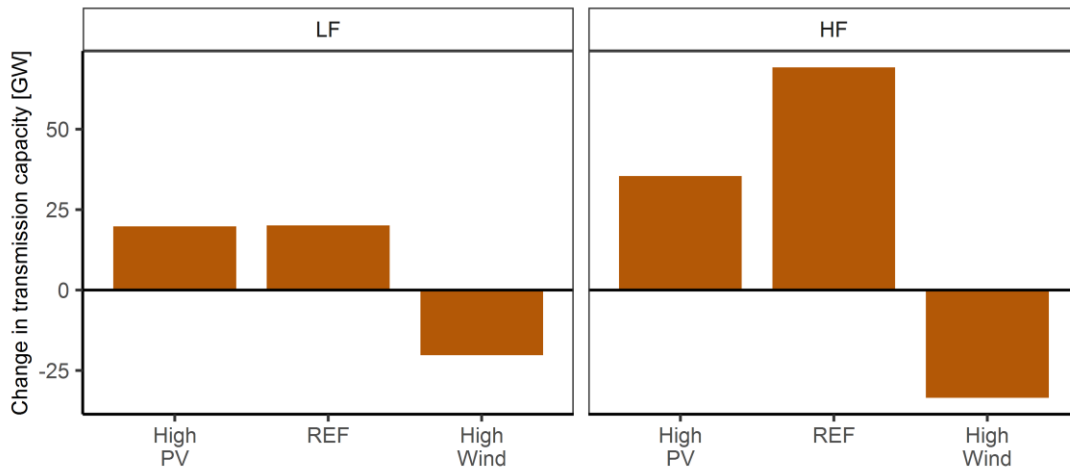


Figure D.17: Absolute change in NTC in *PtX+* compared to the original results (Own illustration)

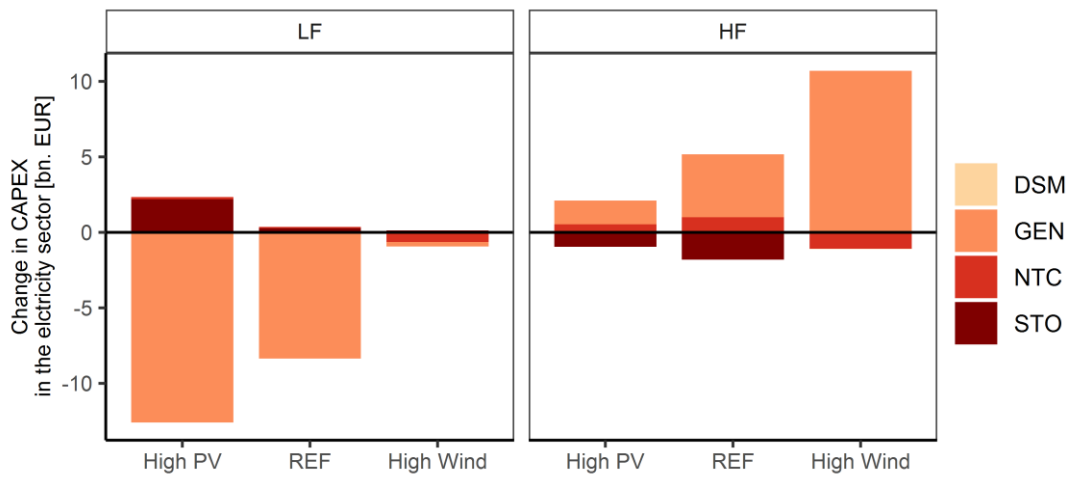


Figure D.18: Absolute change in CAPEX in *PtX+* compared to the original results (Own illustration)

Schriften des Lehrstuhls für Energiewirtschaft, TU Dresden

Technische Universität Dresden
Fakultät Wirtschaftswissenschaften
Lehrstuhl für Energiewirtschaft

In der Schriftenreihe sind auf Qucosa®, dem sächsischen Dokumenten- und Publikationsserver, bisher erschienen:

- Band 1** **Managing Congestion and Intermittent Renewable Generation in Liberalized Electricity Markets**
(Friedrich Kunz)
<http://nbn-resolving.de/urn:nbn:de:bsz:14-qucosa-108793>
- Band 2** **Der Stromausfall in München - Einfluss auf Zahlungsbereitschaften für Versorgungssicherheit und auf die Akzeptanz Erneuerbarer Energien**
(Daniel K. J. Schubert, Thomas Meyer, Alexander von Selasinsky, Adriane Schmidt, Sebastian Thuß, Niels Erdmann und Mark Erndt)
<http://nbn-resolving.de/urn:nbn:de:bsz:14-qucosa-117777>
- Band 3** **Abschätzung der Entwicklung der Netznutzungsentgelte in Deutschland**
(Fabian Hinz, Daniel Iglhaut, Tobias Frevel, Dominik Möst)
<http://nbn-resolving.de/urn:nbn:de:bsz:14-qucosa-141381>
- Band 4** **Potenziale der Elektrizitätserzeugung aus erneuerbaren Ressourcen im Freistaat Sachsen**
(Hannes Hobbie, Vera Schippers, Michael Zipf, Dominik Möst)
<http://nbn-resolving.de/urn:nbn:de:bsz:14-qucosa-153350>
- Band 5** **Energiewende Sachsen - Aktuelle Herausforderungen und Lösungsansätze Beiträge der Abschlusskonferenz des ENERSAX-Projektes**
(Dominik Möst und Peter Schegner (Hrsg.))
<http://nbn-resolving.de/urn:nbn:de:bsz:14-qucosa-156464>
- Band 6** **Electricity transmission line planning: Success factors for transmission system operators to reduce public opposition**
(Stefan Perras)
<http://nbn-resolving.de/urn:nbn:de:bsz:14-qucosa-161770>
- Band 7** **Renewable energy in North Africa: Modeling of future electricity scenarios and the impact on manufacturing and employment**
(Christoph Philipp Kost)
<http://nbn-resolving.de/urn:nbn:de:bsz:14-qucosa-176538>
- Band 8** **Kurzgutachten zur regionalen Ungleichverteilung der Netznutzungsentgelte**
(Dominik Möst, Fabian Hinz, Matthew Schmidt, Christoph Zöphel)
<http://nbn-resolving.de/urn:nbn:de:bsz:14-qucosa-184452>
- Band 9** **The integration of renewable energy sources in continuous intraday markets for electricity**
(Alexander von Selasinsky)
<http://nbn-resolving.de/urn:nbn:de:bsz:14-qucosa-202130>

- Band 10 Bewertung von Szenarien für Energiesysteme**
(Daniel K. J. Schubert)
<http://nbn-resolving.de/urn:nbn:de:bsz:14-qucosa-202226>
- Band 11 Deutschland, ein Solarmärchen? Die Zweite Phase der Energiewende zwischen Richtungsstreit und Systemintegration**
(Sebastian Thuß)
<http://nbn-resolving.de/urn:nbn:de:bsz:14-qucosa-231486>
- Band 12 Voltage Stability and Reactive Power Provision in a Decentralizing Energy System – A Techno-economic Analysis**
(Fabian Hinz)
<http://nbn-resolving.de/urn:nbn:de:bsz:14-qucosa-229585>
- Band 13 Electricity, Heat, and Gas Sector Data for Modeling the German System**
(Friedrich Kunz, Mario Kendziorski, Wolf-Peter Schill, Jens Weibezahn, Jan Zepter, Christian von Hirschhausen, Philipp Hauser, Matthias Zech, Dominik Möst, Sina Heidari, Björn Felten, Christoph Weber)
<http://nbn-resolving.de/urn:nbn:de:bsz:14-qucosa-233511>
- Band 14 Demand Side Management in Deutschland zur Systemintegration erneuerbarer Energien**
(Theresa Ladwig)
<http://nbn-resolving.de/urn:nbn:de:bsz:14-qucosa-236074>
- Band 15 Modellgestützte Wirtschaftlichkeitsbewertung von Betriebskonzepten für Elektrolyseure in einem Energiesystem mit hohen Anteilen erneuerbarer Energien**
(Julia Michaelis)
<http://nbn-resolving.de/urn:nbn:de:bsz:14-qucosa-235773>
- Band 16 Begleitstudie WindNODE – Lastverschiebepotentiale in Dresden**
(Carl-Philipp Anke, Constantin Dierstein, Dirk Hladik, Dominik Möst)
<http://nbn-resolving.de/urn:nbn:de:bsz:14-qucosa2-312491>
- Band 17 Einflussfaktoren auf das Übertragungsnetz im Jahr 2030 für Deutschland - Eine techno-ökonomische Analyse der Wechselwirkungen auf den Umfang des Netzausbaus, die Systemkosten und die Integration erneuerbarer Energien**
(David Gunkel)
<https://nbn-resolving.org/urn:nbn:de:bsz:14-qucosa2-716026>
- Band 18 Auswirkungen der Kopplung von Strom- und Wärmemarkt auf die künftige Integration der erneuerbaren Energien und die CO2-Emissionen in Deutschland**
(Gerda Deac)
<https://nbn-resolving.org/urn:nbn:de:bsz:14-qucosa2-725153>
- Band 19 Fristigkeit und Politik. Konzeptualisierung und Analyse von langfristigkeitsfördernden Institutionen im Kontext energiepolitischer Steuerung**
(Nick Pruditsch)
<https://nbn-resolving.org/urn:nbn:de:bsz:14-qucosa2-748650>

- Band 20 Economics of Ancillary Services for Electricity – Managing Uncertain Power Generation and Grid Operation in the Distribution Network**
(Michael Zipf)
<https://nbn-resolving.org/urn:nbn:de:bsz:14-qucosa2-751856>
- Band 21 Short- and mid-term uncertainties affecting the trade and transmission of electricity with a focus on flow-based market coupling**
(David Josua Schönheit)
<https://nbn-resolving.org/urn:nbn:de:bsz:14-qucosa2-751888>
- Band 22 Quantitative Analysis of the Reduction of Greenhouse Gas Emissions in the Power Sector**
(Carl-Philipp Anke)
<https://nbn-resolving.org/urn:nbn:de:bsz:14-qucosa2-761374>
- Band 23 Flexibility Options in Energy Systems - The influence of Wind - PV ratios and sector coupling on optimal combinations of flexible technologies in a European electricity system**
(Christoph Zöphel)
[https://nbn-resolving.org/urn:nbn:de:bsz:14-qucosa2-781290!](https://nbn-resolving.org/urn:nbn:de:bsz:14-qucosa2-781290)



Kurzzusammenfassung

Im Fokus der vorliegenden Arbeit liegt die Analyse der Wechselwirkungen zwischen Flexibilitätsnachfrage und Flexibilitätsangebot. Dazu werden drei zentrale Herausforderungen im Hinblick auf die zukünftige Transformation des europäischen Energiesystems behandelt. Zunächst wird der Ausbau fluktuierender erneuerbarer Energiequellen (fEE) unter Berücksichtigung der Potenziale von Wind- und PV-Technologien diskutiert. Zur Untersuchung der Unterschiede in der Stromerzeugung zwischen Wind und PV wird ein fEE-Ausbaumodell entwickelt. Mit der Bereitstellung von Flexibilität im Energiesystem wird die zweite zentrale Herausforderung näher beleuchtet. Dazu wird das Strommarktmodell ELTRAMOD um eine Vielzahl von Flexibilitätsoptionen inklusive Sektorkopplungstechnologien mit unterschiedlichen Anwendungsgebieten erweitert. Der dritte Forschungsbereich adressiert darüber hinaus die Sektorkopplung durch Einbeziehung ausgewählter Power-to-X-Technologien. Insbesondere wird die Rolle von Energiespeichern in den Endverbrauchssektoren für eine flexiblere Sektorkopplung betrachtet.

Die Ergebnisse unterstreichen die Bedeutung des Wind-PV-Verhältnisses in der Stromerzeugung bei der Bewertung von Flexibilitätsbedarf und Flexibilitätsangebot in der modellbasierten Energiesystemanalyse. Aufgrund der höheren Saisonalität der solaren Stromerzeugung weisen die Residuallastparameter auf höhere Herausforderungen bei der fEE-Integration hin. Insbesondere die Bereitstellung von räumlicher und zeitlicher Ausgleichsflexibilität wird durch einen höheren Wind- oder PV-Anteil im fEE-Mix deutlich beeinflusst. Mit der Sektorkopplung steigt der Wert der zeitlichen Verschiebung. Stündliche Speicher sind nicht nur sehr sensitiv gegenüber dem Wind-PV-Verhältnis, sondern werden auch stark von der Sektorkopplung beeinflusst. Außerdem erhöht die Sektorkopplung den Bedarf an zusätzlicher Stromerzeugung. Dabei sind für die Bereitstellung von Spitzenlastkapazitäten in der vorliegenden Arbeit Gaskraftwerke optimal, die insbesondere bei hohen PV-Anteilen zu einer Erhöhung der Gesamtemissionen führen.

Autor

Christoph Zöphel schloss das Wirtschaftsingenieur-Studium an der TU Dresden mit den Vertiefungen Energietechnik und Energiewirtschaft ab. Sein Promotionsstudium begann im Juni 2015 im Rahmen des zweiten Boysen-TU Dresden-Graduiertenkollegs. Ab Oktober 2018 war er als wissenschaftlicher Mitarbeiter am Lehrstuhl für Energiewirtschaft der TU Dresden tätig, wo er 2022 seine Promotion erfolgreich beendete.